Electromagnetic Induction in the Earth

Lectures Notes Aarhus 1975

Ulrich Schmucker and Peter Weidelt

Laboratoriet for anvendt geofysik
Aarhus Universitet

Electromagnetic Induction in the Earth

Contents

1. Introduction, basic equations

1.1. General ideas

The following model is the basis of all electromagnetic methods which try to infer the electrical conductivity structure in the Earth's subsurface from an analysis of the natural or artificial electromagnetic surface field: On or above the surface of the Earth is situated a time-dependent electromagnetic source. By Faraday's law the time-varying magnetic field $\dot{\underline{H}}$ induces an electrical field $\underline{E}$ which drives within the conductor a current $\underline{\imath}$. By Ampère's law this current has a magnetic field which again is an inducing agent, and so on. Hence, there is the closed chain

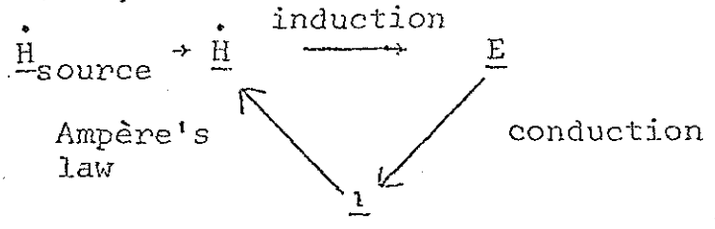

The mathematical expression of this closed chain is a second order partial differential equation resulting after the elimination of two field quantities from the two first order equations $\underline{\imath} \rightarrow \underline{H}$ and $\dot{\underline{H}} \rightarrow \underline{E}$.

At the surface the electromagnetic field of the source is disturbed by the internal fields. This disturbance depends on the conductivity structure and contains information which must be revealed. It is a matter of the particular objective which surface data have to be measured and how the information is extracted from them.

The induced currents try to expel the external field from the conductor leading to a decrease of the electromagnetic field amplitude with depth.

The available period range and average conductivity determine the depth range of a particular method. For a uniform half-space with conductivity σ or resistivity $\rho = 1/\sigma$ the penetration depth (decay on 1/e) is approximately

$$p = 0.5 \sqrt{\rho T}, \text{ where } p \text{ in km, } \rho \text{ in } \Omega m, \text{ and } T \text{ in sec.} \qquad (1a)$$

Alternatively

$$p = 30. \sqrt{\rho T}, \text{ where } T \text{ in } h. \qquad (1b)$$

Eqs. (1a,b) can also be used as a rule of thumb if ρ varies with depth and an average resistivity is inserted.

The natural magnetic source fields of the ionospheric and magnetospheric currents offer periods approximately between 0.1 sec and 20 permitting crustal and upper mantle surveys down to a depth of approximately 800 - 1000 km. On the other side periods between 0.01 and 0.002 sec are most commonly used for sounding of the first 300 m with artificial fields.

Electromagnetic methods are applicable for two objectives:

1) Investigation of the change of conductivity with depth, in particular detection and delineation of horizontal interfaces marking a change of stratigraphy or temperature.
2) Investigation of lateral conductivity variations, in particular search for local regions with abnormal conductivities (e.g. metallic ore deposits, salt domes, sedimentary basins, zones of elevated temperature).

The results of the first investigation are often used to construct a normal conductivity model from which local deviations are measured.

In an interpretation of natural fields the change of the electromagnetic field quantities both with frequency and with position are used. Broadly speaking the dependence on the position provides the lateral resolution and the dependence on frequency gives the resolution with depth.

1.2. Basic equations

Let $\underline{r}$ be the position vector and let $\underline{H}$, $\underline{E}$, and $\underline{\imath}$ be the vectors of the magnetic field, electrical field and current density, respectively. Using SI units and a vacuum permeability μ_0 throughout, the pertinent equations are

$$\text{curl } \underline{H} = \underline{\imath} + \underline{\imath}_e \qquad (1.2)$$

$$\text{curl } \underline{E} = -\mu_0 \underline{H} \qquad (1.3)$$

$$\underline{\imath} = \sigma \underline{E} \qquad (1.4)$$

$$\text{div } \underline{H} = 0 \qquad (1.5)$$

All field quantities are functions of position $\underline{r}$ and time t. Also the (isotropic) conductivity σ is a function of position. $\underline{\imath}_e$ is the current density of the external current sources being different from 0 only at source points. The displacement current $\varepsilon_0 \dot{\underline{E}}$ is generally neglected in induction studies. This is justified as follows: within the conductor the conduction current $\sigma\underline{E}$ exceeds the displacement current even in the case of lowest periods (0.001 sec) and highest resistivities (10^5 Ωm) still 10^2 times. In the vacuum where the conduction current is absent the inclusion of the displacement current merely introduces a slight phase shift of the external field at different points. For in this case the solution of (1.2) and (1.3 (including $\varepsilon_0 \dot{\underline{E}}$ at the RHS of (1.2)) are electromagnetic waves, e.g. the plane wave $e^{i(\underline{k}\cdot\underline{r} - \omega t)}$, where ω is the angular frequency and $\underline{k}$ the wave vector along the direction of propagation. The phase difference between P_1 and P_2 is

$$\omega\Delta t = \frac{\omega\Delta x}{c}\cos\alpha$$

$\simeq 10^{-2}$ in the very pessimistic case of Δx = 1000 km and T = 1se

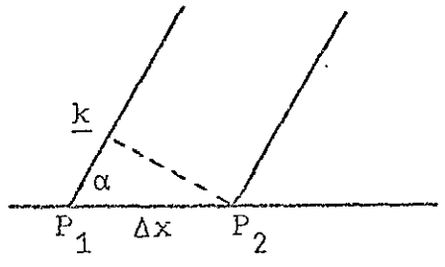

$\underline{H}$ and $\underline{\imath}$ can be eliminated from (1.2) - (1.4). It results

$$\boxed{\text{curl}^2\underline{E} + \mu_0\,\sigma\,\dot{\underline{E}} = -\,\mu_0\,\dot{\underline{\imath}}_e \qquad \text{Induction equation}} \tag{1.6}$$

On using (1.2) and (1.4) the electrical charge density $\rho(\underline{r})$ is given by

$$\rho = \varepsilon_0\,\text{div}\,\underline{E} = -\,\varepsilon_0\,\underline{E}\cdot\text{grad}\log\sigma, \tag{1.7}$$

i.e. there is charge accumulated if an electrical field component parallel to the gradient of the conductivity. Physically this is clear, since the normal component of the current density is continuous whereas the charges account for the corresponding discontinuity of the normal electrical field.

The electrical effect of the changes is very important. They modify by attraction and repulsion the current flow; in particular surface changes deflect the current lines in such a way that the normal current component vanishes at the surface. In contrast the magnetic effect is of the order of that of the displacement current and can be neglected.

2. Electromagnetic induction in 1-dimensional structures

2.1. The general solution

The following vector analytical identities are used in the sequel ($\underline{A}$ is a vector, ϕ a scalar).

$$\text{div curl } \underline{A} = 0 \tag{2.1}$$

$$\text{curl grad } \phi = 0 \tag{2.2}$$

$$\text{div}(\underline{A}\phi) = \phi \text{ div } \underline{A} + \underline{A} \cdot \text{grad } \phi \tag{2.3}$$

$$\text{curl}(\underline{A}\phi) = \phi \text{ curl}\underline{A} - \underline{A} \times \text{grad } \phi \tag{2.4}$$

$$\text{curl}^2\underline{A} = \text{grad div}\underline{A} - \Delta\underline{A} \tag{2.5}$$

$$\text{grad}\phi(\psi) = \frac{\partial\phi}{\partial\psi} \text{grad}\psi \tag{2.6}$$

In this chapter it is assumed that the electrical conductivity σ is a function of depth z (positive downwards) only. In this case the electromagnetic field inside and outside the conductor can be represented in terms of two scalars $\phi_E(\underline{r})$ and $\phi_M(\underline{r})$ denoting the electric and magnetic type of solution. These fields are defined as follows ($\hat{z}$ is the unit vector in z-direction):

$$\underline{H}_M = \text{curl}(\sigma\phi_M\hat{z}), \quad \underline{E}_M = \frac{1}{\sigma}\text{curl}^2(\sigma\phi_M\hat{z}) \tag{2.7a}$$

$$\underline{H}_E = \text{curl}^2(\phi_E\hat{z}), \quad \underline{E}_E = -\mu_o\text{curl}(\phi_E\hat{z}) \tag{2.8a}$$

On using the identity $\text{curl}(\phi\hat{z}) = -\hat{z} \times \text{grad}\phi$ (from (2.4)), it is seen that the M-type solution has no magnetic z-component and the E-type solution has no electrical z-component.

The electric field of the E-type solution is tangential to the planes σ = const. Hence, it is called a TE-mode (tangential electric). Conversely the M-type solution is named a TM-mode. As required from (1.5) the magnetic field of both modes is solenoidal (i.e. $\mathrm{div}\underline{H} = 0$). In addition the E-field of the TE-mode is also solenoidal. In this mode there is no accumulation of charge, all current flow is parallel to the (x,y)-plane.

Now we have to derive the differential equations for the scalars ϕ_E and ϕ_M. The TE-field (2.8a,b) satisfies already (1.3) - (1.5). It remains to satisfy

$$\mathrm{curl}\underline{H}_E = \sigma\, \underline{E}_E.$$

Using (2.5), (2.2), and (2.4) it results

$$\hat{\underline{z}} \times \mathrm{grad}(\Delta\phi_E - \mu_o\sigma\, \dot{\phi}_E) = 0,$$

from which follows

$$\boxed{\Delta\phi_E = \mu_o\sigma\, \dot{\phi}_E} \qquad (2.9)$$

(for if $\partial f/\partial x = 0$ and $\partial f/\partial y = 0$ and $f \to 0$ for $x,y \to \infty$, then $f=0$).

The TM-mode has to satisfy

$$\mathrm{curl}\underline{E}_M = -\mu_o\dot{\underline{H}}_M$$

From this equation follows with the same arguments

$$\boxed{\mathrm{div}\left[\frac{1}{\sigma}\,\mathrm{grad}(\sigma\phi_M)\right] = \mu_o\sigma\, \dot{\phi}_M} \qquad (2.10)$$

In uniform domains, (2.9) and (2.10) agree. Using (2.9), (2.10), (2.5), and (2.4) the TE- and TM-fields in the vacuum outside the sources are

$$\boxed{\begin{aligned} \underline{H}_M &= 0, & \underline{E}_M &= \mathrm{grad}\,\frac{\partial\phi_M}{\partial z} \\ \underline{H}_E &= \mathrm{grad}\,\frac{\partial\phi_E}{\partial z}, & \underline{E}_E &= \mu_o\hat{\underline{z}} \times \mathrm{grad}\,\dot{\phi}_E \end{aligned}} \qquad (2.11)$$

Fields outside the conductor

The variables x,y, and t which do not explicitly occur in (2.9) and (2.10) can be separated from ϕ_E and ϕ_M by exponential factors. Let for ϕ_E or ϕ_M

$$\phi(x,y,z,t) = \int\int\int_{-\infty}^{+\infty} f(z,\underline{\kappa},\omega)e^{i(\underline{\kappa}\cdot\underline{r}+\omega t)}d\kappa_x,\ d\kappa_y\ d\omega \qquad (2.13)$$

where $\underline{\kappa} = \kappa_x \hat{\underline{x}} + \kappa_y \hat{\underline{y}}$ and $\kappa^2 = \underline{\kappa}\cdot\underline{\kappa}$. (2.14a,b)

Then (2.9) and (2.10) read

$$f_E''(z) = \{\kappa^2 + i\omega\mu_o\sigma(z)\}f_E(z) \qquad (2.9a)$$

$$\left(\frac{1}{\sigma}(\sigma f_M(z))'\right)' = \{\kappa^2+i\omega\mu_o\sigma(z)\}f_M(z) \qquad (2.10a)$$

The general solution of (1.2) - (1.5) for a one-dimensional conductivity structure is the superposition of a TE- and TM-field. The total field then reads in components:

$$H_x = \frac{\partial}{\partial y}(\sigma\phi_M) + \frac{\partial^2\phi_E}{\partial x\partial z} \qquad (2.15a)$$

$$H_y = -\frac{\partial}{\partial x}(\sigma\phi_M) + \frac{\partial^2\phi_E}{\partial y\partial z} \qquad (2.15b)$$

$$H_z = -\left(\frac{\partial^2}{\partial x^2} + \frac{\partial^2}{\partial y^2}\right)\phi_E \qquad (2.15c)$$

$$E_x = \frac{1}{\sigma}\frac{\partial^2(\sigma\phi_M)}{\partial x\partial z} - \mu_o\frac{\partial\dot{\phi}_E}{\partial y} \qquad (2.16a)$$

$$E_y = \frac{1}{\sigma}\frac{\partial^2(\sigma\phi_M)}{\partial y\partial z} + \mu_o\frac{\partial\dot{\phi}_E}{\partial x} \qquad (2.16b)$$

$$E_z = -\left(\frac{\partial^2}{\partial x^2} + \frac{\partial^2}{\partial y^2}\right)\phi_M \qquad (2.16c)$$

General expression of field components

At a horizontal discontinuity the tangential components of $\underline{E}$ and $\underline{H}$ and the normal component of H_z are continuous. Let $[\ ]$ denote the jump of a particular quantity. Then from (2.15c) for H_z

$$\left(\frac{\partial^2}{\partial x^2} + \frac{\partial^2}{\partial y^2}\right) [\phi_E] = 0$$

$[\phi_E]$ satisfies the two-dimensional Laplace equation, is bounded and vanishes at infinity because of the finite extent of the sources. Hence, from Liouville's theorem of function theory $[\phi_E] = 0$, i.e. ϕ_E continuous. Differentiating (2.15a) with respect to x and (2.15b) with respect to y and adding we infer along the same lines that $\partial\phi_E/\partial z$ is continuous. Conversely differentiating (2.15a) with respect to y and (2.15b) with respect to x and subtracting one obtains $\sigma\phi_M$ continuous. Finally differentiate (2.16a) with respect to x and (2.16b) with respect to y and add. It results that $(1/\sigma)\ \partial(\sigma\phi_M)/\partial z$ is continuous or $\partial\phi_M/\partial z$ is continous if σ tends to a constant value at both sides.

Summarizing:

$$\phi_E,\ \frac{\partial\phi_E}{\partial z},\ \sigma\phi_M,\ \frac{1}{\sigma}\frac{\partial\sigma\phi_M}{\partial z} \text{ continuous} \qquad (2.17a)$$

Continuity conditions

This result shows that the TE- and TM-field satisfy disjoint boundary conditions. Hence, they are completely independent and not coupled. ingen Kobling

From (2.17c) follows

$$\phi_M(z = +0) = 0 \qquad (2.18)$$

This boundary condition has a serious drawback for the TM-field: As a result within the conductor no TM-field can be excited by external sources.

From (2.18) follows via (2.13) $f_M(o) = 0$. Now

$$\frac{d}{dz}|\sigma f_M|^2 = 2\,\mathrm{Re}\{(\sigma f_M)'(\sigma f_M)^*\} \qquad (2.19$$

Multiplying (2.9a) by $(\sigma f_M)^*$ and integrating over z from 0 to z, integration by parts yields in virtue of $f_M(o) = 0$

$$(\sigma f_M)'(\sigma f_M)^* = \sigma \int_o^z \{\,|(\sigma f_M)'|^2/\sigma + \sigma(\kappa^2 + i\omega\mu_o\sigma)|f_M|^2\}dz \qquad (2.20$$

From (2.20) and (2.19) follows for real frequencies

$$\frac{d}{dz} |\sigma f_M|^2 \geq 0 .$$

On the other hand f_M has to tend to a limit for $z \to \infty$. Hence,

$$f_M(z) \equiv 0, \qquad 0 \leq z < \infty,$$

i.e. there is no externally excited TM-mode.

Outside the conductor the electrical TM-field does not vanish in general. Since ϕ_M vanishes inside the conductor we have $\partial\phi_M/\partial z = 0$ for $z = +o$. The boundary condition (2.17d) then requires that also

$$\partial\phi_M/\partial z = 0 \quad \text{for } z = -0. \tag{2.21}$$

Let $\phi_M^e(x,y,z,t)$ be the TM-potential of the source. It is a solution of $\Delta\phi_M^e = 0$ ((2.10)). Then the mirror potential $\phi_M^e(x,y,-z,t)$ satisfies also (2.10), and the total TM-potential satisfying (2.21) is

$$\phi_M(x,y,z,t) = \phi_M^e(x,y,z,t) + \phi_M^e(x,y,-z,t), \quad z < 0. \tag{2.22}$$

According to (2.11b) and (2.21) the horizontal components of $\underline{E}_M$ vanish at $z = -0$, whereas the vertical component is twice the vertical component of the source field. At the surface $z = -0$ this component is the only indication of a TM-part of the source field, since according to (2.11a) the magnetic TM-field vanishes identically in $z \leq 0$.

We may retain as the most important result of this section that in a horizontally stratified conductor all current flow independently of the source is in horizontal planes and that one scalar function (ϕ_E) is sufficient to represent all fields relevant for the induction process.

2.2 Free modes of decay

Whereas external fields can excite only the TE-mode within the conductor, there exist free modes of current decay for both TE- and TM-fields. Consider the typical potential

$$\phi(x,y,z,t) = \cos\kappa_x x \cdot \cos\kappa_y y \cdot f(z)e^{-\beta t}, \tag{2.23}$$

where ϕ and f stand for ϕ_E, ϕ_M and f_E, f_M, respectively. First it will be shown that the decay constants β (eigenvalues) must be positive quantities. Inserting (2.23) in (2.9) and (2.10) we obtain

$$f_E''(z) = \{\kappa^2 - \beta\mu_o\sigma(z)\} f_E(z), \tag{2.24}$$

$$\{\frac{1}{\sigma(z)}(\sigma(z)f_M(z))'\}' = \{\kappa^2-\beta\mu_o\sigma(z)\}f_M(z), \tag{2.25}$$

where $\kappa^2 = \kappa_x^2 + \kappa_y^2$. The eigenfunctions have to satisfy the boundary conditions

$$f_E = (\pm\infty) = 0, \quad f_M(+o) = 0, \quad f_M'(\infty) = 0 \tag{2.26}$$

If there is a perfect conductor at finite depth d then

$$f_E(d) = 0, \quad f_M'(d) = 0 \tag{2.26a}$$

Multiplying (2.24) and (2.25) by f_E^* and σf_M^* and integrating over z from $-\infty$ to $+\infty$ and 0 to ∞, respectively, we obtain on integrating by parts and using (2.26)

$$\int_{-\infty}^{+\infty} \{|f_E'|^2+\kappa^2|f_E|^2\}dz = \beta\mu_o \int_o^\infty \sigma(z)|f_E(z)|^2dz, \tag{2.27}$$

$$\int_o^\infty \frac{1}{\sigma}\{|(\sigma f_M)'|^2+\kappa^2|\sigma f_M|^2\}dz = \beta\mu_o \int_o^\infty |\sigma f_M|^2dz. \tag{2.28}$$

Hence, all decay constants β are real and positive. The current flow for TE-decays is in horizontal planes, whereas the TM-decay currents flow predominantly in vertical planes.

Example:

$\sigma = 0$ — $z = 0$

$\sigma \neq 0,\infty$

— $z = d$

$\sigma = \infty$

a) TM-mode

From (2.25), (2.26), (2.26a) follows

$$f_M''(z)+\gamma^2 f_M(z) = 0, \quad f_M(o) = f_M'(d)=0, \quad \gamma^2=\beta\mu_o\sigma - \kappa^2.$$

$f_M(o) = 0$ yields $f_M(z) = \sin\gamma z$, whereas $f_M'(d) = 0$ requires $\cos\gamma d=0$. Hence,

$$\gamma_n = \frac{(2n-1)\pi}{2d}, \quad \beta_n = \frac{(2n-1)^2\pi^2+4\kappa^2d^2}{4d^2\mu_o\sigma}, \quad n=1,2,3 \ldots \qquad (2.29)$$

The unnormalized eigenfunctions are

$$f_{M,n}(z) = \sin\frac{(2n-1)\pi z}{2d}, \quad n = 1,2, \ldots$$

There exists also an electrical (potential) field outside the conductor. Find it!

b) TE-mode

From (2.24), (2.26), (2.26a) follows

$$f_E''(z) = \kappa^2 f_E(z), \quad z < 0$$

$$f_E''(z)+\gamma^2 f_E(z)=0, \quad 0 < z < d, \quad \gamma^2=\beta\mu_o\sigma - \kappa^2$$

with $f_E(-\infty) = 0$, f_E, f_E' continuous across $z = 0$, $f_E(d) = 0$.

$$f_E(z) = e^{\kappa z}, \quad z \leq 0$$

$$f_E(z) = \cos\gamma z + (\kappa/\gamma)\sin\gamma z, \quad 0 \leq z \leq d.$$

Then $f_E(d) = 0$ leads to the eigenvalue condition

$$\cos\gamma d + (\kappa/\gamma)\sin\gamma d = 0.$$

For $\kappa = 0$ the eigenvalues agree with those of TM. For $\kappa d \ll 1$ approximately

$$\gamma_n \simeq \frac{(2n-1)\pi}{2d} + \frac{2\kappa}{(2n-1)\pi}, \quad \beta_n \simeq \frac{(2n-1)^2\pi^2}{4d^2\mu_o\sigma} + \frac{2\kappa}{\mu_o\sigma d}. \qquad (2.31)$$

For a current system in the upper mantle of the Earth with $d=500$ km $1/\sigma = 50$ Ωm, the greatest decay time is approximately $1/\beta_1=40$ min.

The TE-decay systems occur as transients to fit the initial conditions, e.g. when an external field is switched on.

2.3. Calculation of $f_E(z)$ for a layered structure

Let the half-space consist of L uniform layers with conductivities $\sigma_1, \sigma_2, \ldots, \sigma_L$, the upper edge of layer m being at $h_m (h_1 = 0)$. Let the index 0 refer to the air half-space.

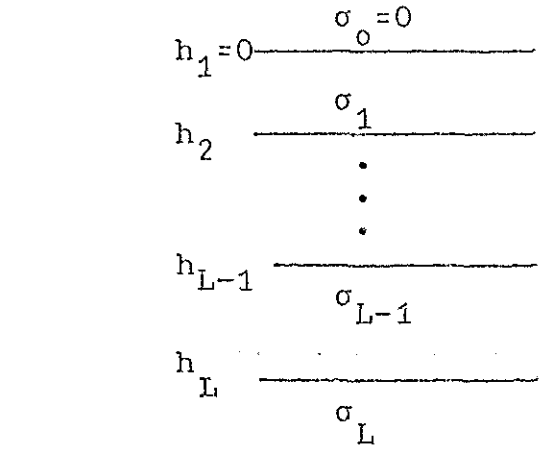

Then given in $z \leq 0$ the potential of the source field

$$f_E^e(z) = f_o^- e^{-\kappa z} \tag{2.32}$$

we have to solve (2.9a), i.e.

$$f_E''(z) = \{\kappa^2 + i\omega\mu_o\sigma(z)\} f_E(z).$$

With the abbreviations

$$\alpha_o^2 = \kappa^2, \quad \alpha_m^2 = \kappa^2 + i\omega\mu_o\sigma_m, \quad m = 1, 2, \ldots, L$$

and the understanding that $h_{L+1} = \infty$, we have

$$f_E(z) = \delta\{B_o^- e^{-\alpha_o z} + B_o^+ e^{\alpha_o z}\}, \quad 0 > z > -h_s \tag{2.33}$$

$$f_E(z) = \delta\{B_m^- e^{-\alpha_m (z-h_m)} + B_m^+ e^{+\alpha_m (z-h_m)}\}, h_m \leq z \leq h_{m+1} \tag{2.33a}$$

$$1 \leq m \leq L$$

In Eq. (2.33) $h_s > 0$ is the height of the lowest source point. Since there are no upward travelling waves in the last layer, $B_L^+ = 0$. The constant δ will be so adjusted that we can choose $B_L^- = 1$. With these starting values the continuity of f_E and f_E' across boundaries yields the backward recurrence relations

$$B_m^+ = (1+\alpha_{m+1}/\alpha_m) g_m^- B_{m+1}^+ + (1-\alpha_{m+1}/\alpha_m) g_m^- B_{m+1}^- \tag{2.34a}$$

$$B_m^- = (1-\alpha_{m+1}/\alpha_m) g_m^+ B_{m+1}^+ + (1+\alpha_{m+1}/\alpha_m) g_m^+ B_{m+1}^- \tag{2.34b}$$

$$L-1 \geq m \geq 0$$

with the abbreviation

$$g_o^{\pm} = \frac{1}{2},\ g_m^{\pm} = \frac{1}{2}\exp\{\pm\alpha_m(h_{m+1}-h_m)\},\quad m = L-1,\ \ldots,\ 1.$$

Having computed B_o^-, Eqs. (2.32) and (2.33) yield

$$\delta = f_o^- / B_o^- .$$

Thus the field is specified.
If we are interested in $f_E(z)$ for $z \leq 0$ only, it is not necessary to calculate B_m^+ and B_m^- separately. Instead only the ratio

$$\gamma_m = B_m^+ / B_m^-$$

is required. Because of (2.33) and (2.32) $f_E(z)$ is given by

$$f_E(z) = f_o^-\{e^{-\kappa z} + \gamma_o e^{+\kappa z}\},\ 0 \leq -z \leq h_s$$

where γ_o is obtained recursively from the ratio (2.34a)/(2.34b), i.e.

$$\gamma_m = \frac{(\alpha_m+\alpha_{m+1})\gamma_{m+1} + (\alpha_m-\alpha_{m+1})}{(\alpha_m-\alpha_{m+1})\gamma_{m+1} + (\alpha_m+\alpha_{m+1})} \exp\{-2\alpha_m(h_{m+1} - h_m)\}$$

$$L-1 \leq m \leq 0$$

starting with $\gamma_L = 0$.

2.4. Particular source fields

Notation: In the sequel only fields with a periodic time function $\exp(i\omega t)$ are considered. For any field quantity $A(\underline{r},t)$ we write $\tilde{A}(\underline{r},\omega)$ with the understanding that the real or imaginary part of $A(\underline{r},t)\exp(i\omega t)$ is meant. Furthermore, since only the TE-mode is of interest we shall drop the subscript "E".

In the last section an algorithm for the calculation of the ϕ-potential in a layered half-space has been given. As input occurs $f^e(z,\underline{\kappa},\omega) = f_o^-(\underline{\kappa},\omega)\exp(-\kappa z)$, the representation of the source potential in the wave-number space. From (2.12a), i.e. $\tilde{\underline{H}}=\text{grad}(\partial\tilde{\phi}/\partial z)$ follows that $-\partial\tilde{\phi}/\partial z$ is the magnetic scalar potential. Between $f_o^-(\underline{\kappa},\omega)$ and the source potential $\tilde{\phi}^e(\underline{r},\omega)$ exist the following reciprocal relations

$$\tilde{\phi}^e(\underline{r},\omega) = \int_{-\infty}^{+\infty}\int f_o^-(\underline{\kappa},\omega)\, e^{i\underline{\kappa}\cdot\underline{r}-\kappa z}\, d\kappa_x\, d\kappa_y \qquad (2.35)$$

$$f_o^-(\underline{\kappa},\omega)\, e^{-\kappa z} = \frac{1}{(2\pi)^2}\int_{-\infty}^{+\infty}\int \tilde{\phi}^e(\underline{r},\omega)\, e^{-i\underline{\kappa}\cdot\underline{r}}\, dx\, dy \qquad (2.36)$$

General field

If $\tilde{\phi}$ is symmetrical with respect to a vertical axis, i.e. $\tilde{\phi}$ is a function of $r = (x^2+y^2)^{1/2}$ only, eqs. (2.35) and (2.36) simplify to

$$\tilde{\phi}^e(r,z,\omega) = 2\pi\int_0^\infty f_o(\kappa,\omega)\, e^{-\kappa z}\, J_o(\kappa r)\,\kappa\, d\kappa \qquad (2.35a)$$

$$f_o(\kappa,\omega)\, e^{-\kappa z} = \frac{1}{2\pi}\int_0^\infty \phi^e(r,z,\omega)\, J_o(\kappa r)\, r\, dr \qquad (2.36a)$$

Cylindrical symmetry

In the derivation of (2.35a) and (2.36a) the cartesian coordinates were replaced by circular polar coordinates

$x = r\cos\theta$, $y = r\sin\theta$, $\kappa_x = \kappa\cos\psi$, $\kappa_y = \kappa\sin\psi$

and use was made of the identity

$$\int_0^{2\pi} e^{-i\kappa r\cos(\theta-\psi)}d\theta=\int_0^{2\pi} e^{-i\kappa r\cos\theta}d\theta=2\int_0^{\pi}\cos(\kappa r\cos\theta)d\theta=2\pi J_o(\kappa r).$$

From (2.35a), (2.36a) follows that if $\tilde{\phi}$ is function of $r=(x^2+y^2)^{1/2}$, then $\bar{f}_o$ is a function of $\kappa = (\kappa_x^2 + \kappa_y^2)^{1/2}$. In certain cases (e.g. example b) below), it is only possible to obtain the potential on the cylindrical axis (r = o) in closed form. Then (2.35a) reads

$$\tilde{\phi}^e(o,z) = 2\pi \int_0^{\infty} \kappa \bar{f}_o(\kappa) e^{-\kappa z}\, d\kappa. \qquad (2.35b)$$

Eq. (2.35b) can be considered as a Laplace-Transform for which the inversion is

$$2\pi\kappa\, \bar{f}_o(\kappa) = \frac{1}{2\pi i}\int_{\varepsilon-i\infty}^{\varepsilon+i\infty} \phi^e(o,z)e^{\kappa z}dz \qquad (2.36b)$$

where ε is an appropriate real constant (thus that all singularities of $\phi^e(o,z)$ are at the left of $z = \varepsilon$). Simpler would be the use of a table of Laplace transforms.

The spectral representation of the source is now calculated for simple sources:

a) Vertical magnetic dipole

Locate the dipole at $\underline{r}_o = (o,o,-h)$, $h \geq o$ and let its moment be $\underline{M} = M\hat{\underline{z}}$. When it is produced by means of a small current loop then M = current x area of the loop. (M is positive if the direction of the current forms with $\hat{\underline{z}}$ a right-handed system, and negative else.)

From the scalar potential

$$\underline{M} \cdot \underline{R}/(4\pi R^3), \quad R = \underline{r} - \underline{r}_o, \quad R = |\underline{R}|$$

follows

$$\frac{\partial\tilde{\phi}^e}{\partial z} = \frac{M(z+h)}{4\pi R^3}, \quad \text{whence} \quad \tilde{\phi}^e = \frac{M}{4\pi R}$$

Since $\tilde{\phi}$ shows cylindrical symmetry, we obtain from (2.36a) on using the result

$$\int_0^{\infty} \frac{r}{R} J_o(\kappa r)dr = \frac{1}{\kappa} e^{-\kappa(z+h)}$$

immediately

$$\bar{f}_o(\kappa) = \frac{M}{8\pi^2\kappa} e^{-\kappa h} \qquad (2.37)$$

Vertical magnetic dipole

b) Circular current loop

Let a and I be the radius and the current of the loop. The potential has cylindrical symmetry, but can be expressed by means of simple functions only on the axis r = 0. For the moment we assume that the current loop is in the plane z = o. For symmetry reasons there is only a H_z component on the axis. Biot-Savart's law yields

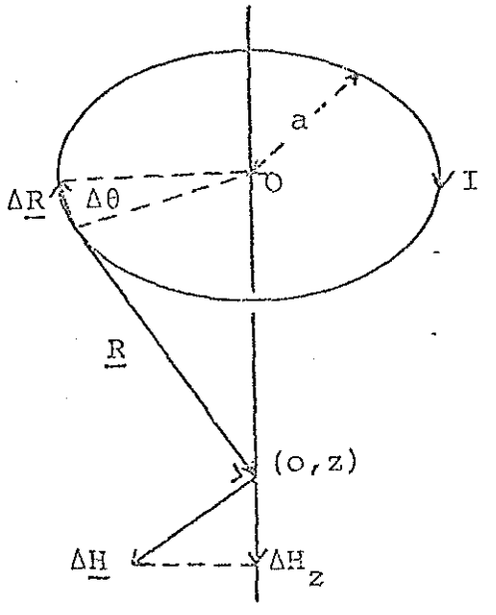

$$\Delta\tilde{\underline{H}} = -\frac{I}{4\pi}\frac{\underline{R}\times\Delta\underline{R}}{R^3},$$

whence

$$\Delta\tilde{H}_z = \frac{I}{4\pi}\cdot\frac{a\,\Delta\theta}{z^2+a^2}\cdot\frac{a}{\sqrt{z^2+a^2}}$$

$$= \frac{Ia^2\,\Delta\theta}{4\pi(z^2+a^2)^{3/2}},$$

$$\tilde{H}_z = \frac{I\,a^2}{2(z^2+a^2)^{3/2}}$$

Now $\tilde{H}_z = -\partial V/\partial z = +\partial^2\tilde{\phi}^e/\partial z^2$. Hence integrating twice on using $V(\infty) = 0 = \tilde{\phi}^e(\infty)$ we obtain

$$\tilde{\phi}^e(o,z) = \frac{I}{2}\frac{a^2}{z+\sqrt{z^2+a^2}}.$$

Now we have to solve (2.35b), i.e.

$$\frac{I}{4\pi}\cdot\frac{a^2}{z+\sqrt{z^2+a^2}} = \int_0^\infty \kappa\, f_o^-(\kappa)\, e^{-\kappa z}\, d\kappa$$

Looking up in a table of Laplace transforms:

$$f_o^-(\kappa) = \frac{I\,a}{4\pi\kappa^2}\,J_1(\kappa a)$$

If the plane of the loop is z = -h, h $\geq$ 0, then a simple change of origin yields

$$\boxed{f_o^-(\kappa) = \frac{I\,a}{4\pi\kappa^2}\,J_1(\kappa a)\,e^{-\kappa h}}$$

Circular current loop (2.38)

In the limit $a \to 0$, $I \to \infty$, $M = \pi a^2 I$ fixed, this leads to the result (2.37) for the vertical magnetic dipole ($J_1(x) = x/2 + O(x^3)$).

c) Horizontal magnetic dipole

Here $\underline{M} = M \hat{\underline{x}}$ and

$$\frac{\partial \tilde{\phi}^e}{\partial z} = -\frac{Mx}{4\pi R^3}, \qquad \tilde{\phi}^e = \frac{Mx}{4\pi R(R+z+h)}$$

With this result, suppressing all further details the evaluation of (2.36) yields

$$\boxed{f_o^-(\underline{\kappa}) = \frac{Mi\kappa_x}{8\pi^2\kappa^2} e^{-\kappa h}}$$

Horizontal magnetic dipole (2.39)

d) Line current

Current I at $y = 0$, $z = -h$. It results the scalar potential

$$V^e(y,z) = -\frac{\partial \tilde{\phi}^e}{\partial z} = \frac{I}{2\pi} \arctan \frac{y}{z+h}.$$

The corresponding source function is

$$\boxed{f_o^-(\kappa) = \frac{2I}{i\kappa_y \kappa} \delta(\kappa_x) e^{-\kappa h}, \quad \kappa = |\kappa_y|}$$

Line current (2.40)

The delta function $\delta(\kappa_x)$ occurs since there is no dependence on x.

e) "Plane wave" (elementary undulated field)

Assume a wavenumber $\kappa_y = w$ and let the scalar magnetic source potential be

$$V^e = -H_o \frac{\sin wy}{w} e^{-|w|z}$$

leading to a magnetic field

$$H_y^e = H_o \cos(wy) e^{-|w|z}, \quad H_z^e = -H_o \sin(wy) e^{-|w|z} \cdot \operatorname{sgn}(w).$$

Hence, $$\tilde{\phi}^e = - H_o \frac{\sin(wy)}{w|w|} e^{-|w|z},$$

and

$$\bar{f}_o(\underline{\kappa}) = \frac{2\pi^2 H_o}{iw|w|} \delta(\kappa_x) \{\delta(\kappa_y+w) - \delta(\kappa_y-w)\} \qquad (2.41)$$

Elementary undulated field

When the source can be considered as elementary harmonic field, as in this case, the Fourier integral representation (2.35) complicates things only.

In the limit $w \to 0$ we obtain a uniform source field in y-direction. For the induction process a strictly uniform source field is useless since only a vertical magnetic field component induces. Hence w must be non-zero, no matter how small. If we confine our attention to a finite part of the infinite horizontal plane, the dimensions of that part being smaller than $1/|w|$, then formally we may put $w = 0$ and can profit from the particularly simple resulting equations. Such a source field is called a quasi-uniform field. To the unrealistic uniform field belongs the source potential

$$\tilde{\phi}^e = H_o\, yz$$

which can no longer be represented in terms of (2.35).

2.5. Definition of the transfer function $C(\omega,\kappa)$

The TE-potential is

$$\tilde{\phi}(\underline{r},\omega) = \int\int_{-\infty}^{+\infty} f(z,\underline{\kappa},\omega)\, e^{i\underline{\kappa}\cdot\underline{r}}\, d\kappa_x d\kappa_y . \tag{2.42}$$

With this potential we define as the basic transfer function for a half-space with one-dimensional conductivity structure

$$\boxed{C(\omega,\kappa) = -\frac{f(0,\underline{\kappa},\omega)}{f'(0,\underline{\kappa},\omega)}} \tag{2.43}$$

Note that f depends on κ_x and κ_y separately via the source function as an amplitude factor. In the ratio f/f' this factor drops out and it remains only the dependence on $\kappa = \sqrt{\kappa_x^2+\kappa_y^2}$, since f is a solution of (2.9a), i.e.

$$f''(z,\underline{\kappa},\omega) = \{\kappa^2 + i\omega\mu_0\sigma(z)\} f(z,\underline{\kappa},\omega). \tag{2.44}$$

How can C be determined from a knowledge of the surface electromagnetic field, at least theoretically?
From (2.8a,b) results

$$\tilde{\underline{H}} = \mathrm{curl}^2(\tilde{\phi}\hat{\underline{z}}) = \int\int_{-\infty}^{+\infty} \{i\underline{\kappa} f' + \kappa^2 f\hat{\underline{z}}\} e^{i\underline{\kappa}\cdot\underline{r}}\, d\kappa_x\, d\kappa_y \tag{2.45a}$$

$$\tilde{\underline{E}} = i\omega\mu_0 \hat{\underline{z}} \times \mathrm{grad}\tilde{\phi} = i\omega\mu_0 \int\int_{-\infty}^{+\infty} \hat{\underline{z}} \times i\underline{\kappa}\, f\, e^{i\underline{\kappa}\cdot\underline{r}}\, d\kappa_x\, d\kappa_y \tag{2.45b}$$

Let

$$\hat{\underline{H}}(\underline{\kappa},\omega) = \frac{1}{(2\pi)^2} \int\int_{-\infty}^{+\infty} \tilde{\underline{H}}(x,y,0,\omega)\, e^{-i\underline{\kappa}\cdot\underline{r}}\, dxdy \tag{2.46a}$$

$$\hat{\underline{E}}(\underline{\kappa},\omega) = \frac{1}{(2\pi)^2} \int\int_{-\infty}^{+\infty} \tilde{\underline{E}}(x,y,0,\omega)\, e^{-i\underline{\kappa}\cdot\underline{r}}\, dxdy \tag{2.46b}$$

denote the surface fields in the wavenumber-frequency space. Then from (2.45a,b), (2.46a,b)

$$\hat{\underline{H}} = i\,\underline{\kappa}\, f' + \kappa^2 f\, \hat{\underline{z}} \tag{2.47a}$$

$$\hat{\underline{E}} = i\omega\mu_0\, \hat{\underline{z}} \times i\underline{\kappa}\, f \tag{2.47b}$$

There are several ways to determine C:

a) From the ratio between two orthogonal components of the horizontal electric and magnetic field

Vectorial multiplication of (2.47a) with $\hat{\underline{z}}$ and use of (2.43) yields

$$\hat{\underline{E}} = -i\omega\mu_o \, C \, \hat{\underline{z}} \times \hat{\underline{H}}$$

or with any horizontal unit vector $\hat{\underline{e}}$

$$C = \frac{\hat{\underline{e}} \cdot \hat{\underline{E}}}{i\omega\mu_o \, (\hat{\underline{z}} \times \hat{\underline{e}}) \cdot \hat{\underline{H}}} \tag{2.48}$$

In particular $\hat{\underline{e}} = \hat{\underline{x}}$ and $\hat{\underline{e}} = \hat{\underline{y}}$ yields

$$\boxed{C = \frac{1}{i\omega\mu_o} \frac{\hat{E}_x}{\hat{H}_y} = \frac{1}{i\omega\mu_o} \frac{\hat{E}_y}{\hat{H}_x}} \tag{2.49a}$$

b) From the ratio of vertical and horizontal magnetic field components

(2.47a) yields immediately

$$\boxed{C = \frac{\hat{\underline{z}} \cdot \hat{\underline{H}}}{i\underline{\kappa} \cdot \hat{\underline{H}}}} \tag{2.50}$$

c) From the ratio of internal to external part of a magnetic horizontal component

In $z \leq 0$ f reads

$$f = f_o^- \, e^{-\kappa z} + f_o^+ \, e^{\kappa z} \tag{2.51}$$

Let $\hat{H}_{xe}$ and $\hat{H}_{xi}$ be the source part and internal part of $\hat{H}_x$. Then from (2.47a) and (2.51)

$$\hat{H}_{xe} + \hat{H}_{xi} = i\kappa_x \kappa (-f_o^- + f_o^+) = i\kappa_x f'$$

$$\hat{H}_{xe} - \hat{H}_{xi} = -i\kappa_x \kappa (f_o^- + f_o^+) = -i\kappa_x \kappa \, f$$

Defining

$$S(\kappa, \omega) = \hat{H}_{xi}(\underline{\kappa}, \omega) / \hat{H}_{xe}(\underline{\kappa}, \omega) \tag{2.52}$$

we arrive at

$$\boxed{C = \frac{1}{\kappa}\ \frac{1-S}{1+S}} \tag{2.53}$$

The same applies to $\hat{H}_y$.

d) From the ratio of vertical gradients at z = +o to the corresponding field components at z=o

Let $\hat{H}'_x(\underline{\kappa},\omega)$ be the vertical gradient of $\hat{H}_x$ at z = +o in the wave-number - frequency domain. Then

$$\hat{H}_x'(\underline{\kappa},\omega)=i\kappa_x f''(O,\underline{\kappa},\omega) = i\kappa_x\{\kappa^2+i\omega\mu_o\sigma(o)\}f_o(O,\underline{\kappa},\omega) \tag{2.54}$$

On applying (2.44) Eq. (2.47a) yields

$$\boxed{C = -\frac{\hat{H}'_x}{\{\kappa^2+i\omega\mu_o\sigma(o)\}\hat{H}_x}} \tag{2.55}$$

The same applies to $\hat{H}_y$. For applications of (2.55) the surface value of σ must be known. C can also be obtained from other field ratios involving vertical gradients.

The methods a) and d) are also applicable for a quasi-uniform source field; b) and c) break down in this case.
The apparent resistivity of magnetotellurics is defined as

$$\rho_a = \frac{1}{\omega\mu_o}\left|\frac{\hat{E}_x}{\hat{H}_y}\right|^2 = \frac{1}{\omega\mu_o}\left|\frac{\hat{E}_y}{\hat{H}_x}\right|^2 \tag{2.56}$$

According to (2.49a,b) its relation to C is

$$\boxed{\rho_a = \omega\mu_o|C|^2} \tag{2.57}$$

2.6. Properties of $C(\omega,\kappa)$

a) Signs, limiting values

According to (2.43) the response function C is defined as

$$C(\omega,\kappa) \overset{/}{=} -\frac{f(o,\kappa,\omega)}{f'(o,\kappa,\omega)}, \qquad (2.58)$$
$$= (2.43)$$

where f satisfies

$$f''(z) = \{\kappa^2 + i\omega\mu_o\sigma(z)\}f(z). \qquad (2.59)$$
$$= (2.44)$$

C has the dimension of a length. Let

$$C = g - ih \quad \text{or} \quad C = |C|e^{-i\psi} \qquad (2.60)$$

Then $\underline{g \geq 0,\ h \geq 0}$ or $\underline{0 \leq \psi \leq \pi/2}$. (2.61a,b)

Proof: Take the complex conjugate of (2.59), multiply by f and integrate over z. Integration by parts yields

$$-f(o)f'^{*}(o) = \int_o^\infty \{|f'|^2 + (\kappa^2 - i\omega\mu_o\sigma)|f|^2\}dz.$$

Division by $|f'(o)|^2$ leads to the result.
The limiting values of C for $\omega \to 0$ and $\omega \to \infty$ are

$$C = \begin{cases} \frac{1}{\kappa}\tanh(\kappa H) & \text{for } \omega\to o \qquad (2.62a) \\ \frac{1}{\sqrt{i\omega\mu_o\sigma(o)}} & \text{for } \omega\to\infty \qquad (2.62b) \end{cases}$$

In (2.62a) H is the depth of a possible perfect conductor. If absent, then $H \to \infty$, $C = 1/\kappa$.
Proof: For $\omega=0$ the solution of (2.59) vanishing at $z=H$ is $f \sim \sinh\kappa(H-z)$, - whence (2.62a). - For high frequencies f tends to the solution for a uniform half-space, i.e. $f \sim \exp\{\sqrt{i\omega\mu_o\sigma}\}$, yield (2.62b). This limit is attained, if the penetration depth for a uniform halfspace with $\sigma = \sigma(o)$,

$$p = \sqrt{\frac{2}{\omega\mu_o\sigma}} \qquad (2.63)$$

is small compared with the scale length $1/\kappa$ of the external field and the scale length $|\sigma(o)/\sigma'(o)|$ of conductivity variation.

b) Computation of C for a layered half-space

When interested in the electric field within a layered structure, we have to compute a set of coefficients $B_m^{\pm}$ according to the rules of Sec. 2.3. These coefficients can be used also to express C:

$$C = \frac{1}{\kappa} \frac{B_o^- + B_o^+}{B_o^- - B_o^+} = \frac{1}{\alpha_1} \frac{B_1^- + B_1^+}{B_1^- - B_1^+} \tag{2.64}$$

The latter form is also applicable for $\kappa=0$, whereas a limiting process is involved in the former one in this case. If we are only interested in C then we may proceed as follows: C can be considered as a continuous function of depth. Then

$$C_m := - \frac{f(h_m)}{f'(h_m)} = \frac{1}{\alpha_m} \frac{B_m^- + B_m^+}{B_m^- - B_m^+} \tag{2.65}$$

From (2.34a,b) follows:

$$B_m^- \pm B_m^+ = (g_m^+ \pm g_m^-)(B_{m+1}^- + B_{m+1}^+) + \frac{\alpha_{m+1}}{\alpha_m}(g_m^+ \mp g_m^-)(B_{m+1}^- - B_{m+1}^+), \tag{2.66}$$

where $g_m^{\pm} = \frac{1}{2} \exp\{\pm\alpha_m d_m\}$, $d_m = h_{m+1} - h_m$, $\alpha_m^2 = \kappa^2 + i\omega\mu_o\sigma_m$.

Hence, (2.65) and (2.66) yield

$$\boxed{C_m = \frac{1}{\alpha_m} \frac{\alpha_m C_{m+1} + \tanh(\alpha_m d_m)}{1 + \alpha_m C_{m+1} \tanh(\alpha_m d_m)}} \tag{2.67}$$

Starting with $C_L = 1/\alpha_L$ backward recursion using (2.67) leads to $C_1 = C$.

c) Approximate interpretation of a one-dimensional conductivity structure

If we can assume $\kappa = 0$, i.e. scale length of external field large compared with penetration depth (as generally done in magnetotellurics) then there exists a simple method to obtain from C a first approximation of the underlying conductivity structure (Schmucker-Kuckes relation):

Let $C = g - ih$. Then a first approximation $\sigma^{\varkappa}(z^{\varkappa})$ of $\sigma(z)$ is obtained by setting

$$\boxed{z^{\varkappa} = g, \quad \sigma^{\varkappa} = \frac{2}{\omega\mu_0 h^2}} \tag{2.68}$$

This cannot be proved rigorously but the following arguments are in favour of it:

1) $z^{\varkappa} = g$ can be considered as the depth of the "centre of gravity" of the in-phase induced current system.
2) It will be shown below that $z^{\varkappa}$ continuously increases when the frequency decreases. According to a) its maximum value is H.
3) For a uniform half-space and $\kappa=0$ we have $h = \sqrt{2/\omega\mu_0\sigma}$. Hence, $\sigma^{\varkappa}$ is correct in this case. For perfect conductions $\sigma^{\varkappa}\to\infty$ since $h\to 0$.

This approximate method performs particularly well when there is a monotone increase in conductivity. The following two figures (p.24) illustrate capabilities and limitations of the method.

d) Properties of C in the complex frequency plane

For the following considerations it is usefull to consider the frequency ω as a complex quantity. Then in the complex frequency plane outside the positive imaginary axis C is an analytical function of frequency. For a proof multiply (2.59) by $f^{\varkappa}$ and integrate over z. Then the integration by parts yields

$$-f^{\varkappa}(0,\omega)f'(0,\omega) = \int_0^{\infty} \{ |f'(z,\omega)|^2 + \{\kappa^2 + i\omega\mu_0\sigma(z)\}|f(z,0)|^2\}dz. \tag{2.69}$$

Hence, for ω not on the positive imaginary axis $f'(0,\omega)$ cannot vanish. There are neither isolated poles nor a dense spectrum of poles (branch cut).
Division of (2.69) by $|f'(0,\omega)|^2$ yields

$$C^{\varkappa}(\omega) = \int_0^{\infty} \{|f'(z)/f'(o)|^2 + \{\kappa^2 + i\omega\mu_0\sigma(z)\}|f(z)/f'(o)|^2\}dz \tag{2.70}$$

We can easily deduce from (2.70) that

$$\operatorname{Re} C(\omega) > 0, \quad \operatorname{Im}(\omega) \leq 0 \tag{2.71a}$$

$$\operatorname{Im} C(\omega) \begin{cases} < 0, & \operatorname{Re}(\omega) > 0 \\ > 0, & \operatorname{Re}(\omega) < 0 \end{cases} \tag{2.71b}$$

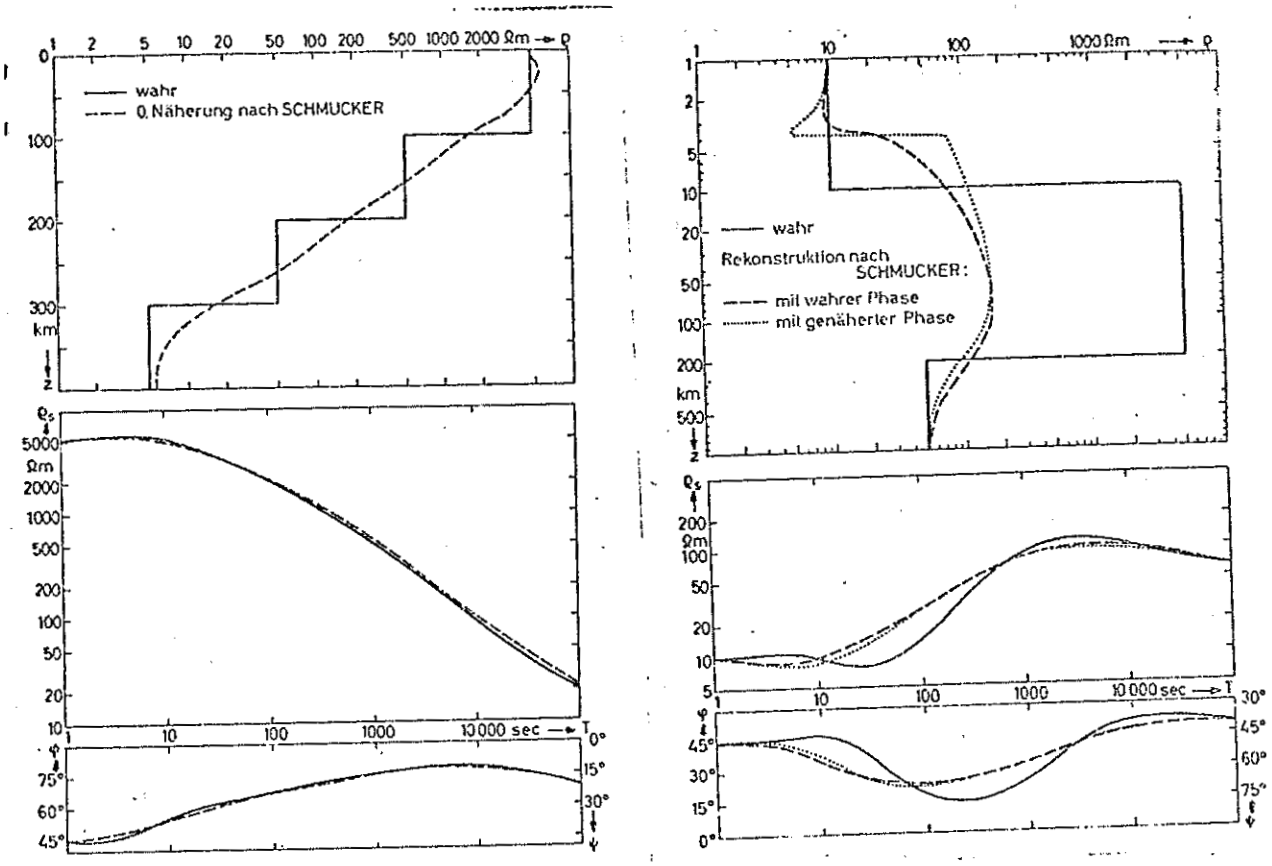

The approximate interpretation of C using (2.68). In the left figure (monotone increase of conductivity) the zero order approximation interpretes the data already completely. When there is a resistive layer (left hand) the zero order interpretation needs refinement. In the dotted line at the left hand, an approximate phase of C was used. This approximate phase has been obtained by differentiation of the double-logarithmic plot of $\rho_a(T)$ (cf. Eq. 2.77).

As a consequence of (2.71a,b) C is also free of zeros outside the positive imaginary axis.

e) Dispersion relations

Because of the analytical properties of C, its real and imaginary part are not independent functions of frequency. Let ω_0 be a point in the upper ω-plane and L be a closed contour consisting of the real axis and a large semi-circle in the lower ω half-plane. Then

$$\frac{1}{\pi i}\int_L \frac{C(\omega')d\omega'}{\omega'-\omega_0} = 0$$

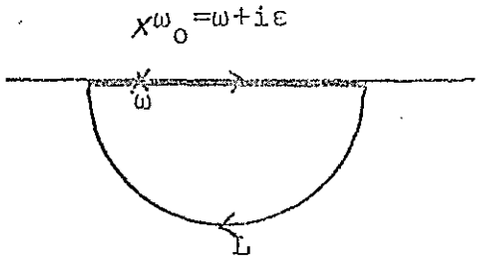

since the integrand is analytical in L. Due to (2.62b) the large semicircle does not contribute and the contour can be confined to the real axis. Here put $\omega'=x$ and let $\omega_0=\omega+i\varepsilon$ (ω real, $\varepsilon > 0$) tend to the real axis. Then

$$0=\lim_{\varepsilon\to+0}\frac{1}{\pi i}\int_{-\infty}^{+\infty}\frac{C(x)dx}{x-\omega-i\varepsilon} = \lim_{\varepsilon\to+0}\left\{\frac{\varepsilon}{\pi}\int_{-\infty}^{+\infty}\frac{C(x)dx}{\varepsilon^2+(x-\omega)^2} + \frac{1}{\pi i}\int_{-\infty}^{+\infty}\frac{(x-\omega)C(x)dx}{\varepsilon^2+(x-\omega)^2}\right\}$$

$$= C(\omega) + \frac{1}{\pi i}\,\text{⨍}_{-\infty}^{+\infty}\frac{C(x)dx}{x-\omega}, \qquad (2.72)$$

where

$$\lim_{\varepsilon\to+0}\frac{1}{\pi}\,\frac{\varepsilon}{\varepsilon^2+(x-\omega)^2} = \delta(x-\omega)$$

has been used. ⨍ denotes the Cauchy principal value of the integral. Let for real frequencies

$$C(\omega) = g(\omega) - ih(\omega).$$

Here g is an even and h an odd function of frequency, i.e.

$$g(-\omega) = g(\omega), \quad h(-\omega) = -h(\omega).$$

This is a consequence of (2.70). Hence a separation of (2.72) in its real and imaginary part yields

$$g(\omega) = \frac{1}{\pi} \int_{-\infty}^{+\infty} \frac{h(x)dx}{x-\omega} = \frac{2}{\pi} \int_{0}^{\infty} \frac{xh(x)dx}{x^2 - \omega^2} \tag{2.73a}$$

$$h(\omega) = \frac{1}{\pi} \int_{-\infty}^{+\infty} \frac{g(x)dx}{x-\omega} = -\frac{2}{\pi} \int_{0}^{\infty} \frac{\omega g(x)dx}{x^2-\omega^2} \tag{2.73b}$$

Dispersion relations

Dispersion relations of this kind occur in many branches of physics. They are a direct consequence of the causality requirement. Relations corresponding to (2.73a,b) exist also for modulus and phase of C. Due to (2.71a) C is also free of zeros in the lower frequency halfplane. Hence the function

$$\log\{\sqrt{i\omega\mu_o\sigma(o)}\ C(\omega)\}$$

is analytical there and vanishes for $|\omega| \to \infty$ due to (2.62b). Let

$$C(\omega) = |C(\omega)|e^{-i\psi(\omega)} \tag{2.74}$$

and assume $\omega > 0$. Then the relation corresponding to (2.73b) is

$$\psi(\omega) - \frac{\pi}{4} = -\frac{2\omega}{\pi} \int_{0}^{\infty} \log\{\sqrt{x\mu_o\sigma(o)}\ |C(x)|\} \frac{dx}{x^2-\omega^2}$$

or introducing the apparent resistivity from (2.57)

$$\psi(\omega) = \frac{\pi}{4} - \frac{\omega}{\pi} \int_{0}^{\infty} \log\{\rho_a(x)/\rho_o\} \frac{dx}{x^2-\omega^2} \tag{2.75}$$

where $\rho_o = 1/\sigma(o)$. There exists a simple approximate version of (2.75). Integration by parts yields

$$\psi(\omega) - \frac{\pi}{4} = \frac{1}{2\pi} \int_{0}^{\infty} \frac{d\log\ \rho_a(x)}{dx} \cdot \log\left|\frac{\omega - x}{\omega + x}\right| dx$$

$$= \frac{1}{2\pi} \int_{0}^{\infty} \frac{d\log\ \rho_a(x)}{d\log\ x} \cdot \log\left|\frac{\omega - x}{\omega + x}\right| \frac{dx}{x}$$

or since $x^{-1} \log\left|\frac{\omega - x}{\omega + x}\right|$ is an integrable function peaked at $\omega=x$, in an approximate evaluation one may draw out of the integral the term $d\log\rho_a/d\log x|_{x=\omega}$. Hence

$$\psi(\omega) - \frac{\pi}{4} \simeq -\frac{\pi}{4} \frac{d\log\ \rho_a(\omega)}{d\log\omega}, \tag{2.76}$$

where the result

$$\int_0^\infty \log\left|\frac{\omega-x}{\omega+x}\right|\frac{dx}{x} = 2\int_0^1 \log\left(\frac{1-t}{1+t}\right)\frac{dt}{t} = -\frac{\pi^2}{2}$$

has been used. With $T = \frac{2\pi}{\omega}$, $d\log\omega = -d\log T$. The final result is

$$\psi(\omega) \simeq \frac{\pi}{4}\left\{1 + \frac{d\log\,\rho_a(T)}{d\log T}\right\} \qquad (2.77)$$

Since in general double-logarithmic plots of $\rho_a(T)$ are used, a first approximation of the phase can immediately be obtained from the slope of a sounding curve. The degree of accuracy can be asserted from two examples given at the left. True phase in broken lines, approximate phase in full lines.

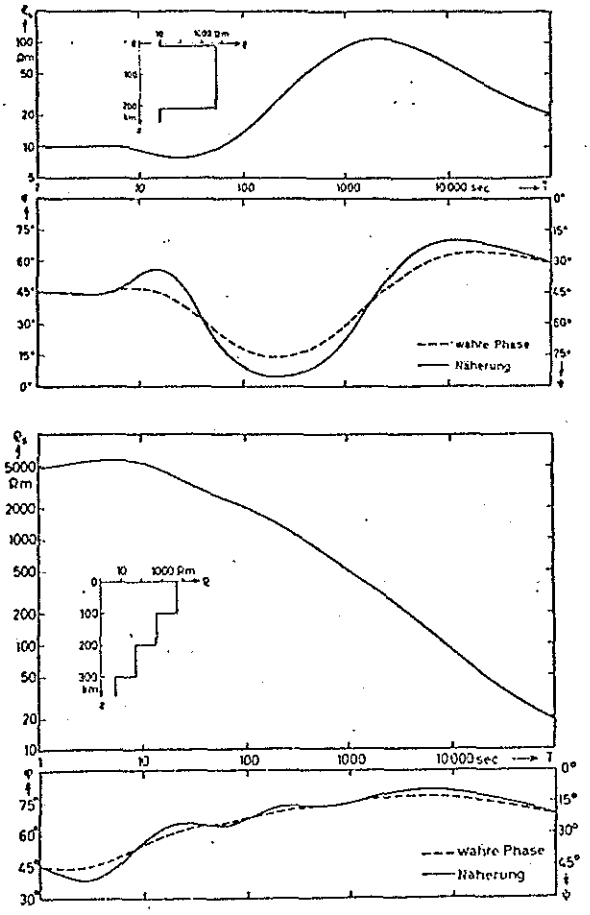

The simple approximate method of inversion described in c) (Schmucker-Kuckes relation) combined with the approximation (2.77) provides an extremely simple tool to derive a zero order approximation of the true conductivity from apparent resistivity.

$$z^* = \sqrt{\frac{\rho_a(\omega)}{\omega\mu_o}}\cos\psi, \quad \sigma^*(z^*) = \frac{2}{\rho_a(\omega)\sin^2\psi} \qquad (2.78)$$

f) Inequalities for the frequency dependence of C

Cauchys formula is

$$C(\omega) = \frac{1}{2\pi i}\int_L \frac{C(\omega')}{\omega'-\omega}\,d\omega', \qquad (2.79)$$

where L is a positively oriented closed contour enclosing only a domain where C is analytical and the point ω. We choose the particular contour shown at the left. When the radius of the circle tends to infinity the circle does not contribute since $C(\omega) = O(1/\sqrt{\omega})$ for $|\omega| \to \infty$. Hence the contour can be confined to both sides of the positive-imaginary axis. On the right hand side put $\omega' = i\lambda + \varepsilon$, $\varepsilon > 0$. Then (2.79) yields

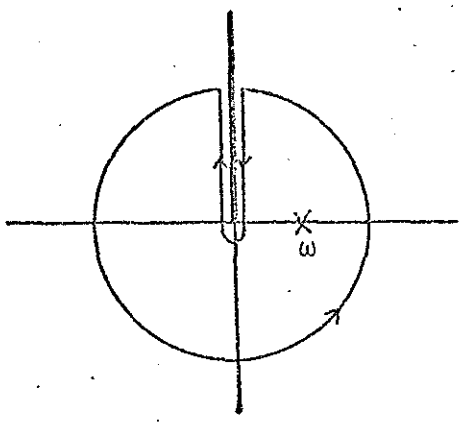

$$C(\omega) = - \lim_{\varepsilon \to +0} \frac{1}{2\pi i} \int_0^\infty \frac{C(i\lambda+\varepsilon) - C^*(i\lambda+\varepsilon)}{\lambda + i\omega} d\lambda =$$

$$= - \lim_{\varepsilon \to +0} \frac{1}{\pi} \int_0^\infty \frac{\mathrm{Im}\, C(i\lambda+\varepsilon)}{\lambda+i\omega} d\lambda = \int_0^\infty \frac{q(\lambda)d\lambda}{\lambda+i\omega},$$

where $q(\lambda) = - \lim_{\varepsilon \to +0} \frac{1}{\pi} \mathrm{Im}\, C(i\lambda+\varepsilon) \geq 0$

in virtue of (2.71b). Summarizing:

$$C(\omega) = \int_0^\infty \frac{q(\lambda)d\lambda}{\lambda + i\omega}, \quad q(\lambda) \geq 0 \tag{2.80}$$

The non-negativity of $q(\lambda)$ has the consequence that C must be a smooth function of frequency. Again let ω be a positive frequency and let

$$C = g - ih.$$

Defining

$$Df := \omega \frac{df}{d\omega} = \frac{df}{d\log\omega} = - \frac{df}{d\log T} \tag{2.81}$$

then the following constraints apply

$g \geq 0$	$h \geq 0$	(2.82a,b)
$\lvert C+DC \rvert \leq g$	$\lvert DC \rvert \leq h$	(2.83a,b)
$\lvert C+2DC+D^2C \rvert \leq g$	$\lvert D^2C \rvert \leq h$	(2.84a,b)

(2.82a,b) simply results when (2.80) is split into real and imaginary; it has already been given above (Eq.(2.61a,b)).(2.83) is proved as follows

$$\underline{|C+DC|} = |C+\omega C'(\omega)| = \left|\int_0^\infty \frac{\lambda q(\lambda)}{(\lambda+i\omega)^2}\, d\lambda\right| \leq \int_0^\infty \left|\frac{1}{\lambda+i\omega}\right|^2 \lambda q(\lambda)\, d\lambda$$

$$= \int_0^\infty \frac{\lambda q(\lambda)}{\lambda^2+\omega^2}\, d\lambda = \underline{g}$$

The other constraints are proved in a similar way. There are other constraints involving second and higher derivatives. In terms of apparent resistivity and phase ψ Eqs. (2.83b,a) read:

$$\frac{1}{4}\left(1 - \frac{D\rho_a}{\rho_a}\right)^2 + (D\psi)^2 \leq \sin^2\psi \qquad (2.85a)$$

$$\frac{1}{4}\left(1 + \frac{D\rho_a}{\rho_a}\right)^2 + (D\psi)^2 \leq \cos^2\psi \qquad (2.85b)$$

The slope of a double-logarithmically plotted sounding curve is $-D\rho_a/\rho_a$. As a consequence of (2.85a,b) we have always

$$\left|\frac{D\rho_a}{\rho_a}\right| \leq 1$$

The monotone decrease of the real part of C with frequency is a consequence of

$$g(\omega) = \int_0^\infty \frac{\lambda q\, d\lambda}{\lambda^2+\omega^2}\,.$$

The following figure shows data (full lines) which are inconsistent on the basis of a one-dimensional model, since the constraints (2.83a,b) are partly violated. Then the least corrections to the data are determined that the inequalities are satisfied. Since this is only a necessary condition, interpretability is not yet granted.

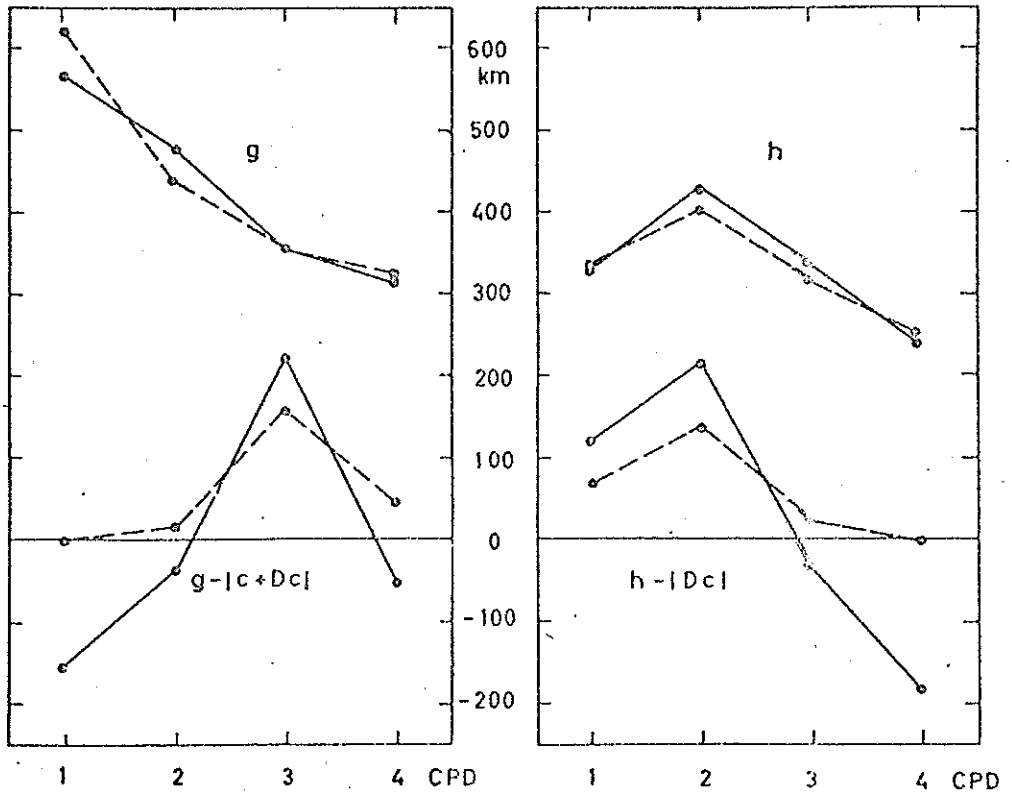

g) Dependence of interpretation on wave-number

The fundamental equation is

$$f''(z,\omega) = \{\kappa^2 + i\omega\mu_0\sigma(z)\}f(z,\omega).$$

By the transformations

$$\tilde{z} = \frac{1}{\kappa}\tanh(\kappa z) \tag{2.86a}$$

$$\tilde{f} = f \cdot \operatorname{sech}(\kappa z) \tag{2.86b}$$

$$\tilde{\sigma} = \sigma \cdot \cosh^4(\kappa z) \tag{2.86c}$$

it is transformed into

$$\tilde{f}''(\tilde{z},\omega) = i\omega\mu_0\tilde{\sigma}(\tilde{z})\tilde{f}(\tilde{z},\omega)$$

in such a way that

$$C(\omega) = -\frac{f(o,\omega)}{f'(o,\omega)} = -\frac{\tilde{f}(o,\omega)}{\tilde{f}'(o,\omega)}$$

remains unchanged. Hence any C can first be interpreted by a uniform external field (κ=o) and the result $\tilde{\sigma}(\tilde{z})$ is then transformed to the true conductivity by

$$\boxed{\sigma(z) = \operatorname{sech}^4(\kappa z)\cdot\tilde{\sigma}\left(\frac{1}{\kappa}\tanh(\kappa z)\right)} \tag{2.87}$$

For this interpretation the condition

$$C(o) \leq \frac{1}{\kappa}$$

has to be satisfied on $C(\omega)$.
An application of (2.87) is given in the following figure.

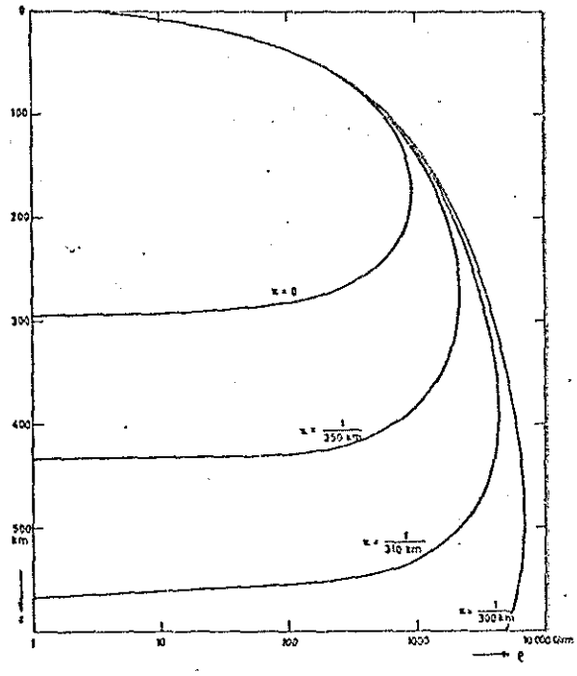

When κ increases attenuation is interpreted by geometrical damping at the expense of electromagnetic damping due to a perfect conductor.

3. Model calculations for two-dimensional structures

3.1. General equations

We are considering now induction problems, where both the conductivity structure and the inducing field are independent of one horizontal coordinate, say x. Compared with Ch. 2, the class of inducing fields has become more restricted, but the class of admitted conductivity structures has been enlarged.
For x-independence, Maxwell's equations

$$\text{curl}\tilde{\underline{H}} = \sigma\tilde{\underline{E}}, \quad \text{curl}\tilde{\underline{E}} = -i\omega\mu_0\tilde{H}$$

are split into two disjoint sets

$\frac{\partial \tilde{H}_z}{\partial y} = \frac{\partial \tilde{H}_y}{\partial z} = \sigma \tilde{E}_x$	$\frac{\partial \tilde{H}_x}{\partial z} = \sigma \tilde{E}_y$	(3.1a,b)
$\frac{\partial \tilde{E}_x}{\partial z} = - i\omega\mu_o \tilde{H}_y$	$\frac{\partial \tilde{H}_x}{\partial y} = - \sigma \tilde{E}_z$	(3.2a,b)
$\frac{\partial \tilde{E}_x}{\partial y} = + i\omega\mu_o \tilde{H}_z$	$\frac{\partial \tilde{E}_y}{\partial z} - \frac{\partial \tilde{E}_z}{\partial y} = i\omega\mu_o \tilde{H}_x$	(3.3a,b)
TE-mode or E-polarization	TM-mode or H-polarization	

The TE-mode has no vertical electric field, the TM-mode has no vertical magnetic field. In the treatment of these modes the use of electromagnetic potentials is not necessary since $\tilde{E}_x$ and $\tilde{H}_x$ can serve as pertinent potentials. For conciseness let

$$H := \tilde{H}_x , \quad E := \tilde{E}_x \qquad (3.4b,a)$$

Then E and H satisfy the equations

$$\Delta E = k^2 E \qquad (3.5a)$$

$$k^2 = i\omega\mu_o\sigma$$

$$\operatorname{div}\left(\frac{1}{k^2}\operatorname{grad} H\right) = H \qquad (3.5b)$$

In uniform domains both equations agree. Eq. (3.5b) resembles the equation of heat conduction in a non-uniform heat conductor.
The continuity of the tangential electric and magnetic field components at conductivity discontinuities leads to the conditions

$$E, \frac{\partial E}{\partial n} \text{ continuous : TE} \qquad (3.6a)$$

$$H, \frac{1}{\sigma}\frac{\partial H}{\partial n} \text{ continuous : TM} \qquad (3.6b)$$

$\frac{\partial}{\partial n}$ is the derivative in direction to the normal of the discontinuity.
The E- and H-polarization shows very different patterns. From (3.1b), (3.2b) follows that $\tilde{H}_x$ is constant in the air half-space (σ=o). Hence the TM-mode admits only a quasi-uniform inducing magnetic field. In contrast in the TE-mode any two-dimensional inducing magnetic field is allowed.
Hence, the source terms to be added on the RHS of (3.1a,b) are

$$j_e(y,z) \quad \text{and} \quad H_o\,\delta(z+h),$$

assuming that the TM magnetic source field is due to a uniform sheet current at height $z = -h$, $h > 0$. This assumption, however, is immaterial for the following.

In the sequel all field quantities are split into a normal and anomalous part, denoted by the subscripts "n" and "a", respectively. The normal part refers to a one-dimensional conductivity structure. Let

$$\sigma(y,z) = \sigma_n(z) + \sigma_a(y,z) \tag{3.7}$$

$$k^2(y,z) = k_n^2(z) + k_a^2(y,z) \tag{3.8}$$

$$E(y,z) = E_n(y,z) + E_a(y,z) \tag{3.9a}$$

$$H(y,z) = H_n(z) + H_a(y,z) \tag{3.9b}$$

E_n and H_n are defined as solutions of the equations

$$\Delta E_n = k_n^2 E_n + j^e \tag{3.10a}$$

$$\frac{d}{dz}\left(\frac{1}{k_n^2}\frac{d}{dz} H_n\right) = H_n, \quad z \geq 0, \qquad H_n(o) = H_o, \tag{3.10b}$$

vanishing for $z \to \infty$.

In virtue of (3.5a,b), (3.9a,b), and (3.10a,b) E_a and H_a satisfy

$$\Delta E_a = k^2 E_a + k_a^2 E_n \tag{3.11a}$$

$$\operatorname{div}\left(\frac{1}{k^2}\operatorname{grad} H_a\right) = H_a + \frac{d}{dz}\left(\frac{1}{k_n^2} - \frac{1}{k^2}\right)\frac{dH_n}{dz}, \quad z \geq 0 \tag{3.11b}$$

If the anomalous domain is of finite extent, E_a has to vanish uniformly at infinity. Under the same condition H_a has to vanish uniformly in the lower half-space. At $z=o$ H_a is zero.

If the anomalous domain is of infinite extent in horizontal direction, we can demand only that E_a, $H_a \to 0$ for $z \to \infty$.

For a numerical solution of (3.11a) the following three choices of a basic domain are possible (boundaries hatched).

In approach A, (3.11a) is solved by finite differences subject to the boundary condition $E_a=0$ or better subject to an inpedance boundary condition (below). In approach B (3.11a) is solved by finite differences only in the anomalous slab. At the horizontal boundaries boundary conditions involicity the normal structure above and below the slab are applied. I approach C (3.11a) is reduced to an integral equation over the anomalous domain. These approaches will now be discussed in details.

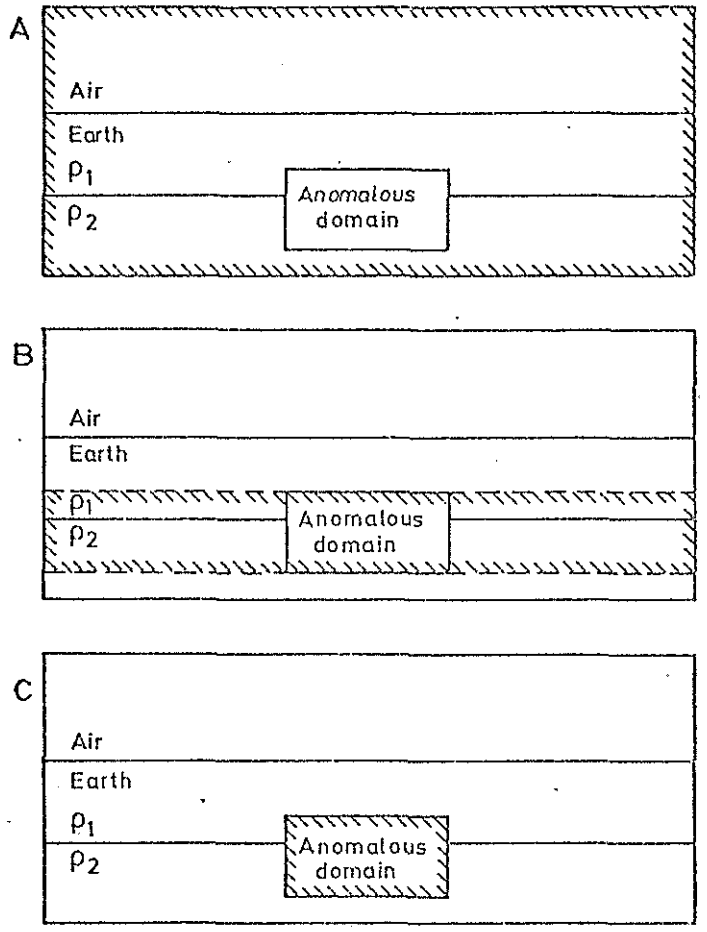

3.2. Air half-space and conductor as basic domain

(Finite difference method)

For the TE- and TM-mode we have to solve the differential equations (3.5a,b), i.e.

$$\Delta E = k^2 E + i\omega\mu_o j^e \quad , \; k^2 = i\omega\mu_o\sigma \tag{3.12a}$$

$$\mathrm{div}\left(\frac{1}{k^2}\,\mathrm{grad}H\right) = H, \; H = H_o \text{ at } z=o \tag{3.12b}$$

with the boundary condition that the differences $E_a=E-E_n$ and $H_a=H-H_n$ vanish at infinity. E_n has to be computed for any given two-dimensional external source field along the lines of Sec.2.3. The H_n-field belongs to a uniform external magnetic field.
In the finite difference method, the differential operators in (3.12a,b) are reduced to finite differences. For simplicity a square grid with grid with h is assumed. Consider the following configuration of a nodal point 0 and its four neighbours:

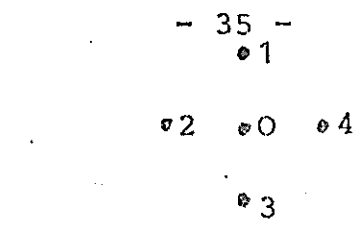

Then the evaluation of (3.12a) in uniform subdomains yields

$$E_1+E_2+E_3+E_4 - 4E_o = h^2k^2E_o$$

or

$$E_o = \frac{1}{4+h^2k^2}\{E_1+E_2+E_3+E_4\} \tag{3.13}$$

Within uniform subdomains the same formula applies to H. Differences occur if the nodal point O is at an interface. Consider as example a vertical discontinuity:

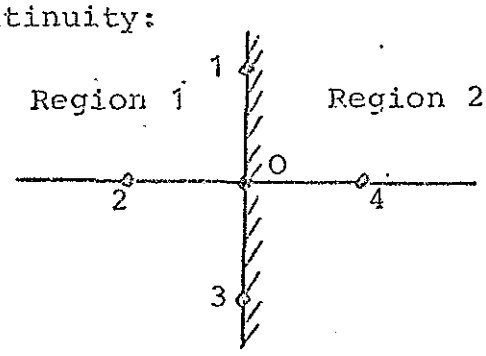

In the absence of region 2 one can write a central difference equation for E at nodal point O as

$$E_1^{(1)}+E_2^{(1)}+E_3^{(1)}+E_4^{(1)} = (4+h^2k_1^2)E_o^{(1)}, \tag{3.14}$$

where the bracketed superscript indicates the region. In the absence of region 1 the central difference equation at O is

$$E_1^{(2)}+E_2^{(2)}+E_3^{(2)}+E_4^{(2)} = (4+h^2k_2^2)E_o^{(2)}. \tag{3.15}$$

At the vertical discontinuity we have because of the continuity of E:

$$E_1^{(1)}=E_1^{(2)}\equiv E_1,\quad E_o^{(1)}=E_o^{(2)}\equiv E_o,\quad E_3^{(1)}=E_3^{(2)}\equiv E_3. \tag{3.16}$$

Since also the normal gradient of E is continuous,

$$E_4^{(1)}-E_2^{(1)} = E_4^{(2)}-E_2^{(2)}. \tag{3.17}$$

The field values $E_2^{(2)}$ and $E_4^{(1)}$ are fictitious and have to be eliminated with the aid of (3.16) and (3.17) from (3.14) and (3.15). The result is

$$\boxed{E_o = \frac{1}{4+h^2(k_1^2+k_2^2)/2}\{E_1+E_2+E_3+E_4\}} \tag{3.18}$$

where $E_2 = E_2^{(1)}$ and $E_4 = E_4^{(2)}$.

Hence, the conductivity is to be averaged in the TE-case. Now consider the TM-case:

$$H_1^{(1)}+H_2^{(1)}+H_3^{(1)}+H_4^{(1)} = (4 + h^2k_1^2)H_o^{(1)} \tag{3.19}$$

$$H_1^{(2)}+H_2^{(2)}+H_3^{(2)}+H_4^{(2)} = (4 + h^2k_2^2)H_o^{(2)} \tag{3.20}$$

The continuity of H and $\frac{1}{\sigma}$ dH/dn yields

$$H_1^{(1)}=H_1^{(2)}\equiv H_1,\ H_o^{(1)}=H_o^{(2)}\equiv H_o,\ H_3^{(1)}=H_3^{(2)}\equiv H_3 \tag{3.21}$$

$$(H_4^{(1)}-H_2^{(1)})/\sigma_1 = (H_4^{(2)}-H_2^{(2)})/\sigma_2, \tag{3.22}$$

from where we obtain on eliminating $H_2^{(2)}$ and $H_4^{(1)}$

$$\boxed{H_o = \frac{H_1 + H_3 + (H_2/k_1^2+H_4/k_2^2)\cdot\overline{k^2}}{4 + h^2\overline{k^2}}} \tag{3.23}$$

where $(\overline{k^2})^{-1} = \frac{1}{2}(\frac{1}{k_1^2} + \frac{1}{k_2^2})$ and $H_2 = H_2^{(1)}$, $H_4=H_4^{(2)}$.

Similar formulae hold for a horizontal discontinuity.

The normal values of E_n and H_n are used as starting as initial values. At the boundaries we have two choices

a) The boundary values are kept fixed, i.e. $E = E_n$,

b) Or free boundary values are used as <u>impedance boundary condition</u>, i.e.

$$\boxed{k_n(\underline{r})\ E_a(\underline{r}) = -\frac{\partial E_a}{\partial n}} \tag{3.24}$$

where n is the direction of the <u>outward</u> normal.

(3.24) is obtained under the assumption that the anomalous fields diffuses in form of plane waves outwards, a valid approximation only if the local penetration depth is small compared with the scale length of conductivity changes. It performs poorly at edges and in isolators. However, better then E_a=0.

Eq. (3.24) yields as condition at the upper edge of the air layer: $\partial E_a/\partial z = 0$ (i.e. constant horizontal magnetic field).

The iteration is carried out either along rows or columns. Generally the Gauß-Seidel iteration procedure is used with a successive over-relaxation factor to speed up convergence.

3.3. Anomalous slab as basic domain

In practice it is not necessary to solve the diffusion equation by finite differences in the total conductor and the air half-space. Instead it is sufficient to treat the equation only in that slab which contains the anomalous domain.
Let the anomalous slab be confined to the depth range $z_1 \leq z \leq z_2$. Within this domain we have to solve the inhomogeneous equation (considering for the moment only the TE-case)

$$\Delta E_a = k^2 E_a + k_a^2 E_n \qquad (3.25)$$
$$= (3.5a)$$

subject to two homogeneous boundary conditions at $z = z_1$ and z_2, which involve σ_n for $z < z_1$ and $z > z_2$ respectively and account for the vanishing anomalous field for $z \to \pm \infty$. When (3.25) is solved by finite differences, the discretization involves also the field values one grid point width above and below the anomalous slab. The idea is to express these values in terms of a line integral over E_a at $z = z_1$ and z_2 respectively.
Let V_1 and V_2 be the half-planes $z \leq z_1$ and $z \geq z_2$, respectively. Let $G^{(m)}(\underline{r}_o|\underline{r})$, $\underline{r}, \underline{r}_o \in V_m$ be Green's functions which satisfy

$$\Delta G^{(m)}(\underline{r}_o|\underline{r}) = k_n^2(\underline{r})\, G^{(m)}(\underline{r}_o|\underline{r}) - \delta(\underline{r} - \underline{r}_o), \quad m=1,2 \qquad (3.26)$$

subject to the boundary condition

$$G^{(m)}(\underline{r}_o|\underline{r}) = 0 \quad \text{at} \quad z = z_m, \quad m = 1,2 \qquad (3.27)$$

In V_1 and V_2, E_a is a solution of

$$\Delta E_a(\underline{r}) = k_n^2(\underline{r})\, E_a(\underline{r}). \qquad (3.28)$$

Now Green's formula for two-dimensions states that

$$\int\{U\Delta V - V\Delta U\}dA = \int\{U\frac{\partial V}{\partial n} - V\frac{\partial U}{\partial n}\}ds \qquad (3.29)$$

The RHS is a closed line integral bordering the area over which the LHS integral is performed. In the RHS differentiation in direction to the outward normal is involved.
From (3.28) and (3.26) follows

$$G\Delta E_a - E_a\Delta G = \delta(\underline{r} - \underline{r}_o)E_a.$$

Identifying U with G, V with E_a, Eq. (3.29) yields in virtue of (3.27)

$$E_a(\underline{r}_o) = -\int_{\text{around } V_m} E_a(\underline{r})\frac{\partial}{\partial n}G^{(m)}(\underline{r}_o|\underline{r})ds.$$

Now $G^{(m)}$ and its normal derivative vanish at infinity. Hence, only the part of the line integral along the axis $z = z_m$ contributes.
For m=1 : $\frac{\partial}{\partial n} = \frac{\partial}{\partial z}$, m=2 : $\frac{\partial}{\partial n} = -\frac{\partial}{\partial z}$.

Hence,

$$\boxed{E_a(\underline{r}_o) = (-1)^m \int_{-\infty}^{+\infty} E_a(y,z_m)\frac{\partial}{\partial z_m}G^{(m)}(\underline{r}_o|y,z_m)dy,\ \underline{r}_o \varepsilon V_m} \qquad (3.30)$$

Because of (3.26), Eq. (3.30) depends only on the difference $y-y_o$.
Defining

$$K^{(m)}(y-y_o,z_o) = (-1)^m\frac{\partial}{\partial z_m}G^{(m)}(\underline{r}_o|y,z_m) \qquad (3.30a)$$

Eq. (3.30) reads shorter

$$E_a(y_o,z_o) = \int_{-\infty}^{+\infty} K^{(m)}(y-y_o,z_o)\,E_a(y,z_m)dy \qquad (3.31)$$

For a layered structure in V_m, the kernels $K^{(m)}$ are easily determined:

Let us first consider the case m = 2. Assume that there are L uniform layers below $z = z_2$ with conductivities $\sigma_1, \sigma_2, \ldots, \sigma_L$, and upper edges at $z = h_1, h_2, \ldots, h_L$ ($h_1 = z_2$). In applications the vertical grid width $z_o - z_2$ will be so small that z_o is in the first uniform layer. Then a solution of (3.26) having the correct singularity is

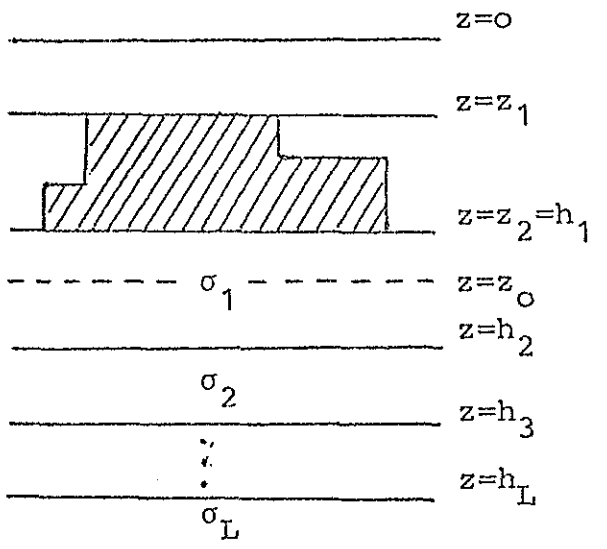

$$\frac{1}{2\pi} K_o(k_1|\underline{r}-\underline{r}_o|) = \frac{1}{2\pi} \int_o^\infty e^{-\alpha_1|z-z_o|} \cos\lambda(y-y_o) \frac{d\lambda}{\alpha_1} \qquad (3.32)$$

$$k_1 = \sqrt{i\omega\mu_o\sigma_1}, \quad \alpha_1 = \sqrt{\lambda^2+k_1^2}$$

However, the boundary condition (3.27) is not yet satisfied and the normal conductivity structure has not yet been taken into account. To achieve this let in

$$z_2 \le z \le z_o : G^{(2)}(\underline{r}_o|\underline{r}) = \int_o^\infty \delta_o \{e^{\alpha_1(z-z_2)} - e^{-\alpha_1(z-z_2)}\} \cos\lambda(y-y_o) d\lambda \qquad (3.33a$$

$$z_o \le z \le h_2 : G^{(2)}(\underline{r}_o|r) = \int_o^\infty \delta_L \{B_1^+ e^{\alpha_1(z-z_2)} + B_1^- e^{-\alpha_1(z-z_2)}\} \cos\lambda(y-y_o) d\lambda \quad (3.$$

$$h_m \le z \le h_{m+1} : G^{(2)}(\underline{r}_o|\underline{r}) = \int_o^\infty \delta_L \{B_m^+ e^{\alpha_m(z-h_m)} + B_m^- e^{-\alpha_m(z-h_m)}\} \cos\lambda(y-y_o) d\lambda \quad (3.$$

$m = 2, \ldots, L$; $h_{L+1} = \infty$ Eq. (3.33a) satisfies already (3.27). Starting with $B_L^+ = 0$, $B_L^- = 1$ the coefficients $B_m^\pm$ are determined from the continuity conditions for $G^{(2)}$ across interfaces as indicated in Sec. (2.3):

$$B_m^\pm = (1 \pm \alpha_{m+1}/\alpha_m) g_m^\pm B_{m+1} + (1 \mp \alpha_{m+1}/\alpha_m) g_m^\mp B_{m+1}^-, \quad m = L-1, \ldots, 1 \qquad (3.34$$

$$g_m^\pm = \frac{1}{2} \exp\{\pm\alpha_m(h_{m+1} - h_m)\}$$

Having determined $B_1^{\pm}$, the coefficients δ_o and δ_L are determined from the fact that the difference between upward (downward) travelling waves of (3.33a) and (3.33b) at $z = z_o$ must be due to the primary excitation given by (3.32). Hence,

$$\delta_L B_1^+ e^{\alpha_1(z_o-z_2)} + \frac{1}{2\pi\alpha_1} = \delta_o e^{\alpha_1(z_o-z_2)}$$

$$- \delta_o e^{-\alpha_1(z_o-z_2)} + \frac{1}{2\pi\alpha_1} = \delta_L B_1^- e^{-\alpha_1(z_o-z_2)}$$

whence

$$\delta_o = \frac{f_1^+ B_1^+ + f_1^- B_1^-}{2\pi\alpha_1(B_1^+ + B_1^-)}, \quad \delta_L = \frac{f_1^+ - f_1^-}{2\pi\alpha_1(B_1^+ + B_1^-)}, \quad f_1^{\pm} = e^{\pm\alpha_1(z_o-z_2)}.$$

From (3.30a)

$$K^{(2)}(y-y_o, z_o) = \frac{1}{\pi} \int_o^\infty \frac{f_1^+ B_1^+ + f_1^- B_1^-}{B_1^+ + B_1^-} \cos\lambda(y-y_o)d\lambda. \qquad (3.35)$$

Since (3.35) involves only the ratio B_1^+/B_1^-, it can be expressed in terms of the transfer function C at $z = z_2$ (cf. (2.64)):

$$\frac{B_1^+}{B_1^-} = \frac{\alpha_1 C - 1}{\alpha_1 C + 1}.$$

For a uniform half space (3.35) is simply

$$\underline{K^{(2)}(y-y_o, z_o)} = \frac{1}{\pi} \int_o^\infty e^{-\alpha_1(z_o-z_2)} \cos\lambda(y-y_o)d\lambda = \underline{\frac{(z_o-z_2)k_1}{\pi|\underline{r}-\underline{r}_o|} K_1(k_1|\underline{r}-\underline{r}_o|)} \qquad (3.36)$$

For $k_1 \to 0$ (isolator) this yields

$$\underline{K^{(2)}(y-y_o, z_o) = \frac{(z_o-z_2)}{\pi\{(y-y_o)^2 + (z_2-z_o)^2\}}}. \qquad (3.36a)$$

The case m = 1 can be treated in a quite analogue way. If the anomalous slab extends till the surface, i.e. $z_1 = 0$, the pertinent kernel is easily derived from (3.36a):

$$K^{(1)}(y-y_o, z_o) = -\frac{z_o}{\pi\{(y-y_o)^2 + z_o^2\}}, \quad z_o < 0 \tag{3.37}$$

(Because of (3.30a) there has been a change of sign.)
If there are more normal layers (in addition to the air half-space), the problem is treated as for m = 2, with the air half-space as last (L-th) layer, we have to calculate δ_L and hence $B_1^{\pm}$ separately. We can't use C.

The kernels $K^{(m)}$ are nicely peaked functions. The halfwidth is approximately $2|z_m - z_o|$, i.e. twice the vertical grid width. For an insulator the tails are comparatively long ($\sim 1/y^2$), for a conductor an exponential decrease is inferred from (3.36). In general two points to the left and the right of the central point will give a satisfactory approximation:

$$E_a(y, z_o) \tilde{=} \sum_{i=-2}^{+2} p_i^{(m)} E_a(y + ih_y, z_m), \tag{3.38}$$

where

$$p_o^{(m)} = 2\int_0^{h_y/2} K^{(m)}(u, z_o)\,du, \quad p_1^{(m)} = \int_{h_y/2}^{3h_y/2} K^{(m)}(u, z_o)\,du, \quad p_2^{(m)} = \int_{3h_y/2}^{\infty} K^{(m)}(u, u_o$$

$p_{-i} = p_i$, $\Sigma\, p_i = 1$, h_y = horizontal grid width.

(3.38) expresses in any application of the finite difference formul the anomalous part of the electric field outside the anomalous slab in terms of anomalous field values at the boundary. At the vertical boundaries the impedance boundary condition (3.24) is applied.

So far only the TE-case has been considered. The TM-mode can be handled similarly, taking only the different boundary condition into account. The approprate formulas can be worked out as an exercise.

3.4. Anomalous region as basic domain

Integral equation method

In the integral equation approach Maxwell's equations are transformed into an integral equation for the electric field over the anomalous domain. With the usual splitting

$$\sigma = \sigma_n + \sigma_a, \quad E = E_n + E_a, \quad k^2 = k_n^2 + k_a^2,$$

we have

$$\Delta E = k^2 E + i\omega\mu_o j^e , \tag{3.39}$$

$$\Delta E_n = k_n^2 E_n + i\omega\mu_o j^e , \tag{3.40}$$

or subtracting

$$\Delta E_a = k_n^2 E_a + k_a^2 E \tag{3.41}$$

Let G_n be Green's function for the normal conductivity structure, i.e.

$$\Delta G_n(\underline{r}_o|\underline{r}) = k_n^2(\underline{r}) G_n(\underline{r}_o|\underline{r}) - \delta(\underline{r} - \underline{r}_o). \tag{3.42}$$

$G_n(\underline{r}_o|\underline{r})$ can be conceived as the electric field of a unit line current placed at $\underline{r}_o$ and observed at $\underline{r}$.
Multiply (3.41) by G_n, (3.42) by E_a, subtract and integrate with respect to $\underline{r}$ over the whole space: It results

$$E_a(\underline{r}_o) = \int k_a^2(\underline{r}) E(\underline{r}) G_n(\underline{r}_o|\underline{r}) dA + \int \{G_n \Delta E_a - E_a \Delta G_n\} dA. \tag{3.43}$$

Green's theorem (3.29) yields

$$\int \{G_n \Delta E_a - E_a \Delta G_n\} dA = \int \{G_n \frac{\partial E_a}{\partial n} - E_a \frac{\partial G_n}{\partial n}\} ds = 0,$$

since E_a and G_n vanish at infinity. Hence, introducing into (3.43) E instead of E_a we obtain the integral equation

$$\boxed{E(\underline{r}_o) = E_n(\underline{r}_o) - \int k_a^2(\underline{r}) E(\underline{r}) G_n(\underline{r}_o|\underline{r}) dA} \tag{3.44}$$

In (3.44), the inhomogeneous term E_n can be computed for a given normal structure and given external field in a well-known way.
It remains to determine the kernel $G_n(\underline{r}_o|\underline{r})$. It satisfies the reciprocity relation

$$\boxed{G_n(\underline{r}_o|\underline{r}) = G_n(\underline{r}|\underline{r}_o),} \tag{3.45}$$

i.e. source and receiver are interchangeable. For a proof write (3.42) for $G_n(\underline{r}_o|\underline{r}')$ and a corresponding equation for $G_n(\underline{r}|\underline{r}')$. Multiply these equations crosswise by $G_n(\underline{r}|\underline{r}')$ and $G_n(\underline{r}_o|\underline{r}')$, subtract and integrate over the full space. Then the result is obtained on using Green's theorem.

For a solution of (3.44) we have to put a line current at each point $\underline{r}_o$ of the anomalous domain and have to compute the resulting electric field at each point of this domain replacing its anomalous structure by the normal conductivity. Assume a rectangular anomalous domain with NY cells in y-direction and NZ cells in z-direction. Because of horizontal isotropy the field depends in horizontal direction only on the distance between source and receiver. Hence, we need field values only for NY horizontal distances. Due to the layering there is no isotropy in vertical direction. Here we have to put the line current into the center of each cell. Because of reciprocity the sorresponding field values have to be calculated in and below the depth of the source. Hence, for the kernel G_n a total of $NY \cdot \frac{1}{2}NZ \cdot (NZ+1)$ field values has to be calculated.

A second set of kernels is required which transform on using (3.44) the electrical field in the anomalous domain into the electromagnetic surface field for all three components E_x, H_y, H_z. The number of required kernel data depends on the range where the field is to be evaluated.

It remains to calculate $G_n(\underline{r}_o|\underline{r})$ for a layered structure. Assume L layers with conductivities $\sigma_o = 0, \sigma_1, \ldots, \sigma_L$ and upper edges $h_1 = 0, h_2, \ldots, h_L, h_{L+1} = \infty$.

Let the source and observation point be placed in the m-th and μ-layer, respectively, and let in the m-th layer

$$G_n^m(\underline{r}_o|\underline{r}) = \int_o^\infty \{P_m^+ + P_m^-\}\cos\lambda(y-y_o)\,d\lambda \tag{3.46}$$

where

$$P_m^\pm = \begin{cases} \delta_o A_m^\pm f_m^\pm(z), & z \leq z_o \\ \delta_L B_m^\pm f_m^\pm(z), & z \geq z_o \end{cases} \tag{3.47}$$

$$f_m^\pm(z) = \exp\{\pm\alpha_m(z-h_m)\},\ \alpha_m^2 = \lambda^2 + i\omega\mu_o\sigma_m.$$

δ_o and δ_L can be so adjusted that $A_o^+ = B_L^- = 1$. Since there are no sources in $z \leq 0$ and in $z \geq z_o$ if z_o is in the L-th layer, $A_o^- = B_L^+ = 0$. With these starting values the continuity of G_n and $\partial G_n/\partial z$ across interfaces yields the forward and backward recurrence relations

$$A_m^{\pm} = (1 \pm \alpha_{m+1}/\alpha_m) g_{m-1}^{+} A_{m-1}^{+} + (1 \mp \alpha_{m-1}/\alpha_m) g_{m-1}^{-} A_{m-1}^{-}, \quad m = 1, \ldots, \mu$$

$$B_m^{\pm} = (1 \pm \alpha_{m+1}/\alpha_m) g_m^{\mp} B_{m+1}^{+} + (1 \mp \alpha_{m+1}/\alpha_m) g_m^{\mp} B_{m+1}^{-}, \quad m = L-1, \ldots, \mu$$

with $\quad g_o^{\pm} = 1/2, \; g_m^{\pm} = (1/2)\exp\{\pm\alpha_m(h_{m+1} - h_m)\}, \; m = 1, \ldots, L-1.$

In the case $\mu = L$ no recurrence is required for the B-terms. The coefficients δ_o and δ_L are determined from the fact that in (3.46) the difference in the upward (downward) travelling waves for $z \geq z_o$ and $z \leq z_o$ must be due to the primary excitation given by

$$\frac{1}{2\pi} K_o(k_\mu |\underline{r} - \underline{r}_o|) = \frac{1}{2\pi} \int_o^\infty e^{-\alpha_\mu |z - z_o|} \cos\lambda(y - y_o) \frac{d\lambda}{\alpha_\mu} .$$

Hence,

$$\delta_o = \frac{1}{2\pi\alpha_\mu} \cdot \frac{B_\mu^- f_\mu^- + B_\mu^+ f_\mu^+}{A_\mu^+ B_\mu^- - A_\mu^- B_\mu^+}, \quad \delta_L = \frac{1}{2\pi\alpha_\mu} \cdot \frac{A_\mu^- f_\mu^- + A_\mu^+ f_\mu^+}{A_\mu^+ B_\mu^- - A_\mu^- B_\mu^+}$$

where $f_\mu^{\pm} = f_\mu^{\pm}(z_o)$. The nominator (including α_μ) is a Wronskian of the differential equation

$$W''(z) = \{\lambda^2 + k_n^2(z)\} W(z)$$

which is a constant thus ensuring reciprocity. (Proof?)

In applications the anomalous domain is split into rectangular cells, the electric field is assumed to be constant within each cell. Then (3.44) reduces to a system of linear equations, which is easily solved because of its dominant diagonal due to the logarithmic singularity of the kernels. Either direct elimination or Gauß-Seidel iteration can be applied, the latter being in general quickly convergent. When E is assumed to be constant within each cell, the integration over the kernel is easily effected by adding in (3.46) the factor

$$4\sin(\lambda h_y/2)\sinh(\alpha_\mu h_z/2)/(\lambda\alpha_\mu),$$

The integral equation method for the H-polarization case looks slightly more complicated. This is related to the fact that even for three-dimensional structures Maxwell's equations look simple when formulated for $\underline{E}$, whereas in the $\underline{H}$-formulation additional gradients of the conductivity arise:

$$\mathrm{curl}^2\underline{\tilde{E}} + i\omega\mu_o\sigma\,\underline{\tilde{E}} = 0, \quad \mathrm{curl}\left(\frac{1}{\sigma}\,\mathrm{curl}\underline{\tilde{H}}\right) + i\omega\mu_o\underline{\tilde{H}} = 0.$$

The pertinent equation for H-polarization is (3.5), i.e.

$$\mathrm{div}\left(\frac{1}{\sigma}\,\mathrm{grad}H\right) = i\omega\mu_o H \tag{3.48}$$

with the usual splitting

$$\sigma = \sigma_n + \sigma_a, \quad H = H_n + H_a$$

and the additional definitions

$$\rho = 1/\sigma, \quad \rho_n = 1/\sigma_n, \quad \rho_a = \rho - \rho_a \tag{3.49a-}$$

the equations for the normal and anomalous part are

$$\frac{d}{dz}\left(\frac{1}{\sigma_n}\,\frac{d}{dz}\,H_n\right) = i\omega\mu_o H_n, \quad H_n(o) = H_o \tag{3.50}$$

and

$$\boxed{\mathrm{div}(\rho_n\,\mathrm{grad}H_a) = i\omega\mu_o H_a - \mathrm{div}(\rho_a\,\mathrm{grad}H)} \tag{3.51}$$

This equation corresponds to (3.41) for the E-polarization case. Green's function appropriate to (3.51) is defined as

$$\mathrm{div}(\rho_n\,\mathrm{grad}G_n) = i\omega\mu_o G_n - \delta(\underline{r} - \underline{r}_o). \tag{3.52}$$

Physically G_n can be interpreted as the magnetic field due to an infinite straight line of oscillating magnetic dipoles along the x-axis.

Multiply (3.51) by G_n and (3.52) by H_a, subtract and integrate over the whole space. Then

$$\int\{G_n\mathrm{div}(\rho_n\mathrm{grad}H_a) - H_a\mathrm{div}(\rho_n\mathrm{grad}G_n)\}dA =$$

$$= -\int G_n\mathrm{div}(\rho_a\mathrm{grad}H)\,dA + H_a \tag{3.53}$$

From the generalized Green's theorem

$$\int\{U\,\mathrm{div}(\psi\,\mathrm{grad}V) - V\,\mathrm{div}(\psi\,\mathrm{grad}U)\,dA = \int \psi\{U\frac{\partial V}{\partial n} - V\frac{\partial U}{\partial n}\}ds \tag{3.54}$$

follows that the LHS of (3.53) vanishes. Applying (3.54) also to the RHS of (3.53) we obtain, introducing $H_a = H - H_n$:

$$H(\underline{r}_o) = H_n(\underline{r}_o) + \int H(\underline{r})\,\mathrm{div}(\rho_a(\underline{r})\,\mathrm{grad}G_n(\underline{r}_o|\underline{r}))\,dA \tag{3.55}$$

This is an integral equation for H_a. It can be cast in a slightly different form, which is particularly suitable for applications since the high degree of singularity due to a two-fold differentiation of G_n at $\underline{r} = \underline{r}_o$ is removed. Because of

$$\mathrm{div}(\rho_a\,\mathrm{grad}G_n) = \frac{\rho_a}{\rho_n}\{i\omega\mu_o G_n - \delta(\underline{r}-\underline{r}_o)\} + \rho_n\,\mathrm{grad}G_n \cdot \mathrm{grad}(\rho_a/\rho_n)$$

Eq. (3.55) reads alternatively

$$H(\underline{r}_o) = \frac{\rho_n(\underline{r}_o)}{\rho(\underline{r}_o)}\left[H_n(\underline{r}_o) + \int H(\underline{r})\{i\omega\mu_o G_n(\underline{r}_o|\underline{r})\frac{\rho_a(\underline{r})}{\rho_n(\underline{r})} + \rho_n(\underline{r})\,\mathrm{grad}G_n(\underline{r}_o|\underline{r}) \cdot \mathrm{grad}\frac{\rho_a(\underline{r})}{\rho_n(\underline{r})}\}dA\right] \tag{3.56}$$

The kernel of the integral equation consists of two parts. The first part takes account of the changing concentration of current lines in anomalous domains. It is a volume effect. The second effect results from the bending of current lines where conductivity changes. It is essentially a surface effect.

In the case of discontinuous changes in conductivity, which is the most common assumption, (3.56) needs a slight modification. Assume that the anomalous domain consists of rectangular cells, where the conductivity is allowed to differ from cell to cell. H is assumed to be constant in each cell.

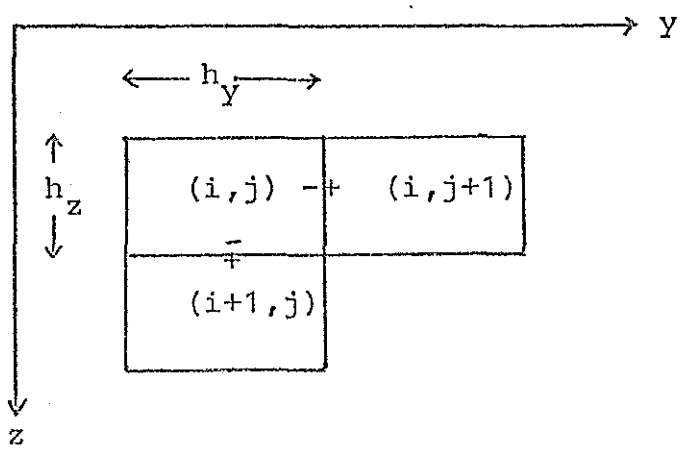

Then the discontinuity between cell (i,j) and (i+1,j) contributes to the integral

$$\frac{1}{2}\{H(i,j)+H(i+1,j)\}\rho_n(i,j)\left.\frac{\partial G_n(\underline{r}_o|i,j)}{\partial z}\right|_{-}\cdot\{\frac{\rho_a(i+1,j)}{\rho_n(i+1,j)}-\frac{\rho_a(i,j)}{\rho_n(i,j)}\}\cdot h_y$$

It has been used that H and $\rho\frac{\partial G}{\partial n}$ are continuous across interfaces. The contribution from the (i,j) → (i,j+1) interface is

$$\frac{1}{2}\{H(i,j)+H(i,j+1)\}\rho_n(i,j)\left.\frac{\partial G_n(\underline{r}_o|i,j)}{\partial y}\right|_{-}\cdot\{\frac{\rho_a(i,j+1)}{\rho_n(i,j+1)}-\frac{\rho_a(i,j)}{\rho_n(i,j)}\}h_z.$$

The integral equation is decomposed into a set of linear equations for the H_a-values at each cell. The electric field is then obtained by differentiating (3.56) with respect to the coordinates of $\underline{r}_o$. - It remains to calculate G_n. At $z = 0$ G_n has to satisfy the boundary condition of H_a, i.e. $H_a = 0$, : $G_n = 0$. The boundary conditions at interfaces are G_n and $(1/\sigma)\partial G_n/\partial z$ continuous. Assume again L uniform layers with conductivities $\sigma_1, \sigma_2, \ldots, \sigma_L$ and upper edges at $h_1 = 0, h_2, \ldots, h_L, h_{L+1} = \infty$.

Let the field in the m-th layer be

$$G_n^m(\underline{r}_o|\underline{r}) = \int_0^\infty \{Q_m^+ + Q_m^-\}\cos\lambda(y-y_o)d\lambda$$

where

$$Q_m^\pm = \begin{cases} \gamma_o\ C_m^\pm f_m^\pm(z), & z \le z_o \\ \gamma_L\ D_m^\pm f_m^\pm(z), & z \ge z_o \end{cases}$$

$$f_m^\pm(z) = \exp\{\pm\alpha_m(z-h_m)\},\quad \alpha_m^2 = \lambda^2 + i\omega\mu_o\sigma_m$$

γ_o and γ_L can again be so adjusted that $C_1^+ = D_L^- = 1$. $G_n = 0$ for $z = 0$ requires then $C_1^- = -1$, and $G_n \to 0$ for $z \to \infty$ demands $D_L^+ = 0$. Starting with these initial values, the boundary conditions yield the forward and backward recurrence relations

$$C_m^{\pm} = (1 \pm \frac{\beta_{m-1}}{\beta_m})\, g_{m-1}^{+}\; C_{m-1}^{+} + (1 \mp \frac{\beta_{m-1}}{\beta_m})\, g_{m-1}^{-}\; C_{m-1}^{-}, \quad 2 \leq m \leq \mu$$

$$D_m^{\pm} = (1 \pm \frac{\beta_{m+1}}{\beta_m})\, g_m^{\mp}\; D_{m+1}^{+} + (1 \mp \frac{\beta_{m+1}}{\beta_m})\, g_m^{\mp}\; D_{m+1}^{-}, \quad L-1 \geq m \geq \mu$$

where

$$\beta_m = \alpha_m/\sigma_m \text{ and } g_m^{\pm} = \frac{1}{2} \exp\{\pm\alpha_m (h_{m+1} - h_m)\}$$

μ is the source layer. There is no recurrence required for the C-term if $\mu = 1$ and for the D-terms if $\mu = L$.
The free factors follow again from the source representation

$$\frac{\sigma_\mu}{2\pi} K_o(k_\mu |\underline{r} - \underline{r}_o|) = \frac{\sigma_\mu}{2\pi} \int_o^\infty e^{-\alpha_\mu |z - z_o|} \cos\lambda(y - y_o)\, \frac{dz}{\alpha_\mu},$$

which must account for the difference for upward and downward travelling waves at $z = z_o$. Hence,

$$\gamma_o = \frac{\sigma_\mu}{2\pi\alpha_\mu} \frac{D_\mu^+ f_\mu^+ + D_\mu^- f_\mu^-}{C_\mu^+ D_\mu^- - C_\mu^- D_\mu^+}, \qquad \gamma_L = \frac{\sigma_\mu}{2\pi\alpha_\mu} \frac{C_\mu^+ f_\mu^+ + C_\mu^- f_\mu^-}{C_\mu^+ D_\mu^+ - C_\mu^- D_\mu^+}.$$

With the present determination of the field G_n satisfies again the reciprocity relation $G_n(\underline{r}_o|r) = G_n(\underline{r}|\underline{r}_o)$. (Proof?)

4. Model calculations for three-dimensional structures

4.1. Introduction

In the three-dimensional case the TE- and TM-mode become mixed and cannot longer be treated separately. Now the differential equation for a vector field instead of a scalar field is to be solved. In numerical solutions questions of storage and computer time become important. Assume as example that in approach A a basic domain with 20 cells in each direction is chosen. In this case, only the storage of the electric field vector would require 48000 locations. For an iterative improvement of one field component at least 0.0005 sec are needed for each cell. This yields 12 sec for a complete iteration, and 20 min for 100 iterations. This appears to be the least time required for this model. Hence methods for a reduction of computer time and storage are particularly appreciated in this case. The equation to be solved is

$$\mathrm{curl}^2 \underline{E}(\underline{r}) + k^2(\underline{r})\underline{E}(\underline{r}) = -i\omega\mu_o \underline{\iota}_e(\underline{r}) \tag{4.1}$$

where $k^2(\underline{r}) = i\omega\mu_o\sigma(\underline{r})$.

$\underline{\iota}_e(\underline{r})$ is the source current density.
After the splitting

$$\sigma = \sigma_n + \sigma_a, \quad k^2 = k_n^2 + k_a^2, \quad \underline{E} = \underline{E}_n + \underline{E}_a, \tag{4.2a-c}$$

where $\underline{E}_n$ is that solution of

$$\mathrm{curl}^2 \underline{E}_n(\underline{r}) + k_n^2(\underline{r})\underline{E}_n(\underline{r}) = -i\omega\mu_o \underline{\iota}_e \tag{4.3}$$

which vanishes at infinity, we obtain for the anomalous field the two alternative equations

$$\mathrm{curl}^2 \underline{E}_a + k_n^2 \underline{E}_a = -k_a^2 E \tag{4.4a}$$

$$\mathrm{curl}^2 \underline{E}_a + k^2 \underline{E}_a = -k_a^2 E_n \tag{4.4b}$$

Eq. (4.4a) is the starting point for the volume integral or integral equation approach, Eq. (4.4b) is the point of starting for the surface integral approach.

4.2. Integral equation method

Let $\underline{G}_i(\underline{r}_o|\underline{r})$, $i = 1,2,3$ be a solution of

$$\mathrm{curl}^2\underline{G}_i(\underline{r}_o|\underline{r}) + k_n^2(\underline{r})\underline{G}_i(\underline{r}_o|\underline{r}) = \hat{\underline{x}}_i\delta(\underline{r}-\underline{r}_o), \tag{4.5}$$

vanishing at infinity. Here, the $\hat{\underline{x}}_i$ are unit vectors along the cartesian coordinate axes: $\hat{\underline{x}}_1=\hat{\underline{x}}$, $\hat{\underline{x}}_2 = \hat{\underline{y}}$, $\hat{\underline{x}}_3 = \hat{\underline{z}}$. Multiply (4.5) by $\underline{E}_a(\underline{r})$ and (4.4a) by $\underline{G}_i(\underline{r}_o|\underline{r})$ and integrate the difference with respect to $\underline{r}$ over the whole space. Green's vector theorem

$$\int\{\underline{U}\cdot\mathrm{curl}^2\underline{V}-\underline{V}\mathrm{curl}^2\underline{U}\}d\tau = \int\{(\hat{\underline{n}}\times\underline{V})\cdot\mathrm{curl}\underline{U}-(\hat{\underline{n}}\times\underline{U})\cdot\mathrm{curl}\underline{V}\}dA, \tag{4.6}$$

where $d\tau$ is a volume element, dA a surface element and $\hat{\underline{n}}$ the outward normal vector, yields

$$\underline{E}_{ai}(\underline{r}_o) = -\int k_a^2(\underline{r})\underline{G}_i(\underline{r}_o|\underline{r})\cdot\underline{E}(\underline{r})d\tau, \quad i = 1,2,3$$

since $\underline{E}_a$ and $\underline{G}_i$ vanish at infinity. After combining all three components and introducing $\underline{E}$ instead of $\underline{E}_a$, the vector integral equation

$$\boxed{\underline{E}(\underline{r}_o) = \underline{E}_n(\underline{r}_o) - \int k_a^2(\underline{r})\,\mathcal{G}(\underline{r}_o|\underline{r})\cdot\underline{E}(\underline{r})d\tau} \tag{4.7}$$

is obtained. Here $\mathcal{G}$ is Green's tensor being defined as

$$\mathcal{G}(\underline{r}_o|\underline{r}) = \sum_{i=1}^{3}\hat{\underline{x}}_i\underline{G}_i(\underline{r}_o|\underline{r}) = \sum_{i,j=1}^{3}G_{ij}(\underline{r}_o|\underline{r})\hat{\underline{x}}_i\,\hat{\underline{x}}_j \tag{4.8}$$

(using dyadic notation). The tensor elements G_{ij} admit a simple physical interpretation: $G_{ij}(\underline{r}_o|\underline{r})$ is the j-th electric field component of an oscillating electric dipole of unit moment pointing in x_i-direction, placed in the normal conductivity structure at $\underline{r}_o$; the point of observation is $\underline{r}$. Note that the first subscript and argument refer to the source, the second subscript and argument to the receiver. Because of the fundamental reciprocity in electromagnetism, source and observer parameters are interchangeable, i.e.

$$\boxed{G_{ij}(\underline{r}_o|\underline{r}) = G_{ji}(\underline{r}|\underline{r}_o)} \tag{4.9}$$

For a proof replace in (4.5) $\underline{r}$ by $\underline{r}'$, write an analogous equation for $\underline{G}_j(\underline{r}|\underline{r}')$, multiply cross-wise by $\underline{G}_j$ and $\underline{G}_i$, integrate the difference with respect to $\underline{r}'$ over the whole space, and obtain (4.9) on using (4.6). Due to (4.9), the equation (4.7) is alternatively written

$$\underline{E}(\underline{r}_o) = \underline{E}_n(\underline{r}_o) - \int k_a^2(\underline{r})\ \underline{E}(\underline{r})\ \mathcal{G}(\underline{r}|\underline{r}_o)\,d\tau \qquad (4.10)$$

Eq. (4.7) involves integration over the coordinates of the receiver, (4.10) requires integration over the coordinates of the source. The kernel G and the inhomogeneous term $\underline{E}_n$ of the integral equation (4.7) or (4.10) depend only on the normal conductivity structure. To determine the kernel $\mathcal{G}$ replace first the conductivity within the anomalous domain by its normal values. Then place at each point of the domain successively two mutually perpendicular horizontal and one vertical dipole and calculate the resulting vector fields at each point of this domain. At a first glance the work involved appears to be prohibitive, but it is sharply reduced by the reciprocity (4.9) and the isotropy of the normal conductor in horizontal direction. Because of (4.9), from the elements of Green's tensor

$$\begin{matrix} G_{xx} & G_{xy} & G_{xz} \\ G_{yx} & G_{yy} & G_{yz} \\ G_{zx} & G_{zy} & G_{zz} \end{matrix}$$

the three elements G_{xz}, G_{xy}, G_{yz} need not to be calculated when G_{zy}, G_{yx}, G_{zy} is computed. From the remaining six elements G_{yy} has the same structure as G_{xx}, only rotated through 90^o. The same relation holds between G_{zy} and G_{zx}. Hence, there are only the four independent elements G_{xx}, G_{yx}, G_{zx}, G_{zz} (say). The particular symmetry of the G_{xx}, G_{yx}, G_{zz}-component in connection with the reciprocity (4.9) then shows that these components need to be evaluated only for points of observation above source points. Consider for example a vertical dipole at $x_o=y_o=0$, z_o. Then (4.9) yields

$$G_{zz}(0,0,z_o|x,y,z) = G_{zz}(x,y,z|0,0,z_o). \qquad (4.11)$$

Because of the isotropy of the conductor in horizontal direction (4.11) is alternatively written

$$G_{zz}(0,0,z_o|x,y,z) = G_{zz}(0,0,z|-x,-y,z_o).$$

Now, G_{zz} has circular symmetry around the z-axis. Hence,

$$G_{zz}(0,0,z_o|x,y,z) = G_{zz}(0,0,z|x,y,z_o).$$

The element G_{zx} is needed for all z and z_o. Assume a rectangular anomalous domain, which is decomposed into cells with quadratic horizontal cross-section. It is sufficient to pose the dipoles in one corner of the anomaly in the (x,y)-plane. Then assuming NX, NY, NZ cells in x,y,z-direction the total number of required kernels is

$$NX \cdot NY \cdot NZ(\frac{5}{2} NZ + \frac{3}{2}).$$

There is still a reduction up to a factor 2 possible, if instead of the corresponding components only some auxiliary functions depending only on the horizontal distance from the sourced are calculated.

The corresponding kernels are most easily computed using a separation into TE- and TM-fields as done in Section 1.
Let the normal structure consist of L uniform layers with conductivities σ_m, m = 1, ..., L with upper edges at $z = h_m$, m = 1, ...,L ($h_1 = 0$).
The Green vector $\underline{G}_i$ satisfies in the m-th layer the equation

$$\mathrm{curl}^2 \underline{G}_i^m + k_m^2 \underline{G}_i^m = \hat{\underline{x}}_i \, \delta(\underline{r} - \underline{r}_o), \quad k_m^2 = i\omega\mu_o\sigma_m.$$

We try a solution in the form

$$\boxed{\underline{G}_i^m = \mathrm{curl}^2(\hat{\underline{z}} \, \phi_i^m) + \mathrm{curl}(\hat{\underline{z}} \, \psi_i^m)} \tag{4.12}$$

where ϕ_i corresponds to the TM-potential and ψ_i to the TE-potential. According to Sec.2.1, at horizontal interfaces ϕ and ψ satisfy the continuity conditions

$$\boxed{\sigma\phi, \ \frac{\partial\phi}{\partial z}, \quad \psi, \ \frac{\partial\psi}{\partial z} \text{ continuous}} \tag{4.13}$$

There is no coupling between ϕ and ψ across boundaries. Within uniform layers, but outside sources ϕ and ψ satisfy identical differential equations

$$\boxed{\Delta\chi_i^m = k_m^2 \chi_i^m, \quad \chi_i^m = \phi_i^m, \ \psi_i^m \ .} \tag{4.14}$$

The behaviour of ϕ and ψ near source points can be obtained from the particular forms, which these functions show in a uniform wholespace:

$$G_{ij}(\underline{r}_o|\underline{r}) = (k^2\delta_{ij} - \partial^2/\partial x_i \partial x_j)\frac{e^{-kR}}{4\pi R k^2}, \quad R = |\underline{r} - \underline{r}_o| \tag{4.15}$$

For a dipole in z-direction this is equal to

$$\underline{G}_z = (k^2\hat{\underline{z}} - \text{grad}\frac{\partial}{\partial z})\frac{e^{-kR}}{4\pi Rk^2} = -\,\text{curl}^2(\hat{\underline{z}}\,\frac{e^{-kR}}{4\pi Rk^2}), \tag{4.16}$$

since

$$\Delta(e^{-kR}/(4\pi R)) = k^2 e^{-kR}/(4\pi R).$$

Comparison of (4.16) and (4.12) shows that for a whole space

$$\phi_z = -\frac{e^{-kR}}{4\pi Rk^2}, \quad \psi_z = 0 \tag{4.17}$$

The absence of a TE-potential is clear from physical reasons, since the magnetic field of a vertical dipole must be confined to horizontal planes (i.e. no vertical magnetic field, which can only be produced by a TE-field).
Using Sommerfeld's integral, (4.17) is written

$$\boxed{\phi_z = -\frac{1}{4\pi k^2}\int_0^\infty \frac{\lambda}{\alpha}\, e^{-\alpha|z-z_o|} J_o(\lambda r)d\lambda, \quad \alpha^2 = \lambda^2+k^2} \tag{4.18}$$

The field of a horizontal electric dipole (in x-direction, say) has both an electric and magnetic component in z-direction. Hence, a TM- and TE-potential are needed.
Since

$$G_{xz} = -(\frac{\partial^2}{\partial x^2} + \frac{\partial^2}{\partial y^2})\phi_x = -\frac{1}{4\pi k^2}\,\frac{\partial^2}{\partial x\partial z}\,\frac{e^{-kR}}{R} = -\frac{1}{4\pi k^2}\int_0^\infty \lambda^2 e^{-\alpha|z-z_o|} J_1(\lambda r)d\lambda\,\cos\phi$$

$$\text{xsign}(z-z_o)$$

and

$$(\frac{\partial^2}{\partial x^2} + \frac{\partial^2}{\partial y^2})J_1(\lambda r)\cos\phi = -\lambda^2 J_1(\lambda r)\cos\phi$$

we have

$$\boxed{\phi_x = -\frac{1}{4\pi k^2}\int_0^\infty e^{-\alpha|z-z_o|} J_1(\lambda r)d\lambda\cos\phi \cdot \text{sign}(z-z_o)} \tag{4.19}$$

and from

$$G_{xy} = \frac{\partial^2}{\partial y\partial z}\,\phi_x - \frac{\partial \psi_x}{\partial x} = -\frac{1}{4\pi k^2}\,\frac{\partial^2}{\partial x\partial y}\,\frac{e^{-kR}}{R}$$

then follows

$$\psi_x = \frac{1}{4\pi}\int_0^\infty e^{-\alpha|z-z_o|} J_1(\lambda r)\frac{d\lambda}{\alpha}\sin\phi \qquad (4.20)$$

With this knowledge of the behaviour of ϕ_z, ϕ_x, ψ_x in the uniform whole-space, these functions for a layered medium can be easily obtained.

Let in the m-th layer $h_m < z < h_{m+1}$

$$\phi_z^m = \int_0^\infty \{P_m^+ + P_m^-\} J_o(\lambda r)d\lambda \qquad (4.21)$$

where
$$P_m^\pm = \begin{cases} \gamma_o A_m^\pm f_m^\pm, & z \le z_o \\ \gamma_L B_m^\pm f_m^\pm, & z \ge z_o \end{cases},$$

$$\psi_x^m = \int_0^\infty \{Q_m^+ + Q_m^-\} J_1(\lambda r)d\lambda \sin\phi$$

where
$$Q_m^\pm = \begin{cases} \delta_o C_m^\pm f_m^\pm, & z \le z_o \\ \delta_L D_m^\pm f_m^\pm, & z \ge z_o \end{cases}, \qquad (4.22)$$

$$\phi_x^m = \int_0^\infty \{R_m^+ + R_m^-\} J_1(\lambda r)d\lambda \cos\phi$$

where
$$R_m^\pm = \begin{cases} \varepsilon_o A_m^\pm f_m^\pm, & z \le z_o \\ \varepsilon_L B_m^\pm f_m^\pm, & z \ge z_o \end{cases} \qquad (4.23)$$

and $f_m^\pm = \exp\{\pm\alpha_m(z-h_m)\}$, $\alpha_m^2 = \lambda^2+k_m^2$. Then starting with

$$A_o^+ = 1,\ A_o^-=0,\ B_L^+=0,\ B_L^-=1,\ C_o^+=1,\ C_o^-=0,\ D_L^+=0,\ D_L^-=1.$$

The boundary conditions (4.13) lead to the recurrence relations

$$\left.\begin{aligned} A_m^{\pm} &= \left(\frac{\sigma_{m-1}}{\sigma_m} \pm \frac{\alpha_{m-1}}{\alpha_m}\right) g_{m-1}^{+} A_{m-1}^{+} + \left(\frac{\sigma_{m-1}}{\sigma_m} \mp \frac{\alpha_{m-1}}{\alpha_m}\right) g_{m-1}^{-} A_{m-1}^{-} \\ C_m^{\pm} &= \left(1 \pm \frac{\alpha_{m-1}}{\alpha_m}\right) g_{m-1}^{+} C_{m-1}^{+} + \left(1 \mp \frac{\alpha_{m-1}}{\alpha_m}\right) g_{m-1}^{-} C_{m-1}^{-} \end{aligned}\right\} \quad m=1, \ldots, \mu$$

$$\left.\begin{aligned} B_m^{\pm} &= \left(\frac{\sigma_{m+1}}{\sigma_m} \pm \frac{\alpha_{m+1}}{\alpha_m}\right) g_m^{\mp} B_{m+1}^{+} + \left(\frac{\sigma_{m+1}}{\sigma_m} \mp \frac{\alpha_{m+1}}{\alpha_m}\right) g_m^{\mp} B_{m+1}^{-} \\ D_m^{\pm} &= \left(1 \pm \frac{\alpha_{m+1}}{\alpha_m}\right) g_m^{\mp} D_{m+1}^{+} + \left(1 \mp \frac{\alpha_{m+1}}{\alpha_m}\right) g_m^{\mp} D_{m+1}^{-} \end{aligned}\right\} \quad m=L-1, \ldots, \mu$$

where $g_m^{\pm} = \exp\{\pm\alpha_m (h_{m+1}-h_m)\}/\lambda$, $g_o^{\pm} = 1/2$ and μ is the layer of the source. In the case $\mu = L$ there is no recurrence required for the B and D terms. The free factors are determined in the usual way simply by comparing upwards and downwards travelling waves at $z = z_o$ taking the source terms (4.18) - (4.20) into account. Dropping the subscript μ on α_μ, k_μ^2, $A_\mu^{\pm}$, $B_\mu^{\pm}$, $C_\mu^{\pm}$, $D_\mu^{\pm}$, $f_\mu^{\pm}$ for conciseness, we obtain from (4.21) and (4.18)

$$\gamma_L B^{+} f^{+} - \frac{\lambda}{4\pi\alpha k^2} = \gamma_o A^{+} f^{+}, \qquad \gamma_o A^{-} f^{-} - \frac{\lambda}{4\pi\alpha k^2} = \gamma_L B^{-} f^{-},$$

whence

$$\gamma_o = -\frac{\lambda}{4\pi\alpha k^2} \frac{B^{+}f^{+} + B^{-}f^{-}}{A^{+}B^{-} - B^{+}A^{-}}, \qquad \gamma_L = -\frac{\lambda}{4\pi\alpha k^2} \frac{A^{+}f^{+} + A^{-}f^{-}}{A^{+}B^{-} - B^{+}A^{-}} \tag{4.24}$$

where $f^{\pm}$ means $f_\mu^{\pm}(z_o)$. From (4.22) and (4.20) follows

$$\delta_L D^{+} f^{+} + \frac{1}{4\pi\alpha_\mu} = \delta_o C^{+} f^{+}, \qquad \delta_o C^{-} f^{-} + \frac{1}{4\pi\alpha} = \delta_L D^{-} f^{-},$$

whence

$$\delta_o = \frac{1}{4\pi\alpha} \frac{D^{+}f^{+} + D^{-}f^{-}}{C^{+}D^{-} - D^{+}C^{-}}, \quad \delta_L = \frac{1}{4\pi\alpha} \frac{C^{+}f^{+} + C^{-}f^{-}}{C^{+}D^{-} - D^{+}C^{-}} \tag{4.25}$$

Because of (4.19) ϕ_x is discontinuous across $z = z_o$. Hence

$$\varepsilon_L B^+ f^+ + \frac{1}{4\pi k_\mu^2} = \varepsilon_o A^+ f^+, \qquad \varepsilon_o A^- f^- - \frac{1}{4\pi k_\mu^2} = \varepsilon_L B^- f^-$$

$$\text{or} \quad \varepsilon_o = -\frac{1}{4\pi k^2} \frac{B^+ f^+ - B^- f^-}{A^+ B^- - B^+ A^-}, \quad \varepsilon_L = -\frac{1}{4\pi k^2} \frac{A^+ f^+ - A^- f^-}{A^+ B^- - A^- B^+} \tag{4.26}$$

After having determined ϕ_z, ψ_x, ϕ_x, Green's tensor G is obtained from (4.12). Also required is the magnetic field in $z \leq 0$. Only the TE-part of a horizontal dipole contributes.
Let $\underline{F}_i\ (\underline{r}_o|\underline{r})$, $i = 1,2$ be the magnetic field at $\underline{r}$ due to a dipole in x_i-direction at $\underline{r}_o$. Then in $z \leq 0$

$$-i\omega\mu_o\, \underline{F}_i^o = \text{curl}^2\,(\hat{\underline{z}}\psi_i^o) = \text{grad}\,\frac{\partial \psi_i^o}{\partial z}\,. \tag{4.27}$$

Now the kernels for the integral equation (4.7) are determined and it remains to discuss how this equation is solved in practice. The simplest way certainly is to decompose the anomalous domain into a set of N rectangular cells and to assume that the electric field is constant within each cell. Then there results from (4.7) a set of 3N linear equations for 3N unknowns. The system has the form

$$\underline{x} = \underline{\underline{A}}\,\underline{x} + \underline{g}\,, \tag{4.28}$$

where $\underline{x}$ is the vector of unknown field components, $\underline{\underline{A}}$ the matrix of coefficients and $\underline{g}$ the given vector of the normal electric field values. A direct inversion of this matrix is only feasible for $N \leq 50$ (say), because of the large amount of storage required. Hence iterative methods must be used in general.
The simplest way would be to start an iterative procedure with $\underline{x}^o = \underline{g}$. This sequence of approximations, however, converges only if the eigenvalue of $\underline{\underline{A}}$ with the largest modulus has a modulus less than 1, a condition which is certainly not satisfied if σ_a is large.

Better convergence properties shows the Gauß-Seidel iterative scheme, using during iteration already the updated approximation and a successive overrelaxation factor:
Let the components of $\underline{\underline{A}}$ be a_{ik}. Then (4.28) reads

$$x_i = \sum_{k=1}^{3N} a_{ik} x_k + g_i, \quad i = 1, \ldots, 3N.$$

Then a new approximation to x_i is obtained by

$$x_i^{new} = x_i^{old} + \frac{\Omega}{1-a_{ii}} \{ \sum_{k=1}^{i-1} a_{ik} x_k^{new} + \sum_{k=i}^{3N} a_{ik} x_k^{old} - x_i^{old} + g_i \} \qquad (4.29)$$

The successive overrelaxation factor $\Omega \geq 1$ has to be chosen suitably. In many cases $\Omega = 1$ (i.e. no overrelaxation) is already a good choice. If the Gauß-Seidel method does not converge then one can apply a spectrum displacement technique: As already mentioned, simple iteration without updating is only convergent, if the largest modulus of the eigenvalues is smaller than 1. Eq. (4.28) is equivalent to

$$\underline{x} = (\underline{\underline{A}} - \alpha \underline{\underline{I}})\underline{x} + \alpha \underline{x} + \underline{g}$$

or

$$\underline{x} = \underline{\underline{B}}\underline{x} + \frac{1}{1-\alpha}\underline{g}\,, \qquad \underline{\underline{B}} = \frac{1}{1-\alpha}(\underline{\underline{A}} - \alpha \underline{\underline{I}}) \qquad (4.30)$$

The iterative procedure (4.30) will be convergent, if α can be chosen in such way that the eigenvalues of $\underline{\underline{B}}$ are of modulus less than 1. If λ is an eigenvalue of $\underline{\underline{A}}$ then $(\lambda-\alpha)/(1-\alpha)$ is an eigenvalue of $\underline{\underline{B}}$. Consider for example the following situation that $\underline{\underline{A}}$ has negative real eigenvalues from 0 to λ_{max}, $|\lambda_{max}| > 1$. Then a choice of $\alpha = -|\lambda_{max}|/2$ is appropriate. The condition

$$\frac{\lambda + |\lambda_{max}|/2}{1 + |\lambda_{max}|/2} < 1$$

is then satisfied for all eigenvalues λ. The requirements which α has satisfied can be put in that form that a circle around α has to include all eigenvalues of $\underline{\underline{A}}$ but has to exclude the point 1. The following figure illustrates the case stated above.

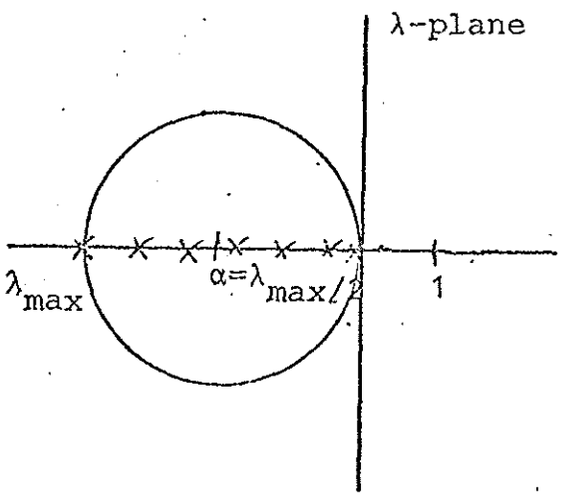

This case applies approximately to the three-dimensional modelli problem, where at least the largest eigenvalues are for a higher conducting insertion to a good approximation negative real. For a poor conducting insertion the largest eigenvalues are essentially positive, but smaller than 1.

4.3. The surface integral approach to the modelling problem

In the surface integral approach, within the anomalous slab the equation (4.4b), i.e.

$$\text{curl}^2 \underline{E}_a + k^2 \underline{E}_a = - k_a^2 \underline{E}_n \tag{4.31}$$

is solved by finite differences or an equivalent method. The required field values one grid point width above the upper horizontal boundary at $z = z_1$ and below the lower boundary at $z = z_L$ are expressed as surface integrals in terms of the tangential component of $\underline{E}_a$ at $z = z_1$ and z_2, respectively.
Let V_1 and V_2 be the half-spaces $z < z_1$ and $z > z_2$ respectively, and let S_m, $m = 1,2$ be the planes $z = z_m$. Let $\underline{G}_i^{(m)}(\underline{r}_o|\underline{r})$, $\underline{r}_o \in V_m$, $\underline{r} \in V_m \cup S_m$ be a solution of

$$\text{curl}^2 \underline{G}_i^{(m)}(\underline{r}_o|\underline{r}) + k_n^2(\underline{r}) \underline{G}_i^{(m)}(\underline{r}_o|\underline{r}) = \hat{\underline{x}}_i \, \delta(\underline{r}-\underline{r}_o) \tag{4.32}$$

$(i=1,2,3;\ m=1,2)$ satisfying for $\underline{r} \in S_m$ the boundary condition

$$\hat{\underline{z}} \times \underline{G}_i^{(m)}(\underline{r}_o|\underline{r}) = 0 \tag{4.33}$$

In V_1 and V_2, $\underline{E}_a$ is a solution of

$$\text{curl}^2 \underline{E}_a + k_n^2 \underline{E}_a = 0 \tag{4.34}$$

Multiply (4.34) by $\underline{G}_i^{(m)}$, (4.32) by $\underline{E}_a$, integrate the difference with respect to $\underline{r}$ over V_m, and obtain on using (4.6), (4.33) and $\underline{E}_a \to 0$ for $\underline{r} \to \infty$:

$$E_{ai}(\underline{r}_o) = (-1)^m \int_{S_m} \text{curl} \underline{G}_i^{(m)}(\underline{r}_o|\underline{r}) \cdot \{\hat{\underline{z}} \times \underline{E}_a(\underline{r})\} dA, \tag{4.35a}$$

$\underline{r}_o \in V_m$, or in tensor notation

$$\boxed{\underline{E}_a(\underline{r}_o) = (-1)^m \int_{S_m} \text{curl} \mathcal{G}^{(m)}(\underline{r}_o|\underline{r}) \cdot \{\hat{\underline{z}} \times \underline{E}_a(r)\} dA} \tag{4.35b}$$

where $\text{curl} \mathcal{G}^{(m)} = \sum_{i=1}^{3} \hat{\underline{x}}_i \, \text{curl} \underline{G}_i^{(m)}$.

Eqs. (4.35a,b) admit a representation of the field values outside the anomalous layer in terms of the boundary values of the continuous tangential component of $\underline{E}_a$.
A physical interpretation of Green's vector $\underline{G}_i^{(m)}$ subject to (4.33) is as follows: Reflect the normal conductivity structure for $z < z_1$ and $z > z_2$ at the planes $z = z_1$ and $z = z_2$ and place a unit dipole in x_i-direction at $\underline{r}_o \in V_m$ and an image dipole at $\underline{r}_o' = \underline{r}_o + 2(z_m - z_o)\hat{\underline{z}}$, the moment being the same for the vertical dipole and the opposite for the two horizontal dipoles. Then the tangential component of $\underline{G}_i^{(m)}$ vanishes at $z = z_m$, and $\underline{G}_i^{(m)}$ is a solution of (4.32) for $\underline{r} \in V_m$.
Hence, if V_m is a uniform half-space, $\underline{G}_i^{(m)}$ is constructed from the whole-space formula (4.15). Eq. (4.35) then reads:

$$E_{ax}(\underline{r}_o) = |z_o - z_m| \int_{S_m} F(R) E_{ax}(\underline{r}) dA, \tag{4.36a}$$

$$E_{ay}(\underline{r}_o) = |z_o - z_m| \int_{S_m} F(R) E_{ay}(\underline{r}) dA, \tag{4.36b}$$

$$E_{az}(\underline{r}_o) = (-1)^m \int_{S_m} F(R)\{(x-x_o)E_{ax}(\underline{r}) + (y-y_o)E_{ay}(\underline{r})\} dA, \tag{4.36c}$$

where $R = |\underline{r} - \underline{r}_o|$, $k^2 = i\omega\mu_o\sigma$

$$F(R) = -\frac{1}{2\pi R}\frac{d}{dR}(e^{-kR}/R) = (1 + kR)e^{-kR}/(2\pi R^3)$$

Eqs. (4.36a-c) contain as important subcase the condition at the air-earth interface ($m = 1$, $z_1 = 0$, $k_o = 0$).

Because of the limited range of the kernels, in applications of the surface integral only a small portion of S_m must be considered. For E_{ax} and E_{ay} the contribution of the region nearest to $\underline{r}_o$ is most important. Assuming E_{ax} and E_{ay} to be constant within a small disc of radius ρ centered perpendicularly over $\underline{r}_o$ the weight from (4.36a,b) is

$$e^{-k\lambda} - (\lambda/\sqrt{\lambda^2+\rho^2})\, e^{-k\sqrt{\lambda^2+\rho^2}},$$

where $\lambda = |z_m - z_o|$. There is a contribution to E_{az} only if E_{ax} and E_{ay} have a gradient along x and y direction respectively.

At the vertical boundaries the condition $\underline{E}_a = 0$ is relaxed to the impedance boundary condition

$$\underline{k E_{at}} = \underline{\hat{n}} \times \text{curl } \underline{E}_a, \quad \underline{\hat{n}} \cdot \underline{E}_a = 0,$$

where $\underline{E}_{at}$ is the tangential component and $\hat{n}$ the outward normal.

5. Conversion formulae for a two-dimensional TE-field

5.1. Separation formulae

In this subsection 5.1. it is assumed that the conductivity does not change in x-direction and that the inducing magnetic field is in the (y,z)-plane, i.e. the conditions for the E-polarization case of Sec. 3.1. Then from a knowledge of the H_y and H_z component along a profile from $-\infty$ to $+\infty$ at $z = o$ it is possible to separate the magnetic field into its parts of internal and external origin without having an additional knowledge of the underlying conductivity structure.

The pertinent differential equation is (3.5a), i.e.

$$\Delta \tilde{E} = i\omega\mu_o \sigma \tilde{E}, \tag{5.1}$$

which reducing in $z \leq 0$ to

$$\Delta \tilde{E} = 0, \tag{5.2}$$

which has the general solution

$$E(y,z) = \int_{-\infty}^{+\infty} \{A_o^-(\kappa) e^{-|\kappa| z} + A_o^+(\kappa) e^{+|\kappa| z}\} e^{i\kappa y} \, d\kappa \tag{5.3}$$

where A_o^- describes the external and A_o^+ the internal part of the fiel

The magnetic field components at $z = 0$ are (cf. (3.2a) and (3.3a)):

$$\frac{\partial \tilde{E}}{\partial z} = -i\omega\mu_o \tilde{H}_y = \int_{-\infty}^{+\infty} |\kappa| \{-A_o^- + A_o^+\} e^{i\kappa y} \, d\kappa \tag{5.4a}$$

$$\frac{\partial \tilde{E}}{\partial y} = +i\omega\mu_o \tilde{H}_z = \int_{-\infty}^{+\infty} i\kappa \{A_o^- + A_o^+\} e^{i\kappa y} \, d\kappa. \tag{5.4b}$$

Let

$$\tilde{H}_y = \tilde{H}_{ye} + \tilde{H}_{yi}, \quad \tilde{H}_z = \tilde{H}_{ze} + \tilde{H}_{zi}, \tag{5.5a,}$$

where the subscripts "e" and "i" denote the parts of external and internal origin at z = o.

Further, let the Fourier transform of any one of the above six quantities be

$$\hat{H}(\kappa) = \frac{1}{2\pi} \int_{-\infty}^{+\infty} \tilde{H}(y,o) e^{-i\kappa y}\, dy. \qquad (5.6)$$

Then (5.4a,b) yields

$$\hat{H}_{ye}/\hat{H}_{ze} = -i\,\mathrm{sgn}(\kappa), \quad \hat{H}_{yi}/\hat{H}_{zi} = +i\,\mathrm{sgn}(\kappa) \qquad (5.7a,b)$$

A product between Fourier transforms in the x-domain transforms to a convolution integral in the y-domain:

$$\hat{F} = \hat{G} \cdot \hat{H} \qquad F(y) = \frac{1}{2\pi} \int_{-\infty}^{+\infty} G(y')H(y-y')dy' = \frac{1}{2\pi}\, G * H$$

Hence we obtain from (5.7a,b)

$$\tilde{H}_{ye} = + K * \tilde{H}_{ze}, \qquad \tilde{H}_{yi} = -K * \tilde{H}_{zi} \qquad (5.8a,b)$$

$$\tilde{H}_{ze} = - K * \tilde{H}_{ye}, \qquad \tilde{H}_{zi} = +K * \tilde{H}_{yi} \qquad (5.8c,d)$$

Here,

$$\underline{K(y)} = \frac{1}{2\pi} \int_{-\infty}^{+\infty} -i\,\mathrm{sgn}(\kappa) e^{i\kappa y}\, d\kappa =$$

$$= \frac{1}{\pi} \int_{o}^{\infty} \sin(\kappa y) d\kappa$$

$$= \lim_{\varepsilon \to +o} \frac{1}{\pi} \int_{o}^{\infty} \sin(\kappa y) e^{-\varepsilon\kappa} d\kappa = \frac{1}{\pi} \lim_{\varepsilon \to +o} \frac{y}{y^2+\varepsilon^2} = \underline{\frac{1}{\pi y}}$$

Convergence was forced by a factor $e^{-\varepsilon\kappa}$. The resulting convolution integral exists only in the sense of a Cauchy principal value, i.e. (5.8a) for example reads explicitly

$$\tilde{H}_{ye}(y) = \int_{-\infty}^{+\infty} K(y-\eta)\tilde{H}_{ze}(\eta)d\eta$$

$$= \frac{1}{\pi} \oint_{-\infty}^{+\infty} \tilde{H}_{ze}(\eta) \frac{d\eta}{y-\eta} = \lim_{\varepsilon \to +o} \frac{1}{\pi} \left\{ \int_{-\infty}^{y-\varepsilon} + \int_{y+\varepsilon}^{\infty} \right\} \tilde{H}_{ze}(\eta)\, \frac{d\eta}{y-\eta}\,.$$

The four equations

$$\hat{H}_{ye} = i\,\mathrm{sgn}(\kappa)\,\hat{H}_{ze}\,, \qquad \hat{H}_{yi} = +\,i\mathrm{sign}(\kappa)\,\hat{H}_{zi}$$

$$\hat{H}_{y} = \hat{H}_{ye} + \hat{H}_{yi}\,, \qquad \hat{H}_{z} = \hat{H}_{ze} + \hat{H}_{zi}$$

can easily be solved for $\hat{H}_{ye}$, $\hat{H}_{ze}$, $\hat{H}_{yi}$, $\hat{H}_{zi}$.

When transformed into the y-domain it results

$$\tilde{H}_{ye} = \frac{1}{2}\,(\tilde{H}_{y} + k \ast \tilde{H}_{z})\,, \qquad \tilde{H}_{ze} = \frac{1}{2}(\tilde{H}_{z} - K \ast \tilde{H}_{y})$$

$$\tilde{H}_{yi} = \frac{1}{2}\,(\tilde{H}_{y} - K \ast \tilde{H}_{z})\,, \qquad \tilde{H}_{zi} = \frac{1}{2}(\tilde{H}_{z} + K \ast \tilde{H}_{y})$$

Two-dimensional separation formulae

For practical purpuses these separation formulae are not very convenient, since the kernel decays rather slowly requiring a long profile to determine the internal and external part at a given surface point.

5.2. Conversion formulae for the field components of a two-dimensional TE-field at the surface of a one-dimensional structure

For the separation of the magnetic field components no knowledge of the two-dimensional conductivity structure is required. However, the conductivity enters if it is attempted to deduce for instance the total vertical component of the magnetic field at the surface from the corresponding tangential component. If the conductivity structure is one-dimensional, the conversion between two components can be effected using a convolution integral, where the kernel is derived from the one-dimensional structure via the transfer function $C(\omega,|\kappa|)$. Sec. (2.5) yields

$$C(|\kappa|,\omega) = \frac{\hat{E}_{x}(o,\kappa,\omega)}{i\omega\mu_{o}\hat{H}_{y}(o,\kappa,\omega)} = \frac{\hat{H}_{z}(o,\kappa,\omega)}{i\kappa\hat{H}_{y}(o,\kappa,\omega)} = \frac{1}{|\kappa|}\cdot\frac{1 - S(|\kappa|,\omega)}{1 + S(|\kappa|,\omega)} \qquad (5.9a$$

where $S(|\kappa|,\omega)$ is the ratio between internal and external part of $\hat{H}_{y}$, i.e. $\hat{H}_{yi}/\hat{H}_{ye}$, in the frequency wavenumber domain.

From (5.9a-c) the various conversion formulas for the durface components can be derived. The following table gives the definition of

the pertinent kernels and their form for two particularly simple structures. Note that in the case of a vanishing conductor (i.e. in the examples $h \to \infty$, or $k \to 0$) the kernels K^- and M have to agree with the kernels of (5.8a) and (5.8c), respectively. The function L_2, occurring in the P-kernel of the uniform half-space model is the modified Struve function of the second order (cf. Abramowitz and Stegun, p. 498).

Conversion		Convolution kernels			
		Perfect conductor at depth h		Uniform half-space with $\sigma=\sigma_0$	
		$C = \tanh(\kappa h)/\kappa$		$C = (\kappa^2 + k^2)^{-1/2}$	
		Abbr.: $u = y/(2h)$		Abbr.: $k = (i\omega\mu_0\sigma_0)^{1/2}$, $V=k\lvert y\rvert$	
		Limiting values		Limiting values	
(κ,ω) domain	(y,ω) domain	$\lvert u\rvert<<1$	$\lvert u\rvert>>1$	$\lvert V\rvert<<1$	$\lvert V\rvert>>1$
$\hat{H}_y = \frac{1}{i\kappa C}\hat{H}_z$	$\tilde{H}_y = K^- \ast \tilde{H}_z$	$\{2h\ \tanh\pi u\}^{-1}$		$\frac{k}{\pi}\{\frac{\pi}{2} + \int_V^\infty K_1(w)w^{-1}dw\}\mathrm{sgn}(y)$	
		$1/(\pi y)$	$1/(2h)\,\mathrm{sgn}(y)$	$1/(\pi y)$	$(k/2)\,\mathrm{sgn}(y)$
$\hat{H}_z = i\kappa C\,\hat{H}_y$	$\tilde{H}_z = M \ast \tilde{H}_y$	$-(2h\ \sinh\pi u)^{-1}$		$-\frac{k}{\pi}K_1(V)\cdot\mathrm{sgn}(y)$	
		$-1/(\pi y)$	$-e^{-\pi\lvert u\rvert}/h\cdot\mathrm{sgn}(y)$	$-1/(\pi y)$	$-ke^{-V}/\sqrt{2\pi V}\cdot\mathrm{sgn}(y)$
$\hat{E}_x = i\omega\mu_0 C\hat{H}_y$	$\tilde{E}_x = i\omega\mu_0 N\ast\tilde{H}_y$	$\frac{1}{\pi}\log\coth(\pi\lvert u\rvert/2)$		$\frac{1}{\pi}K_0(V)$	
		$-\frac{1}{\pi}\log\lvert y\rvert$	$\frac{2}{\pi}e^{-\pi\lvert u\rvert}$	$-\frac{1}{\pi}\log\lvert y\rvert$	$e^{-V}/\sqrt{2\pi V}$
$\hat{H}_{yi} = S\,\hat{H}_{ye}$	$\tilde{H}_{yi} = P \ast \tilde{H}_{ye}$	$\{2\pi h(1+u^2)\}^{-1}$		$\frac{1}{\lvert y\rvert}\{L_2(V) - I_2(V) + \frac{2V}{3\pi}\}$	
		$1/(2\pi h)$	$2h/(\pi y^2)$	$2k/(3\pi)$	$2/(\pi k y^2)$
$\hat{E}_x = i\omega\mu_0(1+S)C\hat{H}_{ye}$	$\tilde{E}_x = i\omega\mu_0 Q\ast\tilde{H}_{ye}$	$\frac{1}{2\pi}\log(1+u^{-2})$		$\frac{2}{\pi V}\{\frac{1}{V} - K_1(V)\}$	
		$-\frac{1}{\pi}\log\lvert y\rvert$	$2h^2/(\pi y^2)$	$-\frac{1}{\pi}\log\lvert y\rvert$	$2/(\pi k^2 y^2)$
$\hat{H}_z = i\kappa(1+S)C\,\hat{H}_{ye}$	$\tilde{H}_z = R \ast \tilde{H}_{ye}$	$-\{\pi y(1+u^2)\}^{-1}$		$\frac{2}{\pi y}\{K_2(V) - \frac{2}{V^2}\}$	
		$-1/(\pi y)$	$-4h^2/(\pi y^3)$	$-1/(\pi y)$	$-4/(\pi k^2 y^3)$

6. Approaches to the inverse problem of electromagnetic induction by linearization

6.1. The Backus-Gilbert method

6.1.1. Introduction

The method of Backus and Gilbert is in the first line a method to estimate the information contents of a given data set; only in the second line it is a method to solve a linear inverse problem. The procedure takes into account that observational errors and incomplete data reduce the reliability of a solution of an inverse problem. It is strictly applicable only to linear inverse problems. Assume that we are going to investigate an "earth model" $m(r)$, where m is a scalar quantity which for simplicity depends only on one coordinate. For the following examples it will be chosen as the distance from the centre of the earth (to be as close as possible to the original approach of Backus and Gilbert). Then in a linear inverse problem there exist N linear functionals ("rules"), which ascribe to $m(r)$ via data kernels $G_i(r)$ numbers $g_i(m)$ in the way

$$g_i(m) = \int_0^a m(r)G_i(r)dr, \quad i = 1, \ldots, N. \tag{6.1}$$

The measured values of $g_i(m)$ are the N data γ_i, $i = 1, \ldots, N$. The "gross earth functionals" $g_i(m)$ are linear in m, since it is assumed that the data kernels $G_i(r)$ are independent of m. The inverse problem consists in choosing $m(r)$ in such a way that the calculated functionals g_i agree with the data γ_i. The Backus-Gilbert method shows how $m(r)$ is constraint by the given data set. Before going into details let us give an example. Assume that we are interested in the density distribution of spherically symmetrical earth, i.e. $m(r) = \rho(r)$, and that our data consist in the mass M and moment of inertia Θ. Then

$$\gamma_1 = M, \quad \gamma_2 = \Theta$$

$$g_1(\rho) = 4\pi \int_0^a \rho(r)r^2dr, \quad g_2(\rho) = \frac{8\pi}{3} \int_0^a \rho(r)r^4dr$$

$$G_1(r) = 4\pi r^2, \quad G_2(r) = \frac{8\pi}{3} r^4$$

6.1.2. The linear inverse problem

The data may have two defects:

a) insufficient

b) inaccurate

Certainly in the above problem the two data M and Θ are insufficient to determine the continuous function $\rho(r)$. Generally, the properties a) and b) are inherent to all real data sets when a continuous function is sought. The lack of data smoothes out details and only some average quantities are available, the observational error introduces statistical uncertainties in the model. (If we were looking for a descrete model with fewer parameters than data, then inconsistency can arise as a third defect.) Because of the lack of data, instead of m at r_o we can obtain only an averaged quantity $<m(r_o)>$, which is still subject to statistical incertainties due to errors in the data. Let

$$< m(r_o) > = \int_o^a A(r_o|r)m(r)dr, \tag{6.2}$$

where a is subject to

$$\int_o^a A(r_o|r)dr = 1 \tag{6.3}$$

The latter condition ensures that <m> agrees with m, if m is a constant. $A(r_o|r)$ is the window, through which the real but unknown function m(r) can be seen. It is the averaging or resolution functio
The more A at r_o resembles a δ-function the better is the resolution at r_o. Resolvable are only the projections of m(r) into the space of the data kernels G_i. The part of m, which is orthogonal to the data kernels cannot be resolved. Hence, it is reasonable to write A as a linear combination of the data kernels

$$A(r_o|r) = \sum_{i=1}^{N} a_i(r_o)G_i(r), \tag{6.4}$$

where the coefficients $a_i(r_o)$ have to be determined in such a way that A is as peaked as possible at r_o. The most obvious choice would be to minimize

$$\int_o^a \{A(r_o|r) - \delta(r - r_o)\}^2 dr, \tag{6.5}$$

subject to (6.3). For computational ease Backus and Gilbert prefer

to minimize the quantity

$$s = 12 \int_0^a A^2(r_o|r)(r-r_o)^2 dr. \tag{6.6}$$

Since $(r-r_o)^2$ is small near r_o, A can be large there. The factor 12 is chosen for the fact that if A is a box-car function of width L

$$A = \begin{cases} \frac{1}{L}, & |r-r_o| \leq L/2 \\ 0, & \text{else} \end{cases}$$

then s = L, i.e. if A is a peaked function then s in the definition of (6.6) gives approximately the width of the peak. $s(r_o)$ is called the spread at r_o.

We have also taken into account that our measurements γ_i have observational errors $\Delta\gamma_i$, i.e.

$$\gamma_i - \Delta\gamma_i \leq g_i(m) \leq \gamma_i + \Delta\gamma_i \tag{6.7}$$

Insertion of (6.4) into (6.2) using (6.1) yields

$$\langle m(r_o)\rangle = \sum_{i=1}^{N} a_i(r_o) \int_o^a m(r) G_i(r) dr = \sum_{i=1}^{N} a_i(r_o) g_i(m) \tag{6.8}$$

From (6.7) and (6.8)

$$\Delta\langle m(r_o)\rangle = \sum_{i=1}^{N} a_i(r_o)\Delta\gamma_i,$$

and the mean variance is

$$\varepsilon^2 = \overline{(\Delta\langle m(r_o)\rangle)^2} = \sum_{i,k=1}^{N} a_i(r_o) a_k(r_o) E_{ik} \tag{6.9}$$

where

$$E_{ik} = \overline{\Delta\gamma_i \, \Delta\gamma_k} \tag{6.10}$$

is the covariance matrix of the data errors, which in general is assumed to be diagonal.

Of course, we would appreciate if the error of $m(r_o)$, i.e. ε^2 would be very small. But also the spread (6.6)

$$s = 12 \int_o^a A^2(r_o|r)(r-r_o)^2 = \sum_{i,k=1}^{N} a_i(r_o) a_k(r_o) S_{ik}(r_o) \tag{6.11}$$

with

$$S_{ik}(r_o) = 12 \int_o^a G_i(r) G_k(r) (r-r_o)^2 dr \tag{6.12}$$

should be small. Hence it required to minimize simultaneously the quadratic forms

$$s = \sum_{i,k=1}^{N} a_i a_k S_{ik} , \qquad \varepsilon^2 = \sum_{i,k=1}^{N} a_i a_k E_{ik} \tag{6.13}$$

subject to the condition (6.3), i.e.

$$\sum_{i=1}^{N} a_i \int_o^a G_i(r)dr = 1 \tag{6.14}$$

There does not exist a set of a_i which minimizes s and ε^2 separately. As a compromise only a combination

$$Q = Ws + (1 - W) \cdot c\varepsilon^2 \tag{6.15}$$

can be minimized. In (6.15), c is an arbitrary positive scaling factor which accounts for the different dimensions of s and ε^2 and W is a parameter

$$0 \leq W \leq 1$$

which weighs the particular importance of s and ε^2. For W = 1 the spread is minimized without regarding the error of the spatially averaged quantity $\langle m(r_o)\rangle$. Conversely for W = 0 the spread s is large and the error ε^2 is a minimum. Hence, in general there is a trade-off between resolution and accuracy, which for a particular r_o is shown in the following figure.

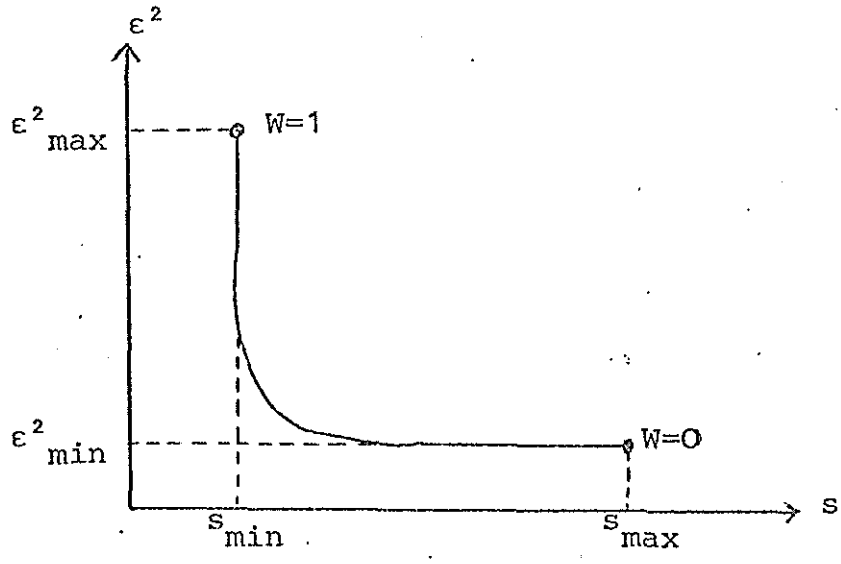

Near $s = s_{min}$ the trade-off curve is rather steep. Hence, a small sacrifice of resolving power will largely reduce the error of the average $\langle m(r_o)\rangle$. This uncertainty relation between resolution and accuracy is the central point of the Backus-Gilbert procedure.

It remains to show a way to minimize Q, subject to (6.15). The way, however, is well-known. One simply introduces as (N+1)-st unknown a Lagrangian parameter λ and minimizes the quantity

$$Q' = Q + \lambda(\Sigma a_i u_i - 1), \quad u_i = \int_o^a G_i(r)dr \tag{6.16}$$

The differentiation of (6.16) with respect to the (N+1) unknowns yields the (N+1) linear equations

$$2 \sum_{i=1}^{N} a_i Q_{ik} + \lambda u_k = 0, \quad k = 1, \ldots, N \tag{6.17a}$$

$$\sum_{i=1}^{N} a_i k_i = 1 \tag{6.17b}$$

where $Q_{ik} = W S_{ik} + (1-W)c E_{ik}$.
This system of equations is easily solved. The meaning of λ is revealed by multiplying (6.17a) by a_k, adding and using (6.17b) and (6.15). It results

$$\lambda = - 2 Q_{min}.$$

In the case W = 1, we have $\lambda = -2s$. With a knowledge of $a_i(r_o)$, $<m(r_o)>$ is obtained from (6.8) with $g_i = \gamma_i$ and ε^2 from (6.9). When $<m(r)>$ is inserted in (6.1) instead of m(r), it will in general not exactly reproduce the data.

The minimization (6.15)

$$Q=Ws+(1-W)c\varepsilon^2, \quad 0\leq W\leq 1, \quad c>0, \quad s = \sum_{k,i=1}^{N} a_i a_k S_{ik}, \quad \varepsilon^2 = \sum_{i,k=1}^{N} a_i a_k E_{ik}$$

subject to the constraint $\sum_{i=1}^{N} a_i u_i = 1$ admits for two data (N=2) a simple geometrical interpretation: For constant s and ε^2 these positive definite quantities are represented by ellipses, the constraint is a line in the (a_1, a_2)-plane. For uncorrelated errors, the principal axes of ε^2 are the a_1 and a_2 axis.

When W varies from 0 to 1 the combinations of (a_1, a_2) on the fat line are obtained. s and ε^2 are determined from the ellipses through these points. Since all s-(ε^2)-ellipses are similar, s and ε^2

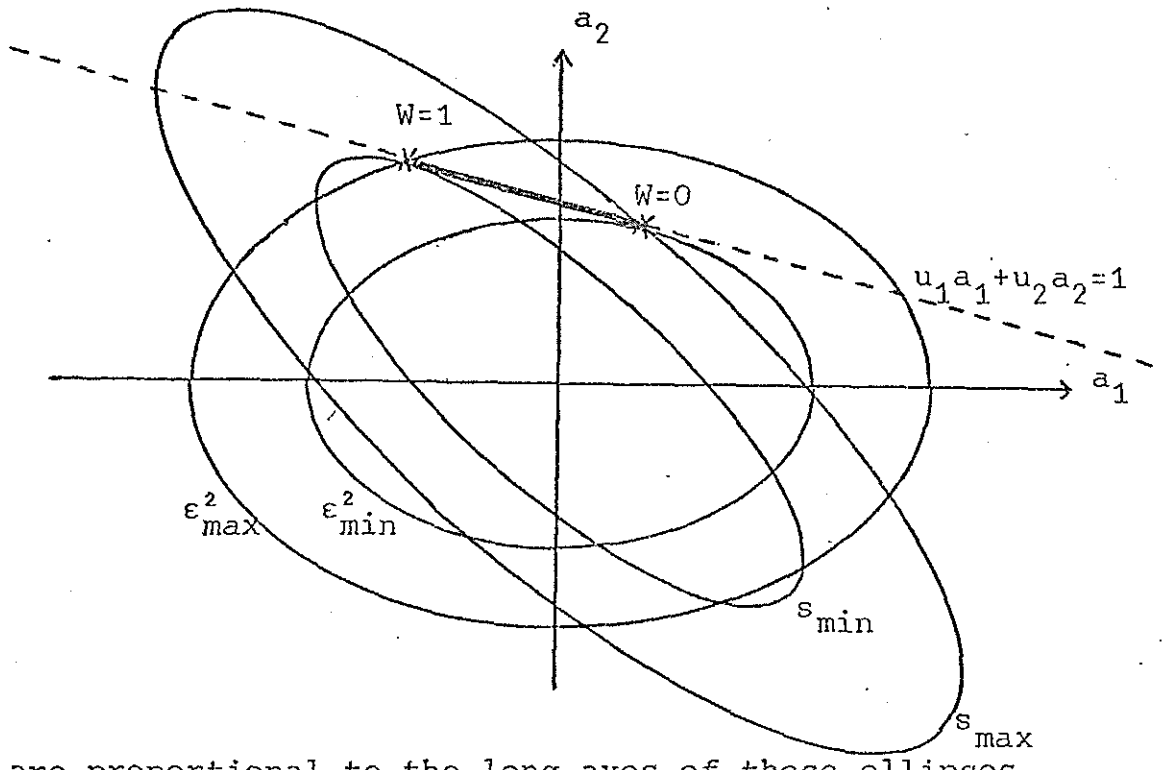

are proportional to the long axes of these ellipses.

6.1.3. The nonlinear inverse problem

The Backus-Gilbert procedure applies only to linear inverse problems, where according to

$$g_i(m) = \int_0^a m(r)G_i(r)dr \qquad (6.18)$$
$$= (6.1\ )$$

the gross earth functionals g_i have the property that

$$g_i(m+m') = g_i(m) + g_i(m'),\ g_i(\lambda m) = \lambda g_i(m).$$

This means for instance that the data are built up in an additive way from different parts of the model, i.e., that there is no coupling between these parts. This certainly does not hold for electromagnetic inverse problem, where each part of the conductor is coupled with all other parts.

In nonlinear problems the data kernel $G_i(r)$ will depend on m. Here it is in general possible to replace (6.18) by

$$g_i(m') - g_i(m) = \int_0^a (m'(r)-m(r))G_i(r,m)dr + O(m'-m)^2, \qquad (6.18a)$$

where m and m' are two earth models. The data kernel $G_i(r,m)$ is called the Frêchet derivative or functional derivative at model m.

Again, from a finite erroneous data set we can extract only averaged estimates with statistical uncertainties, i.e.

$$\langle m(r_o)\rangle = \int_o^a A(r_o|r)m(r)dr. \qquad (6.19) = (6.2)$$

As in the linear case $A(r_o|r)$ is built up from a linear combination of the data kernels

$$A(r_o|r) = \sum_{i=1}^{N} a_i(r_o,m)G_i(r_o,m). \qquad (6.20)$$

Introducing (6.19) into (6.20) we obtain

$$\langle m(r_o)\rangle = \sum_{i=1}^{N} a_i(r_o,m)q_i(m),\ q_i(m) = \int_o^a m(r)G_i(r,m)dr \qquad (6.21)$$

which for nonlinear kernels is different from (6.8), since in this nonlinear case $g_i(m) \neq q_i(m)$.

In the linear case, two models m and m' which both satisfy the data lead to the same average model $\langle m(r_o)\rangle$. In the nonlinear case, the average models are different; the difference, however, is of the second order in (m'-m). (Exercise!)

The Backus-Gilbert procedure in the nonlinear case requires a model which already nearly fits the data. Then it can give an appraisal of the information contents of a given data set.

6.2. Generalized matrix inversion

The generalized matrix inversion is an alternative procedure to the Backus-Gilbert method. It is strictly applicable only to linear problems, where the model under consideration consists of a set of discrete unknown parameters. Nonlinear problems are generally linearized to get in the range of this method. Assume that we want to determine the M component parameter vector $\underline{p}$ with $\underline{p}^T = (p_1,\ldots,p_M)$ and that we have N functionals (rules) g_i, $i = 1, \ldots, N$ which assign to any model $\underline{p}$ a number, which when measured has the average value γ_i and variance $\mathrm{var}(\gamma_i)$:

$$\gamma_i = g_i(\underline{p}),\quad i = 1,2, \ldots, N.$$

Suppose that an approximation $\underline{p}_o$ to $\underline{p}$ is known. Then neglecting terms of order $O(\underline{p} - \underline{p}_o)^2$, we have

$$g_i(\underline{p}_o) + (\underline{p} - \underline{p}_o) \cdot \mathrm{grad}_p\, g_i = \gamma_i$$

or

$$\sum_{k=1}^{M} \frac{\partial g_i}{\partial p_k} (p_k - p_{ko}) = \gamma_i - g_i(\underline{p}_o), \quad i = 1,2, \ldots, N \tag{6.22}$$

Eq. (6.22) constitutes a system of N equations for the M parameter changes $p_k - p_{ko}$. The generalized matrix inversion provides a solution to this system, irrespective of N = M, N < M, or N > M. If the rank of the system matrix $\partial g_i/\partial p_k$ is equal to Min (M, N), the generalized matrix inversion provides in the case M = N (regular system): the ordinary solution, M < N (overconstrained system): the least squares solution, M > N (underdetermined system): the smallest correction vector $\underline{p} - \underline{p}_o$.

The generalized inverse exists also in the case when the rank of $\partial g_i/\partial p_k$ is smaller than Min(M, N).
After solving the system, the correction is applied to $\underline{p}_o$ and this vector in the next step serves as a new approximation to $\underline{p}$, thus starting an iterative scheme.

It is convenient to give all data the same variance σ_o^2, thus defining as new data and matrix elements

$$y_i = \frac{\gamma_i - g_i(p_o)}{\sqrt{\mathrm{var}(\gamma_i)}} \cdot \sigma_o, \qquad G_{ik} = \frac{\partial g_i}{\partial p_k} \cdot \frac{\sigma_o}{\sqrt{\mathrm{var}(\gamma_i)}} \tag{6.23a,b}$$

thus weighing in a least squares solution the residuals according to their accuracy which makes sense. Let

$$\underline{x} = \underline{p} - \underline{p}_o \tag{6.24}$$

be the parameter correction vector. Then (6.22) reads

$$\underline{\underline{G}}\, \underline{x} = \underline{y}. \tag{6.25}$$

($\underline{\underline{G}}$ corresponds to the data kernels $G_i(r)$ in the Backus-Gilbert theory). In the generalized matrix inversion first $\underline{\underline{G}}$ is decomposed into data eigenvectors $\underline{u}_j$ and parameter eigenvectors $\underline{v}_j$:

$$\underline{\underline{G}} = \underline{\underline{U}}\, \underline{\underline{\Lambda}}\, \underline{\underline{V}}^T \tag{6.26}$$

Dimensions: $\underline{\underline{G}}(N,M)$, $\underline{\underline{U}}(N,P)$, $\underline{\underline{\Lambda}}(P,P)$, $\underline{\underline{V}}(M,P)$

Here $\underline{\underline{U}}$ is a N x P matrix containing the P eigenvectors belonging to non-zero eigenvalues of the problem

$$\underline{\underline{G}}\,\underline{\underline{G}}^T\,\underline{u}_j = \lambda_j^2\,\underline{u}_j,\quad j = 1, \ldots, N \tag{6.27}$$

and $\underline{\underline{V}}$ is a M x P matrix with the P eigenvectors of the problem

$$\underline{\underline{G}}^T\underline{\underline{G}}\,\underline{v}_j = \lambda_j^2\,\underline{v}_j,\quad j = 1, \ldots, M \tag{6.28}$$

associated with non-zero eigenvalues. P is the rank of $\underline{\underline{G}}$. Finally $\underline{\underline{\Lambda}}$ is a P x P diagonal matrix containing just the P nonzero eigenvalues λ_j. Then the generalized inverse of $\underline{\underline{G}}$ is

$$\underline{\underline{H}} = \underline{\underline{V}}\,\underline{\underline{\Lambda}}\,\underline{\underline{U}}^T. \tag{6.29}$$

$\underline{\underline{H}}$ always exists. In the cases mentioned above, $\underline{\underline{H}}$ specializes as follows

$$M = N = P:\ \underline{\underline{H}} = \underline{\underline{G}}^{-1}$$

$$P = M \leq N:\ \underline{\underline{H}} = (\underline{\underline{G}}^T\underline{\underline{G}})^{-1}\underline{\underline{G}}^T$$

$$P = N \leq M:\ \underline{\underline{H}} = \underline{\underline{G}}^T(\underline{\underline{G}}\,\underline{\underline{G}}^T)^{-1}$$

For the proof one has to take into account that because of the orthogonality and normalization of the eigenvectors one always has

$$\underline{\underline{V}}^T\underline{\underline{V}} = \underline{\underline{I}}_P \quad (=\text{P-component unit matrix}) \tag{6.30a}$$

$$\underline{\underline{U}}^T\underline{\underline{U}} = \underline{\underline{I}}_P \tag{6.30b}$$

and in addition for

$$P = M:\ \underline{\underline{V}}^T\underline{\underline{V}} = \underline{\underline{I}}_M = \underline{\underline{V}}\,\underline{\underline{V}}^T \tag{6.31a}$$

$$P = N:\ \underline{\underline{U}}^T\underline{\underline{U}} = \underline{\underline{I}}_N = \underline{\underline{U}}\,\underline{\underline{U}}^T \tag{6.31b}$$

For $P < \mathrm{Min}(M,N)$ $\underline{\underline{H}}$ cannot be expressed in terms of $\underline{\underline{G}}$.

The generalized inverse provides a solution vector

$$\langle \underline{x} \rangle = \underline{\underline{H}}\,\underline{y}\ . \tag{6.32}$$

Its relation to the true solution $\underline{x}$ is given by

$$\langle \underline{x} \rangle = \underline{\underline{A}}\,\underline{x}\ ,$$

where $\underline{\underline{A}}$ is the (M x M) resolution matrix

$$\underline{\underline{A}} = \underline{\underline{H}}\,\underline{\underline{G}} = \underline{\underline{V}}\,\underline{\underline{\Lambda}}^{-1}\,\underline{\underline{U}}^T\,\underline{\underline{U}}\,\underline{\underline{\Lambda}}\,\underline{\underline{V}}^T = \underline{\underline{V}}\,\underline{\underline{V}}^T. \tag{6.33}$$

Only for P = M, $\underline{\underline{A}}$ is the M component unit matrix, admitting an exact determination of $\underline{x}$. ($\underline{\underline{A}}$ corresponds approximately to the resolution function $A(r_o|r)$ in the Backus-Gilbert theory. But there are differences: $\underline{\underline{A}}$ is symmetrical, $A(r_o|r)$ not, the norm of $\underline{\underline{A}}$ is small if the resolution is poor, the norm of $A(r_o|r)$ is always 1.)

In generalized matrix inversion exists the same trade-off as in the Backus-Gilbert method. Consider the covariance matrix of the changes of $< \underline{x} >$ due to random changes of $\underline{y}$:

$$\overline{(\Delta <\underline{x}>)(\Delta <x>)^T} = \underline{\underline{V}}\underline{\underline{\Lambda}}^{-1}\underline{\underline{U}}^T \underbrace{\overline{(\Delta \underline{y})(\Delta \underline{y})^T}}_{\sigma_o^2} \underline{\underline{U}}\underline{\underline{\Lambda}}^{-1}\underline{\underline{V}}^T = \sigma_o^2 \, \underline{\underline{V}}\underline{\underline{\Lambda}}^{-2}\underline{\underline{V}}^T. \qquad (6.34)$$

In particular the variance of $<x_k>$ is

$$\mathrm{var}(x_k) = \sigma_o^2 \sum_{j=1}^{P} \left(\frac{V_{kj}}{\lambda_j}\right)^2, \qquad k = 1,2, \ldots, M \qquad (6.35)$$

showing that the variance of x_k is largely due to the small eigenvalues λ_j. By discarding small eigenvalues and the corresponding eigenvectors, the accuracy of x_k can be increased at the expense of the resolution, since $\underline{\underline{A}}$ will deviate more from a (M x M) unit matrix if instead of the required M eigenvectors a smaller number is used. -

The model <x> will in general not reproduce the data. The reproduced data are

$$<\underline{y}> = \underline{\underline{G}} <\underline{x}> = \underline{\underline{G}}\,\underline{\underline{H}}\,\underline{y} = \underline{\underline{B}}\,\underline{y}$$

with the information density matrix

$$\underline{\underline{B}} = \underline{\underline{G}}\,\underline{\underline{H}} = \underline{\underline{U}}\,\underline{\underline{U}}^T. \qquad (6.36)$$

Only in the case N = P, $\underline{\underline{B}}$ is a unit matrix. In particular, $\underline{\underline{B}}$ describes the linear dependence of the data in the overconstrained case. High diagonal values will show that this date contains specific information on the model which is not contained in other data. On the other hand a large off-diagonal value shows that this information is also contained in another data.

Valuable insight in the particular inverse problem can be obtained by considering the parameter eigenvectors corresponding to high and

small eigenvalues. The parameter vector of a high eigenvalue shows the parameter combination which can be resolved well, the parameter eigenvector of a small eigenvalue gives the combination of parameters for which only a poor resolution can be obtained.

The generalized inverse is used both to invert a given data set and to estimate the information contents of this data set when the final solution is reached.
During the inversion procedure one has two tools to stabilize the notable unstable process of linearization:

a) application of only a fraction of the computed parameter correction, leading to a trade-off between convergence rate and stability;
b) decrease of number of eigenvalues taken into account.

In the final estimation of the data contents one might prescribe for each parameter a maximum variance. Then one has to determine from (6.35) the number of eigenvalues leading to a value nearest to the prescribed one. Finally the row of the resolution matrix for this particular parameter is calculated.

6.3. Derivation of the kernels for the linearized inverse problem of electromagnetic induction

6.3.1. The one-dimensional case

Both for the Backus-Gilbert procedure and for the generalized linear inversion a knowledge of the change of the data due to a small change in the conductivity structure is required.
In the one-dimensional case the pertinent differential equation and datum are

$$f''(z,\omega) = \{\kappa^2 + i\omega\mu_o\sigma(z)\}f(z,\omega),$$

$$C(\omega) = -f(o,\omega)/f'(o,\omega).$$

Consider two conductivity profiles σ_1 and σ_2 with corresponding fields f_1 and f_2. Multiplying the equation for f_1 with f_2 and the equation for f_2 with f_1, subtracting the resulting equations and integrating the difference over z from zero to infinity, we obtain

$$\int_o^\infty (f_1''f_2 - f_2''f_1)dz = i\omega\mu_o \int_o^\infty (\sigma_1-\sigma_2) f_1 f_2 \, dz \qquad (6.37)$$

Now

$$\int_0^\infty (f_1''f_2 - f_2''f_1)dz = \int_0^\infty \{(f_1'f_2)' - (f_2'f_1)'\}dz = -f_1'(o)f_2(o) + f_2'(o)f_1(o).$$

Division by $f_1'(o)\cdot f_2'(o)$ yields

$$C_2(\omega) - C_1(\omega) = -i\omega\mu_o \int_0^\infty \{\sigma_2(z) - \sigma_1(z)\} \frac{f_1(z,\omega)}{f_1'(o,\omega)} \cdot \frac{f_2(z,\omega)}{f_2'(o,\omega)} dz .$$

If the difference $\delta\sigma = \sigma_2 - \sigma_1$ is small, f_2 in the integral may be replaced by f_1, since the difference $f_2 - f_1$ is of the order of $\delta\sigma = \sigma_2 - \sigma_1$, leading to a second order term in $\delta C = C_2 - C_1$. Hence to a first order in $\delta\sigma$

$$\boxed{\delta C(\omega) = -i\omega\mu_o \int_0^\infty \delta\sigma(z) \{\frac{f(z,\omega)}{f'(o,\omega)}\}^2 dz} \qquad (6.38)$$

Therefore in the Backus-Gilbert procedure the Fréchet derivative of C is $-i\omega\mu_o\{f(z)/f'(o)\}^2$. In the generalized inversion the derivatives of C with respect to layer conductivities and layer thicknesses is required, if a structure with uniform layers is assumed. Let there be L layers with conductivity σ_m and thickness d_m in the m-th layer, $h_m \leq z \leq h_{m+1}$ ($h_{L+1} = \infty$). Then (6.38) yields

$$\frac{\partial C(\omega)}{\partial \sigma_m} = -i\omega\mu_o \int_{h_m}^{h_{m+1}} \{\frac{f(z,\omega)}{f'(o,\omega)}\}^2 dz, \quad m = 1,\ldots, L \qquad (6.39a)$$

$$\frac{\partial C(\omega)}{\partial d_m} = -i\omega\mu_o \sum_{k=m}^{L-1} (\sigma_{k+1} - \sigma_k) \{\frac{f(h_{k+1},\omega)}{f'(o,\omega)}\}^2, \quad m = 1,\ldots,L-1 \quad (6.3$$

since in the last case all layers below the m-th layer are displaced too.

6.3.2. Partial derivatives in two- and three-dimensions

For two-dimensions only the E-polarization case is considered. The pertinent equation is (cf. (3.5a))

$$\Delta E = i\omega\mu_o\sigma E .$$

Consider again two conductivity structures σ_1 and σ_2.

Then $$\Delta(E_2 - E_1) = i\omega\mu_o\sigma_1(E_2-E_1) + i\omega\mu_o(\sigma_2-\sigma_1)E_2 \qquad (6.40)$$

Let $G_1(\underline{r}'|\underline{r})$ be Green's function for σ_1, i.e.

$$\Delta G_1(\underline{r}'|\underline{r}) = i\omega\mu_o\sigma_1(\underline{r})G_1(\underline{r}'|\underline{r}) - \delta(\underline{r} - \underline{r}'). \qquad (6.41)$$

Multiply (6.41) by $E_2(\underline{r}') - E_1(\underline{r}')$ and (6.40) by $G_1(\underline{r}'|\underline{r})$, integrate the difference with respect to $\underline{r}'$ over the whole (y,z)-plane. Then Green's theorem (3.29) yields

$$E_2(\underline{r})-E_1(\underline{r}) = -i\omega\mu_o \int \{\sigma_2(\underline{r}')-\sigma_1(\underline{r}')\}E_2(\underline{r}')G_1(\underline{r}'|\underline{r})dA'. \qquad (6.42)$$

With the same arguments as in the one-dimensional case we obtain for small conductivity changes, neglecting second order terms,

$$\boxed{\delta E(\underline{r}) = -i\omega\mu_o \int \delta\sigma(\underline{r}')E(\underline{r}')G(\underline{r}'|\underline{r})dA'} \qquad (6.43)$$

The kernel $G(\underline{r}'|\underline{r})$ must be determined from the solution of the integral equation

$$\boxed{G(\underline{r}'|\underline{r}) = G_n(\underline{r}'|\underline{r})-i\omega\mu_o \int \sigma_a(\underline{r}")G_n(\underline{r}'|\underline{r}")G(\underline{r}"|\underline{r})dA"} \qquad (6.44)$$

Eq. (6.44) results from (6.42) by replacing

$\underline{r}'\to\underline{r}"$, $\sigma_2\to\sigma$, $\sigma_1\to\sigma_n$, $E_2(\underline{r})\to G(\underline{r}'|\underline{r})$, $E_1(\underline{r})\to G_n(\underline{r}'|\underline{r})$,

This substitution becomes possible, since the δ-function in the Green's function equations drops out when the difference $\Delta(E_2-E_1)$ is formed.

The changes of the magnetic field components are obtained from (6.43 and (6.44) by differentiation with respect to $\underline{r}$. - Methods for the computation of $G_n(\underline{r}'|\underline{r})$ are given in Sec. 3.4.

In the three-dimensional case one obtains in analogy to (6.43) and (6.44)

$$\delta\underline{E}(\underline{r}) = i\omega\mu_o \int \delta\sigma(\underline{r}')\ \underline{E}(\underline{r}')\cdot\mathcal{G}(\underline{r}'|\underline{r})d\tau \qquad (6.45)$$

where $\mathcal{G}$ is competed by solving the tensor integral equation

$$\mathcal{G}(\underline{r}'|\underline{r})=\mathcal{G}_n(\underline{r}'|\underline{r}) - i\omega\mu_o \int \sigma_a(\underline{r}")\mathcal{G}_n(\underline{r}'|\underline{r}")\cdot\mathcal{G}(\underline{r}"|\underline{r})dA". \qquad (6.46)$$

Again the magnetic field kernels are obtained by taking the curl of (6.45) and (6.46) with respect to $\underline{r}$. Methods for calculating $\mathcal{G}_n$ are given in Sec. 4.2. At the moment, three-dimensional inversion appears to be prohibitive!

6.4. Quasi-linearization of the one-dimensional inverse problem of electromagnetic induction (Schmucker's PSI-algorithm)

In the one-dimensional problem it is possible to a certain extent to linearize the inverse problem by introducing new suitable parameters and data instead of the old ones.

Assume a horizontally layered half-space with L layers having conductivities $\sigma_1, \sigma_2, \ldots \sigma_L$ and thicknesses $d_1, d_2, \ldots, d_{L-1}$ ($d_M = \infty$). Let the upper edge of layer m be at $z = h_m$ and assume that layer conductivities and thicknesses satisfy the condition

$$\sqrt{\sigma_m}\, d_m = \text{const.}, \quad m = 1,2, \ldots, L-1. \tag{6.47}$$

Let $k_m = \sqrt{i\omega\mu_o\sigma_m}$. Then the pertinent equation for a quasi-uniform external field is

$$f_m''(z) = k_m^2 f_m(z), \quad h_m \leq z \leq h_{m+1}.$$

The transfer function is, as usual,

$$C(\omega) = - f_1(o)/f_1'(o) .$$

Introduce instead of f_m the new function

$$\psi_m(z) = 2\log\{-k_m f_m(z)/f_m'(z)\}, \quad h_m \leq z \leq h_{m+1} \tag{6.48}$$

In the TE-case f and f' are continuous across boundaries, i.e.

$$f_m(h_{m+1}) = f_{m+1}(h_{m+1}), \quad f_m'(h_{m+1}) = f_{m+1}'(h_{m+1}) \tag{6.49}$$

As a consequence of (6.48) and (6.49) ψ is discontinuous across boundaries:

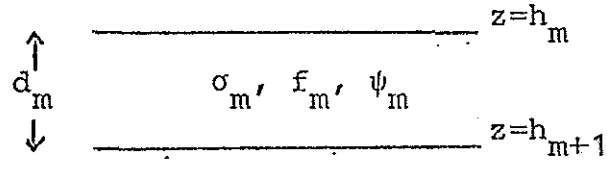

$$\psi_{m+1}(h_{m+1}) - \psi_m(h_{m+1}) = \log(\sigma_{m+1}/\sigma_m) . \tag{6.50}$$

The variation of f_m in the m-th layer is

$$f_m(z) = A_m^- e^{-k_m(z-h_m)} + A_m^+ e^{+k_m(z-h_m)},$$

whence

$$\frac{\psi_m(h_m)}{\psi_m(h_{m+1})} = \frac{\log\left(\dfrac{1 + A_m^+/A_m^-}{1 - A_m^+/A_m^-}\right)}{\log\left(\dfrac{1+(A_m^+/A_m^-)e^{2k_m d_m}}{1-(A_m^+/A_m^-)e^{-2k_m d_m}}\right)} = \frac{\log\left(\frac{1+a\gamma}{1-a\gamma}\right)}{\log\left(\frac{1+a}{1-a}\right)}, \qquad (6.51)$$

where $a = (A_m^+/A_m^-)e^{2k_m d_m}$, $\gamma = e^{-2k_m d_m}$.

Because of the condition (6.47), γ is independent of m.

The quantity $|a|$ is the ratio between the reflected and incident wave at $z = h_{m+1}$. Due to the conservation of energy the amplitude of the reflected wave is never larger than the amplitude of the incident wave. Hence,

$$|a| \leq 1 .$$

Equality applies to a perfect conductor or insulator. For $|a| << 1$ (6.51) yields

$$\frac{\psi_m(h_m)}{\psi_m(h_{m+1})} = \frac{2a\gamma(1+\frac{1}{3}a^2\gamma^2+\ldots)}{2a(1+\frac{1}{3}a^2+\ldots)} = \gamma\{1 + O(a^2)\},$$

or approximately

$$\underline{\psi_m(h_m) = \gamma\,\psi_m(h_{m+1})} \qquad (6.52)$$

Since the neglected term is of order a^2, this is a good approximation for $|a| << 1$. Eqs. (6.50) and (6.52) combined yield

$$\underline{\psi_m(h_m) = \gamma\{\psi_{m+1}(h_{m+1}) + \log(\sigma_m/\sigma_{m+1})\}} . \qquad (6.53)$$

The datum $C(\omega)$ is connected with $\psi_1(h_1,\omega)$ through

$$\psi_1(h_1,\omega) = \psi_1(o,\omega) = 2\log(k_1 C).$$

Introducing the new transfer function

$$\underline{y(\omega) = 2 \log\{\sqrt{i\omega\mu_o\sigma_o}\, C(\omega)\}} \tag{6.54}$$

where σ_o is an arbitrary reference conductivity, we obtain by continued application of (6.53)

$$y(\omega) = \log \frac{\sigma_o}{\sigma_1} + \psi_1(h_1) =$$

$$= \log \frac{\sigma_o}{\sigma_1} + \gamma \log \frac{\sigma_1}{\sigma_2} + \gamma\, \psi_2(h_2)$$

$$= \log \frac{\sigma_o}{\sigma_1} + \gamma \log \frac{\sigma_1}{\sigma_2} + \gamma^2 \log \frac{\sigma_2}{\sigma_3} + \gamma^2\, \psi_3(h_3)$$

$$= \sum_{m=o}^{L-1} \gamma^m \log \frac{\sigma_m}{\sigma_{m+1}}$$

$$\boxed{y(\omega) = (\gamma-1) \sum_{m=1}^{L-1} \gamma^{m-1} \log \frac{\sigma_m}{\sigma_o} - \gamma^{L-1} \log \frac{\sigma_L}{\sigma_o}} \tag{6.55}$$

In the derivation of (6.55) it has been used that $\psi_L(h_L) = 0$. Eq. (6.55) is the desired result: it expresses the new data $y(\omega)$ linearly in terms of the new model parameter $\log(\sigma/\sigma_o)$.

When (6.55) is used for the solution of an inverse problem, one chooses first an arbitrary σ_o, and prescribes the constants $\sqrt{\sigma_m/\sigma_o}\, d_m$ and L. If the occurring conductivity contrasts are not too sharp, the inversion of (6.55) will already give good estimates for the layer conductivities. For these estimates the correct response values are calculated, and with the difference between the data and these values the inversion of (6.55) is repeated, giving corrections $\Delta\log(\sigma_m/\sigma_o)$ to the previous outcome. At the end of the iteration procedure, the true thicknesses of the layers are calculated using (6.47). The errors of σ_m are finally transformed into the errors of d_m.

7. Basic concepts of geomagnetic and magnetotelluric depth sounding

7.1. General characteristics of the method

Two types of geophysical surface data can be distinguished to investigate the distribution of some physical property $m(\underline{r})$ of matter beneath the Earth's surface. The first type is connected with

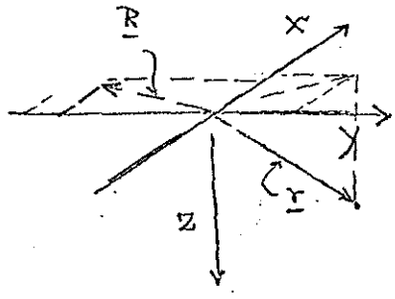

$\underline{r} = (x,y,z)$
$\underline{R} = (x,y,z = 0)$

static or quasi-static phenomena (gravity and magnetic fields), the second type with time-dependent phenomena (seismic wave propagation) or with controlled experiments under variable experimental conditions (DC-geoelectric soundings). Geomagnetic and magnetotelluric soundings utilize the skin-effect of transient electromagnetic fields. Their penetration into the Earth represents a time-dependent diffusion process, thus the observation of these fields at the surface produces data of the second type.

The interpretation of static data $y = y(\underline{R})$ is non-unique and an arbitrary choice can be made among an unlimited number of possible distributions $m(\underline{r})$, explaining $y(\underline{R})$ equally well. The interpretation of transient data is with certain constraints unique in the sense that only <u>one</u> distribution $m(\underline{r})$ can explain the surface data $y = y(R,t)$, basically because one additional variable t (time, variable parameter of controlled experiment) is involved.
If the observation of the transient process or the performance of the experiment is made at a single site, the data $y = y(t)$ permit a <u>vertical sounding</u> of the property $m = m(z)$, assumed to be a sole function of depth z beneath that site. If the observations or ex-

periments are done with profiles or arrays, the data $y = y(\underline{R},t)$ permit a structural sounding of the property $m = \bar{m}(z) + \Delta m(\underline{r})$ with particular emphasis on lateral variations $\Delta m(\underline{r})$.

Here $\bar{m}(z)$ represents either a global or regional mean distribution. It may also be the result of vertical soundings at "normal sites" where the surface data show no indications for lateral variations of m. Since the dependence of $y(\underline{R},t)$ on $m(\underline{r})$ will be non-linear, anomalies $\Delta y(\underline{R},t) = y(R,t) - y_n(t)$ will be dependent on Δm and $\bar{m}(z)$, i.e. the interpretation of second-type-data must proceed on the basis of a known mean or normal distribution $\bar{m}(z)$ consistent with data $y_n(t)$ at a normal site. It should be noted that in the case of static data of the first type usually no interdependence between Δy and $\bar{m}$ will exist, i.e. the interpretation of their anomalies is independent of global or regional mean distributions of the relevant property m.

Suppose that for data of the second type the lateral variations $\Delta m(\underline{r})$ are small in relation to $\bar{m}(z)$. Then the results of vertical soundings at many different single sites may be combined to approximate a structural distribution $m = \bar{m} + \Delta m$. For geomagnetic induction data the relevant property, namely the electrical resistivity has usually substantial lateral variations and a one-dimensional interpretation as in the case of vertical soundings will not be adequate. Instead a truly multi-dimensional interpretation of the data is required which is to be based on "normal data" at selected sites (cf. 8.2). Such normal sites are here rather the exception than the rule.

7.2 The data and physical properties of internal matter which are involved

The Earth's magnetic field is subject to small fluctuations $\underline{H}(r,t)$. They arise from primary sources in the high atmosphere and from secondary sources within the Earth. At the Earth's surface their *

* amplitude is

orders of magnitude smaller than the quasi-static main field. Their depth of penetration into the Earth is limited by the "skin-effect", i.e. by the opposing action of electromagnetically induced eddy currents in conducting matter below the surface . These currents produce the already mentioned secondary component of $\underline{H}$. They are driven by the electric field $\underline{E}(r,t)$ generated by the changing magnetic flux according to Farad y's induction law (cf. 7.3). The time-fluctuations in $\underline{H}$ are referred to "geomagnetic" variations, those in $\underline{E}$ as geo-electric or "telluric" variations.

The connection between $\underline{H}$ and $\underline{E}$ is established by three physical properties of internal matter: the conductivity σ (or its reciprocal the resistivity ρ), the permeability μ and the dielectric constant ε. The permeability of ordinary rocks is very close to unity and the approximation $\mu = 1$ is adequate. The magnetic effect of displacement durrents which is proportional to ε can be neglected within the earth (cf. Sec. 7.3), leaving the conductivity σ as the sole property connecting $\underline{E}$ and $\underline{H}$. Both fields tend to zero at sufficiently great depth, the skin-depth

$$p = \sqrt{\frac{2\rho}{\omega\mu_0}}$$

being a characteristic scale length for the depth of penetration of an oscillatory field $\exp(i\omega t)$ into a medium of resistivity ρ.

Geomagnetic induction data are usually presented in terms of transfer functions which connect as functions of frequency and locations certain components of $\underline{E}$ and $\underline{H}$. Examples are the imagneto-telluric transfer functions between the tangential components E and H and the magnetic transfer functions between the vertical and horizontal components of $\underline{H}$ only. These transfer functions form input data for magneto-telluric and geomagnetic depth soundings, abbreviated MTS and GDS.

Notations and units. Rectangular coordinates (x,y,z) are used with z positive down. If x is towards local magnetic north and y towards local magnetic east, the following notations of the magnetic and electric field components are common:

$$H_x = H \qquad H_y = D$$

$$E_x = E_N \qquad E_y = E_E .$$

The vertical magnetic component H_z is usually simply denoted as Z. All equations are in SI-units, but for $\underline{H}$ the tradional geomagnetic unit $1\gamma = 10^{-5}$ Gauß may be quoted. A convenient unit for the telluric field is (mV/km). The magneto-telluric transfer function between (E_x,E_y) and (H_x,H_y) will have in these units the dimension {mV/km}/γ with the conversion

$$1\ \frac{\text{mV/km}}{\gamma} = \frac{4\pi}{10}\ 10^{-3}\ \Omega$$

to SI-units. Measuring the period $\tau = 2\pi/\omega$ of time-harmonic field variations in seconds,

$$p = \frac{1}{2}\sqrt{\rho\tau}\ \text{km},$$

if τ is measured in hours,

$$p = 30.2\ \sqrt{\rho\tau}\ \text{km},$$

the unit of ρ being in either case (Ωm); $\mu_o = 4\pi \cdot 10^{-7}$ volt sec/Ampm.

7.3 Electromagnetic wave propagation and diffusion through uniform domains

Consider a volume V for which the physical properties μ,ε,σ are constants. Then $\underline{E}$ and $\underline{H}$ are non-divergent within V and connected by Maxwell's field equations ($\dot{} = \partial/\partial t$)

$$\text{rot}\ \underline{H} = \sigma\underline{E} + \varepsilon\varepsilon_o\dot{\underline{E}}$$

$$\text{rot}\ \underline{E} = -\mu\mu_o\dot{\underline{H}} .$$

Elimination of $\underline{E}$ or $\underline{H}$ yields a second order partial differential equation

$$\nabla^2 \underline{F} = \mu\mu_0(\sigma\dot{\underline{F}} + \varepsilon\varepsilon_0\ddot{\underline{F}})$$

where $\underline{F}$ denotes either the electric or the magnetic field vector (div $\underline{F}$ = 0). This equation can be interpreted as a wave equation or as a diffusion equation, depending on the fastness of the field variations in relation to the decay time

$$\tau_0 = \varepsilon\varepsilon_0 / \sigma$$

of free electric charges within V.

Let ω be the angular frequency of harmonic field variations, i.e. $\dot{\underline{F}} = i\omega\underline{F}$ and $\ddot{\underline{F}} = -\omega^2\underline{F}$. Then the basic differential equation is conveniently written as a wave equation

$$\nabla^2 \underline{F} = -(\frac{\omega}{c})^2 \{1 + (i\omega\tau_0)^{-1}\} \underline{F}$$

for $\omega\tau_0 >> 1$ and as a diffusion equation

$$\nabla^2 \underline{F} = \frac{2i}{p^2} \{1 + (i\omega\tau_0)\}\underline{F}$$

for $\omega\tau_0 << 1$. In the first case the field truly propagates through V with the speed

$$c = (\mu\mu_0\varepsilon\varepsilon_0)^{-\frac{1}{2}}$$

and $(i\omega\tau_0)^{-1}$ as absorption factor.
In the second case the field diffuses into V with

$$p = (2\rho/\omega\mu_0)^{\frac{1}{2}}$$

as skin-depth. The diffusion can be regarded as "quasi-stationary" in the sense that the propagation term $(i\omega\tau_0)$ is sufficiently small against unity.
For $\rho = 1/\sigma$ in Ωm $\quad \tau_0 \simeq 10^{-11}\ \rho\ \varepsilon$ (sec),

Since ρ will be less than 10^5 Ωm within the Earth, fields for frequencies up to 10^5 cps possess a quasi-stationary diffusion below

the surface. Only near certain sulfidic ore veins the "effective" decay time τ_o may be in the order of fractions of seconds due to induced polarisation and the propagation term may not be necessarily small against unity.

The air just above the ground has a resistivity in the order of 10^{14} Ωm, yielding a time constant τ_o of about 10 minutes. Hence, fast fluctuations "propagate", while slow variations "diffuse" from their ionospheric sources to the Earth's surface.

For geomagnetic soundings only the field at and below the Earth's surface matters, regardless how the primary field reaches the surface. It is necessary, however, to make one definite assumption about the nature of the primary field in the following sense:

Non-divergent vector fields such as $\underline{E}$ and $\underline{H}$ in uniform domains can be decomposed into two parts

$$\underline{F} = \underline{F}_I + \underline{F}_{II} = \mathrm{rot}(\hat{\underline{r}}T) + \mathrm{rot}\ \mathrm{rot}(\hat{\underline{r}}S)$$

where $\hat{\underline{r}}$ denotes a unit vector in some specified direction, here the z-direction. T and S are scalar functions of position. It is readily seen that the so-called "toroidal" part $\underline{F}_I$ is orthogonal to $\hat{\underline{r}}$, i.e. in the here considered case $\underline{F}_I$ is tangential to planes z = const. The remaining so-called "poloidal" part $\underline{F}_{II}$ of $\underline{F}$ has three components:

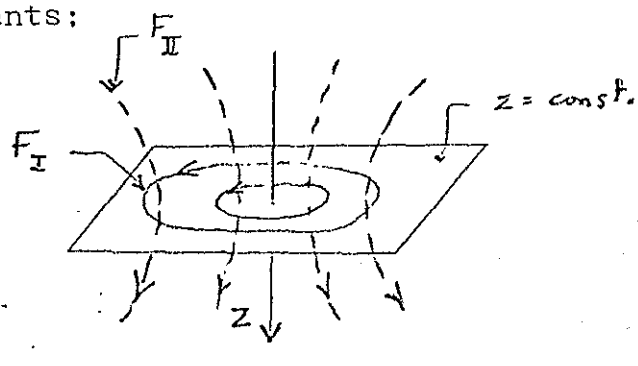

Let now $\underline{P}_I$ and $\underline{P}_{II}$ be a "toroidal" and a "poloidal" diffusion vector, both satisfying

$$\nabla^2\underline{P} = i\omega\mu_o\sigma(1 + \tau_o)\underline{P},$$

from which the toroidal and poloidal parts of $\underline{H}$ are derived by definition as follows:

$$\underline{H}_I = \frac{1}{i\omega\mu_o} \text{ rot } \underline{P}_I; \quad \underline{H}_{II} = \frac{P}{\omega\mu_o(1+i)} \text{ rot rot } \underline{P}_{II}.$$

Observing that

rot rot rot $\underline{P}$ = - rot($\nabla^2\underline{P}$-grad div$\underline{P}$) = $-i\omega\mu_o\sigma$ rot$\underline{P}$, the electric vectors follow then from Maxwell's field equations as

$$\underline{E}_I = \frac{2i}{P^2} \text{ rot rot } \underline{P}_I; \quad \underline{E}_{II} = \frac{P}{i(1+i)} \text{ rot } \underline{P}_{II}.$$

Since the field which is derived from P_I has a tangential magnetic field, it is termed the "TM-mode" of the total field. The field derived from P_{II}, on the other hand, has a tangential electric field and represents the "TE-mode" of the total field.

Suppose that the conductivity is a sole function of depth, $\sigma = \sigma(z)$, and therefore the diffusion vector vertical downward: $\underline{P} = (0,0,P_z)$. Let P_z be in planes z = const. a harmonic oscillating function of x and y with the "wave numbers" k_x and k_y in x and y-direction:

$$P(\underline{r}) = P_o(z)\cdot e^{i\underline{k}\cdot\underline{R}} \text{ with } \underline{k} = (k_x,k_y), \quad \underline{R} = (x,y).$$

Then

$$\text{rot } \underline{P} = (ik_y, -ik_x, 0)\ P_z$$

$$\text{rot rot } \underline{P} = (ik_x/C, iky/C, |k|^2)\ P_z$$

where $\frac{1}{C} = \frac{\partial P_o/\partial z}{P_o}$ and $|k|^2 = k_x^2 + k_y^2$. It can be shown that C is a scale length for the depth of penetration of the field into the uniform domain. Insert now rot $\underline{P}$ and rot rot $\underline{P}$ into the equations as given above and obtain the following relations between field components setting $\omega\tau_o=0$:

TM-mode		TE-mode	
$H_y=\sigma C_I E_x$	$H_x=-\sigma C_I E_y$	$E_x=i\omega\mu_o C_{II} H_y$	$E_y=-i\omega\mu_o C_{II} H_x$
$E_z=ik_x C_I E_x$	$E_z=ik_y C_I E_x$	$H_z=ik_x C_{II} H_X$	$H_z= ik_y C_{II} H_y$

Since C_I and C_{II} cannot be zero for a finite wave number $|k|$, TM-modes will have in the here considered quasi-stationary approximation zero magnetic fields in nonconducting matter as in air above the ground. Hence, the existence of TM-modes within the primary field cannot be ruled out by magnetic observations, since it will be seen above the ground only in the vertical electric field E_z, provided that this vertical electric field is not due to local anomalies of the secondary induced field (s. below). In reality, the detection of a primary E_z will be nearly impossible because changes of the vertical electric field due to changing atmospheric conditions appear to be orders of magnitude greater than those connected with ionospheric sources. Therefore it is an assumption that the primary fields in geomagnetic induction studies are TE-fields.

In that case the secondary induced field above and within a layered substructure $\sigma = \sigma_n(z)$ is likewise a TE-field. The sum of both fields will be referred to as the "normal" field $\underline{H}_n$ and $\underline{E}_n$ for the considered substructure. Its depth of penetration is characterized by the response function $C_{II} = C_n$ which according to the basic relations given above can be derived from the magneto-telluric "impedance" of the field

$$\frac{E_{nx}}{H_{ny}} = -\frac{E_{ny}}{H_{nx}} = i\omega\mu_o C_n \qquad \text{(MTS=magneto telluric sounding)}$$

or from the geomagnetic ratios

$$\frac{H_{nz}}{H_{nx}} = ik_x C_n, \qquad \frac{H_{nz}}{H_{ny}} = ik_y C_n \qquad \text{(GDS=geomagnetic depth sounding)}$$

Suppose the internal resistivity is within a limited range also dependent on one horizontal coordinate, say x:

$$\sigma = \sigma_n(z) + \sigma_a(y,z).$$

Now a local anomaly $H_a(y,z)$ and $E_a(y,z)$ will appear within the secondary field.

Two special types of such anomalies can be distinguished. If the electric vector of the primary fields is linearly polarized in x-direction, i.e.

$$\underline{E}_n = (E_{nx}, 0, 0)$$

and consequently

$$\underline{H}_n = (0, H_{ny}, H_{nz}),$$

the anomaly has an electric vector likewise only in x-direction, because the flow of eddy currents will not be changed in direction. Hence, the anomalous field is a TE-field.

$$\underline{E}_a = (\underline{E}_{ax}, 0, 0)$$

$$\underline{H}_a = (0, H_{ay}, H_{az}).$$

This polarisation of the primary field vector is termed E-polarisati

If the electric vector of the primary field is linearly polarised in y-direction, the normal field is

$$\underline{E}_n = (0, E_{ny}, 0)$$

and consequently

$$\underline{H}_n = (H_{nx}, 0, 0)$$

provided that its depth of penetration is small in comparison to its reciprocal wave number, yielding $H_{nz} = 0$. Only with this constraint is the flow of eddy currents confined to vertical planes $x = \text{const.}$ and the resulting anomalous field will be a TM-field with zero magnetic field above the ground:

$$\underline{E}_a = (0, E_{ay}, E_{az})$$

$$\underline{H}_a = (H_{ax}, 0, 0).$$

This polarisation of the primary field is termed "H-polarisation".

For three-dimensional structures

$$\sigma = \sigma(x,y,z) = \sigma_n(z) + \sigma_a(x,y,z)$$

the anomaly of the induced field will be composed of TE-and TM-fields which cannot be separated by a special choice of coordinates. There is, however, the following possibility to suppress in model calculation the TM-mode of the anomalous field:

Suppose the lateral variations σ_a are confined to a "thin sheet". This sheet may be imbedded into a layered conductor from which it must be separated by thin non-conducting layers. Then no currents can leave or enter the non-uniform sheet and the TM-mode of the induced field is suppressed. Such models are used to describe the induction in oceans, assumed to be separated from zones of high mantle conductivity by a non-conducting crust.

Schematic summary:

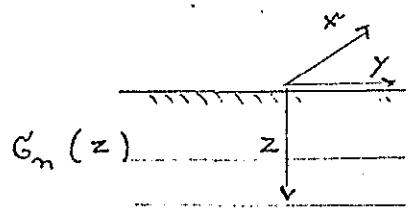

Source field	Induced field: normal	Induced field: anomalous
TE	TE	0
TM	TM	0

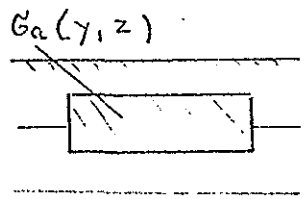

Source field	Induced field: normal	Induced field: anomalous
TE	TE { $TE(H_{nx} = 0)$ / $TM(E_{nx} = 0)$	

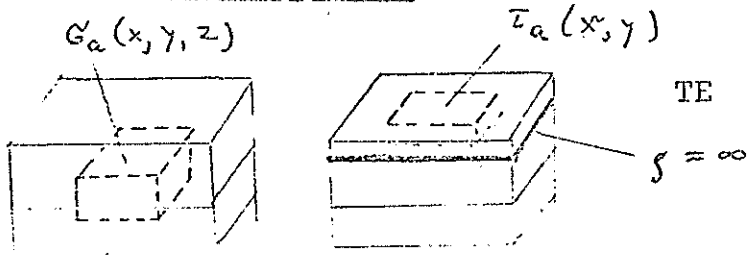

Source field	Induced field: normal	Induced field: anomalous
TE	TE { TE+TM(general) / TE (thin sheet)	

Appendix to 7.3: Recurrence formula for the calculation of the depth of penetration C for a layered substratum (cf. chapter 2)

Definition: $C = -\dfrac{P_o}{\partial P_o/\partial z}$

Differential equation to be solved: $\dfrac{\partial^2 P_o}{\partial z^2} = (i\omega\mu_o\sigma + |k|^2)P_o$

which satisfies $\nabla^2 \underline{P} = i\omega\mu_o\sigma\, \underline{P}$.

Continuity condictions:

1. TE-field: $\underline{H}$ and $\underline{E}$ must be continuous which implies that C is continuous
2. TM-field: $\underline{H}$ and $(E_x, E_y, \sigma E_z)$ are continuous which implies that σC is continuous.

Model:

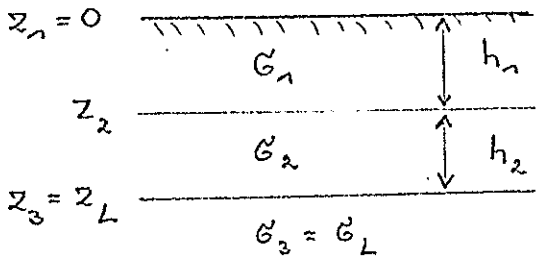

$$\alpha_n = h_n\sqrt{i\omega\mu_o\sigma_n} + |k|^2$$

Solution for uniform half-space: $C_I = C_{II} = \sqrt{i\omega\mu_o\sigma_o} + |k|^2$
$(\sigma = \sigma_o)$

Recurrence formula for layered half-space $\{C_n = C(z_n)\}$:

$$C_{IL} = C_{IIL} = \sqrt{i\omega\mu_o\sigma_L + |k|^2}$$

$$C_{In} = \frac{C_{In+1}\,K_n + \frac{\sigma_n}{\sigma_{n+1}}\tanh(\alpha_n)}{K_n\{\frac{\sigma_n}{\sigma_{n+1}} + C_{I_{n+1}}\,K_n\tanh(\alpha_n)\}}$$

$$C_{IIn} = \frac{C_{IIn+1}\,K_n + \tanh(\alpha_n)}{K_n\{1 + C_{IIn+1}\,K_n\tanh(\alpha_n)}$$

The TE-field within the n'th layer at the depth $z = z_n + \varepsilon$, $z_n < z_n + \varepsilon < z_{n+1}$, can be calculated from its surface value according to:

$$E_x(z_n+\varepsilon) = \{g(z_1,z_2)\cdot g(z_2,z_3) \cdot g(z_n,z_n+\varepsilon)\} \cdot E_x(0)$$

$$H_x(z_n+\varepsilon) = \{h(z_1,z_2)\cdot h(z_2,z_3) \cdot h(z_n,z_n+\varepsilon)\} \cdot H_x(0)$$

with $g(z_r,z_s) = \cosh\beta_{rs} - \sinh\beta_{rs}/(K_rC_r)$

$h(z_r,z_s) = \cosh\beta_{rs} - \sinh\beta_{rs} \cdot K_rC_r$

for $s \leq n$

and $g(z_n, z_n+\varepsilon) = \cosh(K_n\varepsilon) - \sinh(K_n\varepsilon)/K_nC_n$

$h(z_n,z_n+\varepsilon) = \cosh(K_n\varepsilon) - \sinh(K_n\varepsilon) \cdot K_nC_n$

$$\beta_{rs} = K_r(z_s - z_r)$$

$$K_r^2 = \sqrt{i\omega\mu_o\sigma_r} + |k|^2$$

The formula for E_x applies also to E_y and H_z, the formula for H_x also to H_y.

7.4 Penetration depth of various types of geomagnetic variations and the overall distribution of conductivity within the Earth

Three types of conduction which vary by orders of magnitude have to be distinguished:

1. Conduction through rock forming minerals
2. Conduction through fluids in pores and cracks between rockforming minerals
3. Metallic conduction

1.: Since the minerals of crustal and mantle material are expected to be silicates, the conduction through these minerals will be that of semi-conductors. Their resistivity is in the order of 10^5 Ωm at room temperature but decreases with temperature according to

$$\sigma(T) = \sigma_o \, e^{-A/kT} .$$

T is the absolute temperate, k Boltzmann's constant; σ_o and A are pressure-dependent and composition-dependent constants within a limited temperature range, for which one specific mechanism of semi-conduction is predominant. Hence, in plots of ln σ versus T^{-1} the σ-T dependence should be represented by joining segments of straight lines. Laboratory experiments with rocks and minerals at high temperature and varying pressure have confirmed this piece-wise linear dependence of lnσ from T^{-1}. Furthermore, they showed that the composition-dependence of σ is mainly contained in the pre-exponential

parameter σ_o and that the pressure dependence of σ_o and A should not be the determining factor for the conductivity down the depth of several hundred kilometers.

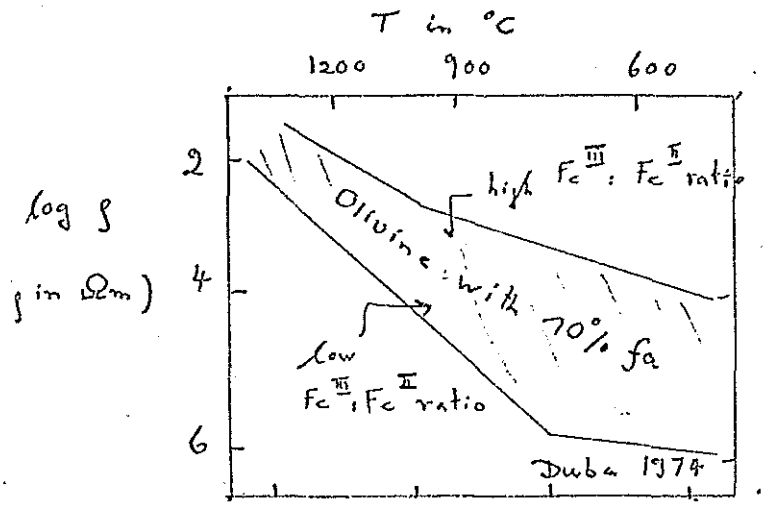

The σ-T dependence of Olivin $(Mg, Fe^{II})_2 SiO_4$ has been extensively investigated by various authors for temperaturs up to 1400°C and pressures up to 30 kbar. This mineral is thought to be the main constituent of the upper mantle with a Mg : Fe ratio of 9 : 1 : $(Mg_{0.9} Fe_{0.1})_2 SiO_4$. The diagram shows the range of σ(T)-curves as obtained for Olivin with 90% Forsterite (Mg_2SiO_4). It is believed that the discrepancies among the curves over orders of magnitude are mainly due to different degrees of oxydation of Fe^{II} to Fe^{III} within the olivin samples used for the measurement. In fact, the samples may have been oxydized in some cases during the heating experiment as evidenced by the irreproducibility of the σ(T)-curves. However, the range of possible conductivities for olivin with 10% forsterite is greatly narrowed in at the high temperature end, where we may expect a resistivity of 10 to 100 Ωm for 1400°C, corresponding to a depth of 100 to 200 km within the mantle.

2.:Electrolytic conduction through salty solutions, filling pores and cracks of unconsolidated rocks, gives clastic sediments resistivities from 1 to 50 Ωm. The resistivity of sea water with 3.5 gr NaCl/liter is 0.25 Ωm. There should be an increase of resistivity by one or two orders of magnitude at the top of the crystalline basement beneath sedimentary basins.

Near to the surface the conduction in crystalline rocks is also electrolytic. Their resistivity may be here as low as 500 Ωm, but it increases rapidly with depth, when the cracks and pores close under increasing pressure. Below the Mohorovicic-discontinuity the conduction through grains can be expected to be more effective than the conduction through pore fluids. If, however, partial

melting occurs, the conduction through even a minor molten fraction of crystalline rocks could lower the resistivity by, say, one order of magnitude.

3.: Metallic conduction is expected to give the material in the oute core a resistivity of 10^{-5} Ωm. This low value is required by dynamo theories for the explanation of the main field of the Earth.

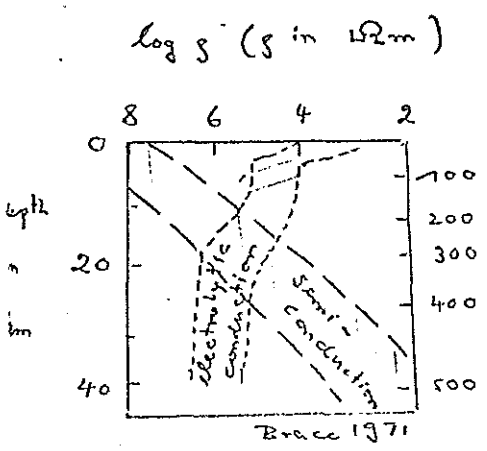

Conduction through crustal material

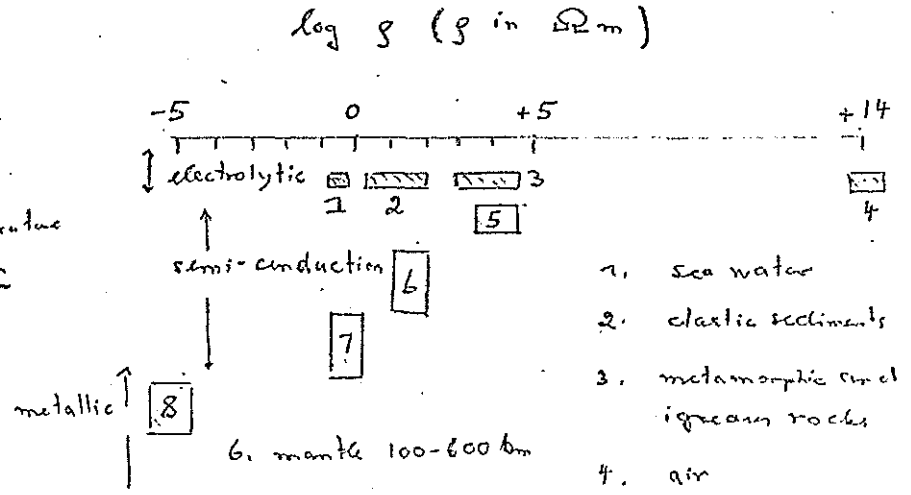

Schematic Summary

The frequency spectrum of geomagnetic variations which can be utilized for induction studies extends from frequencies of fractions of a cycle per day to frequencies of 10 to 100 cycles per second. At the low frequency end an overlap with the spectrum of secular variations occurs which diffuse upwards from primary sources in the Earth's core.

Schematic spectrum of geomagnetic variations:

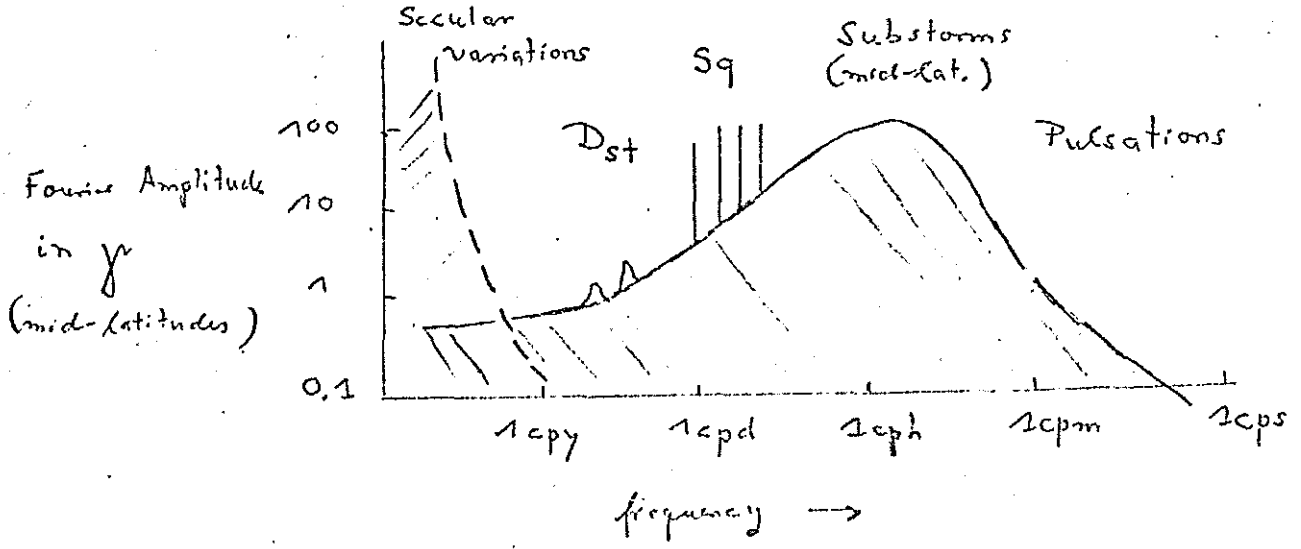

D_{st} (=disturbed)-variations: After magnetic storms the horizontal H-component of the Earth's magnetic field shows a worldwide decrease. Within a week after stormbeginn H returns asymptotically to its pre-storm level. This so-called D_{st}-phase of storms shows negligible longitudinal dependence, while its latitude dependence is well described in geomagnetic coordinates by

$$H_{D_{st}}(\Phi) = - H_o \cos\Phi;$$

Φ is the geomagnetic latitude of the location considered. The source of the D_{st}-phase may be visualized as an equatorial ring current (ERC) which encircles the Earth in the equatorial plane in geomagnetic coordinates:

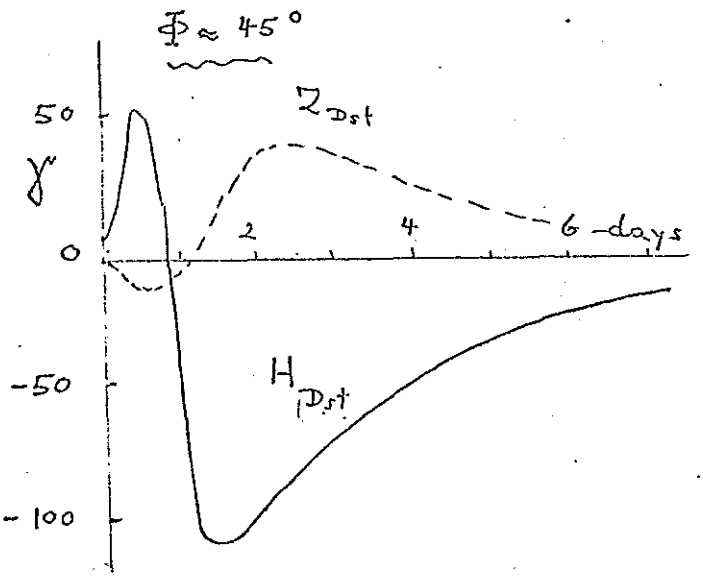

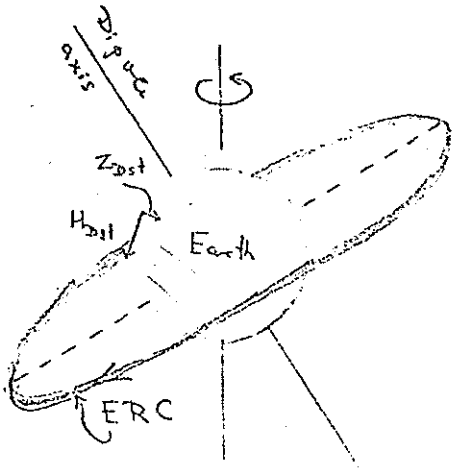

If the interior of the Earth were a perfect insulator and no eddy currents were induced, the vertical D_{st}-component would be $Z_{Dst} = H_o \sin\Phi$. In reality, only one fourth to one fifth of this value is observed due to the field of eddy currents which oppose in Z the primary field of the ERC. Let L_{Dst} denote the inductive scale length of D_{st}, a be the Earth's radius, then for $\Phi = 45^\circ$ (for $\Phi = 45°$)

$$Z_{Dst} = - \frac{2C_{Dst}}{a} H_{Dst}. \qquad \text{(cf. sec. 8.2)}$$

Hence, with $Z_{Dst}/H_{Dst} \simeq 0.2$ the depth of penetration will be 600 km.

SQ (solar quiet) variations: On the day-lit side of the Earth thermal convection in combination with tidal motions generate large-scale wind-systems in the high atmosphere. In the ionosphere these winds produce electric currents which - for an observer fixed to the Earth - move with the sun around the Earth. During equinoxes there will be two current vortices of equal strength in the northern and southern hemisphere, their centers being at roughly 30°N and 30°S. Due to these currents local-time dependent geomagnetic variations will be observed at a fixed site at the Earth's surface. They are repeated from day to day in similar form and are called "diurnal" or Sq-variations:

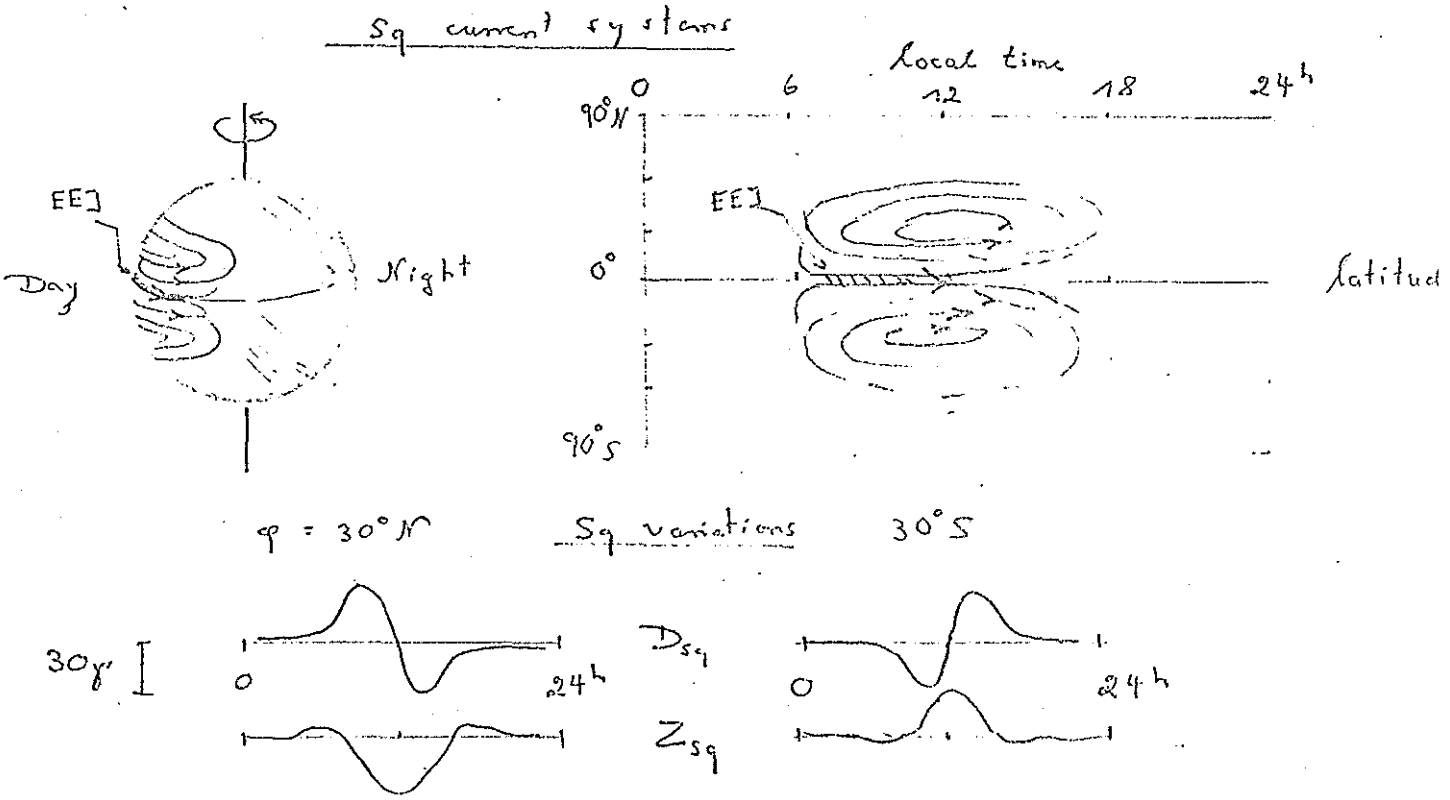

Again the Z_{SQ}-Amplitude is much smaller than to be expected from D_{SQ} for an insulating Earth. If $Z_{SQ}^{(m)}$ and $D_{SQ}^{(m)}$ denote the amplitudes of the m'th subharmonic of the diurnal variations (m=1,2,3,4 corresponding to the periods τ = 24, 12, 8, 6 hours) and $C_{SQ}^{(m)}$ the inductive scale length of this subharmonic,

$$Z_{SQ}^{(m)} = \frac{C_{SQ}}{a} \frac{(m+1)(m+2)}{m \sin\phi} H_{SQ}^{(m)} \qquad \text{(cf. 8.2)}$$

with ϕ as geographic latitude. From the Z_{SQ} : H_{SQ} ratio of continental stations a depth of penetration between 300 and 500 km is inferred. The penetration depth of SQ in the ocean basins is still uncertain.

Bays and Polar Substorms: During the night hours "bay-shaped" deflections of the Earth's magnetic field from the normal level are observed from time to time, lasting about one hour. Their amplitude increases steadily from south to north, reaching its highest value in the auroral zone. Similar variations, but much more intense and rapid, occur during the main phase of magnetic storms, until about one day after stormbegin.

The source of these so-called "polar substorms" is a shifting and oscillating current lineament in the ionosphere of the aurora zone. The current will be partly closed through field alligned currents in the magnetosphere, partly by wide-spread ionospheric return currents in mid latitudes:

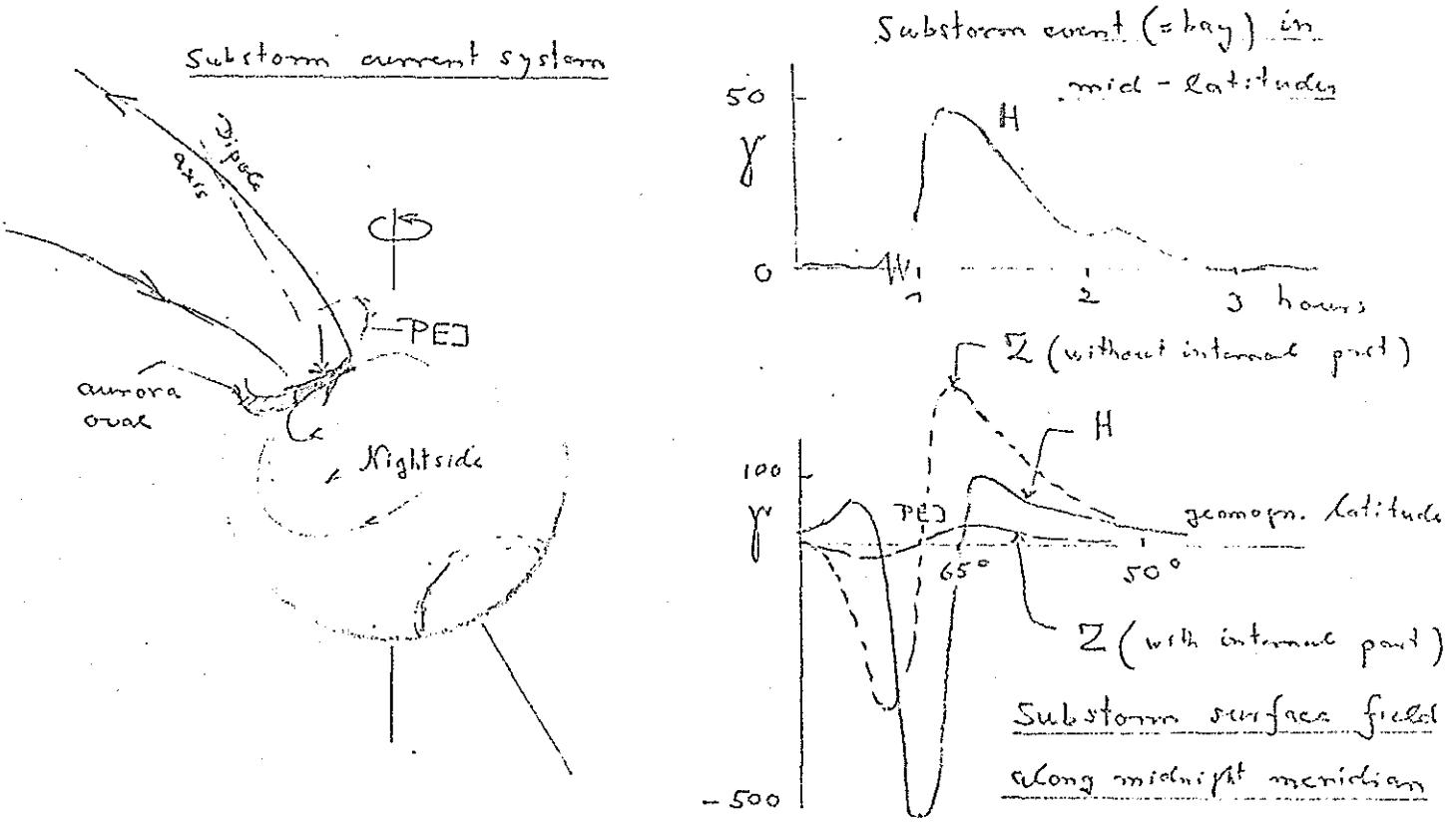

If the Earth were non-conducting, we would observe south of the polar electrojet PEJ strong Z-variations during polar substorms. They would represent the field of a line current and be comparable in amplitude to H- and D-variations, arising from overhead "return currents" in mid-latitudes. In reality, the Z-amplitude during

polar substorms is in mid-latitudes (e.g. Denmark, Germany) much smaller than the amplitudes of H and D because the vertical field of induction currents nearly cancels the vertical field of the polar jet. Under "normal conditions" the Z:H ratio is about 1:10. Assuming for the mid-latitude substorm field an effective wave number of 10- 20 000 km, yielding $k_x \simeq 3\text{-}6 \cdot 10^{-4}$ as wavenumber, depth of penetration is

$$|c_{bay}| = \frac{Z_{bay}}{H_{bay}} \frac{1}{k_x} \simeq 150 \text{ to } 300 \text{ km.}$$

There are indications that the penetration depth of bays into the oceanic substructure is substantially smaller. The ocean itself produces an attenuation of the H-amplitude of about 75% at the ocean bottom, deep basins filled with unconsolidated sediments can yield a comparable attenuation (e.g. North German basin).

Pulsations and VLF-emissions: Rapid oscillations of the Earth's fiel with periods between 5 minutes and 1 second are called pulsations. Their amplitude increases like the amplitude of substorms strongly when approaching the auroral zone. Their typical midlatitude amplitude is 1 gamma. The source field structure of bays and pulsations is similar, the depth of penetration of pulsations being largely dependent on the near-surface conductivity. It may range from many kilometers in exposed shield areas to a few hundred meters and less in sedimentary basins.

The "normal" Z:H ratio of pulsations is too small to be determined with any reliability outside of the auroral zone. However, "anomalou Z-pulsations are frequent and usually of very local charakter. If pulsations occur in the form of lasting harmonic oscillations, often with a beat-frequency, they are called "pulsation trains" pt, single pulsation events are called "pi", pulsations which mark the beginning of a bay disturbance are called "pc". All three types have a clear local time dependence, occuring almost daily:

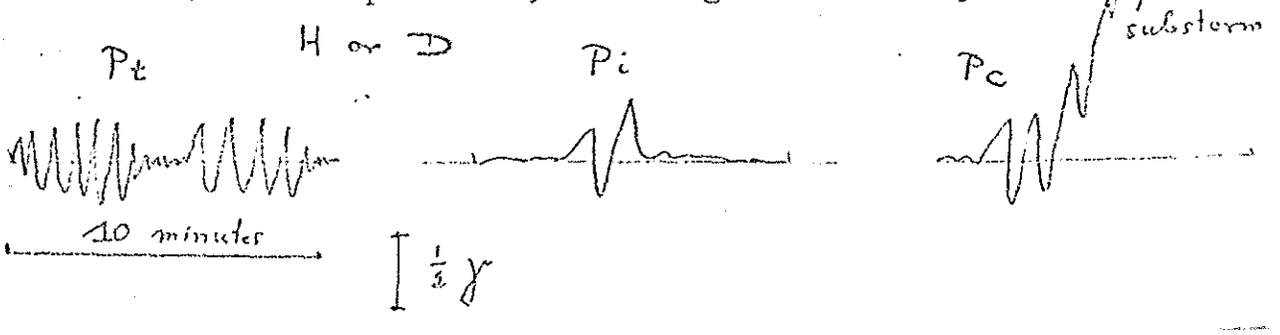

Very rapid oscillations with frequencies between 1 and, say, 100 cps (=Hz) are called - from the radio enginieers point of view - "very low frequency emissions: VLF. Their amplitudes lie well below 1γ. They occur usually intermittendly in "bursts" and are controlled in their intensity by the general magnetic activity. In exposed shield areas they may penetrate downward a few kilometers, but everywhere else they will be totally attenuated within the very surface layers.

Sudden storm commencements and solar flare effects: The begin of a magnetic storm is usually marked by strong deflections in H and Z up to 100γ within one or two minutes. This so-called "sudden storm commencement" SSC, signals the inward motion of the magnetopause (separating the magnetosphere from the interplanetary space) under the impact of a suddenly increased solar wind intensity. SSC's are a world wide, simultaneously occuring phenomenon. They are, however, too rarely occuring events (1 per month) for induction studies.

The momentarily increased solar wave radiation, caused by sun spot eruptions, produces a shortlived (5 minutes) intensification of the Sq-system, its magnetic effect is called a "solar flare event". It measures a few gammas and like the ssc is a rarely observed variation type.

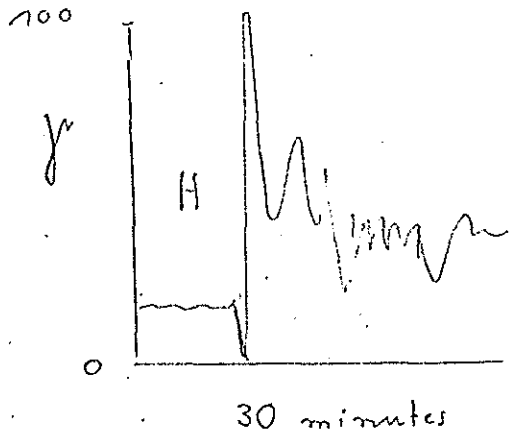

sudden storm commencement

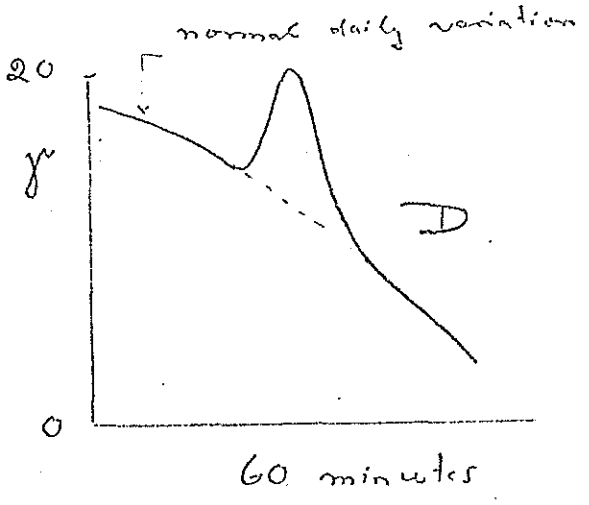

solar flare effect

Overall depth distribution of resistivity

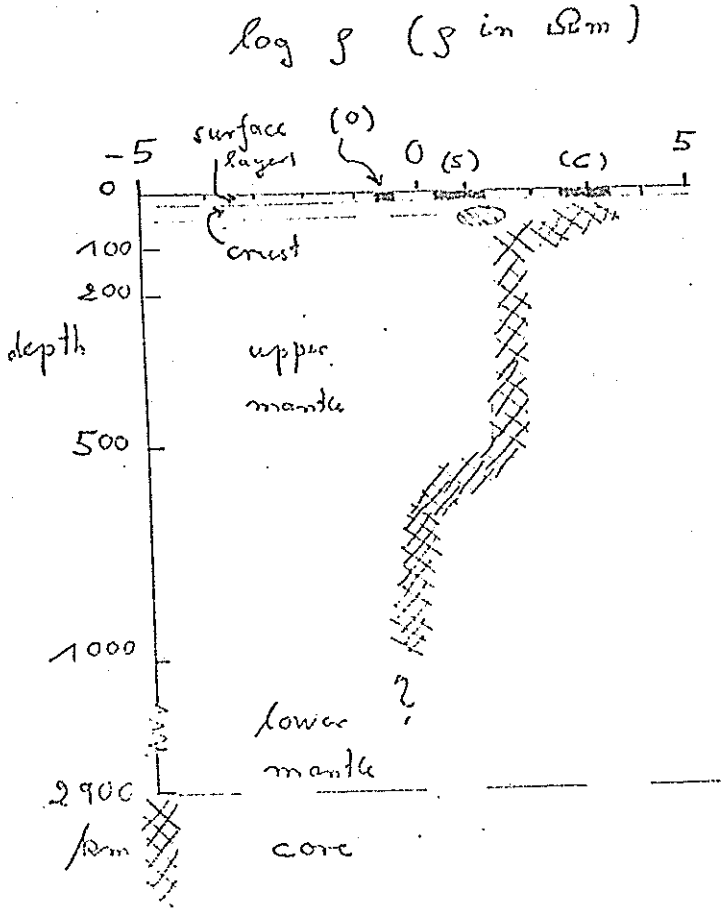

Depth of penetation

(o): oceans

(s): sedimentary basins

(c): exposed crystalline basement

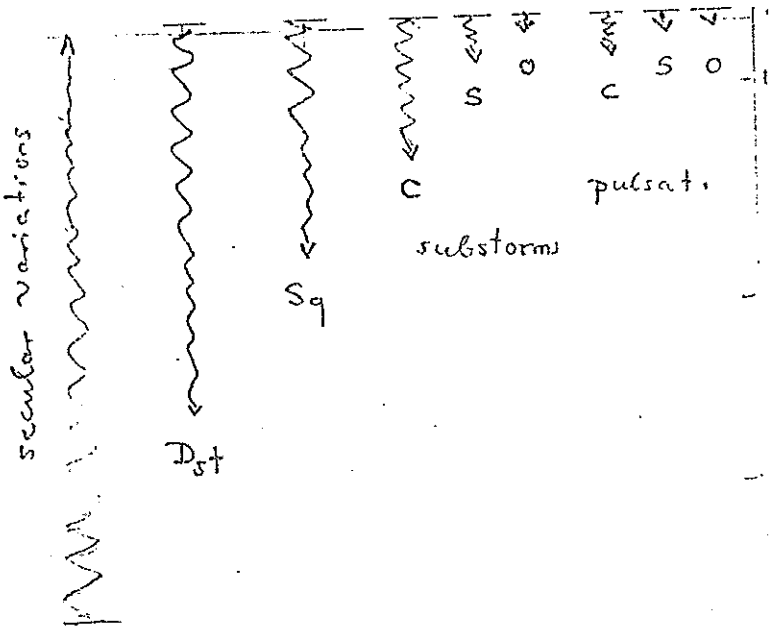

Wavenumber-frequency range of geomagnetic (GDS) and magnetotelluric (MTS) sounding under normal conditions $\rho = \rho(z)$

M : mid-latitude observations

EEJ: equatorial electro

PEJ: polar electrojet

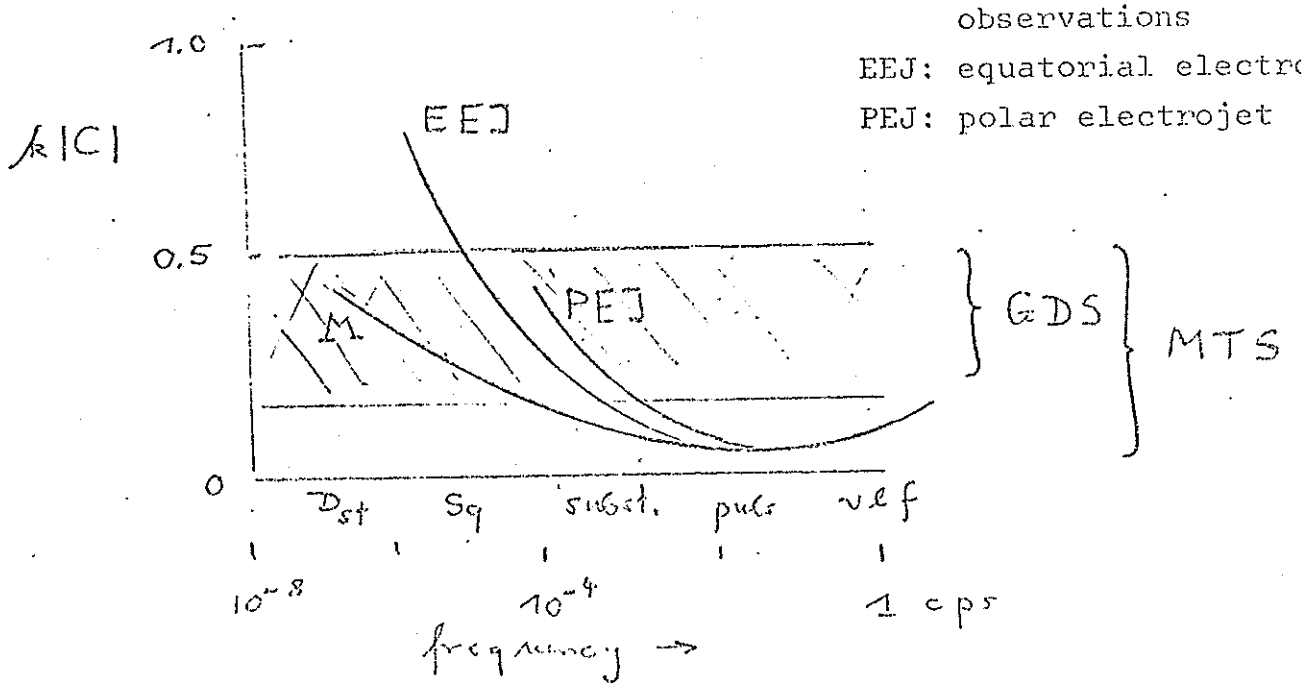

8. Data Collection and Analysis

8.1 Instruments

Magnetic sensors for geomagnetic induction work on land should meet as many as possible of the following requirements:

(1) Sufficient sensitivity and time resolution

(2) Directional characteristics which allow observation of the magnetic variation vector in well-defined, preferably orthogonal components.

(3) Stable compensation of the Earth's permanent field, if required. The sensors should not show "drift" on a time scale comparable to the slowest variations to be analysed.

(4) Compensation of temperature effects or linear temperature dependence with well defined temperature coefficients for subsequent corrections.

(5) Low power consumption to allow field operations on wet or dry-cell batteries (less than 100 mA at 10 to 20 Volts DC continuous power drain).

(6) Minimum maintenance, allowing unattended operations over days, weeks or months, depending on the period range to be investigated.

(7) Electric output signal, adaptable for digital recording

No single sensor system can possibly meet all requirements over the full frequency range of natural geomagnetic variations and the choice of instruments will depend on the type of variations under investigation. They record either the total field $H = H_o + \delta H$ as sum of the steady field H_o and the variation field δH,* by compensation of H_o, the time-derivative $\dot{H} = \delta\dot{H}$ or a combination of δH and $\delta\dot{H}$. In geomagnetic** latitudes the spectral amplitude distribution of δH and $\delta\dot{H}$, averaged over extended periods of moderate magnetic activity, is the following:

* the variation field δH only

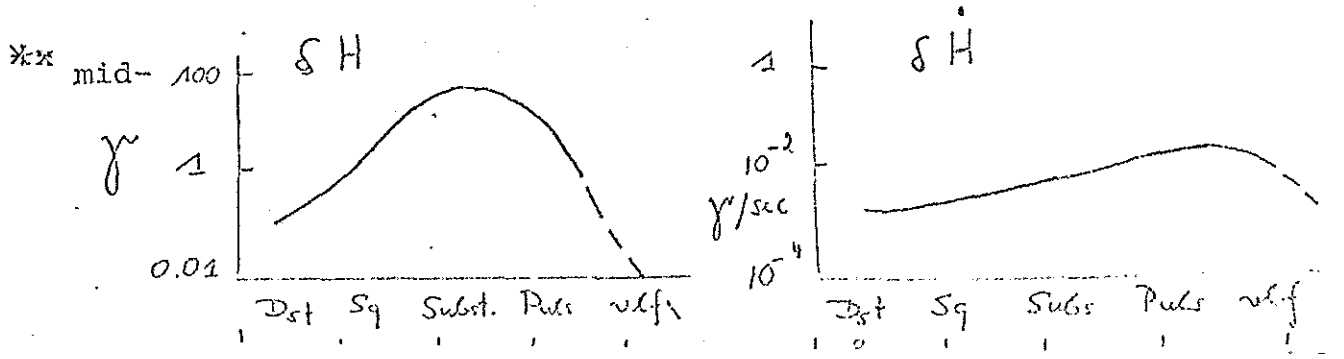

The next diagram shows the resulting spectral range of adequate sensitivity and stability for various magnetic sensors, suitable for geomagnetic studies:

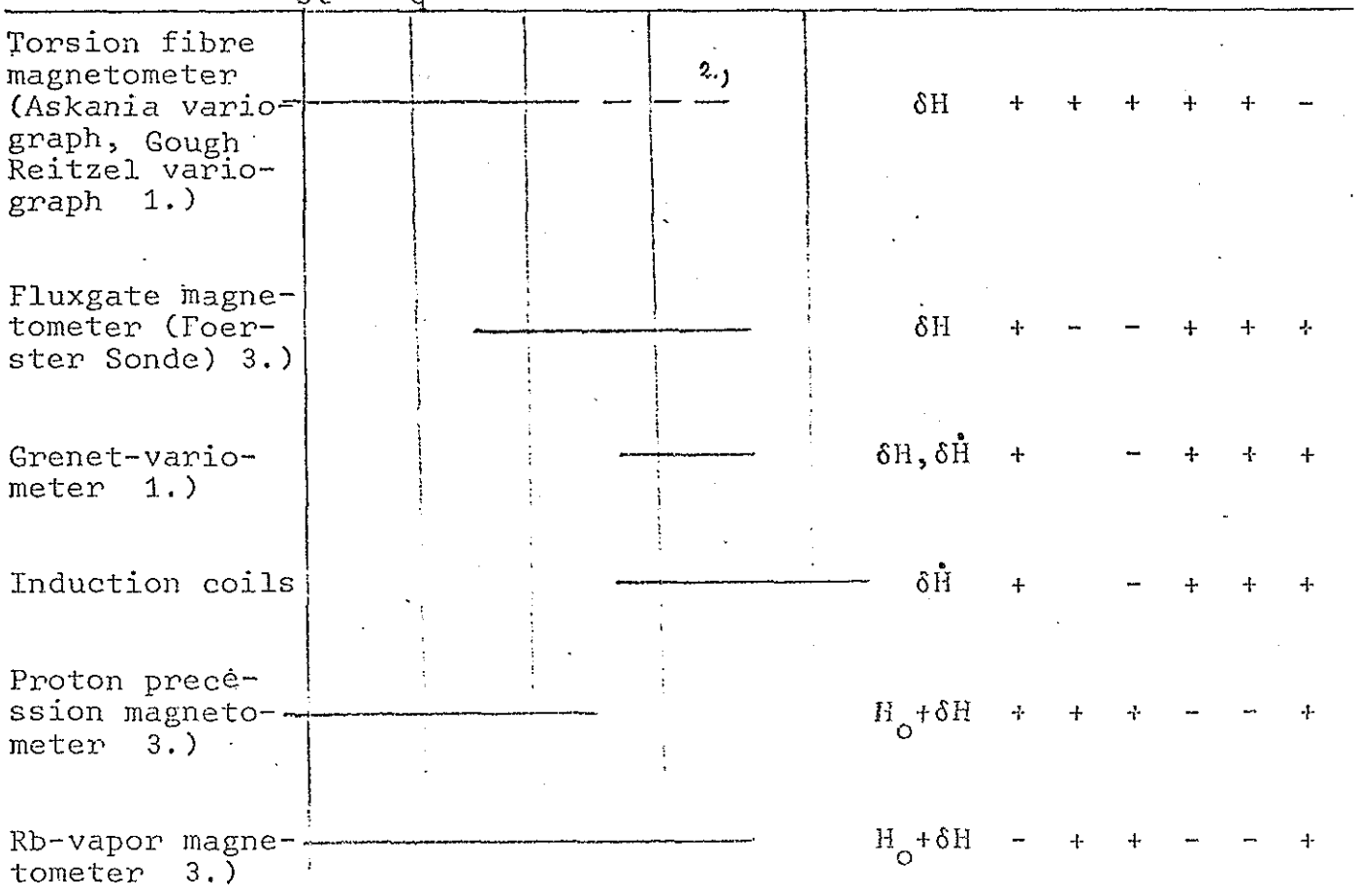

1.) Compensation of H_o by mechanical torque
2.) Bobrov-quartz variometers, Jovilet variometers
3.) Compensation of H_o with bias fields

The horizontal components of the surface electric field E which is connected to δH and δḢ can be estimated either from the knowledge of the depth of penetration C at the period τ or from the knowledge of the resistivity ρ of the upper layers, assumed to be uniform. Measuring H in (γ), C in (km), τ in (sec) and ρ in (Ωm) gives

$$E = \omega\mu_o \, CH = \frac{2\pi C}{\tau} H = \sqrt{\frac{5\rho}{\tau}}\, H \; \left(\frac{mV}{km}\right).$$

Using the spectral amplitudes as given above and C from the previous section, the following spectral amplitudes of E/H and E are obtained for mid-latitudes during moderate magnetic activity:

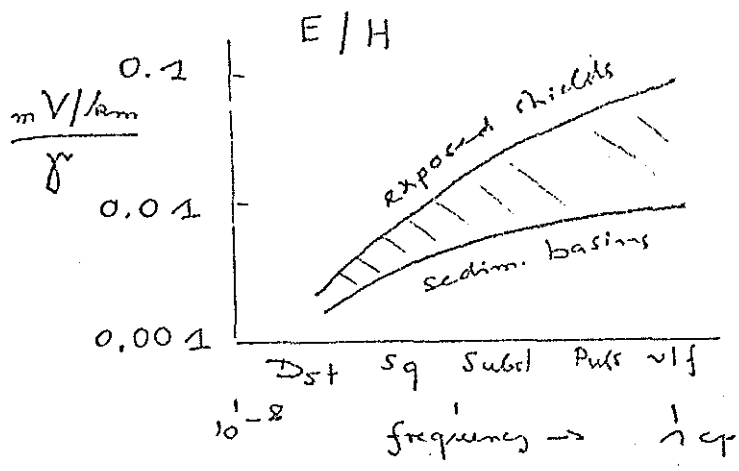

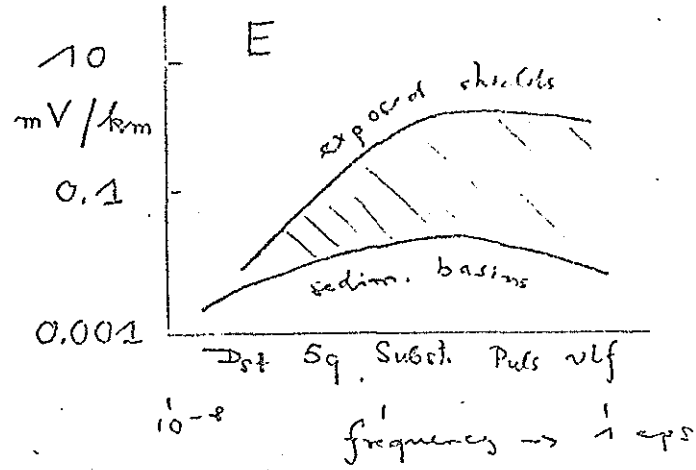

A horizontal electric field component in the direction s is observed as the fluctuating voltage $E_s \cdot d$ between two electrodes in a distance d parallel to s. Due to possible self-polarisation of the electrodes a quasi-steady voltage of considerable size may be superimposed upon the fluctuating voltage, truly connected to geomagnetic variations. This self-potential amounts for electrodes in a salt solution comparable to ocean water to:

> 1 Volt	for	unprotected iron rodes
100 mV		$Cu-CuSO_4$ electrodes
10 mV		Kalomel (= biophysical) electro
0.1 mV		$Ag-AgCl_2$ (=oceanographic) electro

It may vary slowly under changing conditions in the waterbearing soi Hence, it should be as small as possible in comparison to the voltag truly connected to δH and $\delta \dot{H}$. This applies in particular to periods of one hour and more. There are two options to avoid these unwanted electrode effects: Large electrode spacing ($d \geq 10$ km), high-quality electrodes. Preference should be given to the second option, using electrode spacings of, say, 100 m. The use of a large electrode spacing does not imply necessarily that a mean electric field, averaged over local near-surface non-uniformities, will be observed, since the observed voltage may still be largely determined by local conditions near to either one of the electrodes. In any case, the site of the electrode installation should be surveyed with dipol-soundings or DC-geoelectrics to ensure layered conditions at and between electrodes.

8.2 Organisation and objectives of field operations

Geomagnetic induction work can be carried out by (i) single-site soundings, (ii) simultaneous observations along profiles, (iii) simultaneous observations in arrays covering extended areas. It may be possible to replace simultaneous by non-simultaneous observations, provided that the variation field can be "normalized" with respect to the mean regional variation field. This "normal" field may be the field at one fixed site with no indications for the presence of lateral non-uniformities, or it may be the averaged field obtained from distant permanent observatories. Usually the normalisation is performed in the frequency domain, introducing sets of transfer functions.

Single site vertical sounding:

The resistivity structure within the depth-distance range of penetration is regarded a sole function depth: $\rho = \rho(z)$. Its extent is given by the modulus of the inductive scale length $C(\omega)$ at the considered frequency, which increases with the increasing period. If a vertical geomagnetic sounding is to be carried out, the source field wave-number structure as function of frequency, $\underline{k} = \underline{k}(\omega)$, must be known (cf. Sect. 7.3).

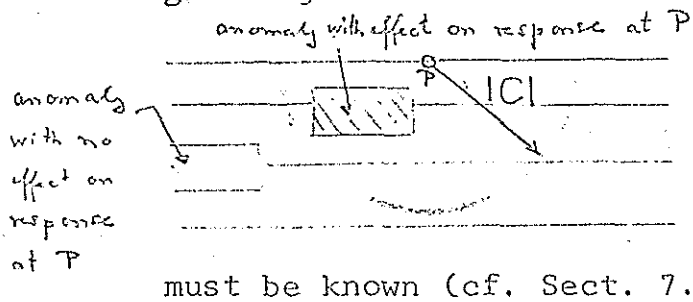

For diurnal Sq-variations, for instance, wave-numbers are derivable from the fact that the Sq-field of the equinoxes is symmetric to the equator and moving with local time from east to west. Hence, the east-west wave-number of the m'th subharmonic of Sq will be m/a with a denoting the Earth's radius.

Magneto-telluric soundings are independent of the wave number, provided that the depth of penetration is sufficiently small in comparison to k^{-1}: $|kC| \ll 1$. Taking the general dependence of C on k into account, it is preferable to stay with vertical soundings in the range in which $C(\omega)$ is independent of k.

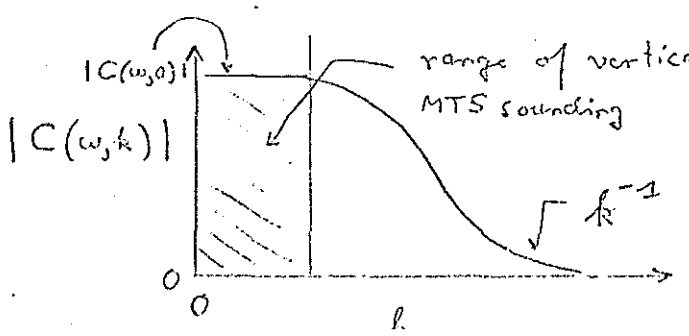

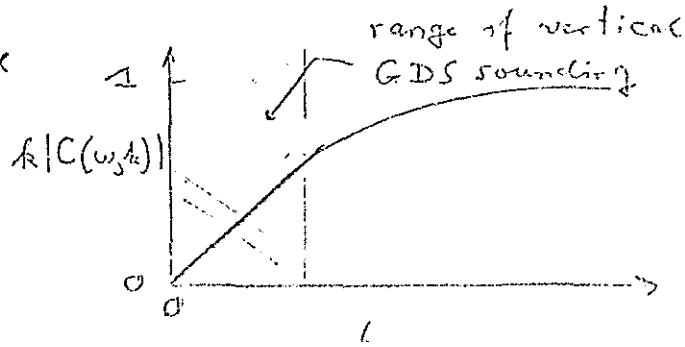

For a data reduction in the frequency domain (cf. Sec. 8.3) the following set of transfer or response functions will be defined:

$$H_{nz} = A_n H_{nx} \qquad E_{nx} = Z_{xy} H_{ny}$$

$$H_{nz} = B_n H_{ny} \qquad E_{ny} = Z_{yx} H_{nx}$$

For a frequency-space factor of the source field

$$\exp\{i(\omega t + \underline{k}\,\underline{R})\}$$

the response function $C(\omega) = C_n$ which characterises the downward depth of penetration is connected to these transferfunctions according to

$$C_n = \frac{A_n}{ik_x} = \frac{Z_{xy}}{i\omega\mu_o}$$

$$C_n = \frac{B_n}{ik_y} = \frac{-Z_{yx}}{i\omega\mu_o} .$$

The Cagniard apparent resistivity if given by

$$\rho_a(\omega) = \omega\mu_o \, |C_n(\omega)|^2 ,$$

the phase of the impedance by

$$\phi(\omega) = \arg(Z_{xy}) = \arg(C_n) + \frac{\pi}{2} ,$$

the modified apparent resistivity by

$$\rho^*(\omega) = 2\,\omega\mu_o \{\mathrm{Im}(C_n)\}^2$$

which can be used as an estimator of the true resistivity at the depth

$$z^*(\omega) = \mathrm{Re}\{C_n\}. \qquad \text{(cf. Sec. 2.5 and 9.1)}$$

A comparison of the various equivalent response functions for a given substructure gives the following display:

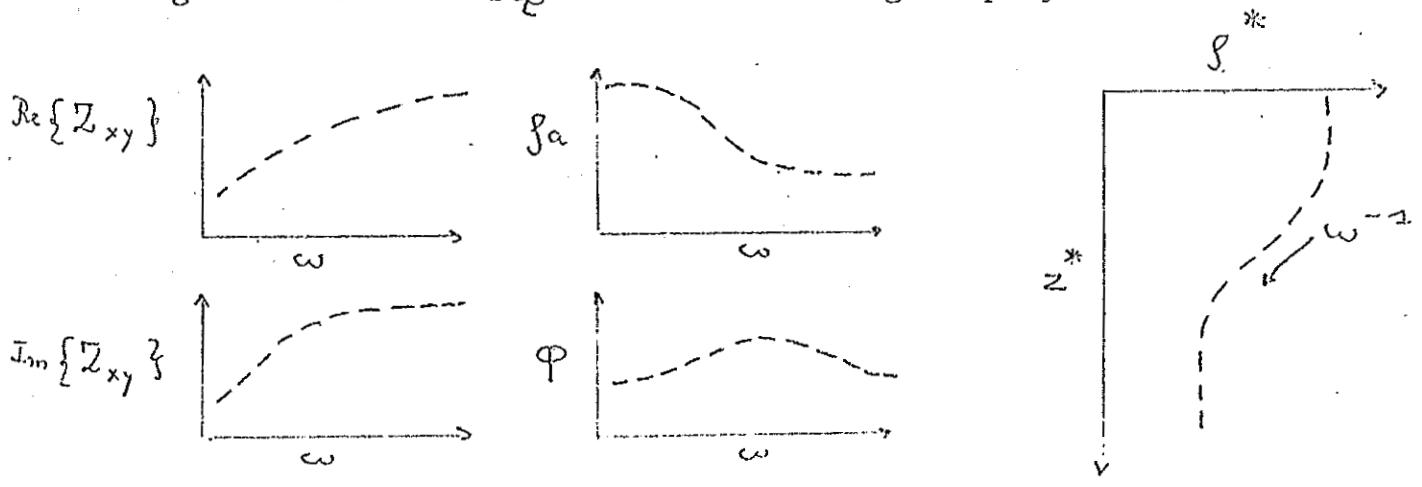

Tests for the assumption of a layered distribution and the source field wavenumber are given by

$$Z_{xy} = - Z_{xy} \qquad \frac{A_n}{B_n} = \frac{k_y}{k_x} .$$

In addition there are certain constraints with regard to modulus, phase and frequency dependence of the transfer functions. (cf. Sec. 2.6).

The compatability of MTS and GDS vertical sounding results can be tested by the requirement that

$$H_{nz} = \omega\mu_o \{k_x E_{ny} - k_y E_{nx}\}$$

as readily seen form the second field equation $\text{rot}\underline{E}_n = -i\omega\mu_o \underline{H}_n$.

If the wave-number structure of the source field is not known, a Horizontal Gradiént GDS can be formed: Observing that

$$-i\omega\mu_o H_{nz} = \frac{\partial E_{ny}}{\partial x} - \frac{\partial E_{nx}}{\partial y} ,$$

the differentation of $E_{nx} = C_n\, i\omega\mu_o\, H_{ny}$ with respect to y and of $E_{ny} = -i\omega\mu_o C_n\, H_{nx}$ with respect to x yields

$$H_{nz} = C_n \{\frac{\partial H_{nx}}{\partial x} + \frac{\partial H_{ny}}{\partial y}\}.$$

Since the electric surface field may be distorted by lateral non-uniformities even when their scale length and depth is small in comparison to the depth of penetration, the E-field observations may be replaced by observing the tangential magnetic field also at some depth d below the surface, i.e. by conducting a Vertical Gradient GDS. No knowledge of the wave-number structure of the source field will be required, but the resistivity ρ_o between the surface and the subsurface points of observations will be required. Assume that the lateral gradients of H_{nz} are small in comparison to the vertical gradients of H_{nx} and H_{ny} in view of the condition $|kC| << 1$. Then it follows readily from the first field equation $\text{rot}\, \underline{H}_n = \sigma_o \underline{E}_n$ for $d < z < 0$ that

$$\frac{\partial H_{ny}}{\partial z} - \frac{\partial H_{nz}}{\partial y} \simeq \frac{\partial H_{ny}}{\partial z} = E_{nx}/\rho_o \quad \text{and} \quad \frac{\partial H_{nx}}{\partial z} = - E_{ny}/\rho_o .$$

Let q be the tranfer function between $H_{nx}(H_{ny})$ at the surface and $H_{nx}(H_{ny})$ at the depth z = d:

$$H_{nx}(d) = q\, H_{nx}(0) \qquad \text{where } |q| < 1.$$

Then $$\frac{\partial H_{nx}}{\partial z} \simeq \frac{q-1}{d} \qquad \text{and} \qquad C_n = \frac{q-1}{i\omega\mu_o\sigma_o d}\,.$$

Single site geomagnetic structural sounding: The source field is regarded as quasi-uniform (k = 0) and the vertical magnetic component therefore as anomalous, arising solely from lateral changes of the resistivity within the depth-distance range of penetration, where

$$\rho = \rho_n(z) + \rho_a(x,y,z)\backslash$$

In this special case the resulting anomalous magnetic vector $\underline{H}_a = (H_{ax}, H_{ay}, H_{az} = H_z)$ is linearly dependent on the quasi-uniform normal magnetic vector $\underline{H}_n = (H_{nx}, H_{ny}, 0)$ in the frequency-distance domain:

$$\underline{H}_a = W\,\underline{H}_n.$$

Here

$$W = \begin{pmatrix} W_{xx} & W_{xy} \\ W_{yx} & W_{yy} \\ W_{zx} & W_{zy} \end{pmatrix}$$

denotes a matrix of linear transfer functions as functions of frequency and surface location. This implies that also linear relations exist between H_z and the total (=observed) horizontal variations:

$$H_{az} = A\,H_x + B\,H_y$$

with

$$H_x = H_{nx} + H_{ax} \qquad H_y = H_{ny} + H_{ay}$$

$$W_{zx} = A(1+W_{xx}) + BW_{yx} \qquad W_{zy} = B(1+W_{yy}) + AW_{xy}.$$

These alternative transfer functions A and B can be derived now from observations at a single site. Their graphical display in the form of Parkinson-Wiese induction arrows indicates the trend of the subsurface resistivity structure which is responsible for the appearance of anomalous Z-variations:

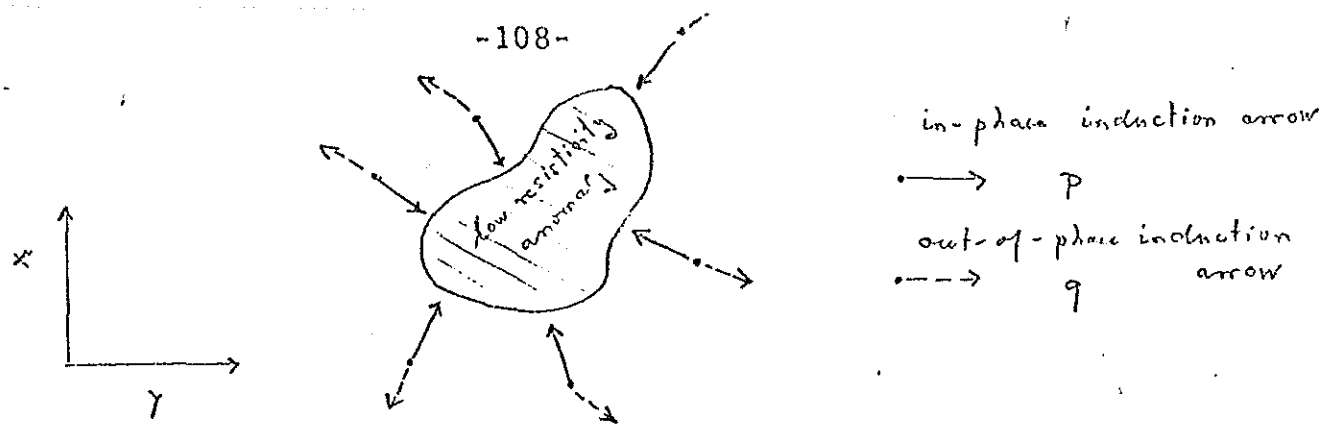

The in-phase induction arrow is defined by (in Parkinson's sense of orientation) by

$$\underline{p} = - \mathrm{Re}\{\hat{x}\, A + \hat{y}\, B\}$$

and the out of-phase arrow by

$$\underline{q} \text{ " } + \mathrm{Imag}\{\hat{x}\, A + \hat{y}\, B\}$$

where $\hat{x}$ and $\hat{y}$ are unit vectors in x- and y-direction. Generally speaking, the in-phase arrows point towards internal concentrations of induced currents, i.e. to zones of lower than "normal" resistivity at one particular depth. They may point also away from high resistivity zones around which the induced currents are diverted.

Vertical soundings with station arrays:

The resistivity structure is regarded as layered, $\rho = \rho(z)$, but the inducing source field as non-uniform. Inducing and induced fields will have matching wave-number spectren with well defined ratios between spectral components in accordance to the subsurface resistivity structure. ~~Beneath the station array under considerations, even though this lateral uniformity may be required only for a limited depth range in which the induced currents mainly flow. (geomagnetic sounding, magnetotelluric sounding in E-polarisation with respect to surface structure).~~

Let U and V be field components of the surface field in the frequency distance domain: $U = U(\omega,R)$, $V = V(\omega,R)$. They are decomposed into the wave-number spectren $\hat{U}(\omega,\underline{k})$, $\hat{V}(\omega,\hat{k})$ according to

$$U(\omega,R) = \int_{-\infty}^{+\infty}\int_{-\infty}^{\infty} \hat{U}(\omega,\underline{k}) e^{i\underline{k}\underline{R}}\, dk_y\, dk_x$$

$$V(\omega,R) = \ldots$$

with

$$\hat{R}(\omega,k) = \frac{\hat{U}(\omega,\underline{k})}{\hat{V}(\omega,\underline{k})}$$

as transfer function between $\hat{A}$ and $\hat{B}$ in the wave number domain, which contains the information about the internal resistivity distribution. A vertical sounding of this distribution is made by considering $\hat{R}$ as a function of frequency, k being fixed, or vice versa.
If the array covers the whole globe, the sphericity of the Earth requires the replacement of the trigonometric functions by spherical harmonics in spherical coordinates (r,θ,λ):

$$U(\omega,\theta,\lambda,r=a) = \sum_{n=1}^{\infty} \sum_{m=o}^{n} U_n^m(\omega)\, P_n^m(\cos\theta) e^{im\lambda}$$

a: Earth's radius; $P_n^m(\cos\theta)$: Associated spherical function. The transfer functions have then the form

$$R_n^m(\omega) = \frac{U_n^m(\omega)}{V_n^m(\omega)}.$$

The first and still basic investigations of the Earth's deep conductivity structure have been carried out by this approach (SCHUSTER, CHAPMAN and PRICE).

If the array of stations covers only a region of limited extent, it may be impracticable to decompose the observed field into wave-spectral components or it may be even impossible because only a small section of the source field structure has been observed. In that case vertical array soundings are carried out preferably with response functions in the frequency-distance domain.

Suppose the source field is quasi-uniform in one horizontal direction, say,

$U = U(\omega,y)$ and $V = V(\omega,y)$. Let

$$R(\omega,y) = \frac{1}{2\pi} \int_{-\infty}^{+\infty} \hat{R}(\omega,k_y) e^{ik_y} \, dk_y$$

be the inverse Fourier transform of $\hat{R}$. Then, if $\hat{V}$ is given by the product of $\hat{R}$ with $\hat{U}$ in the (ω,k) domain, V will be given by a convolution of R with U in the (ω,y) domain:

$$\hat{V}(\omega,k_y) = \hat{R}(\omega,k_y)\cdot U(\omega,k_y) \rightarrow V(\omega,y) = R(\omega,y) \ast U(\omega,y)$$

with $$R \ast U = \int_{-\infty}^{+\infty} R(\omega,y-\eta)\, U(\eta)\, d\eta.$$

If, for instance $E_x = V$ and $H_y = U$, the magnetotelluric relation $\hat{E}_x = \omega\mu_o \, C \, \hat{H}_y$ of the k-ω domain will transform into

$$E_x(\omega,y) = i\omega\mu_o [N(\omega,y) \ast H_y(\omega,y)]$$

with $N(\omega,y)$ as Fourier transform of $C(\omega,k)$. Observe that reversely

$$C(\omega,k) = \int_{-\infty}^{+\infty} N(\omega,y) e^{-iky} \, dy$$

and therefore

$$C(\omega,0) = \int_{-\infty}^{+\infty} N(\omega,y) dy.$$

Hence, if H_y is quasi-uniform within the range of the kernel N,

$$E_x(\omega,y) = i\omega\mu_o \, C(\omega,0) \, H_y(\omega,y)$$

which is the CAGNIARD-TIKHONOV relation commonly used for single site soundings.

In a similar way the magnetic ratio of vertical to horizontal variations can be generalized to

$$H_y(\omega,y) = M(\omega,y) \ast H_y(\omega,y)$$

with $M(\omega,y)$ as Fourier transform of $ik_y \, C(\omega,k_y)$.

The response functions N and M have their highest values close to $y = 0$ and approach zero for distances y which are large in comparison to the modulus of $C(\omega,k=0)$:

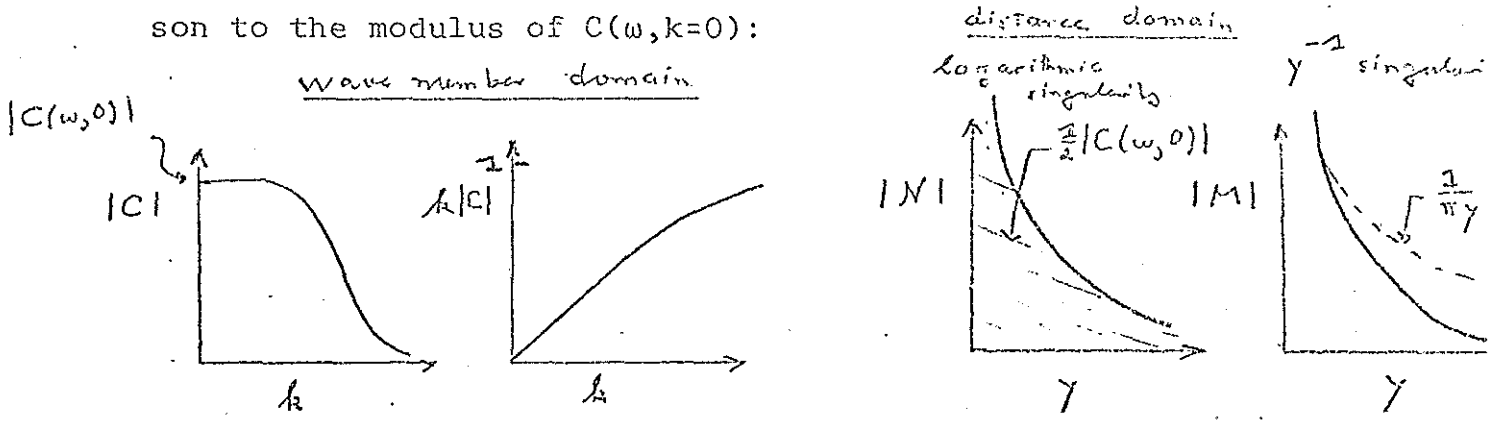

Hence, as to be expected, only the field within a certain distance from the point or area of interest influences the relations between field components used for geomagnetic or magnetotelluric vertical soundings. Consequently, the requirement of a layered structure applies only to this limited depth-distance range as characterized by $|C(\omega,0)|$.

Structural soundings with station arrays: If not only the source field but also the resistivity structure are laterally non-uniform, no generally valid linear relations between normal and anomalous field components exist. In the following it will be assumed that the source field is either quasi-uniform or for a given frequency well represented by a single set of wave numbers. Then the relations between the various field components can be expressed by linear transfer functions in the frequency-distance (ω,R) domain. They can be formulated either for the "normal" horizontal field of the whole array or, if necessary, also for the local horizontal field only. In either case it is necessary to remove from the observed vertical magnetic component its normal part in accordance to the normal resistivity distribution and the source field structure. It is assumed that the normal depth of penetration is small in comparison to the scale length of non-uniformity of the source field, i.e. $H_{nz} << H_{ny}, H_{nx}$ (which implies that) the internal distribution of eddy currents will be independent of the source field structure.

Under these constraints the following linear relations can be formulated:

$$\underline{H}_a = \underline{H} - \underline{H}_n = \begin{pmatrix} H_{ax} \\ H_{ay} \\ H_{az} \end{pmatrix} = \begin{pmatrix} W_{xx} & W_{xy} \\ W_{yx} & W_{yy} \\ W_{zx} & W_{zy} \end{pmatrix} \cdot \begin{pmatrix} H_{nx} \\ H_{ny} \end{pmatrix}$$

$$\begin{pmatrix} E_x \\ E_y \end{pmatrix} = \begin{pmatrix} Z_{xx} & Z_{xy} \\ Z_{yx} & Z_{yy} \end{pmatrix} \cdot \begin{pmatrix} H_{nx} \\ H_{ny} \end{pmatrix}$$

or alternatively

$$H_{az} = A\, H_x + B\, H_y$$

$$\begin{pmatrix} E_x \\ E_y \end{pmatrix} = \begin{pmatrix} Z^*_{xx} & Z^*_{xy} \\ Z^*_{yx} & Z^*_{yy} \end{pmatrix} \cdot \begin{pmatrix} H_x \\ H_y \end{pmatrix} .$$

These sets of transfer functions represent the input for the model calculations to explain the anomalous fields $\underline{H}_a$ or $\underline{E}_a$ in terms of a resistivity anomaly

$$\rho_a(x,y,z) = \rho - \rho_n(z),$$

$\rho_n(z)$ being known.

There exist various constraints about acceptable sets of transfer functions, for examples the functions in either one column of W must describe a magnetic field of solely internal origin as discussed below.

The basic complication in the presence of 3-dimensional structures is due to the fact that the TE and TM mode of the anomalous field cannot be separated. This separation is possible, however, if the resistivity structure is 2-dimensional, say

$$\rho_a = \rho_a(y',z).$$

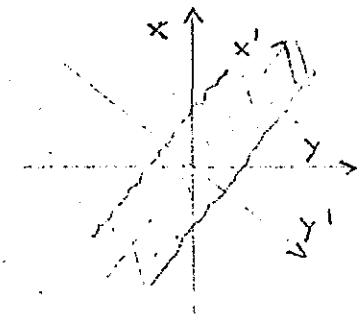

If then the normal E-field is linearly polarised in x'-direction, the anomaly contains only TE modes with $\underline{E}_a$ parallel to x' and $\underline{H}_a$ in planes x'-constant: E-polarisation. If the normal magnetic field is parallel to x', the anomalous field is in the TM mode with zero magnetic fields above the ground. Hence, $\underline{H}_a = 0$ for $z = 0$ and $\underline{E}_a$ lies in planes x'-const.: H-polarisation (cf. Sect. 7.3). The new sets of transfer functions in (x',y',z) coordinates are given by

$$W' = \begin{pmatrix} 0 & 0 \\ 0 & W_{yy'} = W_{n\parallel} \\ 0 & W_{zy'} = W_{z\parallel} \end{pmatrix} \qquad Z' = \begin{pmatrix} 0 & W_{x'y'} = Z_{\parallel} \\ W_{y'x'} = Z_{\perp} & 0 \end{pmatrix}$$

where the subscript ($\parallel$) refers to E-polarisation and the subscript ($\perp$) to H-polarisation. The resulting symmetry relations for W and Z in general (x,y,z) coordinates can be derived as follows: Let

$$T = \begin{pmatrix} c & s \\ -s & c \end{pmatrix} \qquad T_H = \begin{pmatrix} c & s & 0 \\ -s & c & 0 \\ 0 & 0 & 1 \end{pmatrix}$$

be rotation matrices, transforming $\underline{E}$ and $\underline{H}$ from (x,y,z) to (x',y',z) coordinates, $c = \cos\alpha$ and $s = \sin\alpha$:

$$\underline{E}' = \underline{T}\,E \qquad \underline{H}'_h = T\,\underline{H}_n \qquad \underline{H}'_a = T_H\,H_n\,.$$

Since

$$\underline{E}' = Z'\underline{H}'_n = Z'T\underline{H}_n = TZ\underline{H}_n,$$

it follows that

$$Z = T^{-1}\,Z'\,T.$$

In a similar way it is readily verified that

$$W = T_H^{-1}\,W'T.$$

Hence,

$$W = \begin{pmatrix} +\,s^2W_{h\parallel} & -\,scW_{h\parallel} \\ -\,scW_{h\parallel} & c^2W_{h\parallel} \\ -\,s\,W_{z\parallel} & c\,W_{z\parallel} \end{pmatrix} \qquad Z = \begin{pmatrix} -cs\,|Z_{\parallel}+Z_{\perp}| & c^2Z_{\parallel}-s^2Z_{\perp}| \\ c^2Z_{\perp} - s^2Z_{\parallel} & cs\,|Z_{\parallel}+Z_{\perp}| \end{pmatrix}$$

which implies that

$$W_{xx} + W_{yy} = W_{h\parallel} \qquad \text{and} \qquad Z_{xy} - Z_{yx} = Z_{\parallel} - Z_{\perp}$$

are invariant against rotations and that

$$W_{xy} - W_{yx} = 0, \qquad Z_{xx} + Z_{yy} = 0.$$

"Skew" parameters which characterise the deriation from true 2-dimensionality are the moduli of the expressions

$$\frac{W_{xy}-W_{yx}}{W_{xx}+W_{yy}} \qquad \text{and} \qquad \frac{Z_{xx}+Z_{yy}}{Z_{xy}-Z_{yx}}\,.$$

If a geomagnetic sounding at a single site has been performed near such a 2-dimensional structure, the relations which connect A and B with W_{zx} and W_{zy} reduce to

$$-W_{z\parallel}s = A + W_{h\parallel}(As^2 - B\,sc)$$

$$W_{z\parallel}c = B + W_{h\parallel}(Bc^2 - A\,sc).$$

If the first relation is multiplied by c and the second relation by s and then the sum of both is taken, it follows that

$$Ac + Bs = 0 \quad \text{or} \quad B/A = -\,tg\alpha.$$

This implies that the in-phase and out-of-phase induction arrows will be everywhere perpendicular to the trend of the structure, which can thus been found.

In magnetotelluric soundings information about the trend comes from the fact that

$$\frac{-2Z_{xx}}{Z_{xy}+Z_{yx}} = \frac{2\,Z_{yy}}{Z_{xy}+Z_{yx}} = \operatorname{tg} 2\alpha.$$

However, after Z has been rotated into Z' for the thus found angle α, no distinction is possible which one of the off-diagonal elements of Z' refers to E- and H-polarisation. If in addition the direction of the geomagnetic induction arrow is known, such a distinction becomes possible. Furthermore $|Z_{\parallel}| > |Z_{\perp}|$, if the structure is better conducting than its environment and vice versa. Hence, it can be decided whether the induction arrow points toward a well conducting zone or away from a poorly conducting zone.

The distinction between the impedances of E- and H-polarisation is important, if for a first estimate a 1-dimensional interpretation of Z by a layered substratum is made. Such an interpretation may give meaningful results for $Z_{\parallel}$, but in general not for $Z_{\perp}$. A test for the proper choice of the impedance element for a 1-dimensional interpretation comes from the fact that within a given area $Z_{\parallel}$ varies less from place to place than $Z_{\perp}$.

A test for self-consistency of the transfer functions W_h and W_z along a profile y' perpendicular to the strike of a 2-dimensional structure arises from the purely internal origin of the anomaly:

$$W_z = K * W_h \quad \text{and} \quad W_h = -K * W_z$$

where

$$K * f = \frac{1}{\pi} \int_{-\infty}^{+\infty} f(\eta')/(y'-\eta')\,d\eta'$$

denotes a convolution of W_h (or W_z) with the kernel function $1/\pi y$.

8.3 Spectral Analysis of Geomagnetic Induction Data

The objective of the data reduction in the frequency domain is the calculation of transfer functions. They linearly relate functions of frequency for a field component Z to one or more other field components X, Y, ... Let Z(t), X(t) and Y(t) be the observed time variations of Z, X, Y during a time intervall of length T either from

the same or from different sites. Let $\tilde{Z}(\omega)$, $\tilde{X}(\omega)$, $\tilde{Y}(\omega)$ be the Fourier transforms of Z(t), X(t) and Y(t). Then a linear relation of the form

$$\tilde{Z}(\omega) = \tilde{A}(\omega)\,\tilde{X}(\omega) + \tilde{B}(\omega)\,\tilde{Y}(\omega) + \delta\tilde{Z}(\omega)$$

is established in which $\tilde{A}$ and $\tilde{B}$ represent the desired transfer functions between Z on the one side and X and Y on the other side; $\delta\tilde{Z}$ is the uncorrelated "noise" in Z, assuming X and Y to be noise-free.

As the best fitting transfer functions will be considered those which produce minimum noise $< |\delta\tilde{Z}|^2 >$ in the statistical average. Here the average is to be taken either over a number of records or within extended frequency bands of the width $\overline{\Delta f}$ which is L times greater than the ultimate spacing 1/T of individual spectral estimates. The noise: signal ratio defines the residual $\varepsilon(\omega)$, the ratio of related to observed signal the coherence $R(\omega)$:

$$\varepsilon^2 = \frac{<|\delta\tilde{Z}|^2>}{<|\tilde{Z}|^2>} \qquad R^2 = 1 - \varepsilon^2 \ .$$

The coherence in conjunction with the degree of freedom of the averaging procedure establishes confidence limits for the transfer functions $\tilde{A}$ and $\tilde{B}$.

The averaged products of Fourier transforms are denoted as

$S_{zz} = < \tilde{Z}\,\tilde{Z}^{*} >$: power spectrum of Z.

$S_{zy} = < \tilde{Z}\,\tilde{Y}^{*} >$: cross spectrum between Z and Y

with $S_{zy} = S^{*}_{yz}$.

In summary, the data reduction involves the following steps

(a) Fourier transformation of time records
(b) Calculations of power and cross-spectra
(c) Calculation of transfer functions
(d) Calculation of confidence limits for the transferfunctions.

Steps (a) and (b) can be substituted by the following alternatives:

(a^{*}): Calculate auto-correlation functions $R_{zz}(\tau)$, ... and cross-correlation functions $R_{zy}(\tau)$, ... with τ being a time lag, $\tau_{max} << T$:

$$R_{zz}(\tau) = \int_T Z(\tau-t)\, Z(t)dt$$

$$R_{zy}(\tau) = \int_T Z(\tau-t)\, Y(t)dt$$

with $0 < \tau < \tau_{max}$.

(b^*): Take the Fourier transforms of the correlation functions and obtain as in (b) power- and cross-spectral estimates, if the averaging is done within frequency bands of the width $\overline{\Delta f}$. There is a formal correspondence between the maximum lag τ_{max} and $\overline{\Delta f}^{-1}$.

The actual performance of the steps (a) to (d) with one or more sets of records is now described in detail.

a. Fourier transformation. The time series and their spectra are given, respectively to be found, at discrete values of t and ω, which are equally spaced in time and frequency. Let Z_n etc. be an instantenuous value of Z(t) for $t = t_n$, $n = 0,1,2, \ldots N$ with $\Delta t = t_{n+1} - t_n$. Outside of the record, extending from t_o to t_N, Z(t) is assumed to be zero.
Let Z_m be the Fourier transform of Z(t) for the frequency $f = f_m$. Because of the finite length T of the record the lowest resolvable frequency and thereby the frequency spacing will be given by $T^{-1} = \Delta f = f_1$ and f_m has to be a multiple of Δf. Because Z(t) is given at discrete instances of time, Δt apart, the highest resolvable frequency, called the Nyquist frequency, will be the reciprocal of $(\Delta t \cdot 2)$, i.e.

$$f = f_m, m = 0,1,2, \ldots M \quad \text{with } f_{m+1} - f_m = \Delta f$$

and $$f_M = \frac{1}{2\Delta t} = M\Delta f.$$

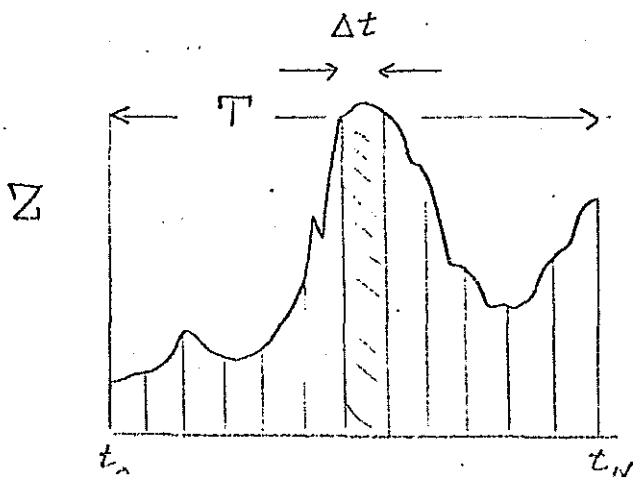

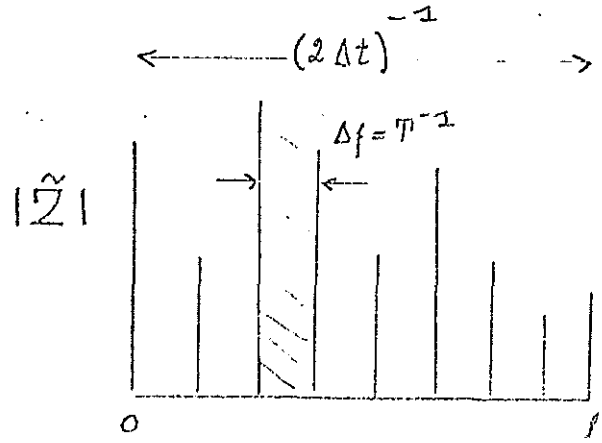

The Fourier integral

$$\tilde{Z}(\omega_n) = \int_{-\infty}^{+\infty} Z(t)e^{-i\omega_n t}\,dt = \int_{0}^{T} Z(t)e^{-i\omega_n t}\,dt$$

will be evaluated numerically according to the trapezoidal formula of approximation. Setting

$$Z_o = \frac{1}{2}[Z(t_o) + Z(t_N)]$$

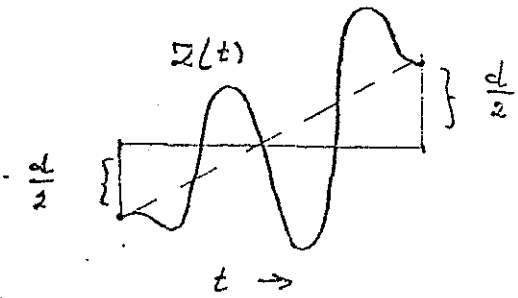

and observing that

$$\omega_m t_n = 2\pi f_m t_n = \frac{2\pi mn}{N}$$

the discrete Fourier transform of Z(t) is

$$\tilde{Z}_m = \Delta t \left\{ \sum_{n=1}^{N-1} Z_n \left(\cos \frac{2\pi nm}{N} - i \sin \frac{2\pi nm}{N}\right)\right\} \quad m = 0,1, \ldots M$$

A linear trend of the record within the chosen interval may be written as

$$Z'(t) = \frac{d}{T}\left(t - t_o - \frac{T}{2}\right) \qquad t_o < t < t_N$$

with $$d = Z(t_N) - Z(t_o).$$

A correction for this trend in the frequency domain implies that the imaginary Fourier transform of Z'(t),

$$\tilde{Z}'(f_m) = (-1)^{m-1}\, i\, \frac{dT}{2\pi m} \quad m = 1,2, \ldots M$$

is substracted from $\tilde{Z}_m$.

A second correction arises from the fact that Z(t) does not vanish necessarily outside of the chosen intervall. In that case the original time function can be multiplied in the time domain with a weight function W(t) which is zero for $t < t_o$ and $t > t_N$. The Fourier transform of the product

$$W(t) \cdot Z(t)$$

is given by a convolution of $\tilde{Z}$ with the Fourier transform of W:

$$\tilde{W}(\omega) * \tilde{Z}(\omega) \simeq \frac{1}{T} \sum_{\hat{m}} \tilde{W}_{m-\hat{m}}\, \tilde{Z}_{\hat{m}} .$$

A frequently used weight function is

$$W(t) = \frac{1}{2}\left[1 + \cos \frac{2\pi}{T}(t - t_o - \frac{T}{2})\right]$$

which has the Fourier transform

$$\tilde{W}(f=f_m) = \begin{cases} \frac{T}{2} & \text{for } m = 0 \\ \frac{T}{4} & \text{for } m = 1 \\ 0 & \text{for } m \geq 1 \end{cases}$$

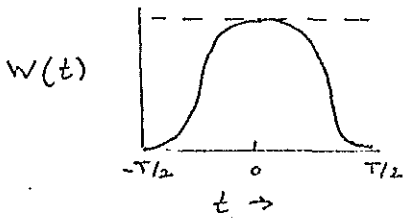

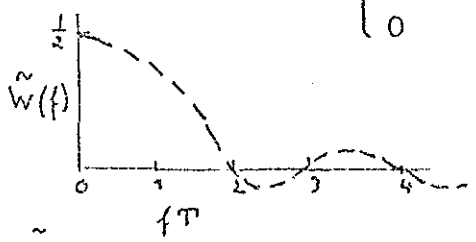

The convolution of $\tilde{W}$ with descrete values of $\tilde{Z}$ reduces then to

$$\langle \tilde{Z}_m \rangle = \frac{1}{T} \sum \tilde{W}_{m-\hat{m}} \cdot \tilde{Z}_{\hat{m}} = \begin{cases} \frac{1}{2}(\tilde{Z}_0 + \tilde{Z}_1) & m = 0 \\ \frac{1}{2}\tilde{Z}_m + \frac{1}{4}(\tilde{Z}_{m+1} + \tilde{Z}_{m-1}) & m = 1, 2, \ldots M-1 \\ \frac{1}{2}(\tilde{Z}_{M-1} + \tilde{Z}_M) & m = M \end{cases}$$

where $\langle \tilde{Z}_m \rangle$ is the discrete Fourier transform of $W(t) \cdot Z(t)$. This smoothing procedure of the original spectrum is called "hanning" after Julius von Hann.

In certain cases it will be necessary to apply a numerical filter to the time series to be analysed before the Fourier transformation. This filtering process consists in a convolution of $Z(t)$ with a filter function $W(t)$ in the time domain and thus corresponds to a multiplication of $\tilde{Z}$ with $\tilde{W}$ in the frequency domain. But because the filtering procedure is intended to prepare the time series for the Fourier transformation it must be carried out in the time domain. If W_n denotes the filter weight for $t = t_n$, the discrete form of the convolution is

$$W \times Z = \sum_{-n_{Max}}^{+n_{Max}} W_{n-\hat{n}} \cdot Z_{\hat{n}} .$$

Usually even filters are employed, $W(t) = W(-t)$, to preserve the correct phase of the Fourier components. The transform of W is chosen in such a way that it acts as a heigh-, low- or bandpass filter for frequency-independent (="white") spectra:

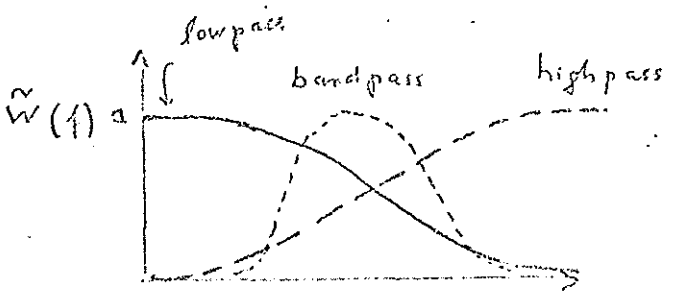

The weight function W is then found by calculating in Fourier transform of $\tilde{W}$:

$$W = \frac{1}{2\pi} \int_{-\infty}^{+\infty} \tilde{W}\, e^{+i\omega t}\, d\omega \ .$$

The purpose of filtering the time series before making a Fourier transformation is

(a) a prewhitening of the spectrum, levelling off peaks and compensating spectral trends

(b) a reduction of unwanted larger spectral values close to zero frequency, arising from a background trend in the time series

(c) a suppression of spectral power beyond the Nyquist frequency to avoid "aliasing". Spectral values for the frequencies

$$f_{2M-r},\ f_r \text{ and } f_{3M-r},\ f_{M+r},\ f_{M-r} \text{ etc.}$$

are undistinguishable (r = 0,1,2, ..., M-1):

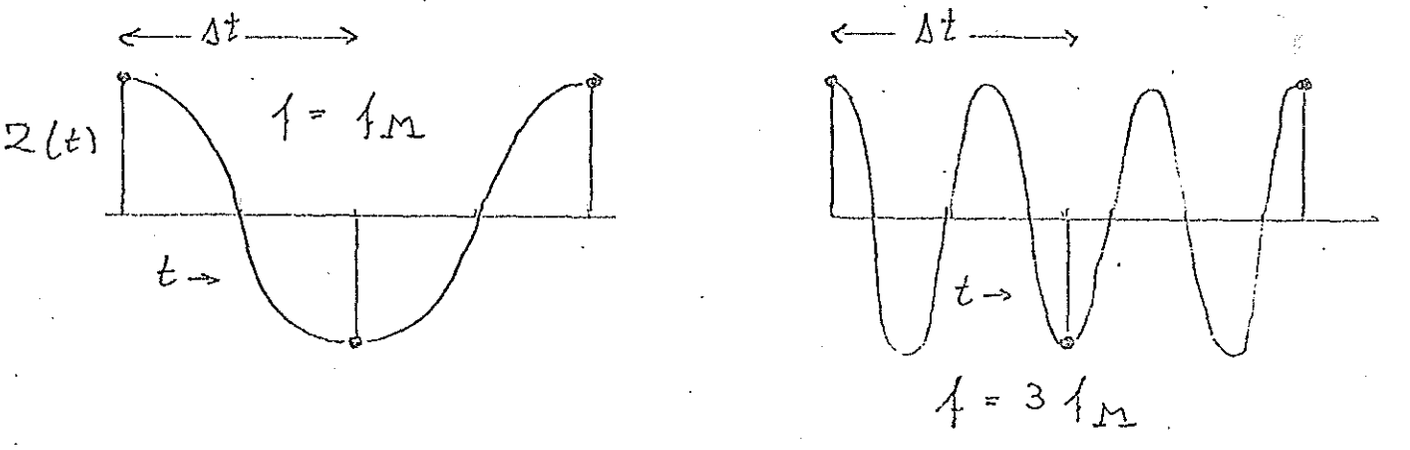

b. Calculation of power and cross spectra: Let P_m denote a product $\tilde{Z}_m Z_m^*$, $\tilde{Z}_m \tilde{Y}_m^*$ etc. for a frequency f_m, m = 1,2 ....M. The calculation of power and cross spectral estimates from real data requires that such products are averaged with a certain degrees of freedom, ν. Suppose that the available record length just gives the desired resolution $\Delta f = T^{-1}$ for the transfer functions to be determined. In this case spectral products P_m have to be derived for a number of individual records and then to be averaged. Average the spectral products and not the spectral values! The resulting mean value

$$S_m = \langle P_m \rangle$$

is the desired power or cross spectral estimate. If L records have been used, ν = 2L because the sine- and cosine transforms of the time series contribute independently to the calculations of S_m.

If the record length T allows a frequency resolution $\Delta f = T^{-1}$ which is much smaller than a meaningful resolution $\overline{\Delta f}$ for the transfer functions under consideration, then P_m can be averayed over $L = \overline{\Delta f}/\Delta f$ spectral values within (M/L-1) frequency bands of width $\overline{\Delta f}$ between $f_o = 0$ and $f_M = M\Delta f$.
Taking the average of P_m within frequency bands implies that a numerical filter Q(f) is applied to P(f), yielding the desired power-cross spectrum by convolution:

$$S_m = Q * P \approx \Delta f \sum_{-M}^{+M} Q_{m-\hat{m}} P_{\hat{m}}$$

($P_{-m} = P_m^*$). The filters to be used are even functions of f, bell-shaped and with zero values outside a range which is smaller then M Δf. Setting Q(f) = 0 för $f > f_Q$,

$$S_m = \Delta f \{ \sum_{\hat{m}=1}^{m_Q} Q_{\hat{m}} (P_{m+\hat{m}} + P_{m-\hat{m}}) + Q_o P_m \} .$$

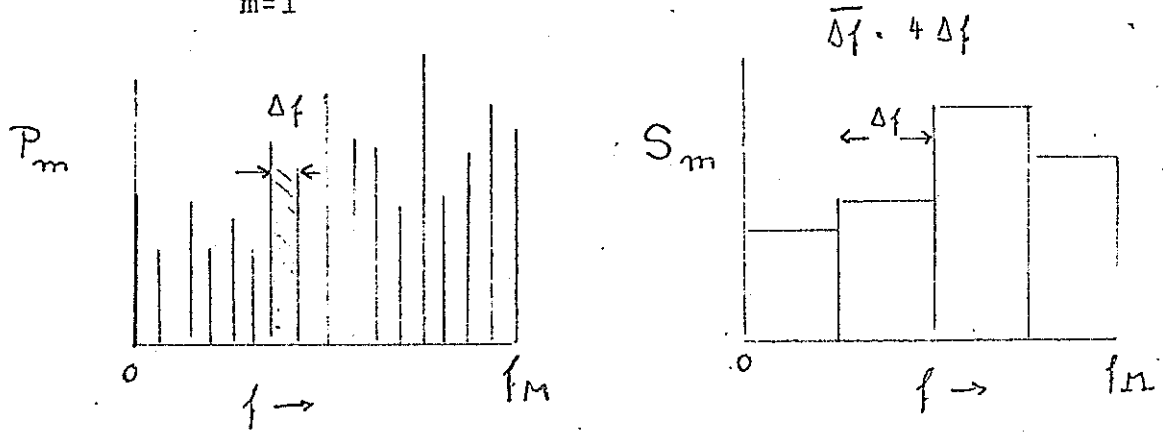

The resulting smoothed spectral estimates S_m have been derived with roughly $L = \overline{\Delta f}/\Delta f$ degrees of freedom. The effective degrees of freedom ν may be somewhat smaller, depending on the frequency dependence of the filter. They are defined as

$$\nu = \frac{2\ \mathrm{var}(u)}{\mathrm{var}\ (uq)}$$

where var(u) denotes the variance (=dispersion) of a random variable u(f) and var(uq) the variance of Q * u, hence

$$\nu = \frac{2}{\int_{-\infty}^{+\infty} Q^2(f)\,df} .$$

Two convenient filters are

the Parzen filter $Q(f) = \frac{3}{4}\,\tau\,(\frac{\sin x}{x})^4$,

the Bartlett filter $Q(f) = \frac{1}{2}\,\tau\,(\frac{\sin x}{x})^2$

with $x = \frac{\pi}{2}\,f\,\tau$. The bandwidth is given by τ^{-1} (Parzen filter), respectivity by $2/\tau$ (Bartlett filter). For the Parzen filter the degrees of freedom are $\nu = 1.84\ L$ and $f_Q = 2/\tau$.

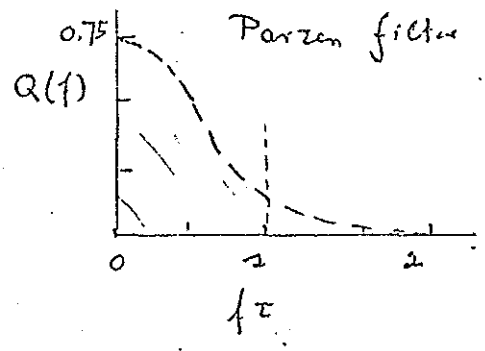

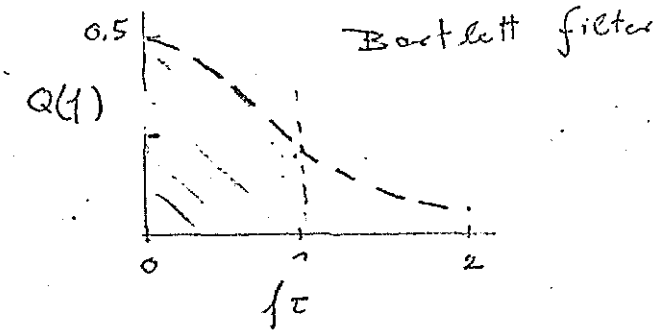

c. Calculation of transfer functions

The non-correlated part of $\tilde{Z}_n$ is

$$\delta\tilde{Z}_m = \tilde{Z}_m - \tilde{A}_m \tilde{X}_m - \tilde{B}_m \tilde{Y}_m$$

for the frequency f_m. In the average over L adjacent frequencies or L individual records the power-spectrum of the non-correlated part in Z shall be a minimum:

$$S_{\delta z \delta z} = < (\delta\tilde{Z}_m \cdot \delta\tilde{Z}_m^{*}) > = \text{Min!}$$

Hence, the derivatives of $S_{\delta z \delta z}$ with respect to the real and imaginary parts of the transfer functions $\tilde{A}_m$ and $\tilde{B}_m$ have to be zero:

$$\frac{\partial S_{\delta z \delta z}}{\partial \mathrm{Re}(A_n)} + i\frac{\partial S_{\delta z \delta z}}{\partial \mathrm{Im}(A_n)} = <(z - A_n X - B_n Y)X^{*}> = 0 \qquad \text{etc.}$$

$$\begin{pmatrix} S_{xx} & S_{yx} \\ S_{xy} & S_{yy} \end{pmatrix} \cdot \begin{pmatrix} A \\ B \end{pmatrix} = \begin{pmatrix} S_{zx} \\ S_{zy} \end{pmatrix}$$

using the notations as introduced above. The subscripts m are ommitted Elimination of either $\tilde{A}$ or $\tilde{B}$ yields the basic formulaes for the determination of transfer functions in geomagnetic and magnetotelluric soundings:

$$\tilde{A} = \frac{S_{zx}S_{yy} - S_{zy}S_{yx}}{S_{xx}S_{yy} - |S_{xy}|^2}$$

$$\tilde{B} = \frac{S_{zy}S_{xx} - S_{zy}S_{xy}}{S_{xx}S_{yy} - |S_{xy}|^2} .$$

The coherence can be derived from

$$R^2 = (\tilde{A}S_{xz} + \tilde{B}S_{yz})/S_{zz}$$

as it is readily seen from

$$S_{\delta z \delta z} = S_{zz} - \tilde{A}S_{xz} - \tilde{B}S_{yz}.$$

If only a relation between Z and X or Y is sought or if X and Y are linearly independent ($S_{xy} = 0$), then the above derived relations reduce to

$$\tilde{A} = \frac{S_{zx}}{S_{xx}} \qquad \tilde{B} = \frac{S_{zy}}{S_{yy}}$$

$$R^2 = \frac{|S_{zx}|^2}{S_{xx}S_{zz}} \qquad R^2 = \frac{|S_{zy}|^2}{S_{yy}S_{zz}}$$

$$R^2 = \frac{S_{yy}|S_{zx}|^2 + S_{xx}|S_{zy}|^2}{S_{xx}S_{yy}S_{zz}}$$

d. Calculation of confidence limits for the transfer functions

In order to establish confidence limits for the transfer functions $\tilde{A}$, $\tilde{B}$ of the previous section it is necessary to find the probability density function ("pd f") of their deviations from their "true" values $\tilde{A}_0$, $\tilde{B}_0$. We assume that estimates of $\tilde{A}$ and $\tilde{B}$ according to the least-square method of the previous section are without bias, i.e. without systematic errors (E = expected value):

$$E(\tilde{A}) = \tilde{A}_0, \qquad E(\tilde{B}) = \tilde{B}_0.$$

Henceforth, random variables will be written with capital letters

(e.g. X), their realizations by observation with lower case letters (e.g. x), and their true values with the subscript "0" (e.g. x_o).

Let f(X) be the pdf of a variable X. Then the probability that a realisation x exceeds a value G is

$$\alpha = \int_G^\infty f(X)dX.$$

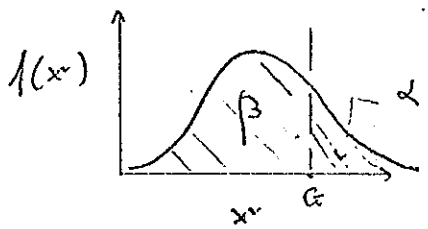

Hence, there is a "confidence" of $\beta = (1-\alpha) \cdot 100\%$ that x does not exceed G.

The following pdf's will be needed in this section:

(1) The "Gaussian Normal Distribution" of a normalized variable with the dispersion 1 and zero mean value:

$$f_N(0,1^2) = \frac{1}{\sqrt{2\pi}} e^{-x^2/2}$$

(2) The χ^2-distribution for ν degrees of freedom:

$$f_\chi(r) = \frac{1}{(\frac{\nu}{2} - 1)!} (\frac{\chi^2}{2})^{\frac{\nu}{2}-1} e^{-\frac{\chi^2}{2}}$$

(3) The Fisher-distribution for ν_1 and ν_2 degrees of freedom:

$$f_F(\nu_1,\nu_2) = \frac{(\frac{\nu_1+\nu_2}{2} - 1)! \nu_1^{\frac{\nu_1}{2}} \nu_2^{\frac{\nu_2}{2}} F^{(\frac{\nu_1}{2}-1)}}{(\frac{\nu_1}{2} - 1)!(\frac{\nu_2}{2} - 1)!(\nu_2 + \nu_1 F)^{(\nu_1+\nu_2)/2}}.$$

These distributions are encountered in the following problems: Consider a random variable X which is normally distributed with a dispersion

$$s_o^2 = E(|X - x_o|^2) = var(X).$$

Let

$$\bar{x} = \frac{1}{n} \sum_{i=1}^{n} x_i$$

be the realized sample mean value of n realizations of X. These mean values are also normally distributed with the dispersion

$$E(|\bar{X} - x_o|^2) = \frac{1}{n^2} \sum_i var(X) = \frac{s_o^2}{n}$$

according to the "central limit theorem".

Let

$$s^2 = \frac{1}{n-1} \sum_i (x_i - \bar{x})^2$$

be the realized dispersion within a sample of n observations. Then the normalized dispersion

$$U = \frac{(n-1)S^2}{s_o^2}$$

will be a random variable with a χ^2 distribution for $\upsilon = n-1$ degrees of freedom. Let S_1^2 and S_2^2 be the dispersions within samples of n_1 and n_2 observations of two different variables X_1 and X_2. Then the ratio of their normalized dispersions

$$F = \frac{S_1^2/s_{o1}^2}{S_2^2/s_{o2}^2}$$

will have a Fisher-probability density distribution $f_F(n-1,n-2)$.

We regard now the Fourier transforms $\tilde{Z}$, $\tilde{X}$, $\tilde{Y}$ as random variables Z, X, Y and denote their realization for a single record or a single frequency component as x, y, z. In a similar way, a and b shall be the realized transfer functions for a limited number of records or a limited frequency band $\overline{\Delta f}$, their true values being a_o and b_o. We assume now that Z depends linearly only on X and that X is observed error-free:

$$E(X) = x_o$$

Then

$$z = a_o x_o + \delta z_o$$

δz_o is the "realized" not correlated part of z for a single record. The variable Z shall be normally distributed with the dispersion

$$\text{var } (Z) = s_o^2,$$

which will be also the dispersion of δZ:

$$E(ZZ^*) = E(\delta Z\ \delta Z^*) = s_o^2$$

By minimizing the uncorrelated power $\langle \delta Z \delta Z^* \rangle = S_{\delta Z \delta Z}$ for a number of records or for a number of frequency lines within a frequency band of the width $\overline{\Delta f}$ a realization of the transfer function A is obtained:

$$a = \frac{\langle Z\ X^* \rangle}{\langle X\ X^* \rangle}$$

Observe that the residual, of which the power has been brought to a minimum, is

$$\delta z = a x_o - z$$

in contrast to the "true" residual

$$\delta z_o = a_o x_o - z.$$

The random variable

$$U = \frac{n \langle |\delta z_o|^2 \rangle}{s_o^2}$$

has a χ^2-distribution with n degrees of freedom, where n is the number of records or the number of lines used to obtain the average.

If a variable U with a χ^2-distribution of ν degrees of freedom is decomposed into two components U_1 and U_2,

$$U = U_1 + U_2,$$

U_1 and U_2 will be likewise χ^2-distributed and the sum of their degrees of freedom will be ν:

$$\nu = \nu_1 + \nu_2.$$

This decomposition will be carried out now with U as defined above: Clearly,

$$\langle |\delta Z_o|^2 \rangle = \langle |Z - a_o x_o|^2 \rangle = \langle |Z - Ax_o + (A - a_o)x_o|^2 \rangle.$$

The power of the averaged residual has been minimised by setting

$$\langle (Z - Ax_o) x_o^* \rangle = 0.$$

Hence,

$$\langle |\delta Z_o|^2 \rangle = \langle |\delta Z|^2 \rangle + |A - a_o|^2 \langle |x_o|^2 \rangle + 0,$$

implying that

$$U_1 = \frac{\langle |\delta Z|^2 \rangle n}{s_o^2}$$

has a χ^2-distribution of n - 2 degrees of freedom because

$$U_2 = \frac{n}{s_o^2} |A - a_o|^2 \langle |x_o|^2 \rangle$$

must be a χ^2-distribution of 2 degrees of freedom in view of the real and imaginary part of $(A - a_o)$. The ratio

$$F = \frac{U_2/2}{U_1/(n-2)} = \frac{|A-a_o|^2 \; <|x_o|^2>}{<|\delta Z|^2>} \cdot \frac{n-2}{2}$$

has a Fisher-distribution $f_F(2, n-2)$. Using the notations from above,

$$<|\delta Z|^2> = S_{\delta z \delta z} = \varepsilon^2 \, S_{zz}$$

$$<|x_o|^2> = S_{xx},$$

and observing that

$$|A|^2 = \frac{|S_{zx}|^2}{(S_{xx})^2} = R^2 \cdot \frac{S_{zz}}{S_{xx}}$$

with $R^2 = |S_{zx}|^2/(S_{zz} \cdot S_{xx})$, the Fisher-distributed ratio becomes

$$F = \frac{n-2}{2} \; \frac{|A-a_o|^2}{|A|^2} \; \frac{R^2}{\varepsilon^2} .$$

We have found now the pdf of the deviation of A from its true value to be in terms of its modulus

$$|A - a_o| = |A| \; \frac{\varepsilon}{R} \sqrt{\frac{2}{n-2} F} .$$

Let

$$\beta = \int_o^G f_F(2, n-2)dF$$

be the probability that F does not exceed the value F = G, observing that f_F is a one-sided pdf. Then there will be the probability β that the modulus of A lies within the confidence limits

$$|\Delta A_\beta| = |A| \; \frac{\varepsilon}{R} \sqrt{\frac{2}{n-2} G}$$

in the complex plane.

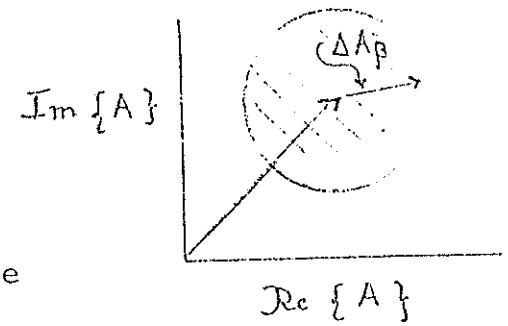

The threshold value G for a desired value of β can be obtained in closed form because

$$f_F(2, n-2) = \left(\frac{m}{m+F}\right)^{m+1} \text{ with } m = \frac{n-2}{2}.$$

Hence,

$$\beta = \int_o^G f_F(2, n-2)dF = 1 - \left(\frac{m}{m+G}\right)^m$$

or $$\frac{2}{n-2} G = \frac{1}{(1-\beta)^{1/m}} - 1 .$$

Example: $n = 12$ and $\beta = 95\%$:

$$\frac{2}{n-2} G = 20^{\frac{1}{5}} - 1 = 0.82$$

or $$|\Delta A_\beta| = |A| \cdot \frac{\varepsilon}{R} \cdot 0.91$$

$n = 12$ and $\beta = 99\%$: $\sqrt{\frac{2}{n-2} G} = \sqrt{100^{\frac{1}{5}} - 1} = \sqrt{1.5} = 1.22$

$n = 12$ and $\beta = 50\%$: $\sqrt{\frac{2}{n-2} G} = \sqrt{2^{\frac{1}{5}} - 1} = \sqrt{.15} = 0.39$

For large n and $m >> \ln\gamma$ ($\gamma = \frac{1}{1-\beta}$), the following approximations are valid:

$$\frac{2}{n-2} G \simeq \frac{2}{n} \ln\gamma$$

$$|\Delta A_\beta| = |A| \frac{\varepsilon}{R\sqrt{n}} \cdot \sqrt{\ln\gamma^2} .$$

This approximation exemplifies the general propagation-of-error law, namely that the errors are reduced proportional to the square root of the number of observations.

In the more general case that Z depends on X and Y with a non-zero coherence between X and Y confidence limits can be obtained in a similar way: Let

$$z = a_o x_o + b_o y_o + \delta z_o ,$$

assuming that now X and Y are realized error free. Then the Fisher-distributed ratio, involving the deviation of A and B from a_o and b_o, turns out to be

$$F = \frac{|A-a_o|^2 S_{xx} + (B-b_o|^2 S_{yy} + Re\{2S_{xy}(A-a_o)(B-b_o)^*\}}{\varepsilon^2 S_{zz}} \frac{n-4}{4}$$

which has a $f_F(4, n-4)$ distribution. The confidence limits for A and B cannot be calculated individually, unless of course S_{xy} is taken to be zero. On the other hand, if we assume that $|A-a_o|$ and $|B-b_o|$ are equal, then

$$F = |A-a_o|^2 \frac{S_{xx} + S_{yy} + Re\{2S_{xy}\}}{\varepsilon^2 S_{zz}} \frac{n-4}{4}$$

which allows the determination of combined confidence limits for A and B. The threshold value of F for a given probability β can be derived from

$$1-\beta = \frac{1}{(1+\frac{2}{m}G)^m}\left(1+\frac{2G}{1+\frac{2}{m}G}\right) \approx \left(\frac{m}{m+2G}\right) \text{ with } m = \frac{n-4}{2}.$$

8.4. Data analysis in the time domain, pilot studies

Suppose the time functions to be related linearly to each other are not oscillatory but more like a one-sided asymtotic return to the undisturbed normal level after a step-wise deflection from it:

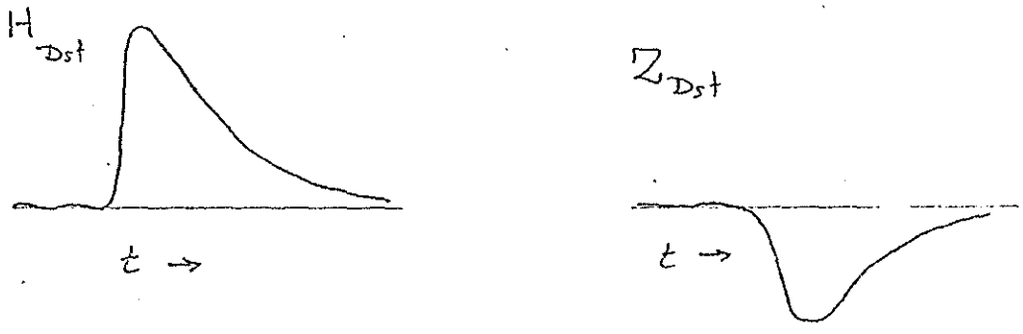

It may then be preferable to avoid a Fourier transformation and to derive inductive response functions in the time domain.

If Z depends linearly only on X, i.e.

$$\tilde{Z}(\omega) = A(\omega) \cdot \tilde{X}(\omega) + \delta Z(\omega)$$

in the frequency domain, then Z(t) will be derived from X(t) in the time domain by a convolution of X(t) with the Fourier transform of A,

$$A(t) = \frac{1}{2\pi}\int_{-\infty}^{+\infty} \tilde{A}(\omega)\, e^{i\omega t}\, d\omega.$$

Since Z(t) cannot depend on X(t) at some future time $\tau > t$, the response function A(t) must be zero for $t < 0$, yielding

$$Z(t)-\delta Z(t) = A(t)*X(t) = \int_{-\infty}^{t} A(t-\tau)\cdot X(t)\,d\tau = \int_{0}^{\infty} A(t')X(t-t')\,dt' .$$

As a consequence, the real and imaginary part of $\tilde{A}(\omega)$ will be related as functions of frequency by a dispersion relation:

$$Re(\tilde{A}) = K \ast Im(\tilde{A})$$

with $K(\omega) = \frac{1}{\pi\omega}$.

The time-domain response A(t) is now determined from a given record of Z(t) between t = 0 and t = T by minimizing $\{\delta Z(t)\}^2$ within this intervall:

$$\int_0^T \{Z(t) - \int_0^\infty A(t') \, X(t-t')dt'\}^2 dt = \text{Min!}$$

It is assumed that X(t) is known also for t < 0. Differentation with respect to $A(t=\hat{t})$ gives

$$\int_0^\infty A(t')\{\int_0^T X(t-t')\cdot X(t-\hat{t})dt\}dt' = \int_0^T Z(t) \, X(t-\hat{t})dt.$$

Let again $Z_n = Z(t = n\cdot\Delta t)$ denote the value of Z at equally spaced instances and let $A_{n'}$ be the value of A(t') for $t' = n'\Delta t$. Then the replacement of the integrals by sums yields a system of linear equations for the determination of the $A_{n'}$, $n' = 0,1, \ldots N$:

$$\sum_{n'=o}^{N'} A_{n'} \{\sum_{n=o}^{N} X_{n-n'} \, X_{n-\hat{n}}\} = \sum_{n=o}^{N} Z_n \, X_{n-\hat{n}}$$

for $\hat{n} = 0,1,2, \ldots \hat{N}$.

Chosing $N < \hat{N}$, the response values can be determined by a least-square fit. Otherwise a generalized inversion of the system of equations can be performed.

Consider the limiting cases that

(1) the frequency response is real and independent of frequency,

(2) the frequency response is imaginary and proportional to ω^{-1}:

$$\tilde{A}_1 = a_o \,. \qquad\qquad \tilde{A}_2 = \frac{b_o}{i\omega}$$

The first case is realized by the inductive scale length C_n above a perfect conductor at the depth $z^\ast$ or by the impedance for a thin

sheet of the conductance τ above a non-conducting substratum: $C_n = z^*$, $Z_n = 1/\tau$. The second case can be realized by the same models, interchanging C_n and Z_n (cf. Sec. 9.1):

$$C_n = \frac{1}{i\omega\mu_o\tau} \; , \qquad Z_n = \frac{h}{i\omega\mu_o} \; .$$

The Fourier transforms of $\tilde{A}_1$ and $\tilde{A}_2$ are

$$A_1(t) = a_o \, \delta(t-0) \qquad\qquad A_2(t) = b_o \int_{-\infty}^{\infty} \frac{\sin\omega t}{\omega} = \mathrm{sgn}(t)\pi b_o$$

$$\text{or} \qquad A_2(t) = \frac{1}{2}\pi b_o \left[1 + \mathrm{sgn}(t)\right].$$

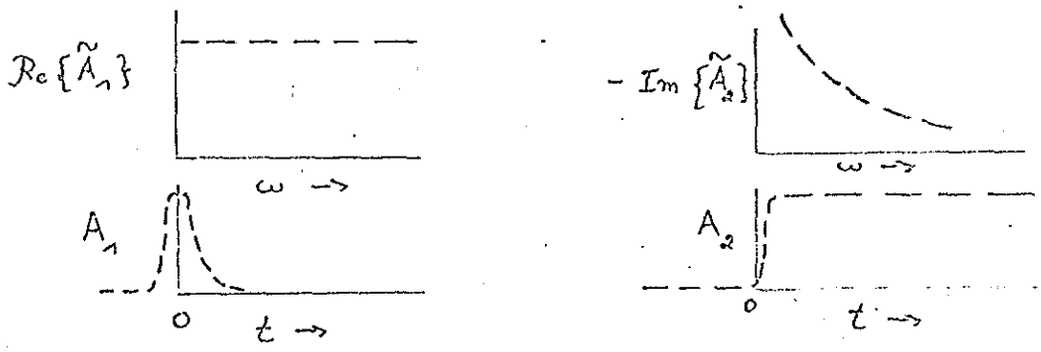

Hence, in the first case Z depends on X at the same instance of time only, in the second case on X with equal weight during the entire past:

$$Z_1(t) = a_o H_1(t) \qquad\qquad Z_2(t) = \pi b_o \int_{-\infty}^{t} X(t')dt'$$

These simple relations are very useful to conduct a pilot reduction of sounding data. Case (1) applies to magnetotelluric soundings in sedimentary basins, underlain by a crystalline basement, to vertical geomagnetic soundings with very long periods, reaching the conductive part of the mantle, and to structural geomagnetic soundings where the perturbed flow of induction currents is in-phase with the normal magnetic field.

The basic linear relation for structural geomagnetic soundings can be written then simply by products in the time domain:

$$H_{az}(t) = A \cdot H_x(t) + B \cdot H_y(t).$$

This relation implies that the local geomagnetic disturbance vector $\underline{H} = (H_x, H_y, H_{az})$ lies at all instances of time in a plane which is fixed in space. The intersecting line q of this plane with the (x,y)-plane gives that polarisation of the normal field vector, for which no anomalous vertical variations are produced. In the case of 2-dimensional structures, this would be the direction of their trends (cf. Sect. 8.2).

Various graphical methods have been developed to find the orientation of this "preferred plane" for the local geomagnetic disturbance vector. In a "Parkinson-plot" the orientation of this vector is displayed for individual events on a unit sphere. They tend to fall onto a plane intersecting the sphere. The projection of the unit vector normal to this plane defines the length and direction of the "Parkinson induction arrow" at the considered site. The orientation is chosen in such a manner that a horizontal disturbance in the direction of the induction arrow is connected with a positive (=downward) anomalous H_{az}:

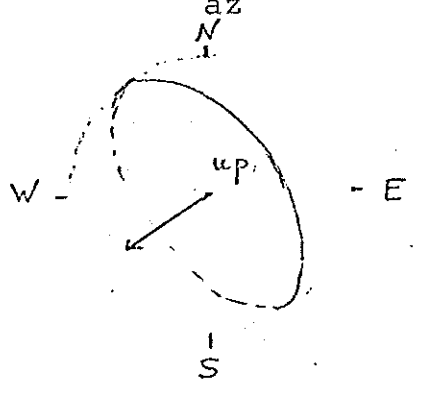

For the construction of a "Wiese-diagram" the ratios

$$u = \frac{H_x}{H_{az}} \quad \text{and} \quad v = \frac{H_y}{H_{az}}$$

are plotted in (x,y)-coordinates for individual events, u in x-direction and v and y-direction. The points (u,v) tend to fall onto a straight line, having the equation

$$1 = A \cdot u + B \cdot v,$$

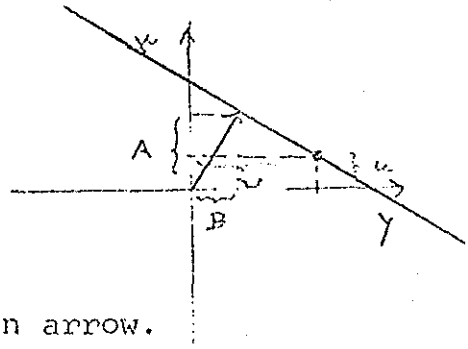

from which the coefficents A and B can be calculated. The "Wiese-induction" arrow with A as x-component and B as y-component is opposite to the Parkinson arrow.

In an "Untiedt diagram" the endpoints of the horizontal disturbance vector ($H_x H_y$) are drawn as a curve in (x,y)-coordinates during a single event. Lines which connect time instances of equal vertical disturbance H_{az} will then be parallel to the intersecting line of the preferred plane with the (x,y)-plane. The "induction arrows" are normal to these lines and their length is given by the ratio of H_{az} to the simultaneous horizontal disturbance vector, projected onto the direction normal to the connecting lines.

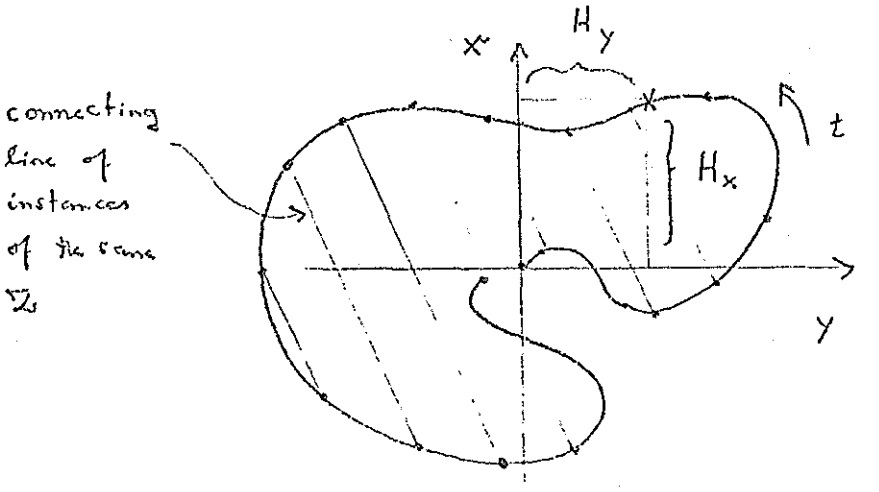

Parkinson and Wiese diagrams which utilize the H_{az}, H_x, H_y relations of numerous individual events can be employed also in the case of 2-dimensional structures with an anomalous field which is not exactly in-phase with the normal field. Then more or less sinusoidal variations are chosen with readings at well defined times, e.g. at the time of maximum deviation of H_{az} from the undisturbed level.

9. Data interpretation on the basis of selected models

9.1 Layered Half-space

The interpretation of geomagnetic sounding data by a layered resistivity distribution $\rho = \rho_n(z)$ is appropiate at those single sites or for those arrays which do not show anomalous magnetic Z-Variations and which have a polarisation-independent magnetotelluric impedance:

$$W = 0, \qquad Z = \begin{pmatrix} 0 & Z_n \\ -Z_n & 0 \end{pmatrix}.$$

The transfer functions to be used for the interpretation are

the inductive scale length for zero wavenumber	$C_n(\omega,0)$
the impedance	$Z_n = i\omega\mu_o C_n$
the ratio of internal to external parts in the wavenumber domain	$S_n = \dfrac{1 - kC_n}{1 + kC_n}$

The transfer function of the Ψ-algorithm to be used for the linearisation of the inverse problem is

$$y_n = 2 \ln(\sqrt{i\omega\mu_o/\rho_o}\, C_n)$$

where ρ_o is arbitrary reference resistivity (cf. chap. 6.4).

Considering these transfer functions at one particular frequency, the parameters of the following models can be derived directly from them. These parameters may then be used to resemble as functions of frequency certain characteristics of the true resistivity distribution. All formulas are readily derived from the formulas for TE-fields at zero wavenumber in chap. 7.3, annex.

(a) Single frequency interpretation of the modulus of transfer-functions (Cagniard-Tikhonov): the model consists of a uniform half-space. Its resistivity is

$$\rho_a = \omega\mu_o |C_n|^2 = \frac{|Z_n|^2}{\omega\mu_o} = 0.2\, \tau \left|\frac{E_x}{H_y}\right|^2 (\Omega m),$$

if the period τ is measured in seconds, E_x in mV/km and H_y in γ. ρ_a is the "Cagniard apparent resistivity" of the substratum at the considered frequency.

(b) Single frequency interpretation of the real part of C_n:

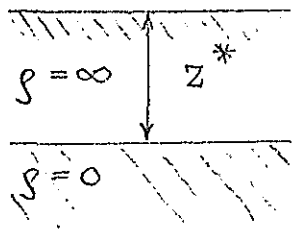

The model consists of a perfect conductor at the depth $z = z^*$ beneath a non-conducting top layer.

$$z^* = \mathrm{Re}\{C_n\} = \frac{\mathrm{Im}(Z_n)}{\omega\mu_o}$$

is the depth of the "perfect substitute conductor" at the considered frequency, indicating the depth of penetration into the substratum at that frequency.

(c) Single frequency interpretation of the imaginary part of C_n:

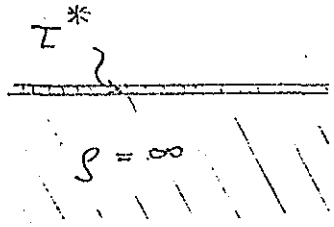

The model consists of a thin conductive top layer of the conductance $\tau^* = \int_0^d \sigma(z)dz$, covering a non-conducting half-space. This apparent conductance is given by

$$\tau^* = \frac{-\mathrm{Im}(C_n)}{\omega\mu_o|C_n|^2} = \frac{-\mathrm{Im}(C_n)}{\rho_a} = \frac{\mathrm{Re}(Z_n)}{|Z_n|^2} .$$

(d) Single frequency interpretation of amplitude and phase of response functions; $\phi = \arg\{Z_n\}$. 1: $0 < \phi < \pi/4$: The model consists of a thin top layer of the conductance τ^* above a uniform substratum of resistivity ρ^{**}:

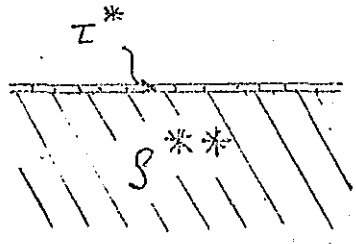

$$\tau^* = \frac{-\mathrm{Im}(C_n) - \mathrm{Real}(C_n)}{\omega\mu_o|C_n|^2} = \frac{\mathrm{Re}(Z_n) - \mathrm{Im}(Z_n)}{|Z_n|^2}$$

$$\rho^{**} = \rho_a \cdot \frac{1 + \cot^2\phi}{2}$$

2: $\pi/4 < \phi < \pi/2$: the model consists of a non-conducting top-layer of thickness h above a uniform substratum of the resistivity ρ^*:

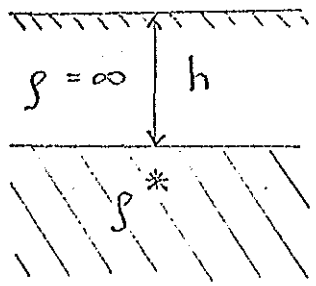

$$h = \mathrm{Real}(C_n) + \mathrm{Im}(C_n) = \frac{\mathrm{Im}(Z_n) - \mathrm{Re}(Z_n)}{\omega\mu_o}$$

$$\rho^* = 2\,\omega\mu_o\{\mathrm{Im}(C_n)\}^2 = \frac{2}{1+\tan^2\phi}\,\rho_a ;$$

The "modified apparent resistivity" ρ^* can be used as an estimator of the resistivity at the depth $z^* = \mathrm{Re}\{C_n\} = h + \frac{1}{2}p^*$ with $p^* = \sqrt{\frac{2\rho^*}{\omega\mu_o}}$ as apparent skin-depth of the substratum. The representation of the true resistivity distribution $\rho(z)$ by the modified apparent resistivity distribution $\rho^*(z^*)$* is usually adequate, if ρ decreases with increasing depth. It is less satisfactory, if ρ increases with depth.

(e) Multiple frequency interpretation with a three-layer model:

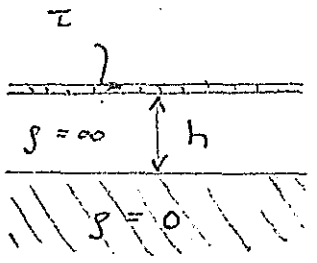

This interpretation combines the single frequency interpretations (b) and (c), i.e. the model consists of a thin top layer with the conductance τ, a non-conducting intermediate layer of the thickness h above a perfectly conducting substratum. Then

$$C_n = \frac{h}{1 + i\eta_s} \quad ;$$

$\eta_s = \omega\mu_o\tau h = \frac{2\,h\,d_1}{p_1^2}$ is the induction parameter of the model with d_1 as thickness of the top layer and $p_1 = \sqrt{\frac{2d_1}{\omega\mu_o\tau}}$ as its skin-depth with the requirement that $p_1 << d_1$.

If $\eta_s >> 1$, implying that $h >>> p_1$, the induction is predominantly in the surface sheet, the response functions

$$C_n = \frac{1}{i\omega\mu_o\tau} \;,\; Z_n = \frac{1}{\tau}$$

are independent of h, thus allowing a unique determination of τ.

In particular,

$$\rho_a = \frac{1}{\omega\mu_o\tau^2} \;.$$

Hence, if $y = \log \rho_a/\rho_o$ and $x = \log T/T_o$ (T = period; ρ_o and T_o are reference values), then

$$y = x - \log(2\pi\mu_o \frac{\rho_o}{T_o}\tau^2),$$

i.e. the ρ_a vs. period curve in log-log presentation is a straight

* with ω as curve parameter

line ascending under 45°, its intersection point on the x-axis given by

$$x_I = \log(2\pi\mu_o \frac{\rho_o}{T_o} \tau^2)$$

or

$$\tau = \sqrt{\frac{T_I}{2\pi\mu_o\rho_o}} = 357 \sqrt{\frac{T_I}{\rho_o}} \ (\Omega^{-1})$$

with $T_I = T_o \cdot 10^{x_I}$ in seconds and ρ_o in Ωm.

If, on the other hand, $\eta_s << 1$, there will be effectively no induction in the thin sheet and

$$C_n = h, \ \rho_a = \omega\mu_o h^2.$$

The log-log plot of ρ_a vs. T is again a straight line, now descending under 45°:

$$y = -x + \log(\frac{2\pi\mu_o h^2}{T_o\rho_o}).$$

The depth h is determined by the intersecting point x_J with the x-axis:

$$h = \sqrt{\frac{T_J\rho_o}{2\pi\mu_o}} = 0.357 \sqrt{T_J\rho_o} \ (\text{km})$$

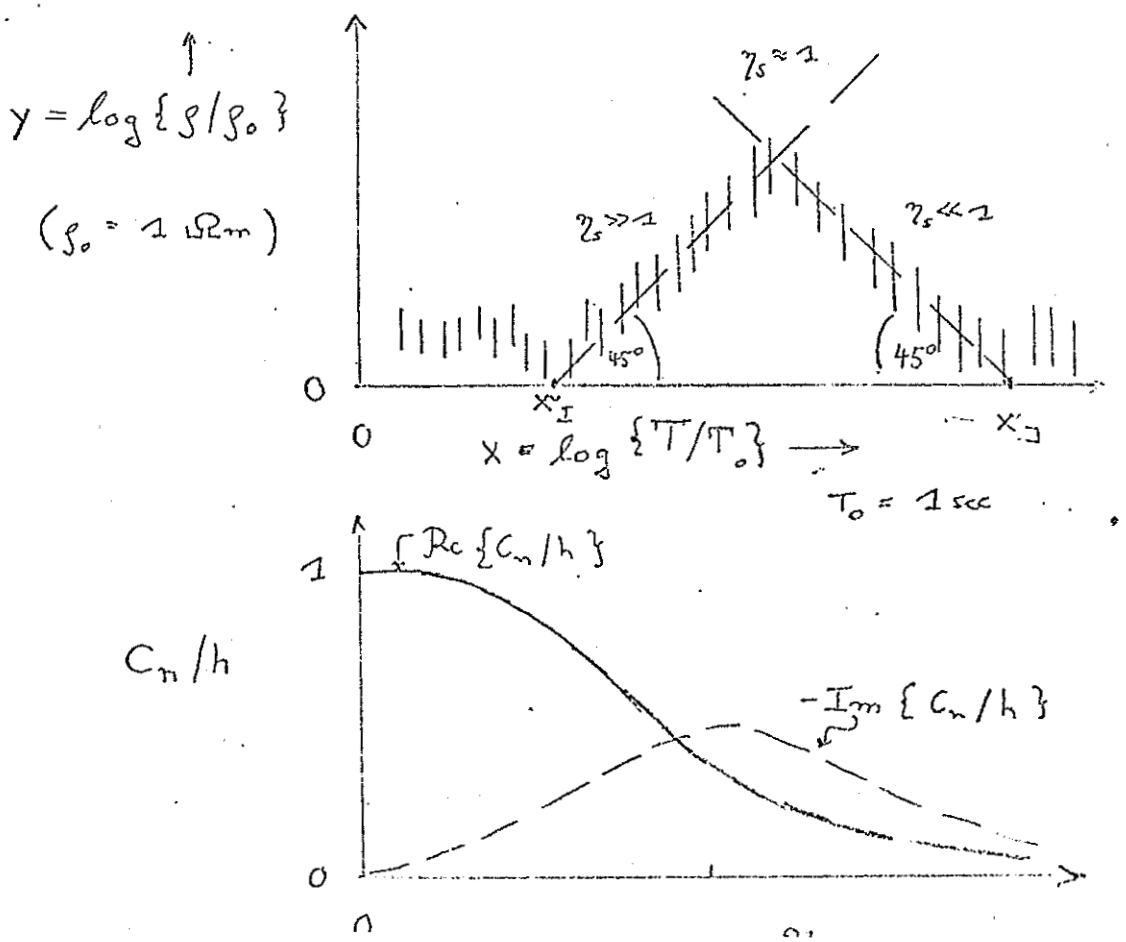

Exercise

Geomagnetic variations in H (north component), D (east component) and Z (vertical component) have been recorded at Goettingen from September 5, 17 h to September 6, 2^h GMT 1957. During the same time intervall records have been obtained also of the telluric field in its northcomponent E_N and its eastcomponent E_E. Scale values and directions of positive change are indicated.

(1) Determine the magneto-telluric impedances E_N/D and E_E/H for fast (period $\tilde{}$ 10 min) and slow (period $\tilde{}$ 1 hour) variations, evaluating peak value readings of pronounced deflections from the smoothed undisturbed level.
Calculate the apparent resistivity ρ_a and estimate the phase ϕ of the impedance (0°, $\pm 45^\circ$, $\pm 90^\circ$). Interpret ρ_a and ϕ with one or two layer models for the two period groups separately. Then search for a model which could explain both period groups by calculating the response function y and solving a system of two to four linear equations.

(2) The magnetogram shows pronounced variations in Z which in view of the low latitude of Goettingen can be interpreted as being due to a resistivity anomaly. Check the correlation of Z with H and D by visual inspection. Then choose effects with distinctly different H : D ratios and determine the coefficient A and B for the anomalous vertical field $Z = AH + BD$.
Interpret the result.

Magnetogramm Göttingen 1957 September 5-6

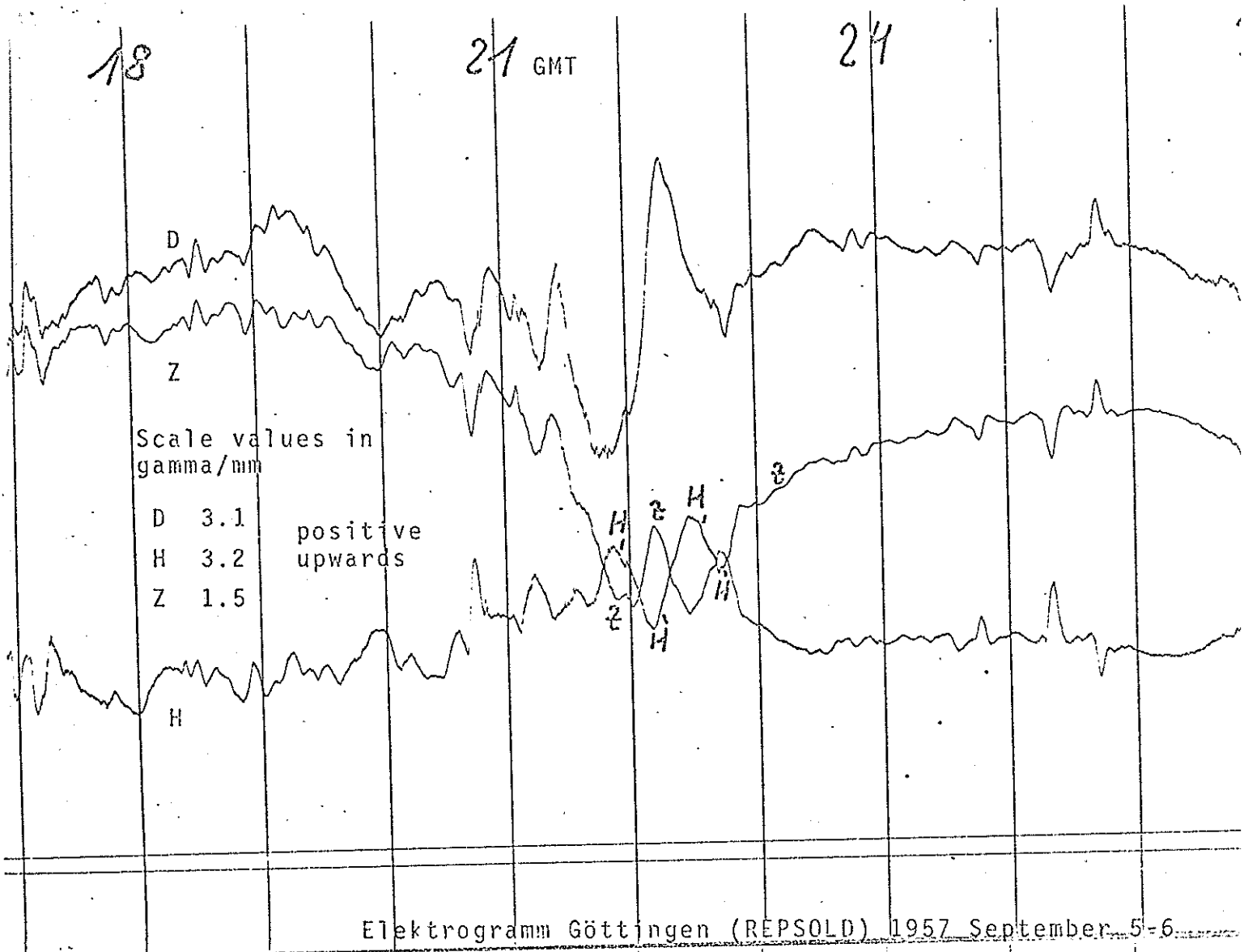

Elektrogramm Göttingen (REPSOLD) 1957 September 5-6

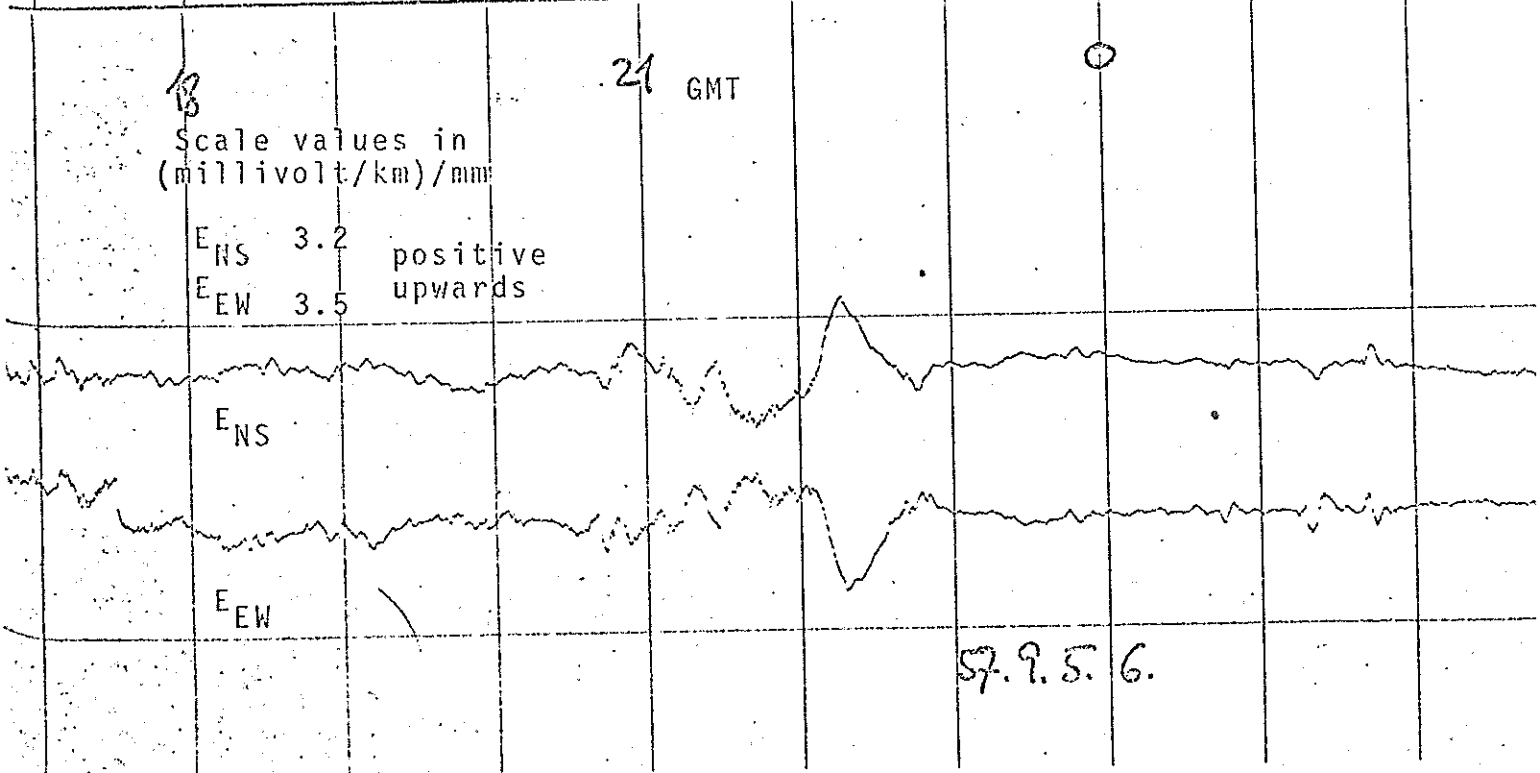

57.9.5.6.

9.2 Layered Sphere

The sphericity of the real Earth has to be taken into account, if for the considered frequency the depth of penetration is comparable to the Earth's radius a divided by N. Here N is the highest value of the degree n of spherical surface harmonics which describe the surface field as functions of latitude and longitude. There is a formal correspondence between the wave number k and n/a or better $\sqrt{n(n+1)}/a$ (s. below).

Only the long-period variations S_q and D_{st} penetrate deeply enough to make a spherical correction of their plane-earth response functions necessary. The D_{st} source field is effectively of the degree $n = 1$, while the Sq source field contains spherical harmonics up to $N = 5$. In fact, the surface field of the m'th Sq subharmonic is well described by a spherical harmonic of the degree $n = m + 1$ when m ranges from one to four. The ratios a/N are therefore roughly 6000 km for D_{st} and 3000 to 1200 km for Sq. These values have to be set in relation to the depth of penetration of D_{st} from 600 to 1000 km and to the depth of penetration of S_q from 300 to 500 km.
Hence, in either case there will be the need of a spherical correction, but it should be noted that it will be bigger for S_q because the greater spatial non-uniformity of S_q outweights the effect of deeper penetration of D_{st}.

The theory of electromagnetic induction in conductors of spherical symmetry surrounded by non-conducting matter can be summarized as follows. Let

$$\underline{H} = (H_\theta, H_\lambda, H_r) \qquad \underline{E} = (E_\theta, E_\lambda, 0)$$

be the magnetic and electric field vectors of time-harmonic TE-mode fields in spherical geocentric coordinates; r is the geocentric distance, λ the angle of longitude and θ the angle of co-latitude (= 90° minus latitude) on a spherical surface. The diffusion vector from Sec. 7.3 points from external sources radially inwards toward r = 0:

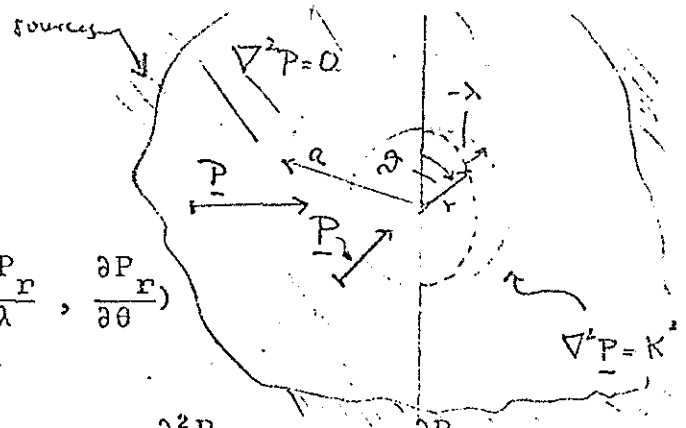

$$\underline{P} = (0,\ 0,\ P_r)$$

with

$$\mathrm{rot}\underline{P} = \frac{1}{r}\left(-\frac{1}{\sin\theta}\frac{\partial P_r}{\partial \lambda},\ \frac{\partial P_r}{\partial \theta}\right)$$

and

$$\mathrm{rot\ rot}\underline{P} = \frac{1}{r}\left(\frac{\partial^2 P_r}{\partial\theta\partial r},\ \frac{1}{\sin\theta}\frac{\partial^2 P_r}{\partial\lambda\partial r},\ -\frac{1}{r\sin\theta}\left\{\frac{1}{\sin\theta}\frac{\partial^2 P_r}{\partial\lambda^2}+\frac{\partial}{\partial\theta}\left[\sin\theta\frac{\partial P_r}{\partial\theta}\right]\right\}\right)$$

P_r is expressed on a surface r = const. by a series of spherical surface harmonics. The diffusion equation $\nabla^2\underline{P} = i\omega\mu_o\sigma_\nu\,\underline{P}$ within the ν'the shell is then solvable by a separation of variables ($K_\nu^2 = i\omega\mu_o\sigma_\nu$):

$$P_r = iK_\nu \sum_{n=1}^{N}\sum_{m=o}^{n} r\, f_n^m(r)\, P_n^m(\cos\theta)e^{im\lambda}$$

where the characteristic radial function f_n^m satisfies the ordinary second order differential equation

$$r^2\frac{d^2 f_n^m}{dr^2} + 2r\frac{df_n^m}{dr} - \{(n+1)n + K_\nu^2\}\, f_n^m = 0.$$

Its general solution are spherical Besselfunctions j_n and η_n of the first and second kind,

$$f_n^m(r) = A_n^m\, j_n(iK_\nu r) + B_n^m\, \eta_n(iK_\nu r)$$

with A_n^m and B_n^m as complex-valued constants of integration. They decribe the in-going (B_n^m) and out-going (A_n^m) solution, the latter being zero below the ultimate shells, surrounding an uniform inner core, because η_n has a singularity at r = o while $j_n \to 0$ for $r \to 0$.

The characteristic scale length of penetration is defined as

$$C_n^m = r\, f_n^m / g_n^m$$

with

$$g_n^m = \frac{d(r\, f_n^m)}{dr}.$$

The field within the conducting sphere, $r \leq a$, is derived from $\underline{P}$ as described in Sec. 7.3. Observing that the radial component of rot rot $\underline{P}$ reduces by the use of spherical harmonics to

$$\frac{iK_\nu}{r} \sum_n \sum_m n(n+1)\, f_n^m\, P_n^m\, e^{im\lambda} ,$$

the field components of the spherical harmonic of degree n and order m are:

$$\left.\begin{aligned} H_\theta &= g_n^m\, dP_n^m/d\theta \\ H_\lambda &= g_n^m\, im\, P_n^m/\sin\theta \\ H_r &= f_n^m\, n(n+1)\, P_n^m \end{aligned}\right\} \quad \frac{e^{im\lambda}}{i\omega\mu_o r}$$

and

$$\left.\begin{aligned} E_\theta &= -\, f_n^m\, im\, P_n^m/\sin\theta \\ E_\lambda &= +\, f_n^m\, dP_n^m/\sin\theta \end{aligned}\right\} \quad e^{im\lambda}$$

$$E_r = 0 .$$

The impedance of the field at spherical surfaces, expressed in terms of C_n^m, is then as in the case of plane conductors given by

$$Z_n^m = E_\lambda/H_\theta = -\, E_\theta/H_\lambda = i\omega\mu_o\, C_n^m .$$

For the field outside of the conducting sphere, $r \geq a$, the solution of the radial function is (in quasi-stationary approximation)

$$f_n^m = A_n^m \left(\frac{a}{r}\right)^{n+1} + B_n^m \left(\frac{r}{a}\right)^n .$$

Hence, the surface value of the characteristic scale length for $r = a$ is found to be

$$C_n^m = \frac{(A+B)a}{A+B-(n+1)A+nB} = \frac{a}{n+1} \cdot \frac{1 + A/B}{1 - \frac{m}{m+1} A/B} .$$

The ratio of internal to external parts of the magnetic surface field is by definition

$$S_n^m = - n A_n^m / (n+1) B_n^m,$$

yielding

$$C_n^m = \frac{a}{n+1} \frac{1 - \frac{n+1}{n} S_n^m}{1 + S_n^m} .$$

The ratio of internal to external parts is therefore derived from C_n^m according to

$$S_n^m = \frac{n}{n+1} \frac{1 - \frac{n+1}{a} C_n^m}{1 + \frac{n}{a} C_n^m}$$

which demonstrates the rôle of n/a, respectively (n+1)/a, as equivalent wavenumber of the source field in spherical coordinates (cf. Sec. 9.1).

The spherical version of the input function for the inverse problem, based on a linearisation according to the ψ-algorithm, is conveniently defined as

$$y_n^m = 2 \ln\{K_o C_n^m\}$$

with $K_o^2 = i\omega\mu_o/\rho_o$. It will be shown that the spherical correction is of the order $(n|C|/a)^2$, if the conductivity is more or less uniform.

If degree and order of the spherical harmonic representation of the source field are independent of frequency (this is true for D_{st} but not for S_q), the inverse problem can be solved by deriving from spherical response functions a preliminary plane-earth model $\hat{\rho}(\hat{z})$. This model is subsequently transformed into a spherical Earth model $\rho(r)$ with WEIDELT's transformation formula:

$$\rho(r) = f^4(r/a) \cdot \hat{\rho}(\hat{z})$$

with

$$f(r/a) = \frac{(n+1)(\frac{a}{r})^n + n(\frac{r}{a})^{n+1}}{2n + 1}$$

and $$\hat{z} = \frac{a\{(\frac{a}{r})^n - (\frac{r}{a})^{n+1}\}}{f(r/a)\cdot(2n+1)}.$$

An algorithm for the direct problem for spherical conductors can be formulated as follows. It is designed not to give the transfer function C_n^m for a given model itself but an auxilary transfer function

$$\hat{C}_n^m(r) = \frac{1}{K_\nu} \cdot \frac{A_n^m j_n + B_n^m \eta_n}{i(A_n^m j_{n-1} + B_n^m \eta_{n-1})},$$

as a direct equivalent to the tranfer function C of plane conductors. To see its connection to C_n^m, differentiate the characteristic depth function f_n^m with respect to r, observing that the differentiation of spherical Besselfunctions with respect to their argument u is

$$\frac{dj_n}{du} = j_{n-1} - \frac{n+1}{u} j_n$$

and the same for η_n. Then

$$\frac{d f_n^m}{dr} = iK_\nu(A_n^m j_{n-1} + B_n^m \eta_{n-1}) - \frac{n+1}{r}(A_n^m j_n + B_n^m \eta_n).$$

Hence,

$$g_n^m = f_n^m + r \frac{d f_n^m}{dr} = f_n^m(r/\hat{C}_n^m - n)$$

or

$$C_n^m = \hat{C}_n^m \cdot (1 - \frac{n\hat{C}_n^m}{r})^{-1}$$

with $n\hat{C}_n^m/r$ as "spherical correction ".

Continuity of the tangential components of the electric and magnetic field requires that C_n^m and thereby $\hat{C}_n^m$ as well are continuous functions of depth. Let r_L be the radius of the inner core of conductivity σ_L, surrounded by (L-1) uniform shells, the γ^{th} shell between r_ν and $r_{\nu+1}$ ($\nu = 1,2, \ldots L$).

Then

$$\hat{C}_n^m(r_L) = \frac{1}{K_L} \frac{j_n(u_L)}{i\, j_{n-1}(u_L)}$$

with $u_L = iK_L r_L$ because the in-going solutions are zero within the core. But $\hat{C}_n^m$ for $r = r_L$ can be expressed also in terms of the general solution of the (L-1)'th shell:

$$\hat{C}_n^m(r_L) = \frac{1}{K_{L-1}} \frac{A_n^m j_n(u_L') + B_n^m \eta_n(u_L')}{i\{A_n^m j_{n-1}(u_L') + B_n^m \eta_{n-1}(u_L')\}}$$

with $u_L' = iK_{L-1} r_L$. As a consequence, $\hat{C}_n^m$ for $r = r_{L-1}$ is now expressible in terms of $\hat{C}_n^m(r_L)$ and thus an algorithm can be established for the calculation of the surface value $\hat{C}_n^m(r_1 = a)$. In numerical evaluation it is preferable not to derive the spherical Besselfunctions for the arguments u_ν and u_ν' themselves, but to reformulate the algorithm by expressing j_n and η_n in terms of hyperbolic functions (cf. Dover Handbook of Mathematical Function, Formula 10.2.12):

$$j_n(u) = i^n\{g_n(z)\sinh(z) + g_{-n-1}(z)\cosh(z)\}$$

$$\eta_n(u) = i^{n+1}\{g_{-n-1}\sinh(z) + g_n(z)\cosh(z)\}$$

with $u = iz$ and the following recurrence formula for the $g_n(n = o, \pm 1, \pm 2 \ldots)$:

$$g_o = z^{-1}, \quad g_1 = -z^{-2}, \quad g_{n+1} = g_{n-1} - \frac{2n+1}{z} g_n .$$

If $|z| >> 1$, the approximations $g_n \simeq z^{-1}$ for $n = \pm 2, \pm 4, \ldots$ and $g_n \simeq -z^2 \cdot (n+1)\cdot n/2$ for $n = \pm 3, \pm 5, \ldots$ are valid; $g_{-1} = 0$.

By making use of the addition theorems of hyperbolic functions the algorithm can be given a form simular to the recurrence formula of plane conductors (cf. Appendix to Sec.7.3)

$$\hat{C}_n^m(r_\nu) = \frac{1}{K_\nu} \frac{\beta_\nu a_1 + \varepsilon_1 + \tanh(\alpha_r)\{a_2 + \beta_\nu \varepsilon_2\}}{a_3 + \beta_\nu \varepsilon_3 + \tanh(\alpha_r)\{\beta_\nu a_4 + \varepsilon_4\}}$$

with

$$\alpha_\nu = (r_\nu - r_{\nu+1})K_\nu \qquad \beta_\nu = \hat{C}_n^m(r_{\nu+1}) \cdot K_\nu$$

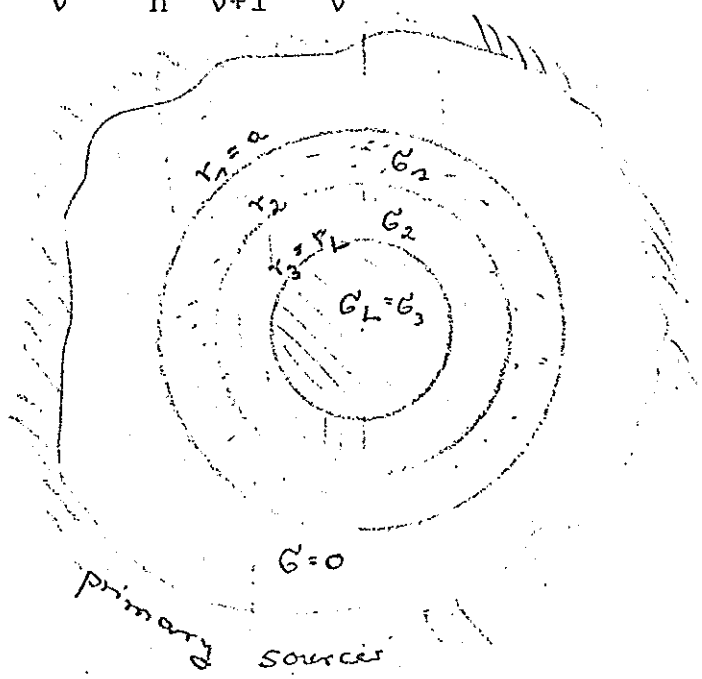

and

$$a_1 = g_n g'_{-n} - g_{-n-1} g'_{n-1}$$

$$a_2 = g_n g'_n - g_{-n-1} g'_{-n-1}$$

$$a_3 = g_{-n} g'_n - g_{n-1} g'_{-n-1}$$

$$a_4 = g_{-n} g'_{-n} - g_{n-1} g'_{n-1}$$

$$\varepsilon_1 = g_{-n-1} g'_n - g_n g'_{-n-1}$$

$$\varepsilon_2 = g_{-n-1} g'_{-n} - g_n g'_{n-1}$$

$$\varepsilon_3 = g_{n-1} g'_{-n} - g_{-n} g'_{n-1}$$

$$\varepsilon_4 = g_{n-1} g'_n - g_{-n} g'_{-n-1} .$$

The argument of g_n is $u_\nu = iK_\nu r_\nu$, the argument of g'_n is $u'_\nu = iK_\nu r_{\nu+1}$. If $|u_\nu|$ and $|u'_\nu|$ are large compared to unity, i.e. if the mean radius is much larger than the skin-depth of the ν'th shell, the coefficients a_n are of the order $\pm(u_\nu\, u'_\nu)^{-1}$, the spherical correction coefficients ε_n of the order $u_\nu^{-2}\, u'^{-1}_\nu$ or $u_\nu^{-1}\, u'^{-2}_\nu$.

Consider for example the case of a uniform sphere of the radius a, the conductivity σ, $K = i\omega\mu_0\sigma$ and $u = iKa$. Then

$$\hat{C}_n^m(r=a) = \frac{1}{K} \cdot \frac{g_{-n-1} + g_n \cdot \tanh(u)}{g_{n-1} + g_{-n} \cdot \tanh(u)} .$$

Assuming the skin-depth to be small in comparison to a, ($|u| \gg 1$), $\tanh(u) \simeq 1$ and with $z = u/i = Ka$

$$\hat{C}_n^m(a) \simeq \frac{1}{K} \frac{1 - \frac{n(n+1)}{2z}}{1 - \frac{n(n-1)}{2z}} \simeq \frac{1}{K}\left(1 - \frac{n}{z}\right) .$$

The resulting approximate spherical transfer function

$$C_n^m(a) = \frac{1}{K} \frac{1 - n/z}{1 - n/z(1-n/z)} \simeq \frac{1}{K}$$

has its plane-halfspace value except for a spherical correction of the order $(n/z)^2$.

9.3. Non-uniform thin sheets above a layered substructure

The thin-sheet approximation has been introduced by PRICE to geomagnetic induction problems. It applies to those variation anomalies for which there is reason to believe that they arise from lateral changes of resistivity close to the surface. For instance, highly resistive basement rocks may be covered by well conducting sediments of fairly uniform resistivity ρ_s but variable thickness d.

Two conditions have to be satisfied, if this surface cover is to be treated as a "thin sheet" of variable conductance $\tau = d/\rho_s$:

(i) Its skin-depth $\sqrt{2\rho_s/\omega\mu_o}$ at the considered frequency must exceed the maximum thickness d_{max} by at least a factor of 2.

(ii) The inductive scala-length $C_n^-(\omega,0)$ for the matter below the surface cover, assumed to be a layered half-space, must be large in comparison to d_{max}.

Under these conditions the electric field within the "thin sheet" may be regarded as constant for $0 < z < d$, reducing the first field equation to its thin-sheet approximation

$$\underline{H}^{+}_{tg} - \underline{H}^{-}_{tg} = -\hat{\underline{z}} \times \underline{j}$$

with

$$\underline{j} = \tau \underline{E}$$

as sheet current density; $\underline{H}^{+}_{tg}$ is the tangential magnetic field above the sheet at z = 0, $\underline{H}^{-}_{tg}$ the tangential magnetic field below the sheet at z = d; $\hat{\underline{z}}$ is the unit vector downward.

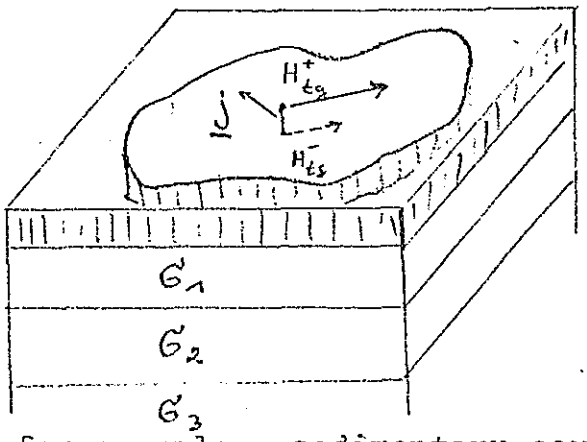

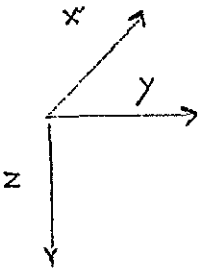

Consider for example a sedimentary cover with ρ_s = 2Ωm, nowhere exceeding 4 km in thickness. Then condition (i) will be satisfied for periods up to 2 minutes and condition (ii) for deep resistivities in excess of, say, 50 Ωm.

The response functions for the normal field above the sheet at z = 0 are readily found from

$$C^{+}_{n} = \frac{Z^{+}_{n}}{i\omega\mu_o} = \frac{C^{-}_{n}}{1 + i\omega\mu_o \tau_n C^{-}}$$

where τ_n is the constant normal part of τ, while C^{-}_{n} has to be derived from the given substructure resistivity profile. The field equations to be considered for the evaluation of the variation anomaly are

$$\underline{H}^{+}_{atg} - \underline{H}^{-}_{atg} = -\hat{\underline{z}} \times \underline{j}_a$$

with

$$\underline{j}_a = \underline{E}_n \tau_a + \underline{E}_a (\tau_n + \tau_a)$$

$$\mathrm{rot}_z \underline{E}_a = i\omega\mu_o H_{az}$$

The second field equation implies that the vertical magnetic field is also to be regarded as a constant between z = 0 and z = d.
In addition there are boundary conditions for the anomalous field, arising from the fact that its primary sourced lie within the sheet.

Pilot interpretation: In many cases the anomalous field has no inductive coupling with the substructure because its half-width is small in comparison to $|C_n^-|$. In that case no currents are induced by $\underline{H}_a$ in the substructure and the anomalous magnetic field is solely due to the anomalous sheet current j_a within the sheet. For reasons of symmetry

$$H^+_{atg} = - H^-_{atg}$$

or

$$\underline{H}^+_{atg} = -\frac{1}{2} \{\hat{\underline{z}} \times (\underline{E}_n \tau_a + \underline{E}_a \tau)\}.$$

Observe that the inductive coupling of the normal field has not been neglected, i.e. its internal sources lie within the sheet as well as within the substructure. Assuming that τ_n is known and that it is possible to identify the normal part of the total electric field $\underline{E} = \underline{E}_n + \underline{E}_a$ either by calculation or by observations outside of the anomaly, the anomalous part of the conductance τ_a is readily found from observations of $\underline{H}^+_{atg}$ and $\underline{E}_a$. In this way, using the example from above, the variable depth of the basement below the sediments,

$$d = d_n + d_a = \rho_s(\tau_n + \tau_a),$$

can be estimated.
If an elongated structure is in H-polarisation with respect to the normal field, the magnetic variation anomaly will disappear (cf. Sec.7.3). The pilot investigation of the conductance is done n even more simply because the sheet current density must be a constant in the direction normal to the trend:

$$E_{\perp}\tau = j_{\perp} = \text{const.} \quad \text{or} \quad E_{n\perp}\tau_a + E_{a\perp}\tau = j_a = 0.$$

This approach has been used by HAACK to obtain a fairly reliable conductance cross-section through the Rhinegraben.

In the case of E-polarisation a different kind of simplification may be in order: Suppose the half-width of the anomaly is sufficiently small in comparison to $(\omega\mu_o\tau)^{-1}$ everwhere. Then no significant local self-induction due to H_{az} which produces $\underline{E}_a$ takes places, i.e. the electric field driving the anomalous current will be the large-scale induced normal field only:

$$H^+_{a\perp} \approx \frac{\tau_a}{2}\,(\hat{z} \times E_{n\parallel}).$$

Assuming $\underline{E}_{n\parallel}$ again to be known, the conductance anomaly is now derived from the observation of the tangential magnetic variation anomaly normal to the trend,

In the actual performance with real data all field components may be expressed in terms of their transfer functions W and Z and thus be normalised with regard to H^+_{ntg}.

Direct problem for 2-dimensional structures

Let τ be variable only in one horizontal direction, say, in y-direction which implies that the anomalous field is also variable only in that direction, obeying the field equations

(E-polarisation)

$$H^+_{ay} - H^-_{ay} = j_{ax}$$

$$j_{ax} = E_{nx}\tau_a + E_{ax}\tau$$

$$\partial E_{ax}/\partial y = i\omega\mu_o H_{az}$$

(H-polarisation)

$$H^-_{ax} - H^+_{ax} = j_{ay}$$

$$j_{ay} = E_{ny}\tau_a + E_{ay}\tau$$

$$\partial H^-_{ax}/\partial y = -\sigma_o E^-_{az}.$$

with

and

Here σ_o denotes the conductivity at the top of the substratum and E^-_{az} the anomalous vertical field at z = d which is responsible for driving currents upwards from the substructure to the sheet and vice versa.

The boundary conditions, reflecting the "thin-sheet origin" of the variation anomaly, are

	(E-polarisation)	(H-polarisation)
for z = 0:	$H^+_{ay} = -K * H_{az}$	$H^+_{ax} = 0,$
for z = d:	$H^-_{ay} = L_{II} * H_{az}$	$E_{ay} = L_I * E^-_{az}.$

The kernel function of the convolution integrals are

$$K(y) = \frac{1}{\pi y}$$

$$L_{II}(\omega,y) = \frac{1}{\pi}\int_0^{+\infty} \frac{\sin(y\,k_y)}{ik_y\, C^-_{nII}(\omega,k_y)}\, dk_y$$

$$L_I(\omega,y) = \frac{1}{\pi}\int_0^{\infty} \frac{\sin(y\,k_y)}{ik_y\, C^-_{nI}(\omega,k_y)}\, d\,k_y .$$

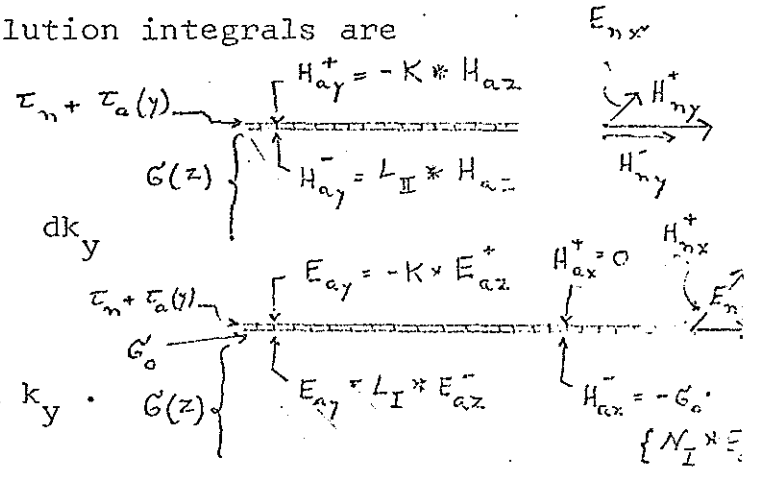

Here C^-_{nII} is the response function of the substructure for the anomalous TE-field in the case of E-polarisation and C^-_{nI} the response function of the substructure for the anomalous TM-field in the case of H-polarisation.

The kernel K is the separation kernel, introduced in Sec.5.1. It connects H^+_{ay} and H_{az} in such a manner that the source of the anomaly is "internal" when seen from above the sheet. The kernels L are the Fourier transforms of the response functions, introduced in Sec.7.3, which connect the tangential and horizontal field components above a layered half-space. Their application to the anomalous field at z = d implies that $\underline{H}_a$ and $\underline{E}_a$ diffuse downward into the substructure and disappear for $z \to \infty$. They represent the inductive coupling of the anomalous field with the substructure.

Field equations and boundary condition together constitute a set of four linear equations for an equal number of unknown field components. They are uniquely determined in this way. A solution toward the anomalous tangential electric field in E-polarisation, for instance, gives

$$-(L_{II}+K) * \frac{\partial E_{ax}}{\partial y} = i\omega\mu_o(E_{nx}\tau_a + E_{ax}\tau).$$

A similar solution toward the anomalous current density in H-polarisation gives

$$j_{ay} = j_{ny}\frac{\tau_a}{\tau_n} - (L_I * \frac{\partial j_{ay}}{\partial y}) \cdot \frac{\tau}{\sigma_o} .$$

For a given model-distribution these equations are solved numerically by setting up a system of linear equations for the unknown field components at a finite number of grid points along y. The convolution integrals, involving derivatives of the unknown field components with respect to y, are preferably treated by partial integration which in effect leads to a convolution of the unknown field components themselves with the derivatives of the kernels. It should be noted that the kernels L approach for $y \to \infty$ finite limiting values, given by $\{2C_n^-(\omega,0)\}^{-1}$.

Inverse problem for two-dimensional structures

It is also possible to consider the anomalous conductance τ_a as the unknown quantity to be determined from an observed elongated variation anomaly, in the actual calculations to be represented by a set of respective transfer functions. The normal sheet conductance τ_n and the resistivity of the substructure, for which the kernels L have to be determined, enter into the calculations as free model parameters. They can be varied to get the best agreement in $\tau_a(y)$ when using more than one frequency of the variation anomaly.

Another point of concern is the reality of the resulting numerical values of τ_a. Usually empirical data will give complex values and the free parameters should be adjusted also to minimize the imaginary part of the calculated conductance.

In E-polarisation the elimination of H^-_{ay} gives

$$\tau_a = \frac{H^+_{ay} - L_{II} * H_{az} - E_{ax}\,\tau_n}{E_{nx} + E_{ax}} .$$

We can then eliminate either H^+_{ay} and H_{az}, if τ_a is to be determined from anomalous electric field, or we can derive τ_a from the anomalous magnetic field by observing that

$$E_{ax}(y) = \frac{i\omega\mu_o}{2} \int_{-\infty}^{+\infty} H_{az}(y-\hat{y}) \cdot \operatorname{sgn}(\hat{y})\, d\hat{y}$$

by integration of the second field equation. The normal electric field is derived from the normal magnetic field by setting

$$E_{nx} = i\omega\mu_o\, C^+_n(\omega,0)\, H^+_{ny}$$

when the source field is quasi-uniform and

$$E_{nx} = i\omega\mu_o\, N_{II} * H^+_{ny}$$

when the source field is non-uniform; $N_{II}(\omega,y)$ is the Fourier transform of $C^*_{nII}(\omega,k)$. Cf. Sec.8.2, "Vertical soundings with station arrays".

In H-polarisation only the anomalous electric field is observable at the surface. For the elimination of the anomalous magnetic field at the lower face of the sheet from the field equations we use the generalized impedance boundary condition for the anomalous TM-field at the surface of the substructure (cf. Sec.7.3 und 8.2):

$$\bar{H}_{ax} = j_{ay} = - \sigma_o (N_I * E_{ay})$$

with $N_I(\omega,y)$ being the Fourier transform of $\bar{C}_{nI}(\omega,k_y)$. Insertion above gives

$$\tau_a(y) = - \frac{\sigma_o (N_I * E_{ay}) + E_{ay}\ \tau_n}{E_{ny} + E_{ay}} \quad .$$

9.4 Non-uniform layers above and within a layered structure

The source of the surface variation anomaly is assumed to be an anomalous slab between $z = z_o$ and $z = z_o + D$ in which the resistivity changes in vertical and horizontal direction: $\rho=\rho_n+\rho_a$. The region above and below the slab are taken to be layered, $\rho = \rho_n$ being here a sole function of depth (cf. Sec.3).

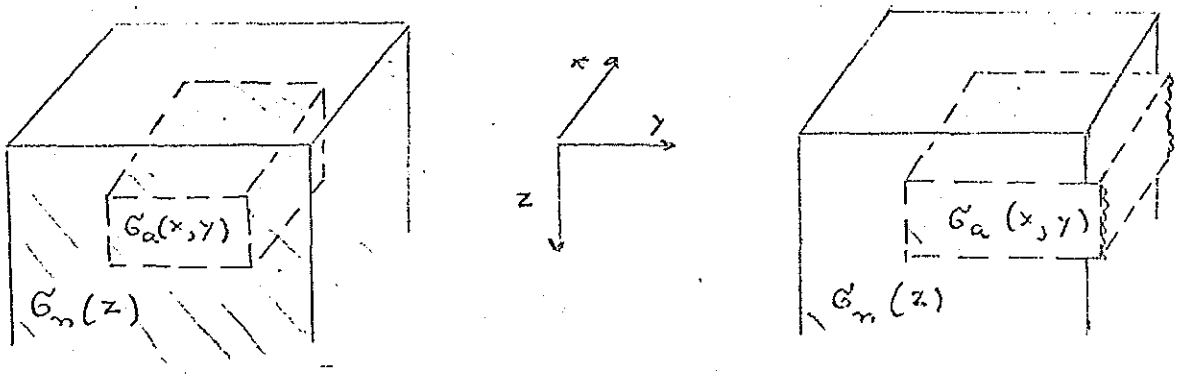

The response functions for the normal variation field are defined for the normal structure as given by ρ_n. If the anomaly lies at the transition between two extended normal regions, two normal solutions have to be formulated. It should be noted that in that case the anomalous field will not disappear but converge outside of the anomaly toward the difference of the two normal solutions.

Henceforth, the normal structure , the normal response functions, and the normal fields $\underline{H}_n$ and $\underline{E}_n$ will be assumed to be known throughout the lower conducting half-space. The source-field will be regarded as quasi-uniform except for source fields in E-polari-

sation in the case of longated anomalies when a non-uniform source can be permitted (cf. Sec. 9.3, calculation of E_{nx} from H_{ny}!).

The principal problem in basing the interpretation of actual field data on this type of model consists in a proper choice of the upper and lower bounds of the anomalous slab. The following arguments may be useful for a sensible choice:

The anomalous region must be reached by the normal variation field, i.e. z_o should not be made larger than the depth of penetration of the normal field as given by $|C_n(\omega,0)|$ at the highest frequency of an anomalous response. A lower bound for the depth of the slab is not as readly formulated because the anomalous response does not disappear necessarily when the depth of penetration is much larger than $z_o + D$, i.e. when no significant normal induction takes places within the anomalous slab. Only if the anomaly is elongated and the source field in E-polarisation, can it be said that the depth $z_o + D$ must be at least comparable to the normal depth of penetration at the lowest frequency of an anomalous response.

Pilot studies: In section 8.2 the general properties of the impedance tensor Z above a non-layered structure have been discussed and the following rule for elongated anomalies was established: The impedance for E-polarisation does not diverge markedly from the impedance of a hypothetical one-dimensional response for the local resistivity-depth profile, while the impedance for H-polarisation will do so unless the depth of penetration is small in comparison to the depth of the internal resistivity anomaly and the inductive response nearly normal anyway.

Suppose then that an impedance tensor has been obtained at a location y on a profile across a quasi-twodimensional anomaly which by rotation of coordinates has zero or almost zero diagonal elements and that a distinction of the offdiagonal elements for E- and H-polarisation can be made (cf.Sec.8.2). Regarding the E-polarisation response for a first approximation as quasi-normal, a local inductive scale length

$$C_{\parallel}(\omega,y) = \frac{1}{i\omega\mu_o} E_{\parallel}(\omega,y)/H_{\perp}(\omega,y)$$

is calculated as function of frequency and location. It is converted into an apparent CAGNIARD resistivity and phase:

$$\rho_{\parallel}(\omega,y) = \omega\mu_o|C_{\parallel}|^2 \quad , \quad \phi_{\parallel}(\omega,y) = \arg\{C_{\parallel}\}$$

or alternatively into the depth of a perfect substitute conductor and a modified apparent resistivity :

$$z^*_{\parallel}(\omega,y) = \mathrm{Re}\{C_{\parallel}\} \quad , \quad \rho^*_{\parallel}(\omega,y) = 2\omega\mu_o(\mathrm{Im}\{C_{\parallel}\})^2$$

which can be combined into a local depth versus apparent resistivity profile $\rho^*_{\parallel}(z^*_{\parallel}, y)$.

If the magnetic variation anomaly rather than the geoelectric field has been observed, the anomalous part of $E_{\parallel}$ can be derived by integration over the anomaly of the vertical magnetic variations, while the normal part of $E_{\parallel}$ is calculated from the normal impedance outside of the anomaly or derived theoretically for a hypothetical normal resistivity model:

$$E_{\parallel}(\omega,y) = i\omega\mu_o\{C_n H_n + \int_{-\infty}^{+\infty} \mathrm{sgn}(y-\hat{y})\, H_{az}(\hat{y})\, d\hat{y}\}$$

or in terms of transfer functions with respect to $H_{n\perp}$,

$$C_{\parallel}(\omega,y) = i\omega\mu_o\{C_n + \int_{-\infty}^{+\infty} \mathrm{sgn}(y-\hat{y})\, W_{z\parallel}(\hat{y})\, d\hat{y}\} \ ,$$

using for the transfer function of H_{az} the notations of page 113.

Magnetotelluric and geomagnetic depth sounding data along a profile are in this way readily converted either into CAGNIARD resistivity and phase-contours in frequency-distance coordinates, into lines of depth-of-penetration z^* at a given frequency, or into modified apparent-resistivity-contours in a z^*-distance cross-section Either one of these plots will outline the frequency range, respectively the depth range, in which the source of the anomaly can be expected to lie, and provide a rough idea about the resistivities likely to occur within the anomalous zone.

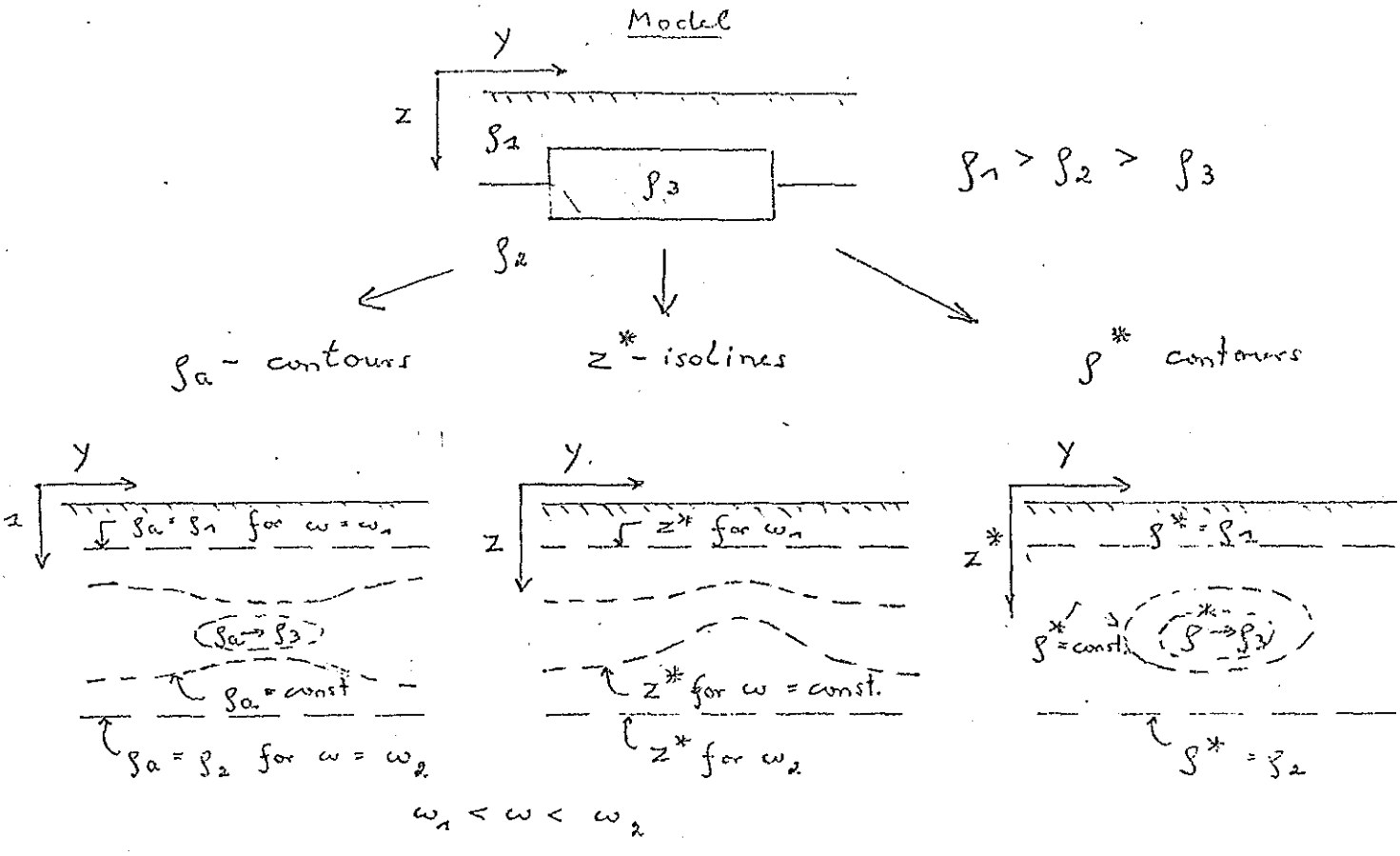

Single frequency interpretation by perfect conductors at variable depth

Geomagnetic variations anomalies show frequently nearly zero phase with respect to the normal field, the transfer functions which connect the components of $\underline{H}_a$ and $\underline{H}_n$ being real functions of frequency and locations. This applies in particular to two types of anomalies. Firstly to those which arise from a non-uniform surface layer, thin enough to allow the "thin-sheet" approximation of the previous section with predominant induction within the sheet ($\eta_s >> 1$). Secondly, it applies to anomalies above a highly conductive subsurface layer at variable depth beneath an effectively non-conducting cover.

In the first case E_n will be in-phase with H_n, in the second case out-of-phase (cf. Sec. 9.1). But it is important to note that the anomalous variation field H_a will be in either case roughly in-phase with H_n.

Both types of anomaly can be explained at a given frequency by the undulating surface S of a perfect conductor below non-conducting matter. Its variable depth below the surface point (x,y) will be denoted as $h^*(x,y)$. Outside of the anomaly h^* shall be constant and equal to the real part of C_n at the considered frequency.

This kind of interpretation is intended to demonstrate the effect of lateral changes of internal resistivity on the depth of penetration as a function of frequency and location. It does not provide, however, quantitative information about the resistivities involved nor does it allow a distinction of the two types of anomalies mentioned above.

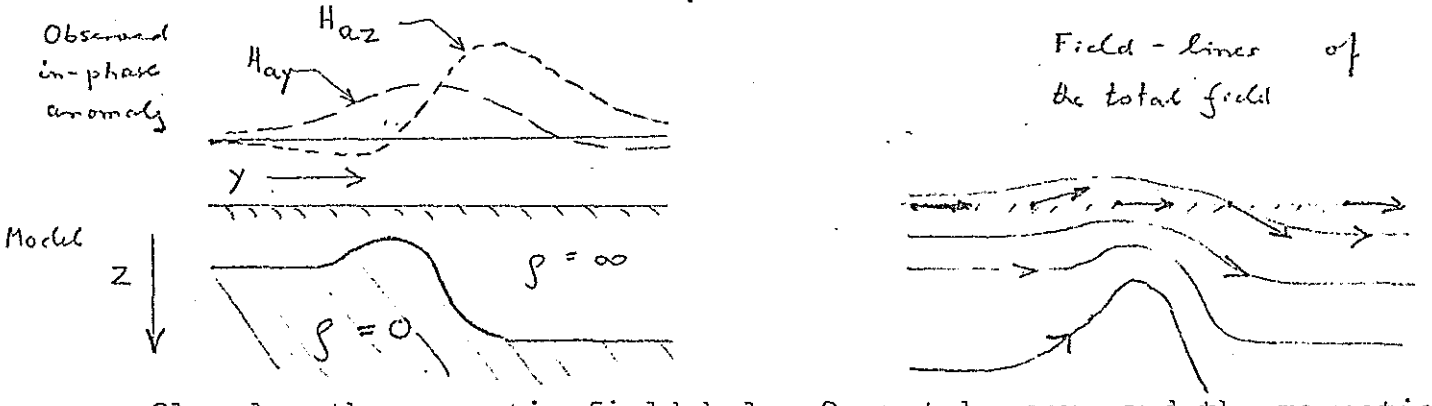

Clearly, the magnetic field below S must be zero and the magnetic field vector on S tangential with respect to S because the continuity condition for the field component normal to S requires that this component vanishes just above S.

Direct model problem: For a given shape of S the anomalous surface field can be found with the methods of potential field theory, since $\underline{H}_a$ will be irrotational and of internal origin above S. If in particular S has a simple shape independent of x, the field lines for E-polarisation in the (y,z)-plane for $z \leq h^*(y)$ can be found by conformal mapping as follows:

Let $w(y,z) = y(y',z') + i \cdot z(y',z')$ be an analytic function which maps the line $z'=0$ of rectangular (y',z') coordinates into the line $z=h^*(y)$ of rectangular (y,z) coordinates. Lines $z' = \text{const.}$ are interpreted as magnetic field lines of a uniform field above a perfect conductor at constant depth, their image in the (y,z)-plane as field lines of a distorted field above a perfect conductor at the variable

depth $h^*(y)$, the image of the ultimate field line $z'=0$ being tangential to the surface of the conductor as required.

If $\underline{H}_n = (H_{ny}, 0)$ denotes the uniform horizontal field vector at a point in the original (y',z') coordinates, the components of the field vector $\underline{H} = (H_y, H_z)$ at the image point in the (y,z) coordinates can be shown to be given by

$$H_y = \frac{\partial y/\partial y'}{r^2} \cdot H_n, \qquad H_z = \frac{-\partial z/\partial y'}{r^2} H_n$$

with

$$r^2 = (\partial y/\partial y')^2 + (\partial z/\partial y')^2 \quad .$$

The difference $\underline{H} - \underline{H}_n$ represents the anomalous field to be determined.

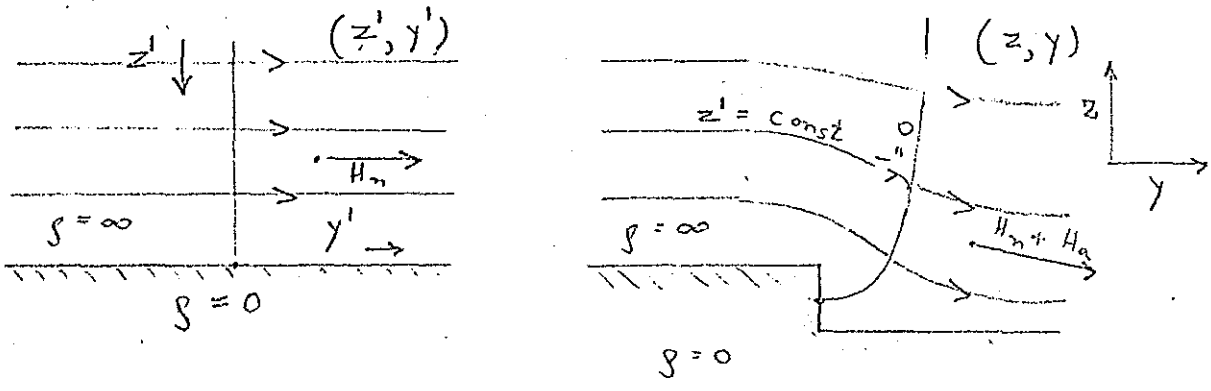

Inverse problem: The shape of the surface S can be found inversely from a given surface anomaly by constructing the internal field lines of the field $\underline{H}_n + \underline{H}_a$. Field lines which have at some distance of the anomaly the required normal depth $\mathrm{Re}(C_n)$ define the surface S, provided of course that the surface thus found does not intersect the Earth's surface anywhere.

The actual calculation of internal field lines requires a downward extension of the anomaly through the non-conducting matter above the perfect conductor, using the well developed methods of potential field continuation towards its sources. In order to obtain sufficien stability of the numerical process, the anomaly has to be low-pass filtered prior to the downward continuation with a cut-off at a reciprocal spatial wave number comparable to the maximum depth of intended downward extrapolation.

A field line segment with the horizontal increments dx and dy has then the vertical increment

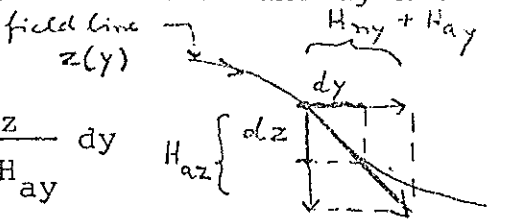

$$dz = \frac{\partial z}{\partial x}\,dx + \frac{\partial z}{\partial y}\,dy = \frac{H_{az}}{H_{nx}+H_{ax}}\,dx + \frac{H_{az}}{H_{ny}+H_{ay}}\,dy$$

and the entire field line is then constructed by numerical integration.

An analytically solvable inverse problem: Suppose the observed anomaly is 2-dimensional and sinusoidal,

$$H_{ay}(y,z=0) = c\,\sin(k\cdot y)\,H_{ny}\ .$$

Because of the internal origin of the anomaly

$$H_{az}(y,z) = -c\,\cos(k\cdot y)H_{ny}\ ,$$

the internal field increasing exponentially with depth,

$$\underline{H}_a(y,z) = \underline{H}_a(y,0)\cdot e^{k\cdot z}\ .$$

Hence, the slope of field lines at the depth z is

$$\frac{dz}{dy} = \frac{-c\,\cos(k\cdot y)\cdot e^{k\cdot z}}{1+c\,\sin(k\cdot y)\cdot e^{k\cdot z}}\ ,$$

yielding by integration

$$z(y) = z_o - c/k\cdot\sin(k\cdot y)\cdot e^{k\cdot z(y)}$$

as the implicit solution with z_o as the constant of integration. Here it will be chosen in such a way that the highest point of the field line is still below the Earth's surface z=0.

We infer from the field line equation z(y) that field lines above sinusoidal anomalies oscillate non-symmetrically around the depth $z=z_o$ with $L=2\pi/k$ as spatial wave length. Their deepest points $z=z^+$ are at $y=L/4,-3L/4,\pm.....$, their highest points $z=z^-$ at $y=-L/4,3L/4,\mp....$.

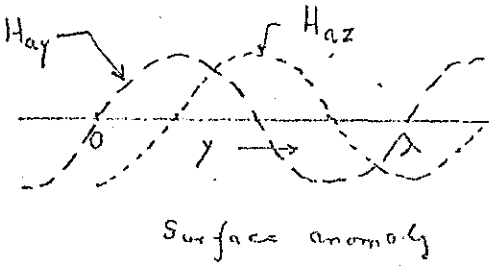

Surface anomaly

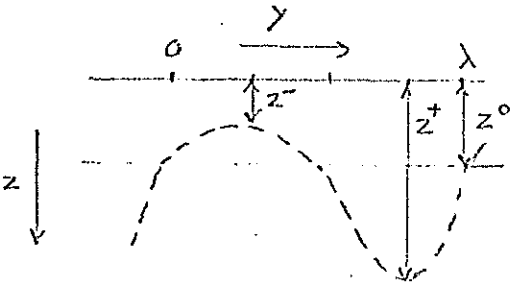

Field line

Suppose the spatial wave length of the anomaly is large in comparison to the deepest point of penetration z^+. Then the approximate field line equation

$$z(y) = \frac{z_o - c/k \cdot \sin(k \cdot y)}{1 + c \cdot \sin(k \cdot y)}$$

can be used with the requirement that z_o is equal to or larger than c/k. The mean amplitude of the field line oscillations is readily expressed now in terms of the amplitude of the observed surface anomaly as given by the factor c, namely

$$\frac{1}{2}(z^+ - z^-) = \frac{c}{1 - c^2}(z_o + k^{-1}) .$$

If, for example, a moderate anomaly has the amplitude c=0.25 and a wave length of 628 km, the mean amplitude of the field line oscillations are given by $(z_o+100)/4$ km, $z_o \geq 25$ km. Using z_o=30 km gives a mean amplitude of 33 km and the field line oscillates between 4 km and 70 km. This numerical example demonstrates that even minor anomalies require rather large undulations in the depth of a perfect substitute conductor.

Multi-frequency interpretation by local induction in isolated bodies

Most geomagnetic induction anomalies arise from a local rearrangement of large-scale induced currents. In some cases, however, it may be justified to assume that the source of the anomaly is a conducting body which is isolated by non-conducting matter from the large-scale current systems. Such a body can be, for instance, a crustal lense of high conductivity within the normally highly resistive crust.

The direct problem: Consider a body of (variable) conductivity between $z=z_1$ and $z=_2$. The surrounding matter at the same depth is effectively non-conducting at the considered frequency, i.e. large-scale induced currents which flow in the normal structure above and

below can neither enter nor leave this body.

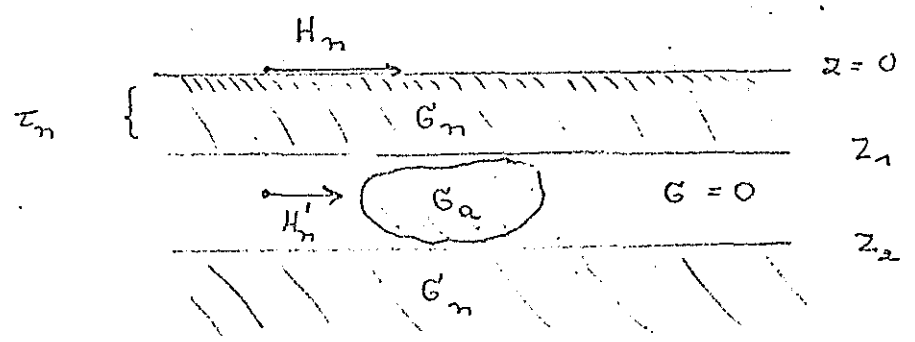

The inducing field is the normal field H_n' between z_1 and z_2, regarded as uniform. For simplicity it is assumed that the normal structure between z=0 and z_1 represents a "thin sheet" of the conductance τ_n. Then the attenuation of H_n' with respect to the normal field H_n at the surface z=0 is given by

$$(H_n - H_n')/H_n = i\eta_s/(1 + i\eta_s)$$

$$\eta_s = \omega\mu_o C_n^- \tau_n$$

as thin-sheet induction parameter (Sect.9.3 and Appendix to 7.3).

Three aspects of the arising induction problem have to be considered: (i) the local induction by H_n' within the body, (ii) the electromagnetic coupling of this body with the normal substructure below z_2, (iii) the coupling of the body with the surface cover above. In order to make problem (i) solvable in a straightforward manner uniform bodies of simple shape such as spheres and horizontal cylinders of infinite length have to be selected. The anomalous field due to the induction in these bodies is of frequency-independent geometry. This fact permits simple solutions of the inverse problem as seen below.

Consider the case of a horizontal cylinder of infinite length, the radius R and the conductivity σ_Z; its axis is parallel to x and intersects the (y,z)-plane at the point $(0,z_o)$. The normal horizontal field is parallel to y and produces by induction currents which flow parallel to x in the upper halve and anti-parallel to x in the lower halve of the cylinder. Their magnetic field outside the cylinder is the field of a central 2-dimensional dipole of the moment

m antiparallel to y. It has the components

$$H_{ay}(y,z) = m\cos(2\theta)\cdot r^{-2}, \quad H_{az}(y,z) = -m\sin(2\theta)\cdot r^{-2}$$

with $r^2 = y^2 + (z_o - z)^2$ and $\cos\theta = z_o/r$, $\sin\theta = y/r$.

The dependence of the dipole moment on the inducing field will be expressed in terms of a response function. Let m_∞ be the dipol moment of a perfectly conducting cylinder which shields the external field completely from its interior. Hence, the induced field at the point $(0, z_o - R)$ just above the cylinder must be equal to H_n', i.e.

$$m_\infty = R^2 H_n',$$

which implies that it cancels H_n' within the cylinder as required.

The response function of the cylinder with respect to a uniform inducing field perpendicular to the axis is now defined as the complex-valued ratio

$$f(\eta_Z) = m/m_\infty$$

which can be shown to be a sole function of the dimensionless induction parameter

$$\eta_Z = \omega\mu_o\sigma_Z R^2 .$$

The modulus of $f(\eta_Z)$ will approach zero for $\eta_Z << 1$ and unity for $\eta_Z >> 1$, its argument changing from 90° for $\eta_Z \to 0$ to 0° for $\eta_Z \to \infty$. Hence, at sufficiently high frequencies the anomalous field from the cylinder will be in-phase with H_n' and not increase beyond a certain "inductive limit", while at sufficiently low frequencies the anomalous field will be out-of-phase and small in comparison to the field at the inductive limit.

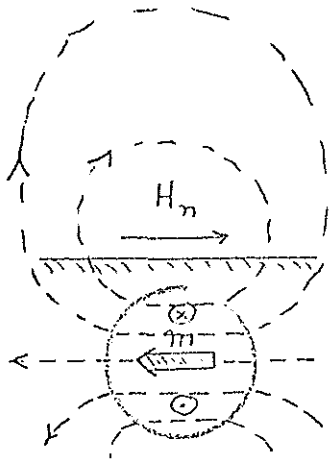

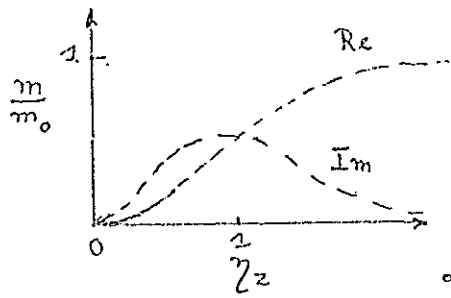

Induction curves

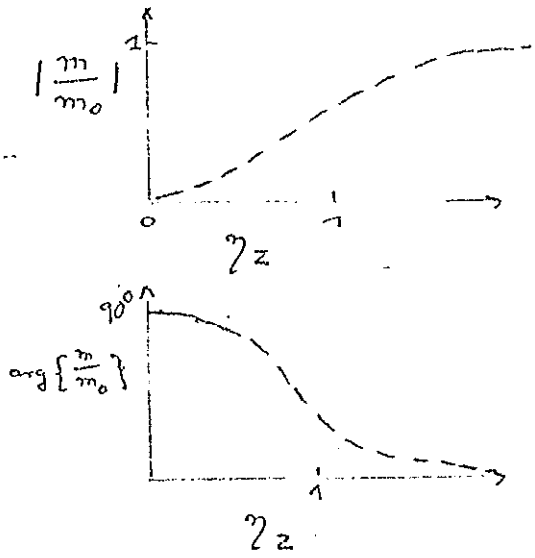

The transfer function between the anomalous and normal field are now readily expressed in terms of a frequency-dependent response function, a frequency-independent geometric factor, and a frequency-dependent attenuation factor Q' for the normal field:

$$H_{ay} = f(\eta_Z)\ \cos(2\theta)\cdot(R/r)^2\cdot Q'\ H_n$$

$$H_{az} = -f(\eta_Z)\ \sin(2\theta)(R/r)^2\cdot Q'\ H_n$$

with

$$Q' = (1 + i\ \eta_Z)^{-1}\ .$$

An approximate solution of problem (ii) can be obtained by representing the conductive substructure below the surface sheet by a perfect conductor at the (frequency-dependent) depth $Re(C_n^-)$ and by adding to the anomalous dipole field the field of an image dipole of the moment R^2H_n' at the depth $2\cdot Re(C_n^-)-z_o$.

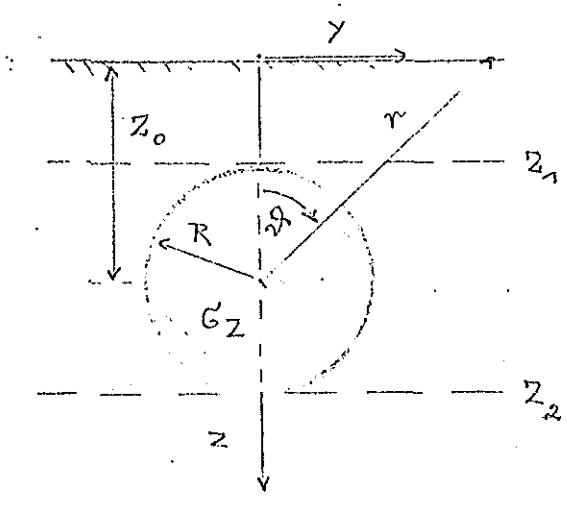

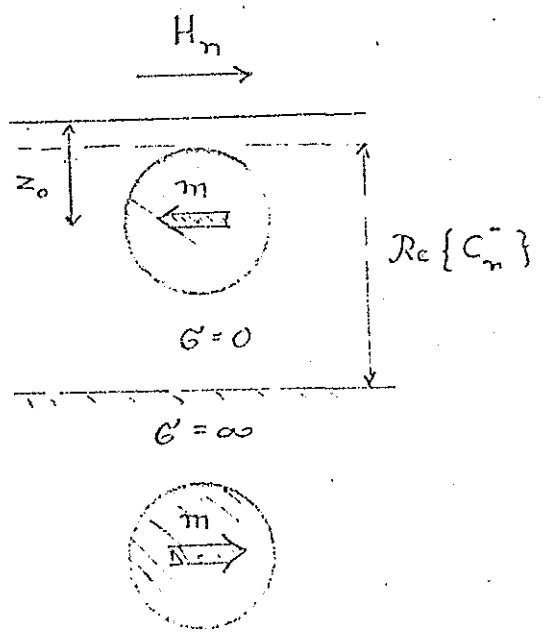

Problem (iii) involves mainly the attenuation of the upward diffusing anomaly $\underline{H}_a$ by uniform surface layers. This attenuation is, however, a second order effect and can be neglected, if at the considered frequency the widespread normal field penetrates the surface layers to any extent, i.e. if the modulus of Q' is sufficiently close to unity.

The inverse problem: Assuming the anomalous body to be a uniform cylinder, the model parameters z_o, R, σ_R can be uniquely inferred from surface observations, providing the transfer functions for H_{ay} and H_{az} are known for at least two locations and frequencies. Forming here the ratios

$$H_{az}/H_{ay} = \tan(2\theta)$$

the angles θ and thereby the position of the cylinder can be found. The depth of the cylinder axis being known, the dipole moment $R^2 f(\eta)$ can be calculated. Its argument fixes the size of the induction parameter η_Z and two determinations of η_Z at different frequencies the radius R and the conductivity σ_Z. Now R and z_o being known, the field of the image dipole can be calculated. The inverse procedure is repeated now with the observed surface anomaly minus the field of the image dipole until convergence of the model parameters has been reached.

Interpretation with BIOT-SAVART's law

Let $\hat{\underline{i}}$ be the current density vector within a volume dV at the point $\hat{\underline{r}} = (\hat{x}, \hat{y}, \hat{z})$. Then according to BIOT-SAVART's law in SI units the magnetic field vector at the point $\underline{r} = (x, y, z)$ due to the line-current element $\hat{i}dV$ is

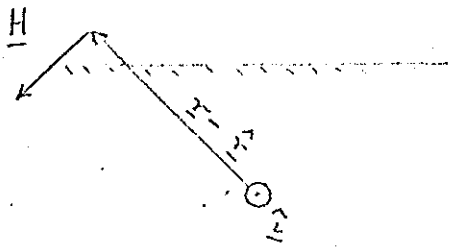

$$\underline{H} = \frac{1}{4\pi} \frac{\hat{\underline{i}} \times (\underline{r} - \hat{\underline{r}})}{|\underline{r} - \hat{\underline{r}}|^3} dV.$$

This law can be used to interpret an observed surface anomaly of geomagnetic variations in terms of a subsurface distribution of anomalous induction currents, which in turn are related to an internal conductivity anomaly σ_a, i.e. to local deviations of σ from a normal layered distribution $\sigma_n(z)$.

It has been pointed out in Sec.8.3 that the anomalous part of the geomagnetic and geoelectric variation field can be split into TE and TM modes (= tangential electric and tangential magnetic modes) and that only the TE modes produce an observable magnetic variation anomaly at the Earth's surface. Consequently, only a TE anomalous current density distribution $\underline{\hat{i}}_{aII}$ can be related to the anomalous magnetic surface field $\underline{H}_a$, the subscript "II" refering to the solution II of the diffusion equation.

Denoting the tangential components of $\underline{\hat{i}}_{aII}$ simply with $\hat{i}_{ax}$ and $\hat{i}_{ay}$, the components of the anomalous surface field are given by

$$H_{ax}(x,y,0) = \frac{1}{4\pi} \int_V \frac{-\hat{i}_{ax}\,\hat{z}}{r^2}\,dV$$

$$H_{ay}(x,y,0) = \frac{1}{4\pi} \int_V \frac{i_{ay}\,\hat{z}}{r^2}\,dV$$

$$H_{az}(x,y,0) = \frac{1}{4\pi} \int_V \frac{\hat{i}_{ax}(y-\hat{y}) - \hat{i}_{ay}(x-\hat{x})}{r^2}\,dV$$

with $r^2 = (x-\hat{x})^2 + (y-\hat{y})^2 + \hat{z}^2$. The inverse problem, namely to find from a given surface anomaly the internal anomalous current distribution, has no unique solution. Within certain constraints, however, it can be made unique, at least in principle. For instance, it is assumed that the anomalous current flow is limited to a certain depth range which implies that the matter between this depth range and the surface is regarded as non-conducting at the considered frequency.

The surface anomaly can be extended now downward to the top of the anomalous depth range with standard methods which require

only adequate smoothing of the observed anomalous surface field. Then a certain well defined depth dependence of the anomalous current density is adopted as discussed below and the anomalous current distribution can be derived in a straightforward manner.

Suppose an observed anomaly $\underline{H}_a$ at a given frequency has been explained in this way by a distribution of anomalous internal currents. Its connection to the internal conductivity is established by the normal and anomalous electric field vector according to

$$\underline{i}_{aII} = \sigma_a \underline{E}_n + (\sigma_n + \sigma_a) \cdot \underline{E}_{aII} \cdot$$

Assuming the normal conductivity distribution $\sigma_n(z)$ to be known, $\underline{E}_n$ as a function of depth is readily calculated. There is no simple way, however, to derive the anomalous electric field of the TE mode except by numerical models as discussed below. There is in particular no justification to regard it as small in comparison to the normal electric field and thus to drop the second term in the above relation. Instead the following argumentation has to be used:

The anomalous electric field in the TE mode can be thought to contain two distinct components. The first component may be regarded as the result of local self-induction due to $\underline{H}_{aII}$. It can be neglected at sufficiently low frequencies, when the half-width of the anomaly is small in comparison to the minimum skin-depth value within the anomalous zone.

The second component arises from electric charges at boundaries and in zones of gradually changing conductivity. These charges produce a quasi-static electric field normal to boundaries and parallel to internal conductivity gradients which ensures the continuity of the current across boundaries and internal gradient zones. Hence, this second component of the anomalous electric field does not disappear, when the frequency becomes small.

It vanishes, however, if anomalous internal currents do not cross boundaries of gradient zones, i.e. when the normal field is in E-polarisation with respect to the trend of elongated structures.

Only in this special case will be justification to neglect the term σE_a at low frequencies and to use the approximation

$$\underline{i}_{aII} = \sigma_a \underline{E}_n$$

to calculate the internal conductivity anomaly σ_a from the anomalous current density and the normal electric field. It will be advisable to regard here σ_a as a sole function of x and y and thus to postulate the same depth dependence for the anomalous current and the normal electric field.

Interpretation with numerical models

So far idealized models for a laterally non-uniform substructure have been considered. They allowed a simplified treatment of the induction problem and had in common that only few free parameters were involved. Once numerical values were attached to them, the observed surface anomaly of the variation field could be converted rather easily into variable model parameters to characterize the internal change of subsurface conductivity at some given depth from site to site.

The introduction of more realistic models leads to a substantial increase of the numerical work involved and should be considered only, if transfer functions for the anomalous surface field are known with high accuracy. The inverse problem to derive a set of variable model parameters directly from observations can be solved by linearisation, i.e. by the introduction of a linear data kernel, connecting changes of the surface response to changes in the subsurface conductivity structure (cf. Sec.6).

As before a normal structure σ_n outside of the anomaly is given, the variable model parameters representing only lateral changes of σ with respect to σ_n within the range of the anomaly. Unless

stated otherwise, source fields of lateral homogeneity are assumed, yielding in conjunction with σ_n the normal fields H_n and E_n as known functions of depth.

Conductivity anomalies $\sigma_a = \sigma - \sigma_n$ are restricted to an anomalous slab above or within a laterally uniform structure, extending in depth from z_1 to z_2. Within this slab two basic types of conductivity anomalies may be distinguished:
(i) slabs with gradually changing conductivities in horizontal direction or (ii) slabs which consist of uniform blocs or regions, separated by plane or curved boundaries.

In the first case electric changes are distributed within the slab, yielding closed current circuits $\mathrm{div}\hat{i} = 0$ as required in quasi-stationary approximation. Consequently, $\mathrm{div}\underline{E} = -(E \cdot \mathrm{grad}\sigma)/\sigma$ will not be zero. In the second case only bloc boundaries carry free surface changes and the electric field will be non-divergent within the blocs. In either case a solution of the diffusion equation for $\underline{H}_a$ or $\underline{E}_a$ has to be found under the condition that the anomalous field approaches zero with increasing distance from the anomalous slab.

Numerical methods for the actual solution of the <u>direct problem</u>, when σ_a is given and H_a or E_a are to be found, have been discussed in Sec. 2 and 3. Here some additional comments: Models should be set up in such a way that either the shape of the anomalous body or the anomalous conductivity is the variable to be described by a set of model parameters. After fixing the free parameters, in particular z_1 and z_2, the model parameters for the description of the anomaly are varied until agreement is reached between the observed and calculated transfer functions.

Suppose that models of type (ii) are used, that only vertical and horizontal boundaries are permitted, and that the anomalous slab is subdivided by equally spaced horizontal boundaries into layers. Then the variable model parameters are either the positions of vertical boundaries, enclosing a body of constant

anomalous conductivity σ_{ac} or the anomalous conductivity values σ_{am} of the blocs m = 1,2, ... M, separated by equally spaced vertical boundaries:

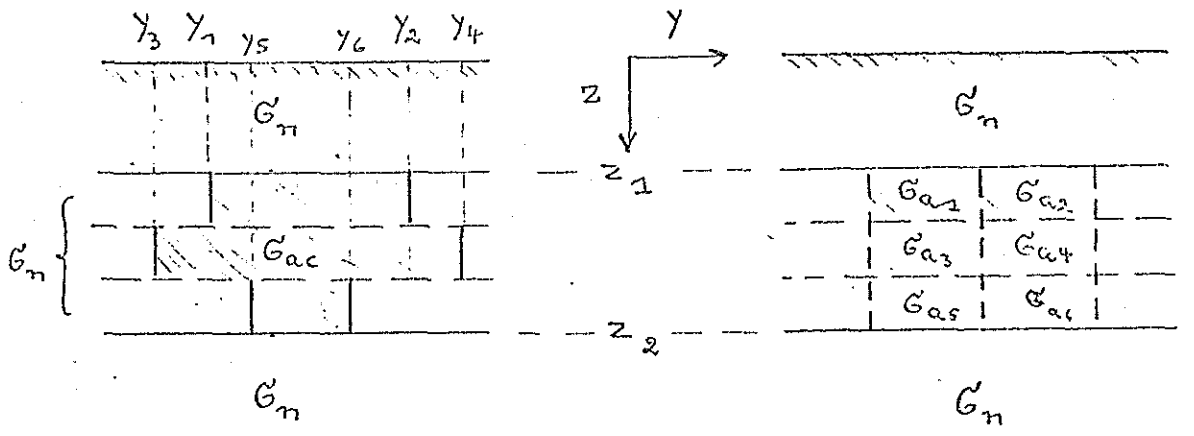

If the search for a best fitting set of model parameters is to be done by an iterative inverse method rather than by trial-and-error, the linear data kernel matrix $G = (g_{nm})$ has to be found for an initial model. In this matrix the element g_{nm} represents the change y_n of the anomalous transfer function at a certain surface point and frequency R_n which arises in linear approximation from a change x_m of the model parameter in the m'th bloc of the starting model. The resulting system of linear equations $y_n = \sum_m g_{nm} x_m$ is solved with the methods of Sec.6. Its solution represents the improvement of the initial model, if y_n is the misfit between observed and calculated transfer functions for the initial model. The process is repeated with the improved models until the necessary improvements x_m are small enough to justify a linear approximation.

Which complications arise in the general case that not only the internal conductivity structure but also the inducing source field are laterally non-uniform? First of all, in addition to σ_n as a function of depth the magnetic field $H^{(e)}$ of the external source must be a known function of surface location. In the special case of the equatorial jet field this source field configuration will be more or less the same for all day-time variations and thus a normalisation of the observed surface field by the

field at some distinguished surface point will be possible, for instance by the horizontal field at the dip equator.

The conversion formulas of Sec. 5.2 and the methods described in Sec. 8.2 ("Vertical soundings with station arrays") are now used to find the internal part $H_n^{(i)}$ of the normal magnetic field and the normal electric field E_n as functions of the surface location and frequency. Finally, the normal surface field is extended downward by consideration with the spatial Fourier transforms of the downward extension factors as given in the Appendix to Sec. 7.3.

Now the normal field within the anomalous slab is known and the diffusion equation for the anomalous field can be solved numerically in the same way as before, when the slab or the anomalous region themselves are chosen as basic domains for the numerical calculations. Here a final schematic summary of the various steps of the calculations, when the source is the combined field of the equatorial jet and the low-latitude Sq:

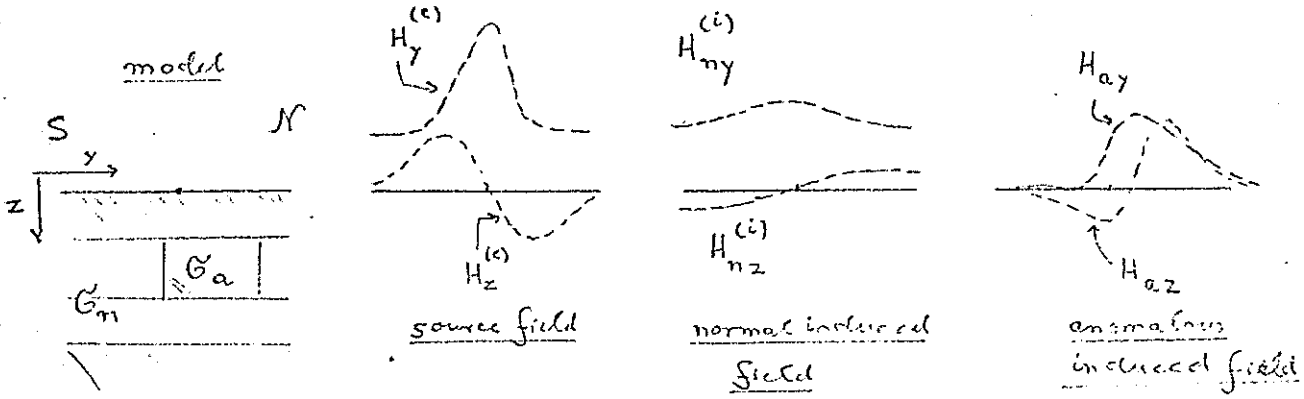

Interpretation with scale model experiments

Numerical model calculations may be too elaborate, if the induction by a non-uniform source in a three-dimensional anomalous structure has to be considered. An example is the coast effect of the equatorial jet, when the dip equator crosses the coastline under an angle. – No complications arise at those places, when the dip equator is parallel to the coast and the jet field in E-polarisation (s. above). –

In situation of great complexity the qualitative and even quantitative understanding of surface observations may be furthered by laboratory scale model experiments, simulating the natural induction process on a reduced scale. Invariance of the electro-

the product $\omega\sigma L^2$ constant with L denoting the length scale.

The primary inducing field is produced by an oscillating dipole source or by extended current loops, situated as "ionospheric sources" above an arrangement of conductors which represent the conducting material below the Earth's surface. Alternatively, the conductors as a whole can be placed into the interior of coils, say Helmholtz coils, and thus be exposed to a uniform source field.

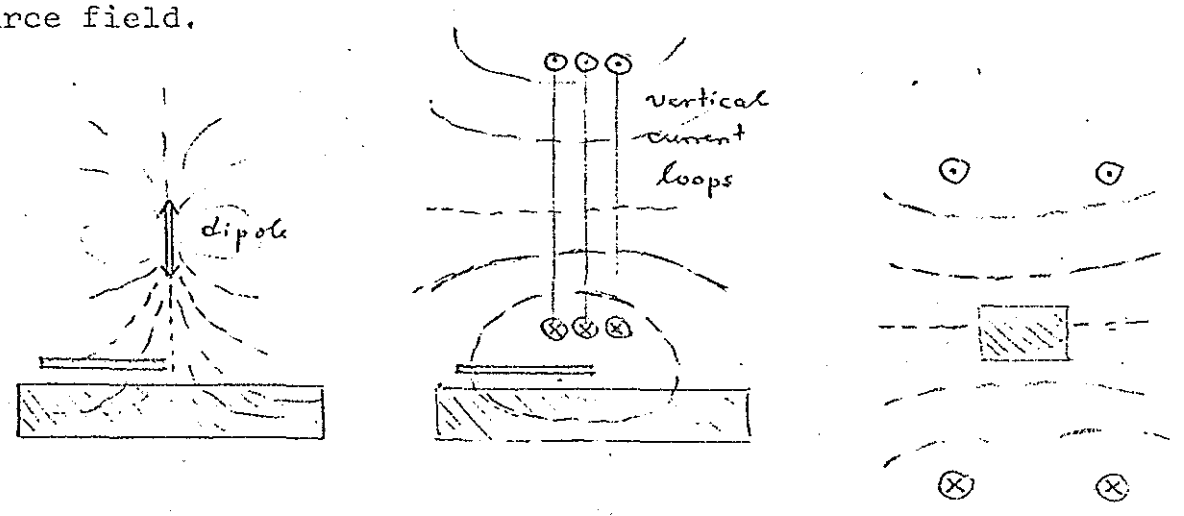

The magnetic source field at the surface of the conductors is exactly known. Hence, by substrating it from the observed field, measured with small triaxial pick-up coils, the induced field from the conductors can be investigated. The electric field can be measured also by submerging, for instance, an arrangement of metalic conductors into a much less conducting electrolyte (s. below).

A basic difficulty in conducting a scale model experiment, which is truly equivalent to the induction process in nature, arises from the necessarily finite dimensions of the conductors in the scale model. If the conductors are placed below the source of the inducing field, their finite downward extent represents no problem because the ultimate conductor can be dimensioned in such a way that the electromagnetic field is completely shielded from the space beneath the scale model. Their finite length and

width, however, forces the induced currents to flow in loops which in strength and phase may be totally controlled by the edges of the conductor. In order to avoid this unwanted effect the source field at the level of the conductors should die away before reaching the edges of the scale model. For instance, if a line current source is used, the half-width of the line current field on the surface of the scale model should be considerably smaller then the width of the model.

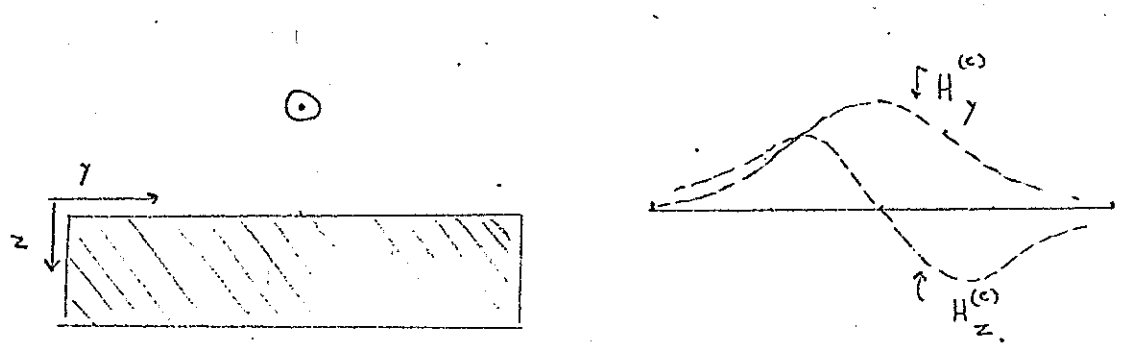

These complications do not arise of course, when no attempt is made to simulate local anomalies of a large-scale induced current system, i.e. when the scale model is placed into the interior of coils in order to simulate local induction in isolated bodies (cf. subsection on this topic in Sec. 9.4).

Here are to mention the scale model experiments by GRENET and LAUNAY who showed how a large-scale induction can be simulated also by the induction in the interior of coils. Their objective was to make a scale model of the coast effect at complicated coastlines. They noted that the inductive coupling between the ocean and highly conducting material at some depth within the Earth is well represented by a system of image currents at the level $2 \cdot h^*$ below the ocean. Here h^* is again the depth of a perfect substitute conductor for the oceanic substructure at the considered frequency.

GRENET and LAUNAY use as model conductors two thin metallic plates which are connected along two edges by vertical conducting strips.

One of the thin plates represents the ocean and one of its edges is given the shape of a certain coastline to be studied. The second plate represents the level of the image currents. The whole arrangement of conductors is placed into a Helmholtz coil in such a way that the vertical strips are parallel to the magnetic field. Plates and strips now form a loop normal to the magnetic flux within the Helmholtz coil and thus currents are induced which flow in the "oceanic" plate parallel to the "coastline".

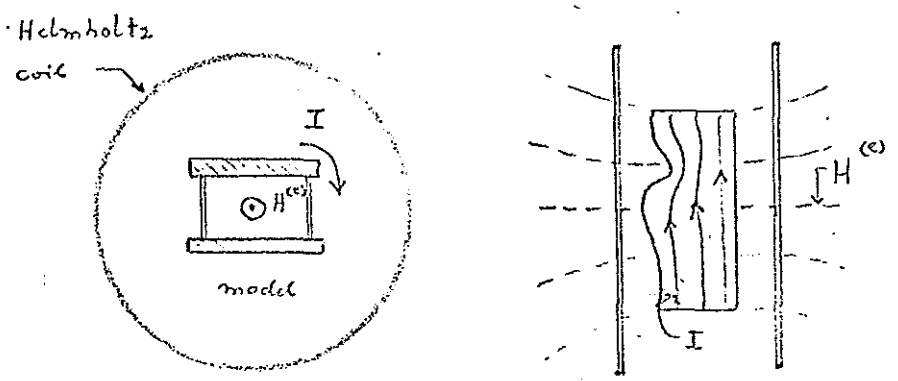

side view top view

In SPITTA's arrangement for the study of the coast effect the conductors are placed below a horizontal band-current closed by a large vertical loop. The oceanic and continental substructure is represented by a thick metalic plate, the oceans by a thin metalic sheet which partially covers the plate. The thickness of the plate is large in comparison to the skin depth and its width about twice the half-width of the field of the band-current at the level of the plate. The induced current systems form closed loops within plate and sheet and can be assumed to be largely horizontal. By placing one edge of the covering sheet below the center of the band-current the coast effect of an ionospheric jet can be studied for any angle between coast and jet.

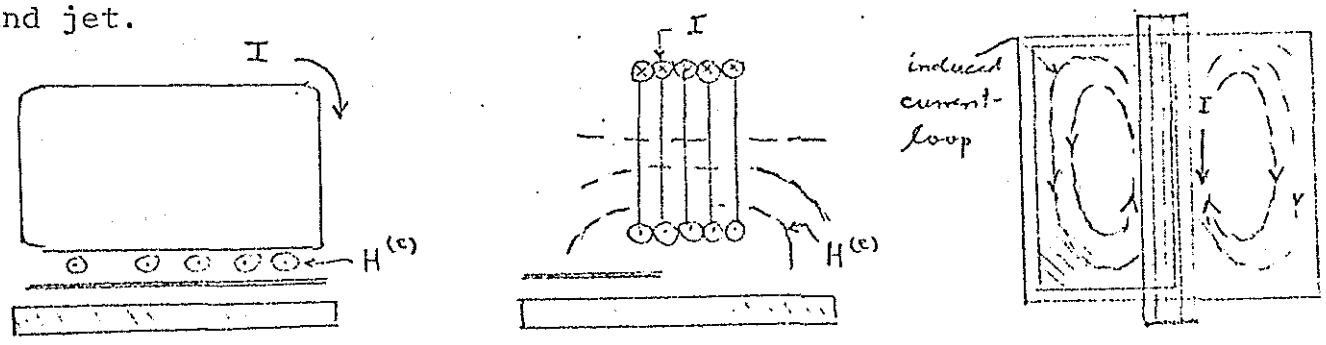

side view top view

(edge of thin sheet in E-polarization)

The ratio of the length-scales model: nature should be in the order 1 : 10^6 or 1 : 10^7. In this way current loops of some 1000 km in nature can be reproduced. In SPITTA's experiment the ratio of length-scales is 1 : $4 \cdot 10^6$. A 4 km thick ocean is represented by an aluminium sheet of 1 mm thickness, a highly conducting layer in the mantle at 360 km depth by an aluminum plate 9 cm below the sheet. The width of this plate is 2 m and is equivalent to 8000 km in nature.

Model conductors may be chosen from the following materials:

Cu - AL - Pb	7 ——— $0.5 \cdot 10^7$	$(\Omega m)^{-1}$
Graphite	$3 \cdot 10^4$	"
(saturated) NaCl solution	20	"
H_2SO_4, HNO_3, HCl-solution (concentration of maximum conductivity)	60	"

In SPITTA's experiment the conductivity-ratio model: nature is $2 \cdot 10^7 : 4$. Hence, with a ratio of length scales of $1/4 \cdot 10^{-6}$ a frequency of 1 kHz in the model corresponds to $1/32 \cdot 10^{-2}$ Hz ≈1cph in nature.

DOSSO uses graphite to represent the oceans and highly conducting material in the deeper mantle, saturated NaCl-solution to represent the continental surface layers and the poorly conducting portions of crust and uppermost mantle. Since his model frequencies are only slightly higher (1 to 60 kHz), a one order of magnitude greater ratio of length-scales (1:10^5) has to be used to simulate natural frequencies between 1 cph and 1 cpm.

The lists of available model conductors shows that it is difficult to simulate conductivity contrasts of 1:10 or 1:100 which are of particular importance in the natural induction process. Only salt solutions of variable concentration could provide a sufficient range in model conductivity, but their relatively

low conductivity requires the use of very high frequencies (10^3 kHz) and extremely large model dimensions (10 m).

In conclusion it should be pointed out that even those scale model experiments which do not reproduce the natural induction in a strict quantitative sense may be useful for a descriptive interpretation of complicated variation fields. In those cases only the impedance or the relative changes of the magnetic field with respect to the field at one distinguished point above the model will be considered and compared with actual data.

10. Geophysical and geological relevance of geomagnetic induction studies

In exploration geophysics the magnetotelluric method, preferably in combination with geomagnetic depth sounding, has been applied with some success to investigate the conductivity structure of sedimentary basins. Electromagnetic soundings with artificial sources as well as DC soundings which truly penetrate through a sedimentary cover of even moderate thickness are difficult to conduct on a routine basis. Hence, it seems that electromagnetic soundings with natural fields are more efficient than any other geoelectric methods in exploring the overall distribution of conductivity in deep basins.

In particular the integrated conductivity τ of sediments above a crystalline basement is well defined by the inductive surface response to natural EM fields and can be mapped by a survey with magnetic and geoelectric recording stations. If in addition some estimate about the mean conductivity of the sediments can be made from high frequency soundings, the depth of the crystalline follows directly from τ.

If structural details of sedimentary basins are the main interest of the exploration, a mapping of the electric field only according to strength and direction for a given polarisation of the regional horizontal magnetic field will be adequate. The inter-

pretation is handled like a direct current problem in a thin conducting plate of variable conductivity. This so-called "telluric method" represents a very simple kind of inductive sounding, but the preferential direction of the superficial currents thus found usually gives a surprisingly clear impression about the trend of structural elements like grabens, anticlines etc. The usefulness of this method arises from the fact that these structural elements can be detected even when they are buried beneath an undisturbed cover of younger sediments.

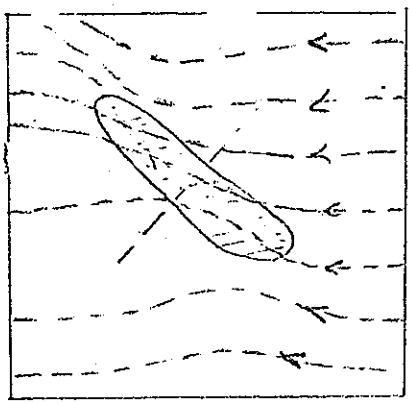

Current distortion by sedimentary filling of buried graben

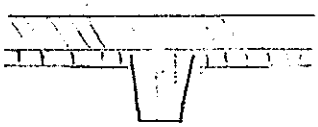

Geomagnetic and magnetotelluric soundings are less useful for exploration in areas of high surface resistivity, in particular in crystalline regions. Even pulsations penetrate here too deeply to yield enough resolution in the shallow depth range of interest for mining. Audio-frequency soundings with artificial or even natural sources will be better adapted and are widely used in mineral exploration.

The probing of deeper parts of crust and mantle with natural electromagnetic fields will eventually lead to a detailed knowledge of the internal conductivity distribution down to about 1000 km depth. Its relation to the downward rise in temperature is obvious, in fact electromagnetic soundings provide the only, even though indirect method to derive present-day temperatures in the upper mantle.

Other derivable properties of mantle material like density and elastic parameters are largely determined by the downward increase in pressure with only a second-order dependence on temperature, which is hardly of any use for estimates of mantle temperatures.

The remarkable rise of conductivity between 600 and 800 km depth, however, should not be understood as temperature-related but as indication for a gradual phase change of the mantle minerals, possibly with a minor change in chemical composition, this is with a slight increase of the Fe:Mg ratio of the olivine-spinell mineral assembly.

The conductivity beneath the continental upper mantle from 100 km down to about 600 km is suprisingly uniform and seems to indicate that in this depth range the temperature gradient cannot be far away from its adiabatic value of roughly 0.5° C/km. The mysterious appearance of highly conducting layers in the uppermost mantle may be connected to magma chambers of partially molten material and to regional mantle zones of higher than normal temperatures in general. The expected correlation of high mantle conductivity, high terrestrial heatflow and magmatic activity clearly exists in the Rocky Mountains of North America.

There are also some indication for high conductivities beneath local thermal areas. The Geysers in California, Owens Valley in Nevada, possibly Yellowstone and the Hungarian plains are examples. It should be pointed out, however, that there exist also regions of high subcrustal conductivity with absolutely no correlation to high heatflow or recent magmatic activity. The most prominent inland anomaly of geomagnetic variations, which has been found so far, namely the Great Plains or Black Hills anomaly in North America, lacks still any reasonable explanation or correlation to other geophysical observations.

One great unsolved problem in geomagnetic inductions studies is the depth of penetration of slow variations into the mantle below ocean basins. There are definite reasons to believe

that the upper mantle beneath oceans is hotter than the mantle beneath continents down to a depth of a few hundred kilometers. If this is so, a correspondingly higher conductivity should exist beneath oceans which could be recognised from a reduced depth of penetration in comparison to continents. Once a characteristic conductivity difference between an oceanic and a continental substructure has been established, this could be used to recognize former oceanic mantle material beneath present-day continents and vice versa.

First soundings with recording instruments at the bottom of the sea have been carried out. They confirmed to some extent the expectation of high conductivities at extremely shallow depth, but these punctual soundings may not be representative for the oceans as a whole. Here the development of new experimental techniques for expedient seafloor operations of magnetic and geolectric instruments has to be awaited.

Observations on mid-oceanic islands provide a less expensive way to study the induction in the oceans which in the case of substorms and Sq is strongly coupled to the crustal and subcrustal conductivities beneath the oceans. But again oceanic islands are usually volcanic and their substructure may differ from that of ordinary parts of ocean basins.

The island-effect itself is no obstacle for soundings into the deep structure. In fact, this effect represents a powerful tool to investigate the inductive response in the surrounding open ocean, since the theoretical distortion of the variation fields due to the islands can be regarded at sufficiently low frequency as a direct current problem for a given pattern of oceanic induction currents at some distance from the island. Setting the density of these currents in relation to the observed magnetic field on the island gives the impedance of the variation field for the surrounding ocean of known integrated conductivity. To a first approximation induced currents in the ocean do not contribute to the horizontal magnetic field on the island. Hence, by knowing their density the horizontal magnetic field on the sea floor can be calculated from which the inductive response function for the oceanic substructure follows.

11. References for general reading

Electromagnetic induction in the earth and planets. Special issue of Physics of the Earth and Planet. Interiors, 7, No.3, 227-400, 1973.

BERDICHEVSKII, M.N., (Electrical sounding with the method of magneto-telluric profiling), Nedra Press, Moscow 1968.

FRAZER, M.C.: Geomagnetic depth sounding with arrays of magnetometers. Rev. Geophys. Space Phys. 12, 401-420, 1974.

JANKOWSKI, J., Techniques and results of magnetotelluric and geomagnetic deep soundings, Publications of the Institute of Geophysics, Polish Academy of Sciences, vol.54, Warsaw 1972.

KELLER, G.V. and FRISCHKNECHT, F.C.: Electrical methods in Geophysical prospecting. Int. Ser. Monogr. im Electromagnetic Waves, 10, 1-517, 1966.

PORATH, H. and DZIEWONSKI, A.: Crustal resistivity anomalies from geomagnetic depth-sounding studies. Rev. Geophys. Space Phys. 9, 891-915, 1971.

RIKITAKE, T.: Electromagnetism and the Earth's interior. Developments in Solid Earth Geophys. 2, 1-308, 1976.

SCHMUCKER, U.: Anomalies of geomagnetic variations in the southwestern United States. Bull. Scripps Inst. Oceanogr. 13, 1-165, 1970.

WARD, S.H.: Electromagnetic theory for geophysical application. In: D.A. Hansen et al. (Eds.), Mining Geophysics, The Soc. of Expl. Geophysicists, Tulsa, Oklahoma, 1967.

WARD, S.H., PEEPLES, W.J., and RAN, J.: Analysis of geoelectromagnetic data. Methods in Computational Physics 13, 163-238, 1973.